GILL BLOOD FLOW IN TELEOSTS

by

ANTHONY PETER FARRELL

B.Sc., University of Bath, 1974

A THESIS SUBMITTED IN PARTIAL FULFILMENT OF

THE REQUIREMENTS FOR THE DEGREE OF

DOCTOR OF PHILOSOPHY

in

THE FACULTY OF GRADUATE STUDIES

(Zoology)

We accept this thesis as conforming

to the required standard

THE UNIVERSITY OF BRITISH COLUMBIA

June, 1979

In presenting this thesis in partial fulfilment of the requirements for an advanced degree at the University of British Columbia, I agree that the Library shall make it freely available for reference and study. I further agree that permission for extensive copying of this thesis for scholarly purposes may be granted by the Head of my Department or by his representatives. It is understood that copying or publication of this thesis for financial gain shall not be allowed without my written permission.

Department of Zoology

The University of British Columbia
2075 Wesbrook Place
Vancouver, Canada
V6T 1W5

Date 20th July 1979

ABSTRACT

Unlike the respiratory organs of airbreathing vertebrates where gas exchange is perfusion limited, gas transfer across fish gills is diffusion limited. Fish can therefore enhance gas exchange by increasing the gill diffusing capacity. Previous suggestions indicate that fish may achieve this by altering the pattern of gill blood flow to increase the area of gill perfused and to reduce the blood-water diffusion barrier. To verify these suggestions an investigation of the patterns of gill blood flow, their regulation and their significance in gas exchange in the ling cod, Ophiodon elongatus, was undertaken.

The circulatory arrangement in the gill filament of the ling cod consists of an arterio-arterial respiratory network and an arterio-venous venolymphatic system. All cardiac output passes through the respiratory exchange sites, the lamellae. Blood flow through lamellae is described by sheet blood flow equations, where flow is proportional to the vascular sheet thickness (h). The lamellar vascular sheet is very compliant and h increases with transmural pressure (ΔP_{lam}). It is predicted that if ΔP_{lam} and flow are raised, then intralamellar shunting of blood flow and a reduction of the blood-water barrier will result, thereby increasing the gill diffusing capacity.

Not all lamellae appear to be equally perfused under certain in vivo conditions. Furthermore, if resting perfusion

conditions are simulated, only 67% of the more proximal lamellae are perfused. Thus the total gill area is not utilised at rest. To account for this situation it is proposed that the critical closing pressures associated with distal lamellar units are greater than those for the proximal lamellae. The afferent arterioles were determined to be the major resistance site in the gills and they therefore control flow to lamellae. Elevations in flow and lamellar input pressure will reduce the likelihood of critical closing and more lamellae will be perfused. Lamellar recruitment increases the gill diffusing capacity.

The demonstrated changes in flow patterns to and within lamellae are effected by elevated flow and input pressures (or ΔP_{lam}). Changes in cardiac performance and in the pressure profile of the gills alter flow and pressure. Cardiac performance in ling cod is influenced by intrinsic, cholinergic and adrenergic controls which alter stroke volume and heart rate. The pressure profile of the gills can be altered by cholinergically or adrenergically mediated changes in vessel dimensions. The gill outflow arteries vasoconstrict in localised regions with cholinergic stimulation and thereby increasing gill resistance (Rg) and lamellar input pressures. Afferent vessels apparently dilate with β-adrenergic stimulation and thereby lower Rg.

Cardiovascular changes are associated with conditions of reduced oxygen availability (hypoxia) and of increased oxygen demand (struggling) in ling cod. The cardiovascular changes are

such that they alter the pattern of gill blood flow and increase the gill diffusing capacity. Increased oxygen uptake, cardiac output and gill ventilation are associated with hypoxia and struggling. The quantitative increases in cardiac output *per se* associated with these conditions does not fully account for the observed increase in oxygen uptake. It is concluded that changes in gill diffusing capacity through alterations in gill blood flow patterns are important in enhancing oxygen uptake across the gills.

TABLE OF CONTENTS

ACKNOWLEDGEMENTS

During the course of this work I received help, advice, encouragement and technical assistance from many people. I am grateful. I would like to acknowledge the following in particular:

Dr. David Randall, for giving me the opportunity to perform this research and for providing subtle guidance throughout my endeavours.

Dr. David Jones, whose tenacity always provided me with an incentive.

Dr. Sidney Sobin, for the use of the facilities in his laboratory in Los Angeles.

Dr. David Smith, for his assistance in some of the micropressure experiments.

Charles Daxboeck, for his assistance in the oxygen uptake determinations and gill perfusion studies.

Colin Parkinson, Fergus O'Hara, Laslo Veto and Susin Crosby of the U.B.C. Zoology Department for their technical assistance.

Gerry Bance and Paul Nitishin of the University of New Brunswick Biology Department, for their technical assistance.

Dr. Colin Mailer of the University of New Brunswick Physics Department, for his help in developing the equation to describe resistance in the afferent filament artery.

Susan Harrison, for her assistance in developing and running the programs for the PDP II.

All the post-graduates and post-doctorates in D.J.R.'s laboratory, for their friendship and support, as well as intellectual interchange. Tony Harmen, for the many discussions with him on the properties of blood vessels.

Anna MacDonald, for her typing skills in preparing this manuscript.

Miriam, for her patience during the writing of this thesis.

I was supported at U.B.C. by a U.B.C. graduate fellowship and teaching assistantships. I was able to complete my writing while I was a lecturer in the U.N.B. Biology Department. The equipment for my research was supplied through N.R.C. operating grants to D.J.R.

GENERAL INTRODUCTION

In recent years patterns of blood flow through the gill filament and lamellae in teleost fish has received some attention. A number of these studies base their conclusions completely or largely on the anatomical arrangements of blood vessels (e.g. Mott, 1950; Steen and Kruysse, 1964; Hughes and Grimstone, 1965; Richards and Fromm, 1969; Morgan and Tovell, 1973). Such studies have been valuable, but confusion over precise vascular arrangements has invalidated some of their conclusions. Furthermore, they generally lacked any consideration of the physical properties of blood vessels, for which considerable literature now exists (Bergel, 1972; Attinger and Attinger, 1973, Kaley and Altura, 1977). Blood vessels are not simple rigid tubes especially when conducting pulsatile blood flow. They have a compliance which is dependent in part on the radius/wall thickness ratio which may vary with absolute blood pressure and pulse frequency. Thus the resistance of a vessel will vary depending on the conditions of the input and output flow. For instance, vessels will collapse at above ambient pressures, their 'critical closure pressure', (Burton, 1951; Nicol, et al., 1951). The resistance and compliance of vessels are largely passive properties, but they can be influenced neurally or humorally, e.g. adrenergic and/or cholinergic actions. The actions may be tonic effects, i.e. to enable the vessel to maintain a given diameter over a range of pressures, or be directed at specific sites e.g. sphincters to control blood pressure and flow to certain regions. To evaluate the relative

importance of these passive and active vascular changes information on vascular innervation is necessary. With the exception of Gannon's (1972) extensive work on the adrenergic innervation of trout heart and gills, this information is lacking. It is therefore not surprising that previous descriptions of gill blood flow based on anatomy alone are somewhat limited.

Physiological studies of gill blood flow have leaned heavily on *in vitro* perfusion studies (See later for numerous references), which date back to the Keys and Bateman (1932) perfused heart-gill preparation. At best it is difficult to mimic *in vivo* conditions *in vitro*. We also lack a detailed knowledge of the individual importance that each of the various *in vitro* perfusion conditions has upon patterns of flow through the gill. Once we establish their importance, it is likely that a number of conclusions from previous *in vitro* work will need reinterpretation because of neglect surrounding the selection of perfusion conditions.

In vivo information of gill blood flow is not vast. Other than the studies of Davis (1972) and Booth (1978), which established that only a portion of all gill lamellae were perfused in trout at rest, there has been no study directed towards establishing patterns of blood flow through the gill. Certain detailed *in vivo* investigations of cardiovascular function have been helpful in ascertaining some characteristics of pre- and post-branchial blood flow (Jones *et al.*, 1974;

Stevens et al., 1972). Many other in vivo studies have measured blood pressures and heart rate in teleosts, but Stevens and Randall (1967b), Holeton and Randall (1967b), and Kiceniuk and Jones (1977) only have estimated values for cardiac output for resting teleosts. Randall et al. (1967) noted at that time that the data on circulation and respiration in fish were fragmentary; the same might now be said for the information on specific blood flow patterns in the gills.

Why are patterns of gill blood flow so interesting? Saunders' (1962) observed that in several teleosts that O_2 uptake (Mo_2), predicted from total gill area, was nearer to the elevated levels measured during swimming rather than those measured at rest. This is surprising since O_2 transfer at the gills is considered to be a passive process. Steen and Kruysse (1964) attempted to explain the findings in terms of anatomical shunts which they developed from Riess' (1881) original concept of two blood pathways in gill filaments. Their choice of eels as an experimental fish was unfortunate to explain the findings of Saunders since the eel gill vasculature differs in a very important respect from the trout and many other fish. All cardiac output goes through the gills in trout (Gannon et al., 1973) unlike in eels where blood can enter non-respiratory channels and by-pass the lamellae. As a consequence, arterial blood in eels is fully saturated only during exercise, whilst arterial blood in trout is fully oxygenated at rest (Randall et al., 1967). Clearly the explanation of Steen and Kruysse cannot be applied to the findings of Saunders. Steen and Kruysse,

however, made the important observation that alterations in blood flow can alter $\dot{M}o_2$ in eels. In trout the pattern of gill blood flow can change. Only 60% of all lamellae are perfused at rest (Booth, 1978); a situation predicted by Randall et al. (1967) and Morgan and Tovel (1973). Perfusion of more lamellae would increase the surface area for gaseous exchange, which could increase the rate of oxygen transfer. Trout, however, increase Mo_2 by 5 to 10 times during exercise (Saunders, 1962; Stevens and Randall, 1967a; Kiceniuk and Jones, 1977) and thus lamellar recruitment from 60% to even 100% cannot fully account for this change. Thus Randall et al. (1967) have suggested that increased blood volume in the gill respiratory circulation, shunting of blood closer to the surface of the gills and a decrease in the thickness of lamellae may all be important in altering Mo_2. There have also been postulates that flow changes within individual lamellae (intralamellar shunting) (Hughes and Grimstone, 1965). It is, therefore, clear that various patterns of gill blood flow must occur and they have fundamental effects on the rate of Mo_2 in teleosts. However the specific nature of these changes and their control is largely unknown. Thus I will examine various gill blood flow patterns, indicating how they are affected or effected by adrenergic, cholinergic or passive mechanisms and suggesting how they may effect O_2 exchange.

This study approached the problem from physiological and morphological standpoints using a number of recently developed

techniques in addition to established ones. The experimental fish was Ophiodon elongatus (ling cod) because of its suitability for the in vivo surgery. Nothing is known of the vascular pathways in this fish, thus, in Section I, there were examined using histological and morphological thchniques and 3-D observations of plastic vascular corrosion casts (Gannon et al., 1973). I used equations to describe the lamellar blood flow after first determining the vascular dimensions and the passive properties of the vessels with respect to pressure. I also predicted the major gill resistance sites and possible flow control sites from the vascular geometry and then tested these predictions using blood pressure measurements in the gill filament. I also established the importance of active (humoral or neural) cardiovascular controls in controlling gill blood flow using in vitro and in vivo experiments. The passive properties of the gill vessels and how they influence the number of lamellae perfused were examined. In the final Section, the cardiovascular responses of the fish to reduced oxygen demand, hypoxia, and to increased oxygen requirements, struggling, were examined and interpreted based on the previous observations and conclusions. The final outcome was a more complete analysis of blood flow in a teleost which enabled a description of branchial blood flow patterns and their probable mode of regulation.

GENERAL MATERIALS AND METHODS

Fish supply and holding facilities

Salines

Routine surgery

Experimental aquaria

Isolated perfused holobranch preparation

Recording systems

In vivo monitoring

Fish supply and holding facilities

Ling cod, Ophiodon elongatus, were caught by local fishermen, transported to U.B.C. and held in large aquaria supplied with flowing, aerated water. The water temperature was maintained between 9 and 11°C. The fish were fed a maintenance diet of live rainbow trout, but were starved for at least several days prior to an experiment. A total of 69 ling cod were used in these experiments with weights ranging from 2.5 to 6.5 kg (average weight = 4.6 kg).

Rainbow trout, Salmo gairdneri, (300 to 600 g) were used in one series of experiments. They were obtained from a local fish hatchery and held in large aquaria supplied with flowing, aerated, dechlorinated Vancouver tap water at U.B.C. The water temperature fluctuated between 7 and 12°C depending on the season. The trout were fed daily with commercial trout pellets.

All experiments were performed at water temperatures between 10 and 11°C.

Salines

Cortland salines for saltwater and freshwater fish (Wolf, 1963) were used in all experiments. The composition in $g.l^{-1}$ of the freshwater fish saline was: 7.25 g NaCl; 0.38g KCl; 0.162 g $CaCl_2$; 0.23 g $MgSO_4.7H_2O$; 1.0 g $NaHCO_3$; 0.4 g $NaH_2PO_4.2H_2O$ (or 0.36 g $NaH_2PO_4.H_2O$); 1.0 g glucose.
The saline for saltwater fish contains an additional 3.25 g NaCl

and has an osmolality of 373 m Osm. Salines used for in vivo experiments were heparinised (10 $IU.ml^{-1}$) and the glucose was excluded.

Routine surgical protocol to allow in vivo measurements of cardiac output, pre- and post-branchial blood pressure and ventilation

Ling cod were deeply anaesthetised (0.02% MS222, trimethane sulphonate), placed ventral side up in an operating sling and cooled with an ice pack on the body. The gills were continuously irrigated with cool (8 to 14°C), recirculating seawater containing anaesthetic (0.005% MS222). A 4-6 cm incision was made in the skin along the inside of the opercular cavity wall in line with, but slightly ventral to the ventral aorta. The muscle mass, which is thinnest in this area, was carefully teased aside to expose the pericardium and the more ventral hypobranchial artery. The pericardium surrounding the ventral aorta was opened and a pneumatic cuff (Shoukas, 1977) was implanted around the anterior end of the ventral aorta. A cuff-type electromagnetic flow probe (Biotronics) was selected for good fit on the ventral aorta (10-20% vessel constriction, Langille, pers. comm.) and was implanted near to the bulbus arteriosus. The pneumatic cuff and the flow probe were, therefore, maximally separated on the vessel. Both cuffs were anchored to their adjacent muscle masses with several silk thread sutures. The bevelled tip of a non-occlusive catheter

(50 cm of polyethylene (PE) tubing, PE 60) was introduced upstream into the ventral aorta with the aid of a Medicut cannula (Aloe Medical, St. Louis). All catheters were prefilled with heparinised saline. The catheter was secured to the body of the flow probe and to the adjacent muscle mass. The wound in the muscle mass and in the skin were closed separately with silk thread sutures. The dorsal aorta was cannulated via the efferent banchial artery of one of the 4th gill arches (Jones et al., 1974). The catheter, 50 cm of PE 100 tubing, was introduced downstream of the ligated efferent vessel and advanced 2-5 cm towards the dorsal aorta. The vessel was tied around the catheter and the skin incision closed around the catheter which was anchored in place to the tissue. The buccal and opercular cavities were also cannulated in some experiments using methods similar to those described by Holeton and Randall (1967a) using PE 200 tubing. These surgical procedures routinely lasted approximately one hour and were accomplished with minimal blood loss from the fish.

Recovery of the fish from anaesthetic was begun during the final stages of the surgery by removing the ice pack and commencing gill irrigation with fresh saltwater. When strong opercular movements had began, usually within 5 minutes, the fish was placed in the experimental holding aquarium fitted with a temporary gill irrigation tube. Fish were sufficiently revived after 5 to 10 minutes to swim off the irrigation tube and sustain their own gill ventilation.

The experimental aquarium (Fig. 1) was a darkened, covered plexiglass box, which limited forward and lateral movements. The saltwater supply was flow-through, aerated and at 10-11°C, but it could also be diverted through a gas exchanger to generate hypoxic or hyperoxic water. A constant temperature recirculating system was also in line and this was used to recirculate water containing anaesthetics e.g. 0.7% urethane (ethyl carbonate) during in vivo micropressure experiments. In experiments where oxygen consumption was measured, the plexiglass box was replaced by an air tight, darkened plexiglass cylinder that had a much reduced water dead space.

Isolated, perfused holobranch preparation

The heart and ventral aorta were exposed by an 8-10 cm ventral midline incision in deeply anaesthetised ling cod (0.02% MS222). The circulating blood was heparinised with an intracardiac injection of sodium heparin (1,000 IU.kg^{-1}). The bulbus arteriosus (bulbus) was cannulated occlusively through an incision in the ventricle with a short, heat flared PE 200 catheter. The branchial vessels were cleared of blood with approximately 200 ml of pre-filtered (Millipore, 0.45μ), heparinised saline infused via the catheter. The best clearing results were obtained when rapid pulsations were applied to the perfusion syringe, and when the gills were completely submerged and irrigated with the salt water at 10°C during the perfusion. The filament tips and the small filaments at either end of the

FIGURE I

A schematic diagram of the experimental holding aquarium displaying the three alternative water supplies that were utilised. ⊕ = a three way tap which controlled the direction of flow. Gas = gas supply; either air, 100% N_2 or 100% O_2. The aquarium was covered with a loose fitting lid when the fish was inside.

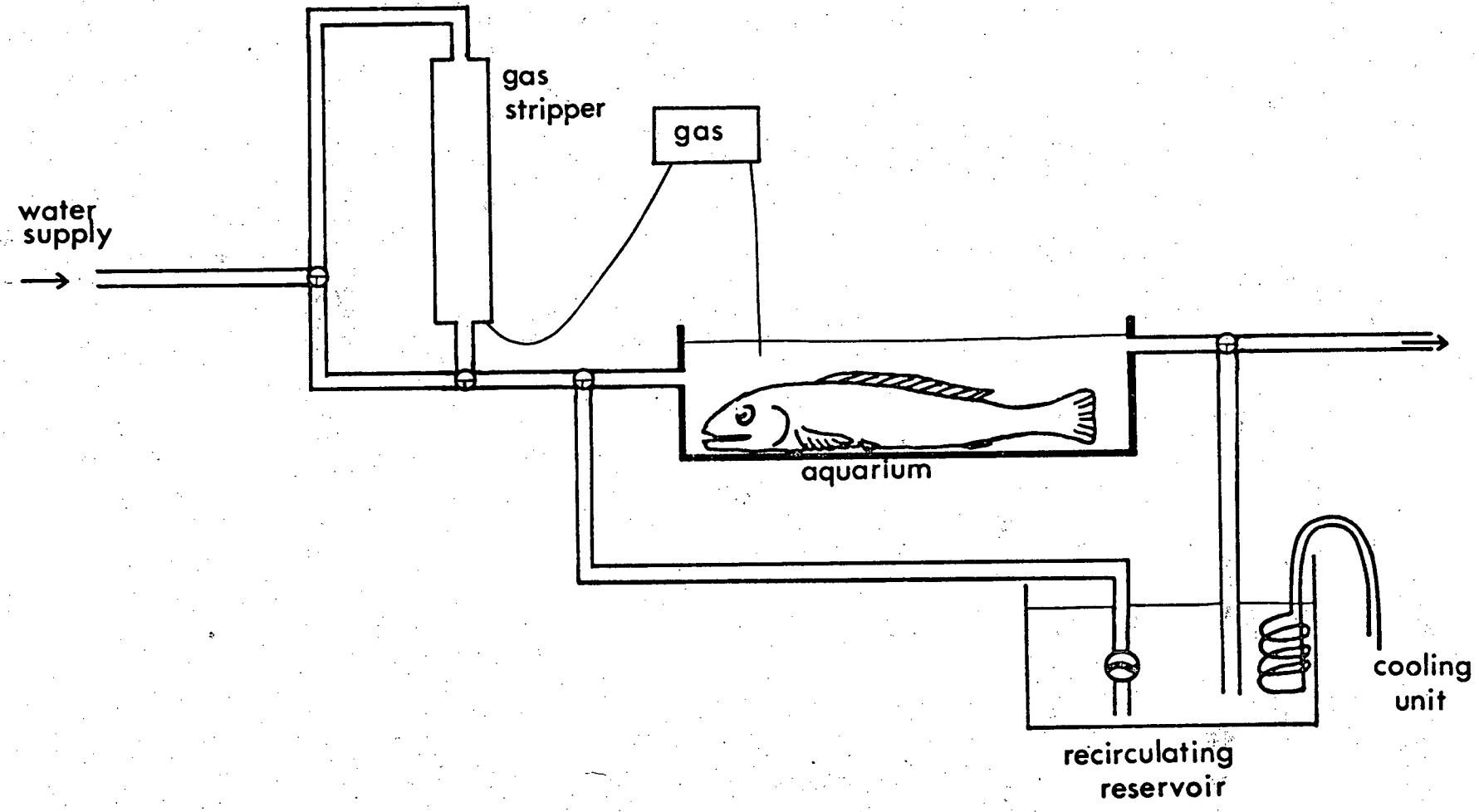
gas
stripper
gas
water
supply
aquarium
cooling
unit
recirculating
reservoir

arch were always difficult to clear at this stage. The tips and any unclear filaments were later cleared, either by saline perfusion after the afferent branchial artery was cannulated, or, more commonly, during the initial perfusion period of the experiment. Clearing blood lowered gill resistance to perfusion. The whole branchial basket was excised and then individual holobranchs were dissected free. Isolated holobranchs were stored in aerated (95% O_2; 5% CO_2) saline, on ice, until required for cannulation.

The afferent and efferent arch vessels were exposed at either end of the holobranch and cannulated with blunted and shortened 18 G, thin walled hypodermic needles. In early experiments 0.5 mm lengths of PE 100 were used as catheters. The arch was kept ice-cooled during cannulations. The gill arch and free filaments distal to the cannulation site were ligated as near to the catheter as possible. Hence a minimal amount of cut or exposed tissue was perfused and the poorly cleared filaments were excluded from the preparation. It was estimated that at least 95% of the remaining filaments were clear of blood. These arch ligations also reduced, but did not completely stop, venous and lymphatic outflow which would have otherwise proceeded at an unrestricted rate. The arterial perfusion pathway was further isolated by also ligating the hypobranchial artery at the afferent end of the arch. Cannulated arches were stored in the same ice-cold saline as above and were always used within 3h of their removal from the fish.

Recording Systems

Blood and water pressures were detected using saline filled Statham pressure transducers (P23Db, P23BB and P23V) connected to saline filled catheters. For micropressure measurements the P23Db pressure transducer was oil filled. The transducers were calibrated against pressures generated by a static water column before the experiment (1 cm H_2O = 0.098 kPascals). The transducers were always balanced to a zero signal at the appropriate water or saline level. This balance point was checked frequently throughout the course of an experiment. The transducers faithfully reproduced oscillating pressures in the range being monitored since the frequency response of the fluid filled transducers and their associated catheters was in excess of 10 Hz, as determined by the Hanson "pop" test (McDonald, 1960). Pulsatile ventral aortic blood flow (cardiac output, Q) was monitored with a BL610 flow meter (Biotronix Ltd.), set for a 12.5 Hz frequency response, using the signals of the implanted electromagnetic flow probe. A zero flow calibration signal was obtained *in vivo* by either, briefly occluding the ventral aorta distal to the flow probe by inflating the pneumatic cuff, by disturbing the fish in the aquarium, or by an intravascular Carbachol (K+K) injection (0.01 to 0.1 μg.ml blood^{-1}) (See later Figs. 16 and 40). The latter two procedures produced a bradycardia during which ventral aortic blood flow stopped briefly. Any major flow probe movement would change the zero signal level. Such changes, whilst a nuisance, were easily

corrected for, or a new zero signal was established using one of the above techniques. Drift of the flow probe signal during lengthy recording periods was not extensive between zero calibrations and was ignored. The signals from individual flow probes were calibrated either *in situ* or *in vitro* with measured saline perfusions. Beat to beat heart rate was monitored in some experiments using a rate meter triggered by the pulsatile blood flow signal.

All electrical signals were suitably amplified for monitoring on chart recorders. Initially a Beckman R four channel chart recorder was used to continuously display records during an experiment. Later a Brush 260 six channel chart recorder was used in conjunction with a Tanberg series 115 tape recorder (equipped with a flutter compensation device). With this latter system all signals were recorded directly onto the chart recorder and the blood pressures and blood flow signals were also stored directly onto magnetic tape. The stored information was used for subsequent analyses, when the signals were replayed through 5Hz band pass filters onto the chart recorder. The filters reduced background electrical noise produced by the tape recorder, but did not alter the signal waveform significantly.

Oxygen concentration was monitored continuously in the inflowing water with a Beckman 0260 O_2 analyser that had automatic temperature compensation. The signals from the oxygen analyser were only recorded on the Brush recorder during hypoxic or hyperoxic exposure experiments. For oxygen uptake experiments

the oxygen partial pressure, Po_2, in water samples was measured with a Radiometer PHM72 system with associated electrodes and water jackets. The oxygen electrodes were calibrated using zero oxygen solutions (saturated sodium sulphite or N_2 equilibrated seawater) and air, or 100% O_2 equilibrated seawater.

In vivo monitoring of blood flow and ventilation in Ophiodon elongatus.

Q, blood pressures and ventilation pressures were monitored in vivo on individual ling cod after recovery from routine surgical procedures and acclimation to the aquarium for 12 to 24 hours. Records were collected for up to 6 days and often continuously for 10 to 15 hours in any one day. On occasion monitoring was continued over night on an undisturbed fish. Noise was minimised and kept constant (white noise) during experimentation. The fish were usually in one of three states. The majority of the time fish were "resting" when the environment was constant, and this state corresponded to steady state recordings. Fish usually became "disturbed" when the environment suddenly changed and here the recordings altered in an unpredictable fashion. A "struggle" involved visible or audible tail movements and it was accompanied by a particular pattern of cardiovascular and respiratory events. Struggling usually followed a disturbance but sometimes it apparently occurred spontaneously. All experiments commenced only when the fish were considered to be in a resting state. If the fish struggled or were disturbed during the experiment the results

were not analysed. An exception to this rule was during hypoxic exposure when fish often struggled and in this case the struggle response was analysed separately.

SECTION I

THE MORPHOLOGY AND VASCULAR PATHWAYS OF THE GILLS IN LING COD

Gross morphology and morphometrics of ling cod gills.

Plastic corrosion casting of the gill vasculature.

The properties of the lamellar capillary bed as revealed by silicone elastomer casting of the capillaries under known transcapillary pressure gradients.

Predictions on gill blood flow.

INTRODUCTION

In order to interpret physiological experiments concerning blood flow it is essential to first establish the nature of the vascular pathways under observation. This has not always been the situation in the past. For instance, a controversy concerning arterio-venous shunts in gills was only recently resolved when the correct vascular networks of gill filaments were established (see Steen and Kruysse, 1964; Richards and Fromm, 1969; Gannon *et al.*, 1973; Morgan and Tovell, 1973; Vogel *et al.*, 1973, 1974 and 1976; Cameron, 1974; Laurent and Dunel, 1976; Smith, 1976). Three points emerged from this controversy. First, whilst teleosts all have the same basic pattern of gill blood vessels, many important species differences exist. Second, some of the techniques used for visualising the complex 3-dimensional patterns of vessels were on occasion misleading. The development of methyl methacrylate vascular corrosion casting by Murakami (1971) has, however, allowed 3-dimensional analysis of vascular beds using the scanning electron microscope. Gannon *et al.* (1973) adopted this technique to examine the vasculature in *Salmo gairdneri*. Since then the gill vessels of other teleost species have been examined using a similar technique (Dunel and Laurent, 1977; Olsen, pers. comm.). Lastly, the wealth of previous literature dating back almost two centuries was somewhat ignored. The anatomical works of Munro (1785), Doellinger (1837), Hyrtl (1838), Muller (1839),

Riess (1881) on fish gill vasculature have now been well reviewed by Smith (1976), Laurent and Dunel (1976) and Campbell et al. (in preparation). Ironically it is Muller's (1839) major conclusions that have in fact been verified using modern techniques. Fundamentally, two vascular systems exist in the gills: a respiratory system with arterio-arterial pathways and a nutritive system with arterio-venous pathways. Whether the nutritive supply is derived only from efferent arterial vessels, as in Salmo gairdneri, or both afferent and efferent arterial vessels, as in Anguilla, is an important species difference since in the former situation all the cardiac output must pass through the respiratory exchange area, the secondary lamellae.

Vessel geometry is helpful in establishing theoretical patterns of flow through the vasculature. Vessel resistance can be calculated from vessel geometry by assuming Poiseuillean flow and knowing certain physiological blood flow variables. In a parallel network of vessels, such as the gills, resistance sites are valuable in predicting flow patterns. Unfortunately, theoretical analysis of blood flow in capillary beds where vessel diameters approach vessel length, e.g. respiratory exchange sites, is difficult using Poiseuillean equations (Weibel, 1963). Sheet blood flow equations, however, allow a better description of such capillary blood flow. With sheet blood flow equations, and given the properties of the vascular bed, predictions of volumes, resistances and flow patterns can be made relatively

easily. Sheet blood flow equations have been used to describe alveolar blood flow (Fung and Sobin, 1969 and 1977). The derived equations for sheet blood flow describe the capillary sheet by its thickness (h), its area (expressed as a ratio of vascular area to that of the tissue) and its vascular compliance. Characteristically, h is dependent upon the transmural pressure gradient (ΔP_{alv}), but the planar dimensions, however, remain constant. The degree to which h changes is set by α, the compliance coefficient. For alveolar capillaries α is at least an order of magnitude greater than for systemic capillaries, i.e. the alveolar vascular sheet thickness is very sensitive to the transmural pressure.

The respiratory exchange site in fish is the gill lamellae. The lamellae are erect epithelial folds encasing a dense capillary network. The epithelial folds do not separate under blood pressure because pillar cells extend between the two epithelial sheets at regular intervals. The pillar cells form the capillary endothelium. The lamellae, therefore, show some structural similarities with mammalian alveoli with the pillar cells of lamellae being analogous to the avascular posts of alveoli. Capillary blood flow in lamellae might then be similar to sheet flow in alveoli. Scheid and Piiper (1976) have suggested that "sheet flow" be adopted for lamellar flow in elasmobranch fish. The lamellar shape is certainly sheet-like in elasmobranchs, as it is in teleost fish. Kempton (1969) preferred the term lamellar sheet to lamellar capillaries when

describing the dogfish gill anatomy. If sheet flow theory were applicable to lamellar blood flow, clear similarities would exist between blood flow in vertebrate respiratory organs.

Similarities between mammalian pulmonary and teleost gill blood flow are indeed apparent. The distribution of pulmonary blood flow (Permutt et al., 1962; West, 1977), and gill blood flow (Booth, 1978) may alter to meet respiratory oxygen demands. In an upright human only about 2/3rds of the lung is perfused at rest, but during exercise there is increased lung perfusion associated with elevated arterial blood pressures and increased cardiac output. In resting trout only 60% of gill lamellae are perfused (Booth, 1978). It is expected that the number of lamellae perfused can be increased given a change in metabolic demand, e.g. exercise, or in water quality, e.g. hypoxia, since gaseous exchange at the gills is apparently diffusion limited (Randall et al., 1967; Fisher et al., 1969; Randall, 1976), unlike the lungs where perfusion limitations exist. If this were not the case then the increased oxygen delivery (Vg) and removal (Q) from the gill which are also associated with these two situations would be pointless. Saunders (1962), Steen and Kruysse (1964) and Hughes and Grimstone (1965) have suggested that the effective gill exchange area can be increased and more lamellae are indeed recruited during hypoxia in trout (Booth, pers. comm). Exercising trout, however, increase oxygen uptake as much as 5 fold (Randall et al., 1967); but lamellar recruitment will only increase oxygen uptake by about 50%. Thus

other factors which affect gaseous diffusion must contribute to increase oxygen uptake. Randall et al. (1967) concluded that shunting of blood closer to the surface of the gill and a reduction of lamellar thickness might be operative during hypoxia. With a detailed knowledge of the pattern of flow in gill lamellae it is predicted that we will be able to understand how lamellar flow patterns may affect diffusion.

Sheet blood flow equations have not been applied to the teleost gill lamellae. I established the properties of the lamellar vasculature in ling cod to determine whether sheet flow equations could be applied and intralamellar flow patterns could subsequently be predicted from these equations. Neither gill vascular pathways nor gill morphometrics have been studied previously in ling cod, so these studies were carried out here. Methyl methacrylate plastic vascular corrosion casting and scanning electron microscopy were the major tools used to determine vascular pathways. Having established vascular pathways and geometry, predictions were made on gill blood flow using Poiseuillian equations for the input and output vessels and equations for sheet blood flow for the gill lamellae.

MATERIALS AND METHODS

Gross morphology and morphometrics on fixed gill tissue

In 15 freshly killed ling cod (weight range 2.7 to 6.3 kg.) the whole branchial basket was excised and fixed in Bouin's fixative for 12 to 24 hours. The gills were examined and measured with the aid of a Leitz operating microscope either immediately post fixation or after storage in 70% EtOH. Arch lengths were measured at the base of the filaments. This length approximates to that of the arch arteries. The total number of filaments were counted on each arch and the mean filament length determined by measuring the length of every 10th filament. Only the posterior hemibranchs from the 4 arches on one side of the fish were usually examined, since investigation of the whole gill apparatus showed bilateral symmetry existed between the gill arches and that anterior and posterior hemibranchs were similar.

Some gill filaments were also examined histologically. Complete filaments were removed from the central region of the second gill arch and embedded in paraffin blocks. Histological 5 μ serial sections were taken in the transverse, sagittal and longitudinal planes. The sections were mounted on slides and stained with haemotoxylin and eosin.

Vascular casting using methyl methacrylate plastic

The techniques used were essentially those described by Murakami (1971) and modified by Gannon (1979). The branchial vasculature was completely or partially cast by injection

with the pre-polymerising plastic fluid in 8 fish. Prior to the injection the gills were cleared of blood using heparinised saline (see general methods). The polymerising plastic cocktail, which permitted a 10 to 15 minute working time, was prepared just prior to infusion from a kit (Polysciences Inc., Warrington, Pa.). Care was taken to exclude air bubbles from the catheter when the plastic infusion was started. All infusions were made from a 50 ml syringe. Up to 10 minutes were taken to infuse 10 to 20 ml of methyl methacrylate into the gill bed to prevent a high capillary pressure developing due to the relatively high viscosity (50 to 80 cp) of the unpolymerised methyl methacrylate. Excessive capillary pressures would rupture the lamellar vessels.

After completing the perfusion the catheters were occluded and the gills left submerged and undisturbed for two hours whilst the plastic polymerised and hardened. The tissue was dissolved from around the corrosion cast by first soaking in warm water (<50°C) overnight and then by daily changes of 20% NaOH solutions. The cast was finally cleaned in distilled water in an ultrasonic bath and dried with 100% EtOH.

Cast examination and analysis

The methyl methacrylate casts were first examined macroscopically and with a light microscope. For scanning electron microscopy small areas of interest were carefully dissected from the cast, gold coated and examined with a

Cambridge Stereoscan microscope. A 10 kV accelerating voltage was used on the microscope to minimise volatilisation of the plastic cast (Gannon, 1978). Some scanning electron microscopy was performed at the University of New Brunswick, Fredericton using a Cambridge Stereoscan S4-10 and a 5 kV accelerating voltage. The great depth of focus of the scanning electron microscope (SEM) at high magnifications greatly aided the observation and tracing of vascular networks in the gill filament.

Detailed measurements and weighings were made on a complete orthograde cast of the second gill arch of a 4 kg ling cod. For every 10th filament the length and the total number of lamellae and their spacing were recorded (See Plate 5). The diameters of the afferent and efferent filament arteries were measured at various locations a known distance from the base of the filament. Two or three individual lamellae were carefully dissected free at five to eight locations a known distance from the filament base. Only nine filaments were used, but they were selected to include the complete range of filament lengths found on a 4 kg ling cod. The afferent and efferent lamellar arterioles were measured and photomicrographs taken of the individual lamellae for surface area determinations.

Filament and lamellar volumes were estimated by weighing intact filaments and then weighing all the lamellae removed from them. Pairs of filaments from both hemibranchs were combined to increase the accuracy of the weighings. Weights were determined

for every 10th pair of filaments neighbouring those used for the morphometric analysis described above. The weights were compared to that of a known volume of methyl methacrylate which had received the same treatment after polymerisation. Cast shrinkage was less than 1%.

Types of casts made

Several modes of plastic injection were used. They involved orthograde and retrograde perfusions via major arteries and veins.

A. Orthograde arterial gill perfusions were made via the ventral aortic catheter (as above). B. Retrograde arterial gill perfusions were made via an occulsive, retrograde dorsal aortic catheter. This catheter (5 cm PE 200 tubing) was implanted in the vessel through a ventral body wall incision. Visceral arteries were ligated to allow preferential retrograde flow to the gills. C. Retrograde venous perfusions were performed via the gill venous return vessel, which is located in the pericardial cavity dorsad to the ventral aorta. An occlusive catheter was also implanted in this vessel.

D. Double infusions were performed in which a partial orthograde infusion was followed by one of the two retrograde infusions. Differential colouring of the plastic compound distinguished the two infusions. This technique allowed better filling of the venous and lymphatic networks, since the arterial outlet for the retrograde filling was essentially blocked, and, in addition, permitted the tracing of vessels to their afferent, efferent or venous origins.

Silicone elastomer casting of lamellar capillaries under constant transmural pressures

The silicone elastomer microvascular casting technique, as developed for the pulmonary capillary bed and fully described by Sobin et al. (1970), was adapted for microvascular casting in the fish gills. The silicone polymers, catalyst and accelerator used were those especially supplied to Dr. Sobin's laboratory by G.E.C. (Waterford, N.Y.).

Casting Procedure: Three ling cod of similar weight (3.3, 3.6 and 3.8 kg) were used. Individual fish were lightly anaesthetised and prepared with a ventral aortic catheter for perfusion (see general methods). The gills were submerged and irrigated with sea water at all times. The pre-polymerised silicone elastomer was prepared just prior to perfusion and had a working time of 20 min. It was introduced at a constant pressure head of 70 cm H_2O without any pre-perfusion with saline. Thus the silicone formed an interface with the heparinised blood. Once perfusion had started, the dorsal aorta was bisected and the elastomer flowed freely from the vessel. After about 10 min perfusion at a pressure head of 70 cm H_2O, at least the proximal two-thirds of all centrally located filaments were completely clear of blood. At this time the pressure head was reduced to create a transmural pressure gradient of 20 cm H_2O for a selected region of the arch. This region was the central filaments near to the bend of the arch and these filaments lay

parallel to the water surface. To achieve a transmural pressure of 20 cm H_2O the perfusion head was set at a height of 20 cm H_2O above these filaments. Perfusion was maintained at this transmural pressure gradient for one minute, then through-flow was stopped in one gill arch by clamping the dorsal end of the arch. The static pressure gradient was maintained for 0.5 min before the elastomer was held within the arch, at this given transmural pressure, by clamping the afferent end of the arch as well. Now the perfusion pressure was raised by 10 cm H_2O and the protocol repeated on a different arch. Six gill arches were cast at different pressures for each fish at 10 cm H_2O transmural pressure increments up to 70 cm H_2O i.e. 20, 30, 40, 50, 60 and 70 cm H_2O. The 4th gill arches were not used. After completion of the casting the gills were left submerged and undisturbed for the 2 hours required for catalytic hardening of the elastomer.

Tissue preparation: After the elastomer had hardened the intact gill basket was excised and the tissue fixed overnight in a 10% buffered formalin solution. Four neighbouring filaments from the selected area in each gill arch were dissected free and embedded in blocks of gelatin. The filaments were all between 19 and 21 mm in length. The region 5 mm from the filament base was sectioned in a cryostat. The 10μ and 20μ thick sections were stained with cresyl violet, using cooled solutions mounted on slides in glycerol gelatin and subsequently covered and sealed. The stain was basement membrane specific and sharply defined the

lamellar microvasculature against the opaque silicone which filled the vessels. This definition was seen in the plan view and in cross-section.

Measurement techniques: Automated measurements were made from a video screen displaying microscope images of the sectioned material. These measurements were performed in Dr. Sobin's laboratory in Los Angeles and the techniques used were those fully described by Sobin et al. (1970). The vascular space to tissue ratio (VSTR) was determined from the plan sections of the lamellae (Plate 1). In a given microscopic field 6 to 12 clearly visible pillar cells outlines were traced from the video image onto transparent plastic. The area occupied by the pillar cells was determined and substracted from the total area that they occupied (vascular plus tissue cell area) i.e. the VSTR. Areas of the outlines were measured with an automatic planimeter (loaned by Lasico, Los Angeles, Ca.). The vascular sheet thickness (h) was measured using a split image device on the video screen. The diameters of afferent and efferent arteries were also measured in the same way. Measurements of h were made at all transmural pressures, but only lamellar cross-sections with all lamellar channels filled were analysed. VSTR measurements were made largely at the 20 and 70 cm H_2O transmural pressures. Artery diameters were only measured at 20 and 70 cm H_2O transmural pressures. The lamellar transmural pressure is here after referred to as ΔP_{lam}.

PLATE 1

A plan view of a secondary lamella from a ling cod that had been perfused with polymerising silicone elastomer. The tissue was stained for the basement membrane and the pillar cells (pc) are indicated. The section thickness is 20μ such that the lamella sheet is almost completely intact. For VSTR analysis groups of clearly visible pillar cells were isolated, as indicated, and the total area of the enclosure determined. The area of the pillar cells enclosed was combined and substracted from the total area to yield the VSTR. (Magnification = 785x: calibration bar = 20μ).

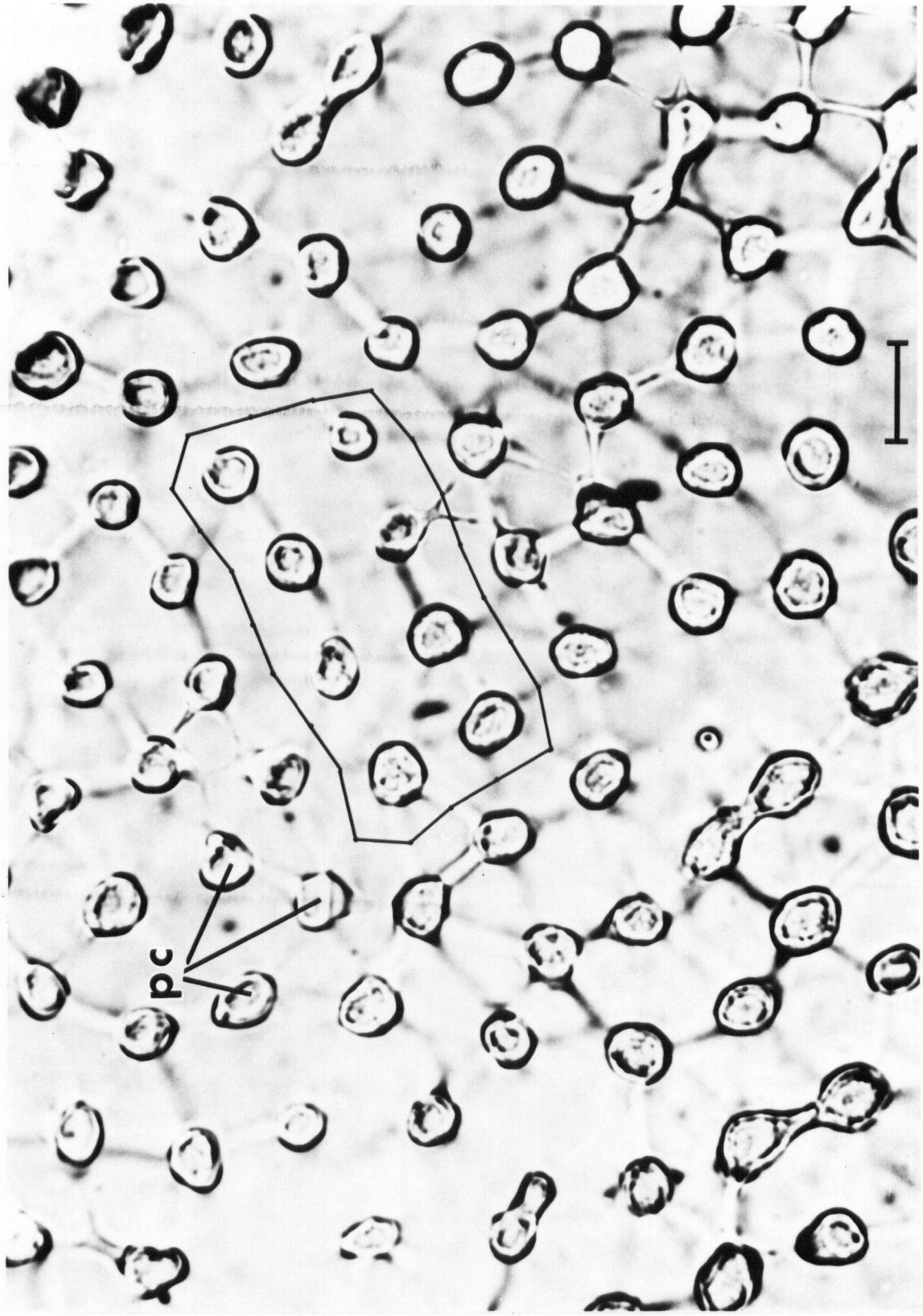
pc

Abbreviations commonly used in the text morphological and vascular descriptions.

ABA	=	afferent branchial artery
AAA	=	afferent arch artery
AFA	=	afferent filament artery
ALA	=	afferent lamellar arteriole
ELA	=	efferent lamellar arteriole
EFA	=	efferent filament artery
EAA	=	efferent arch artery
EBA	=	efferent branchial artery
DA	=	dorsal aorta
CM	=	coeliaco-mesentery artery
CART	=	filament cartilage
CS	=	central sinus
CVL	=	central venolymphatics
EVC	=	efferent companion vessel
ACV	=	afferent companion vessel
LAM	=	lamellar vascular sheet
"lamellar unit"	=	LAM plus ALA and ELA
b	=	basal peripheral blood channel of LAM
m	=	marginal peripheral blood channel of LAM
a	=	afferent
e	=	efferent
α	=	compliance coefficient of LAM vascular sheet
	=	mean LAM thickness
ΔP	=	lamellar transmural pressure
ΔP	=	alveolar transmural pressure
VSTR	=	vascular space to tissue ratio

RESULTS

In general the morphology and major arterial pathways of the ling cod gills differ only in detail from the well established descriptions for other teleosts, notably Salmo gairdneri. An emphasis is therefore placed on additional information and contrasting results. To avoid confusion, the terms gill filament (= primary lamella) and lamella (= secondary lamella) are used here.

Gill morphology and morphometrics

Gill arches and filaments: The branchial basket is bilaterally symmetrical. The four gill arches (holobranchs) on either side support two arrays of gill filaments (hemibranchs). The filaments of each hemibranch of a holobranch interdigitate and their septa are not fused. A number of shorter filaments are located at either end of the arch (Plate 2). The four gill arches have different lengths (Fig. 2A) and support different numbers of filaments (Fig. 2B). Gill arches 1, 2 and 3 support approximately the same total length of filaments since gill arch 3 supports filaments of greater length on average than arches 1 and 2 (Table I). The fourth gill arch is reduced in size. The increase in gill size (total filament length) with increasing body weight is due largely to longer filaments (Fig. 3) rather than greater filament numbers (Fig. 2B).

PLATE 2

A. The general arrangement of the gill filaments in the centre of the gill arch as revealed by methyl methacrylate corrosion casting. White arrows indicate the recurrent venolymphatic channels of the arch. Black arrow indicates efferent filament artery junction with efferent arch artery (Calibration marker = 2 cm).

B, C and D. Surface views of gill lamellae *in situ* on the filament after critical point drying. B = center of filament, C = filament tip and D = filament base and septum (sep). Arrows indicate direction of water flow. (B = 94x, bar = 200 ; C and D = 38x, bar = 500μ).

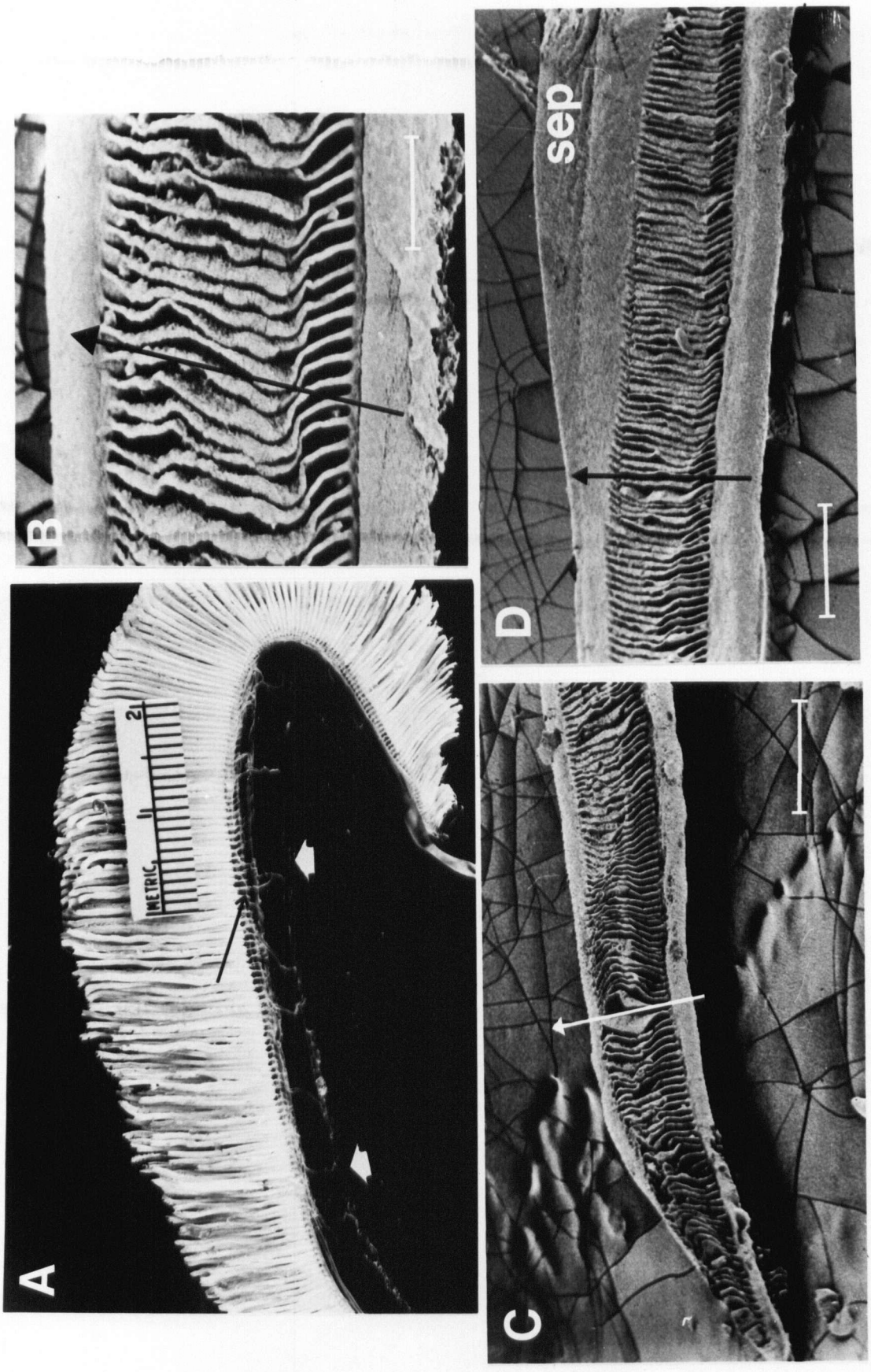
A
METRIC
21
B
C
D
sep

FIGURE 2A

The relationship between gill arch length (mm) for individual gill arches and fish weight. For clarity individual data points are given for gill arches 1 and 4 only (solid regression lines). The regression lines for gill arches 2 and 3 are the non-continuous lines. The regression line equations are:

Arch 1 = 9.34 Wt. + 107.1

Arch 2 = 9.19 Wt. + 104.7

Arch 3 = 9.78 Wt. + 86.5

Arch 4 = 6.38 Wt. + 77.7

FIGURE 2B

The relationship between the number of filaments supported on one gill hemibranch of each of the 4 arches and fish weight. The notation used is the same as for 2A. The regression line equations are:

Arch 1 = 2.89 Wt. + 243.2

Arch 2 = 3.26 Wt. + 241.3

Arch 3 = 4.72 Wt. + 213.8

Arch 4 = 3.11 Wt. + 186.8

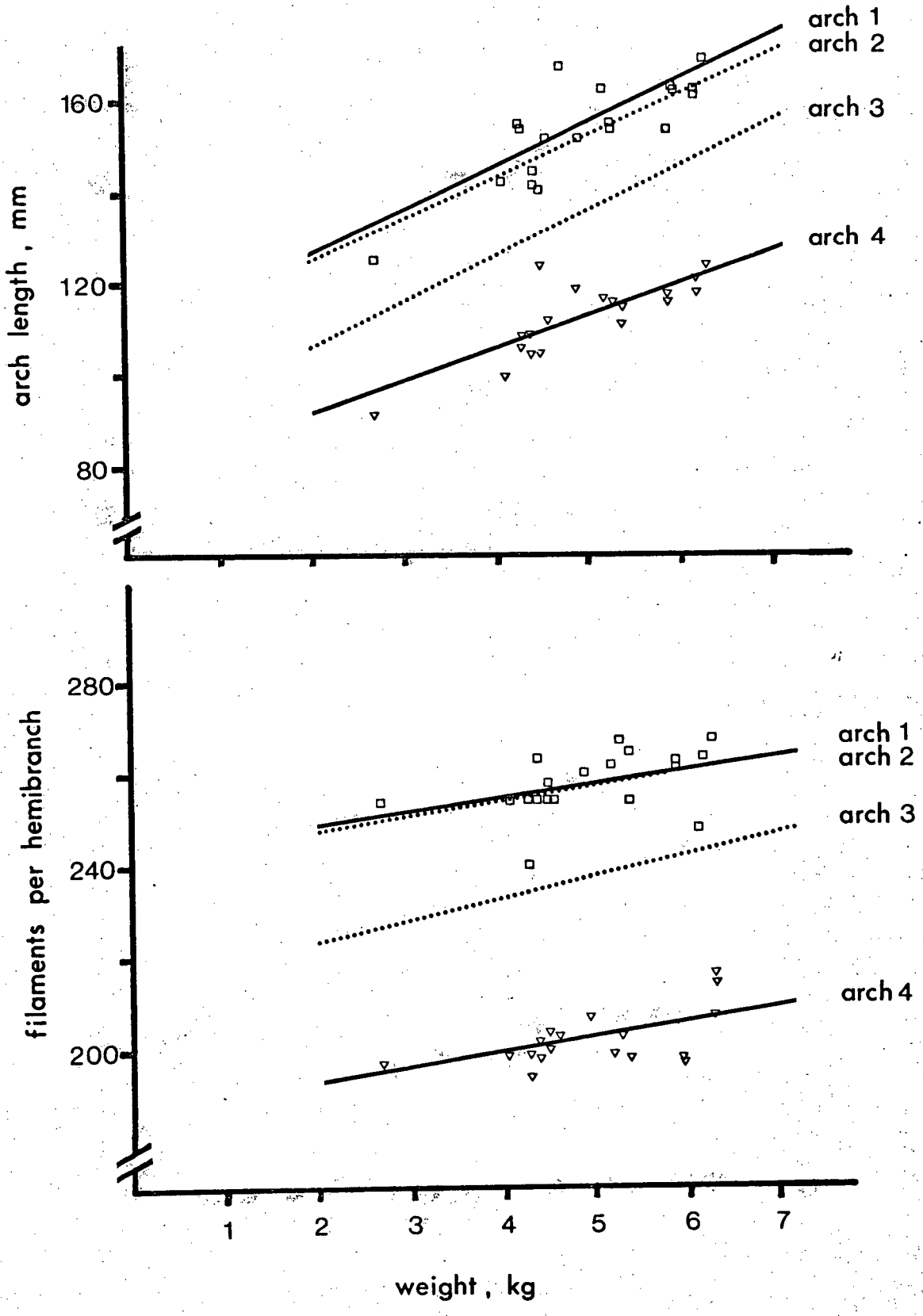
arch 1
arch 2
arch 3
arch 4
160
120
80
arch length , mm
280
240
200
filaments per hemibranch
1
2
3
4
5
6
7
weight , kg

TABLE I

A summary of the morphometric analysis of the gill arches and gill filaments from 15 ling cod (wt range = 4.0 to 6.2 kg; mean = 5.1 ± 0.2 kg). The mean values standard error were calculated from measured values for each fish (n = number of fish). The mean filament spacing and the total filament length of the gills are based on calculations from the mean values for individual fish.

TABLE I

Morphometric	Arch 1	Arch 2	Arch 3	Arch 4
Arch length (mm (n = 18)	155 ± 9	152 ± 9	136 ± 10	113 ± 7
# filaments/holbranch (n = 18)	258 ± 7	258 ± 12	238 ± 12	202 ± 6
Mean filament spacing (mm)	0.60	0.59	0.57	0.56
Mean filament length (mm) (n = 8)	15.3 ± 0.9	16.4 ± 1.1	16.7 ± 0.8	16.9 ± 0.8
Total filament length (m)	0.790	0.846	0.745	0.683

FIGURE 3

A) Mean filament length for the whole gill basket versus fish weight.

B) Total filament length for the whole gill structure in ling cod for a range of fish weights.

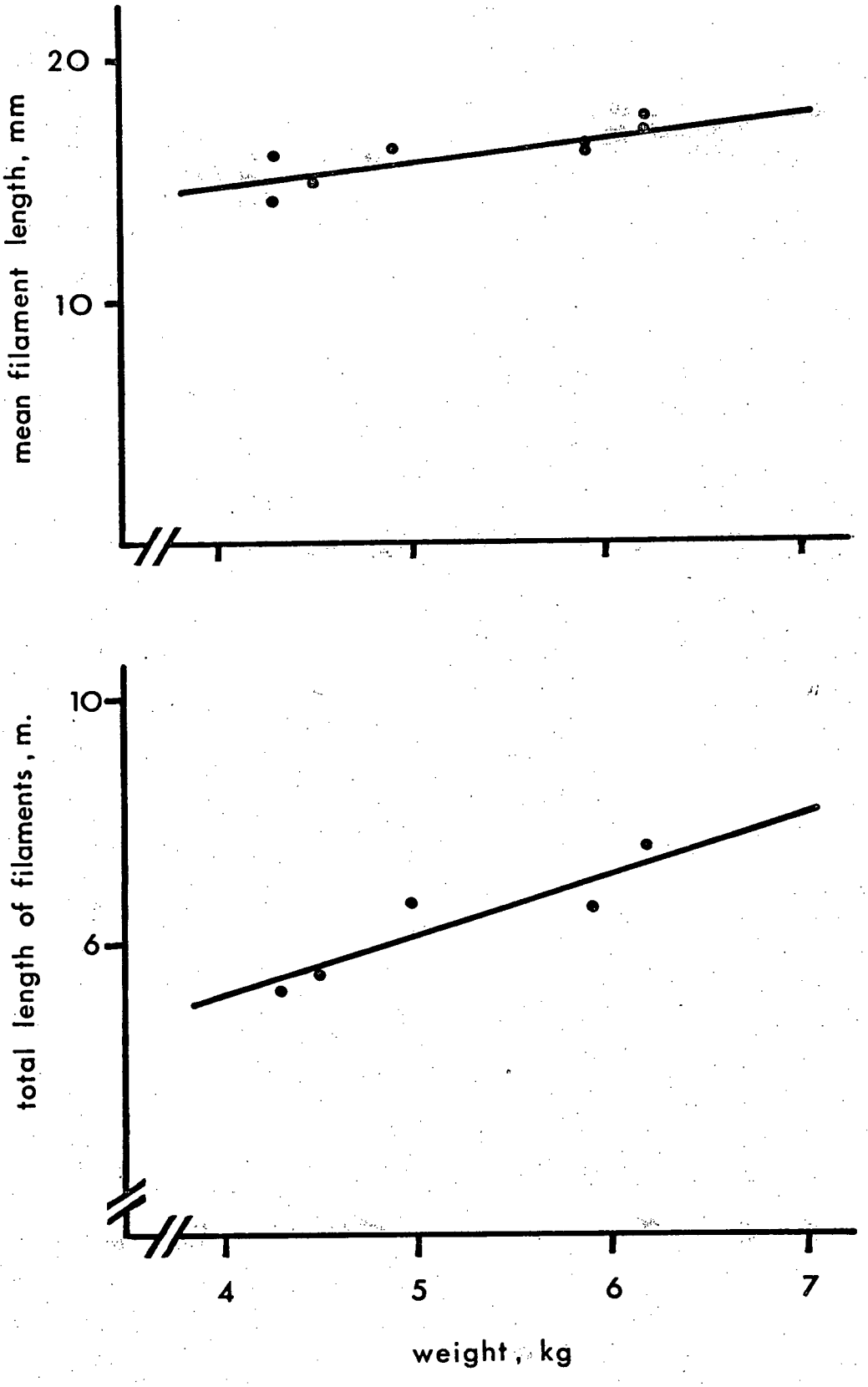
20
10
mean filament length, mm
10
6
total length of filaments, m.
4
5
6
7
weight, kg

Lamellae: These are the respiratory exchange sites. They are regularly arranged on both sides of the filaments (Plates 2 and 3), extend across the width of the filament and have a variety of shapes that resemble triangles. The shortest edge of the "triangle" is anterior and faces the water flow (Plate 3). The lamellae are unsupported epithelial folds that are held together under the strain of internal blood pressure by regularly spaced pillar cells, which form the endothelial lining of the lamellar capillaries (Plate 4). A noticable interstitial/lymphatic space is located between the epithelium and the pillar cells. This space was swollen considerably in some preparations. The epithelium is one cell thick except at the base of the lamella (the junction with the filament) where it is thickened. Some lamellar capillaries are buried within the filament epithelium (Plate 4), and this occurs more extensively on the efferent side of the lamella. Clearly the blood to water epithelial barrier is much greater in these basal regions than elsewhere on the lamella.

The lamellae are regularly spaced along the filament length and filaments of different lengths have similar lamellar spacings in the 4 kg specimen examined (Fig 4). Lamellae are spaced slightly closer together at the tip and base of the filament, but these regions are limited and contribute little to the overall lamellae numbers in the long filaments of these large fish.

PLATE 3

The general relief of the filament with dorsal and ventral lamellae as shown by a 20μ thick histological cross section. The section was prepared for VSTR analysis. afa = afferent filament artery; ala = afferent lamellar artery; cart = filament support cartilage; lam = lamellar with b = basal blood channel and m = marginal blood channel; ela = efferent lamella arteriole; efa = efferent filament artery and ecv = main efferent companion vessel. acv = main afferent companion vessel. (120x, bar = 200 μ).

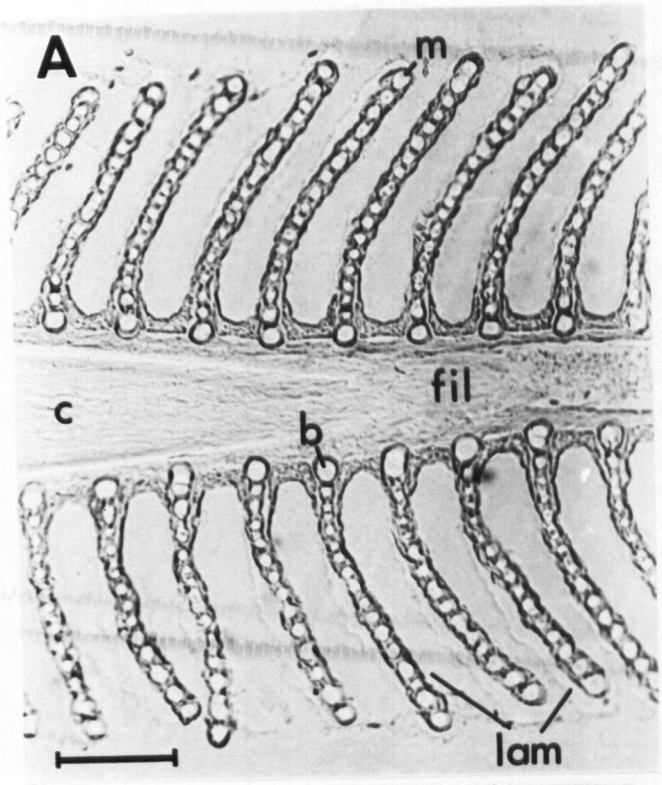
A
m
fil
c
b
lam

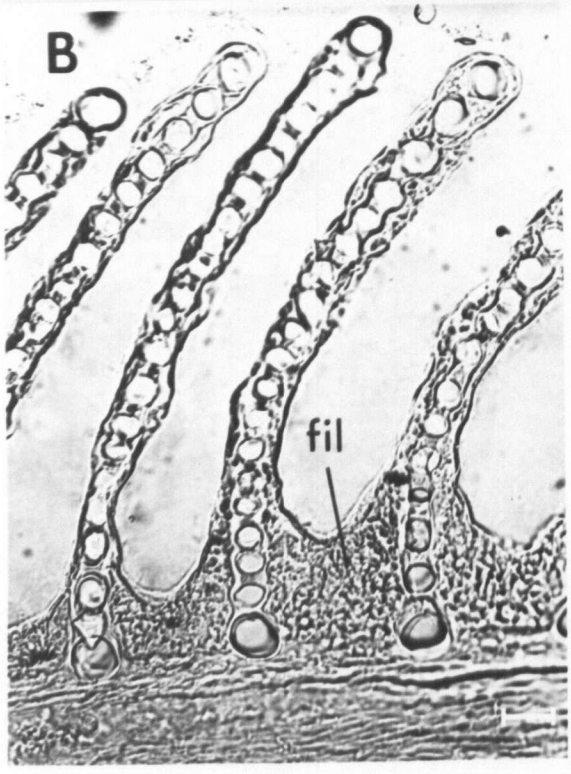
B
fil

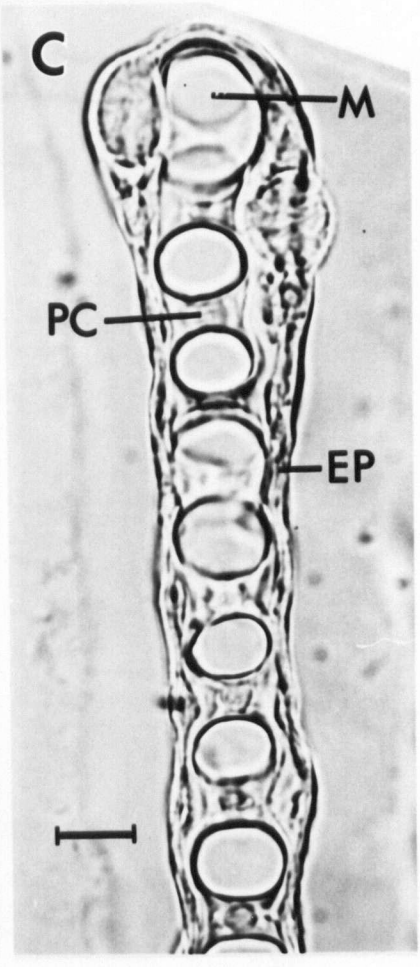
C
M
PC
EP

PLATE 4

Histological sections of the gill lamella (lam) in cross section and the filament (fil) in sagittal section. b = basal lamellar blood channel, m = marginal lamellar blood channel, PC = pillar cell, EP = lamella epithelium and c = cartilage. Note how the basal lamella blood channels are buried in filament epithelium (B). (10μ sections as prepared for VSTR analysis. Magnifications: A = 155x, B = 354x and C = 1040x. Calibration bars: A = 100 µ , B = 20 µ and C = 10 µ).

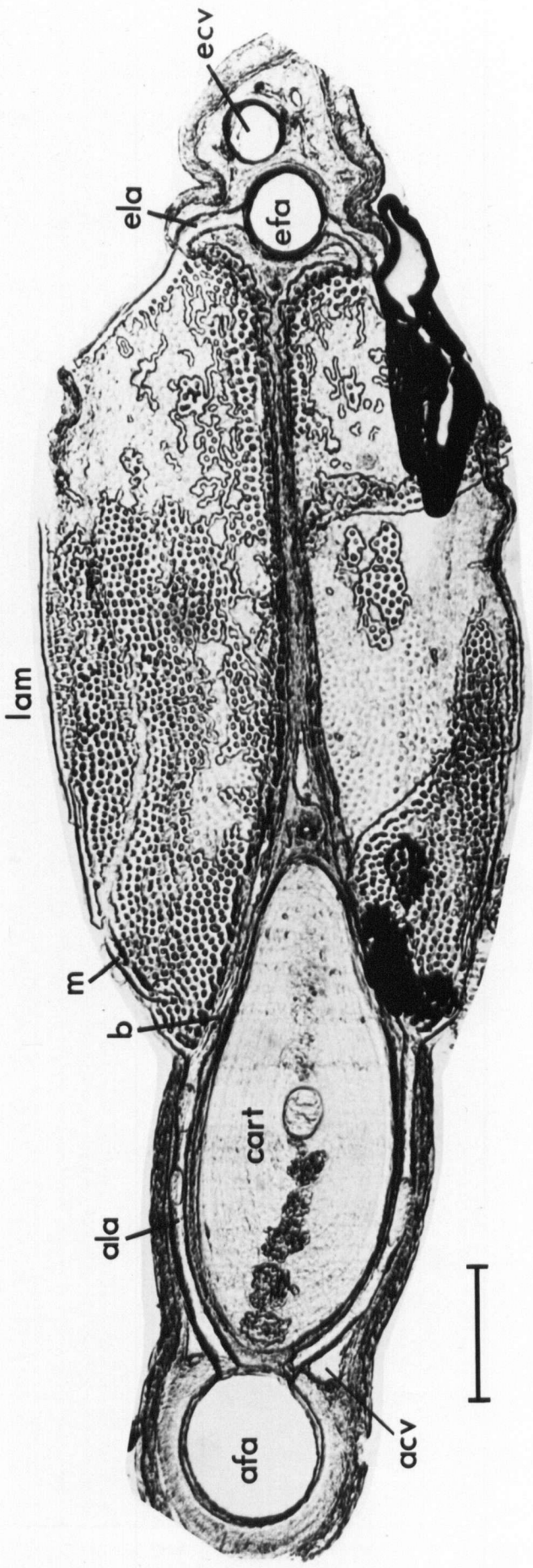
ecv
ela
efa
lam
m
b
cart
ala
afa
acv

FIGURE 4

The lamellar spacing determined from vascular casts for a complete range of filament lengths from a 4 kg ling cod. Filaments shorter than 8mm were not numerous and were not examined.

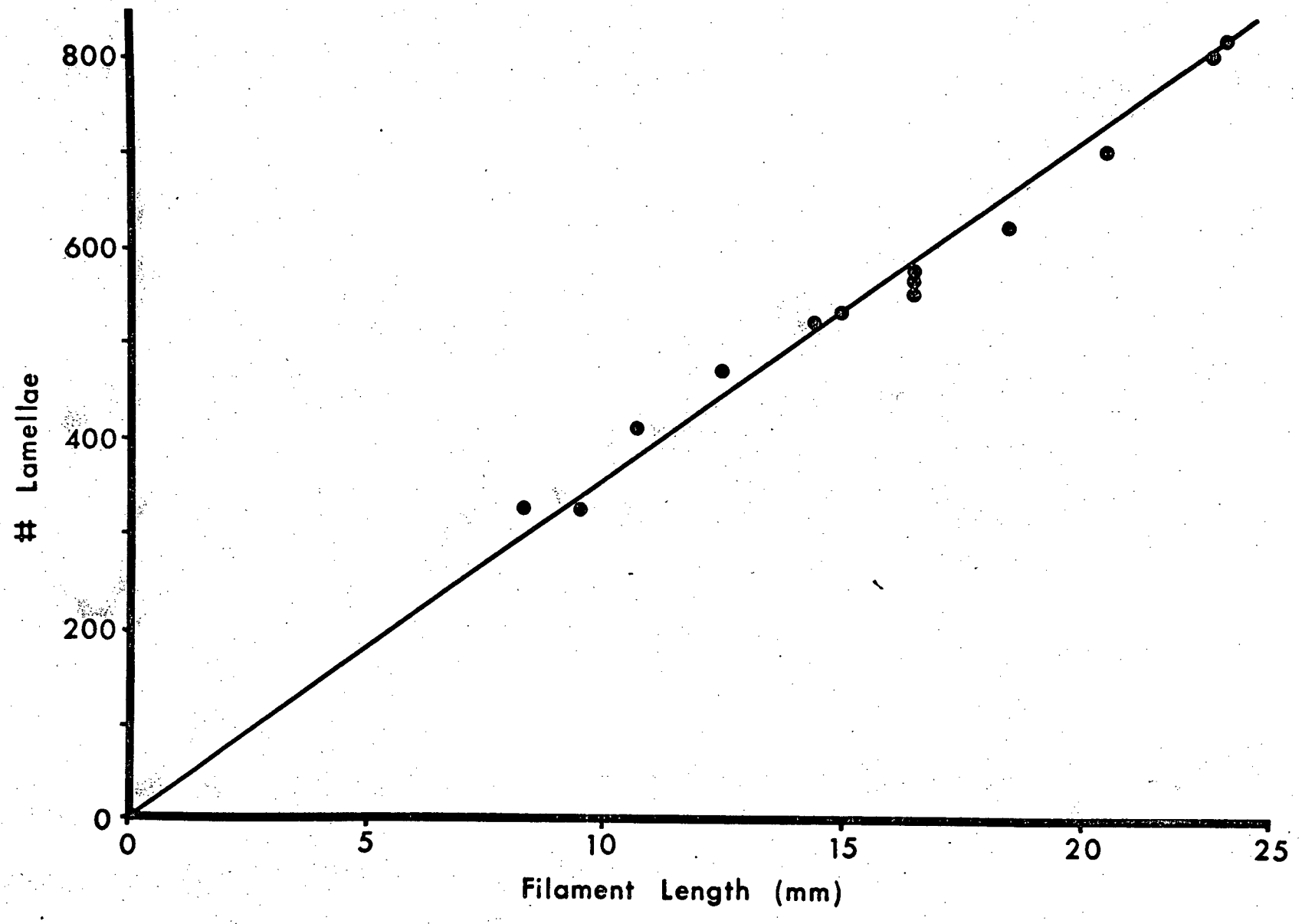
800
600
400
200
0
Lamellae
0
5
10
15
20
25
Filament Length (mm)

Vascular pathways in ling cod

The following description is a synthesis of the observations made on plastic corrosion casts, on histologically sectioned material and from many dissections.

The bulbus arteriosus and ventral aorta have muscular walls; the wall of the bulbus is trabeculated. The ventral aorta is long (3 cm in a 4 kg fish) and divides into 8 afferent branchial arteries (Plate 5).

Gill arch vessels: The afferent branchial artery (ABA) extends dorsally along the arch and bifurcates to form the afferent arch arteries (AAA)(Plate 5). Each AAA in turn forms a parallel series of right angled branches which correspond to the alternating afferent filament arteries of each hemibranch. The AAA is somewhat compressed laterally and tapers along its length. The efferent vessels have a similar, but reversed, arborescent pattern. The parallel series of efferent filament arteries unite perpendicularly to an efferent arch artery (EAA). The EAAs are paired at either end of the holobranch (one for each hemibranch), but they form a single vessel centrally. An efferent branchial artery (EBA) extends dorsally in each arch. The two posterior EBAs unite as do the two anterior EBAs; thus two efferent epibranchials are formed on either side of the pharynx (Plate 6). The epibranchial arteries unite to form the dorsal aorta.

The formation of the dorsal aorta is not a simple

unification of the four efferent epibranchial arteries. The epibranchials from the posterior arches certainly unite with the dorsal aorta, but at the same time they appear continuous with the coeliaco-mesenteric artery. The confluence of the left and right epibranchials from the posterior arches is predominantly on the left side of the dorsal aorta i.e. the right efferent epibranchial actually passes ventrally to the dorsal aorta (Plate 6). In the same region on the right side of the dorsal aorta the coeliaco-mesenteric artery is derived. In this localised region, the arterial walls have deep smooth muscle coats.

A gill arch in cross section reveals that the EAA lies in between the anteriorly located branchial arteries and the more posteriorly located AAA (Fig. 5). Two major venolymphatic channels are also located in the arch, one in between the AAA and EAA, the other anterior to the EAA (Plate 2).

The carotid and afferent pseudobranch arteries are formed from a single branch of the EBA of the first gill arch before it forms the epibranchial artery. The single hypobranchial artery is derived from branches of the EAA in gill arches 2 and 3 and passes along the pericardial cavity to supply the hypobranchial musculature. A relatively small branch from the hypobranchial artery forms the vasa vasorum of the ventral aorta, the bulbus arteriosus and possibly the ventricle. There was no other coronary supply to the heart seen in ling cod.

Respiratory network of the gill filament

Arterial vessels: A single afferent filament artery (AFA) extends with a gradual taper towards the tip of each filament and is parallel to the posterior edge of the filament. The efferent filament artery (EFA) is similarly arranged, but on the anterior edge of the filament. The EFA is slightly longer than the AFA at its base since it extends over the AAA before uniting with the EAA. A constriction in the corrosion cast of the EFA was consistantly seen at the base of the EFA where it unites with the AAA (Plate 7).

Lamellar capillary beds extend between the AFA and EFA to form a parallel, ladder-like network of vessels along the filament length (Plate 8). A lamellar capillary sheet and its associated arterioles are termed a "lamellar unit" (Plate 9).

Lamellar unit: The nature of the afferent lamellar arteriole (ALA) is variable. Proximal ALAs differ from distal ALAs. Some generalisations can, however, be made. The ALA extends almost completely over the width of the filament support cartilage before forming the lamellar capillaries (Plates 3 and 10). In distal regions the AFA length is reduced and corresponds to the narrower filament cartilage. Individual ALAs usually supply individual lamellae on either side of the filament. However, some ALAs may divide along their length to supply two lamellae on the same side of the filament. The origins of the ALA for the

dorsal and ventral sides of the filament are quite separate at the base of the filament. However, more distally the ALA origins become much closer and about mid-filament the dorsal and ventral ALAs share a short, common vessel origin (Plate 11). Analysis of plastic casts also showed that the diameter of distal ALAs was 3 to 6μ smaller than proximal ones. The efferent lamellar arterioles (ELA), by contrast, are always short and undivided. Even in its short length the ELA has a noticable bulbar region (Plates 8, 9, 10 and 12). Both the ALA and ELA have smooth muscle in their vessel walls. The various "triangular" shapes of lamellar capillary sheets and the regular locations of pillar cells (holes in the corrosion cast) can clearly be seen in Plate 8. The distinct peripheral channels of the lamella are larger than the central capillaries. On each lamella, the outside "marginal" channel is continuous whilst the lower "basal" channel often tapers towards the efferent side, where the vessel also lies more deeply in the filament tissues (See Plates 3 and 4).

Venolymphatic networks of the gill filament

In addition to the respiratory network, another vascular complex exists within the gill filaments: the venolymphatics. No vessels other than the ALAsare derived from the afferent filament artery. Thus the venolymphatic circulation is derived totally from the efferent circulation and the formation of lymph. The major venolymphatic vessels are the afferent and efferent companion vessels, which lie parallel to the AFA and EFA respectively, and the large central sinus that lies in the filament body. These vessels are all interconnected and have thin, non-muscular walls that appear very distensible.

Efferent companion vessels (ECV): A major vessel lies parallel to and outside of the EFA, with which it also has short connections (Plate 12). The connections are spaced about every 600μ i.e. every 12 lamellae or so, and they have smooth muscle in their walls which is a continuation of that found in the EFA. Several inter-connected ECVs of a smaller diameter also extend along the filament length but in a more meandering fashion (Plate 12). The smaller vessels are connected to the main ECV, and they also have regular short, narrow, 10μ diameter inter-connections to the central sinus. These are the only inter-connections to the central sinus on the efferent side of the filament and they pass around the EFA and in between the ELAs (Plate 12).

Central sinus: A large sinus occupies the center of the filament between the EFA and the filament cartilage. The dimensions of the central sinus were always much greater in retrograde corrosion casts made with retrograde filling (Plate 13). The whole central sinus is connected to the ECV (as described above) and to the afferent companion vessels by long vessels that extend either side of and the whole width of the filament cartilage (Plates 8 and 11). No direct connections to either the EFA or the AFA were seen. A small, separate, more diffuse and blind ending system is also located in the filament body between the central sinus and the lamellar base (Plate 13). This system is more pronounced in the region immediately underneath a lamella and it is connected to the central sinus near to the cartilage. It has no other connections, and is consequently thought to represent the lymphatic drainage system of the lamellae.

Afferent companion vessels (ACV): These paired vessels lie parallel to the inside of the AFA, both dorsad and ventrad (Plate 11). As well as their own connections to the central sinus, they themselves are inter-connected by a varicose capillary network around the outside of the AFA (Plate 11). The ACV was the most poorly cast of the filament vessels and often only the section in the center of the filament was filled, whilst at other times the cast had a segmented appearance along its length due to partial filling at different levels along the filament.

The drainage of the filament venolymphatic system into the arch and subsequently from the arch was not examined in great detail. There are no direct connections of the central sinus *per se* to the arch. The ACVs are united with the major venolymphatic vessels in between the AAA and EFA. A quite dense, intertwining network of vessels exists at the base of the filament and in the filament septum. It has origins from the EFA base and is often inter-connected with neighbouring filaments (Plate 7). This and the ECVs appear to connect with the venolymphatic vessels surrounding the anterior of the EAA. Some of the venolymphatic arch vessels, at least, were connected to the sinus venosus by the anterior venous return vessel located in the pericardial cavity, as indicated by successful retrograde gill injections via this vessel.

PLATE 5

General form and arrangment of the afferent vessels to the gills as shown by methyl methacrylate corrosion casts.

a) A cast of the bulbus arteriosus and ventral aorta.

b) The afferent branchial arteries and part of the ventral aorta.

c) The 4 gill arches (holobranchs) with filaments in situ. Arch 2 has every 10th filament missing to show sampling areas.

d) The afferent arch artery with branchial artery from the first and the fourth (shorter) gill arches. Some afferent arteries are partially cast on the fourth gill arch.

Calibration marker = 2 cm).

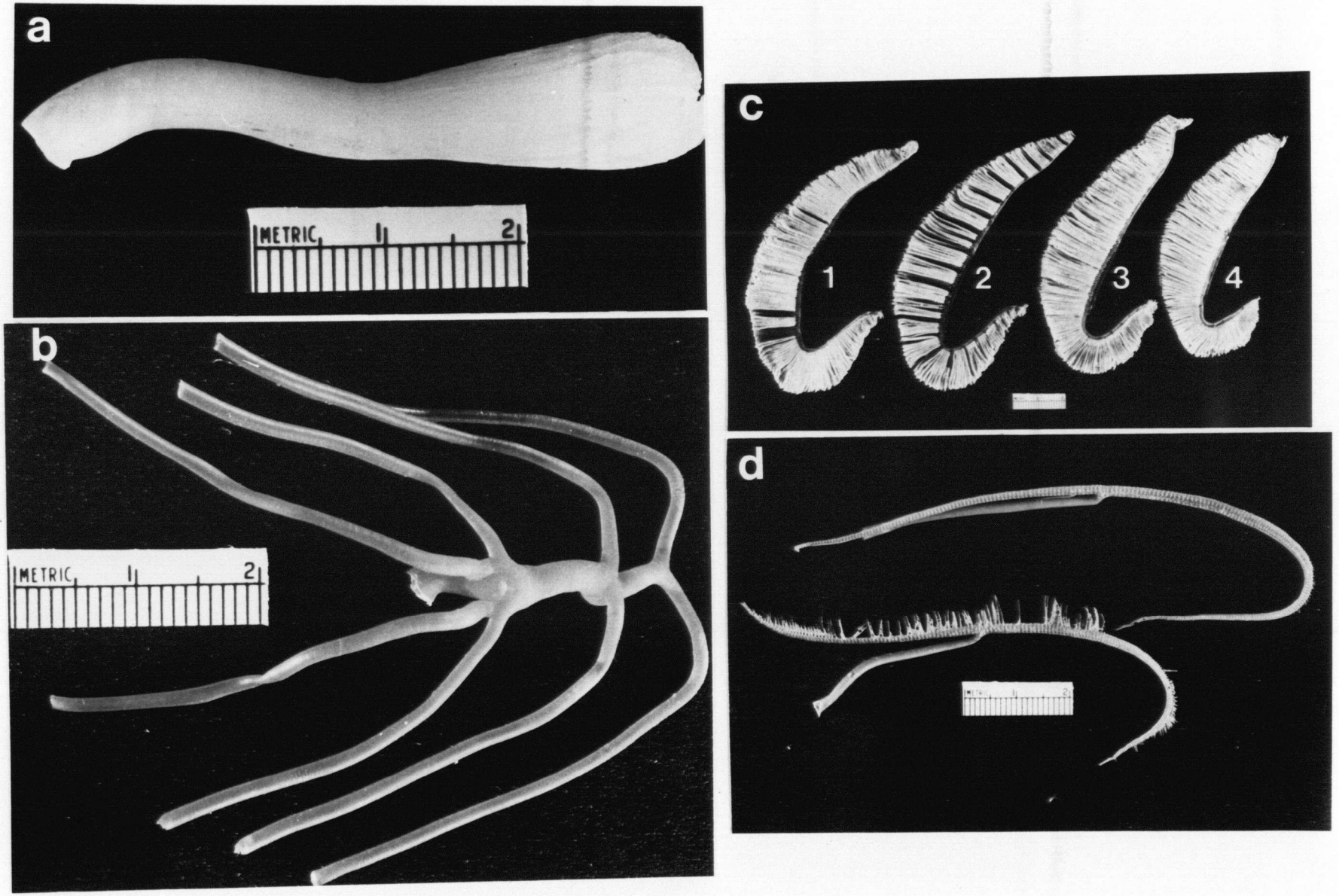
a
METRIC 1 2
b
METRIC 1 2
c
1
2
3
4
d

PLATE 6

The general arrangement of the four (1,2,3,4) efferent branchial arteries as revealed by a methyl methacrylate corrosion cast. da = dorsal aorta (which was almost totally removed) cm = coeliaco-mesenteric artery. Note the confluence of the branchial arteries to form the 2 pairs of epibranchials, and also the confluence of the epibranchials (see text). A = dorsal view B = ventral view. (Calibration bar = 2 mm).

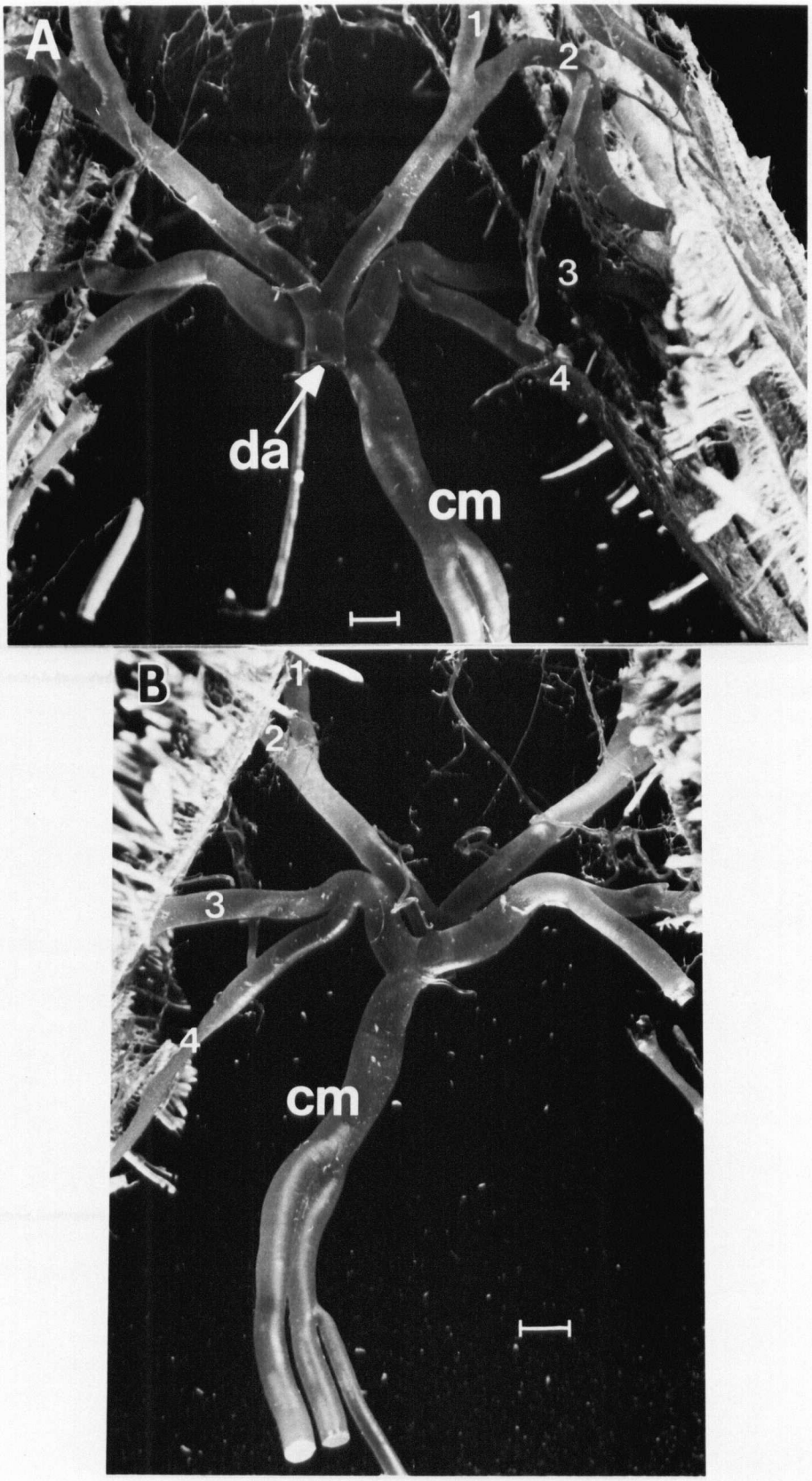
A
1
2
3
4
da
cm
B
1
2
3
4
cm

FIGURE 5

A schematic line diagram of the vascular arrangement in the gill arch and proximal region of a gill filament of a ling cod. L = lymphatic vessels; BA = branchial artery; EAA = paired efferent arch arteries; AAA = afferent arch artery; efa = efferent filament artery; afa = afferent filament artery; acv = afferent companion vessel.

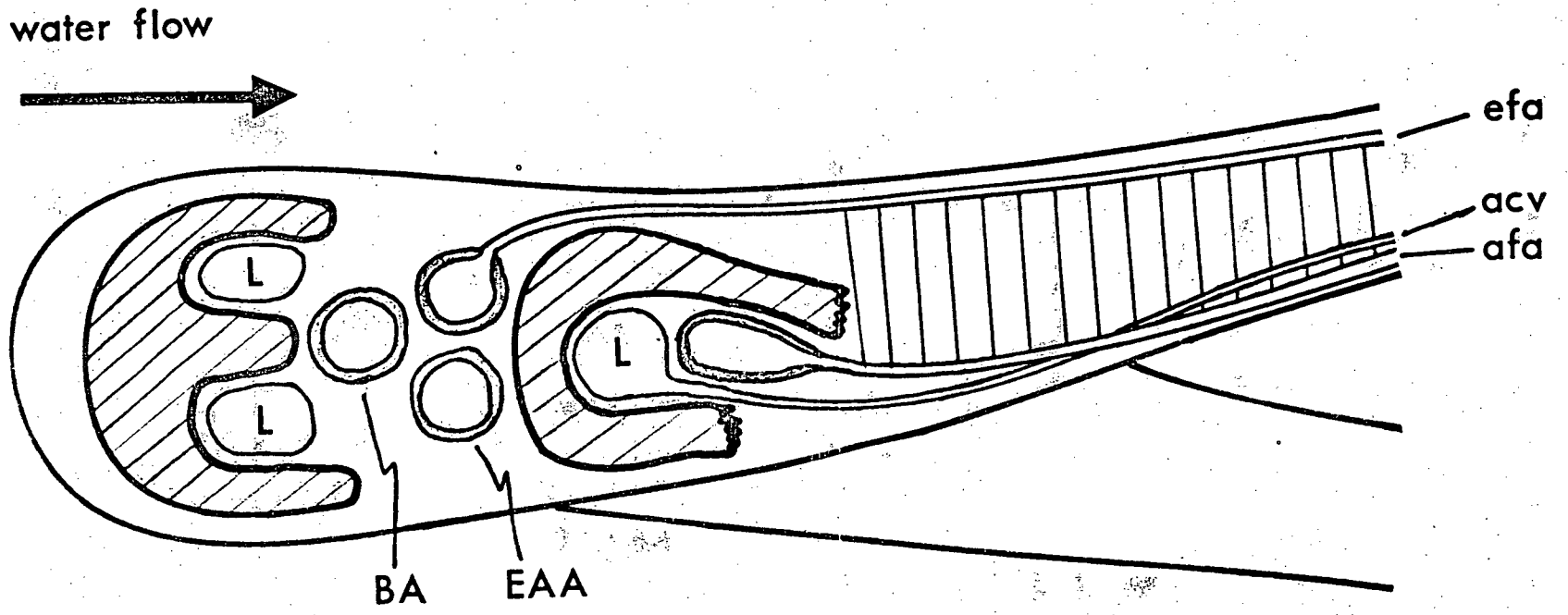

ARCH CROSS-SECTION

PLATE 7

Two views of the base of the efferent filament artery (efa) near to its junction with the efferent arch artery (eaa). These demonstrate the constriction (arrows) in the corrosion cast of the EFAs. Note the plexus of venolymphatic (vl) vessels at the base of the filament. (A = 78x : B = 50x. Calibration bars = 200μ).

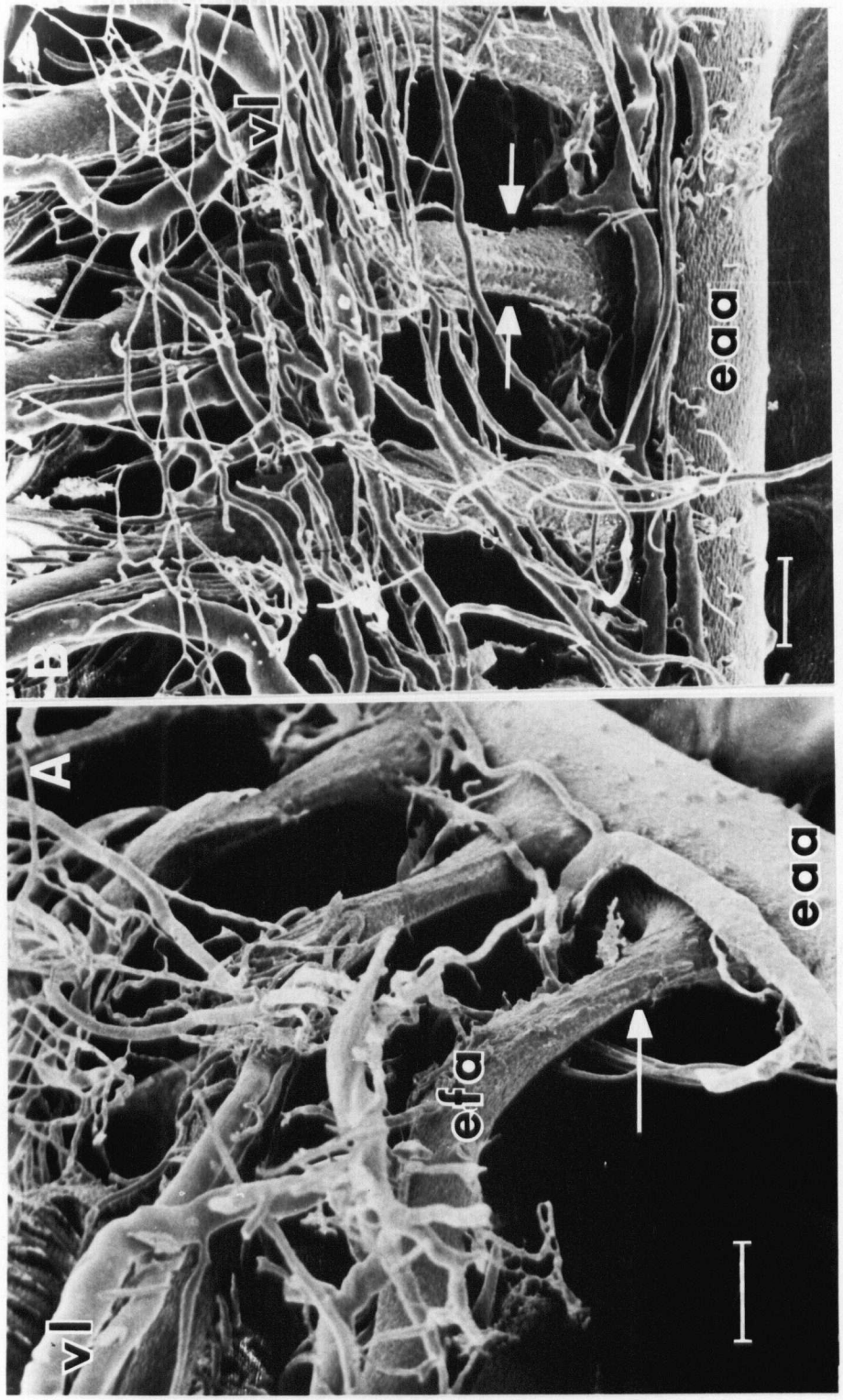
A
vl
efa
eaa
B
vl
eaa

PLATE 8

Methyl methacrylate casts of gill lamellae. 1 to 5 are a series to show the various shapes and sizes of lamellae. They progress from a basal filament location (1) to a distal filament location (5). a = afferent; e = efferent. 6, 7 and 8 are the afferent, central/marginal and efferent regions of a lamella, respectively, in more detail (Magnifications : 1 = 74x, 2 = 64x, 3 = 66x, 4 = 74x, 5 = 61x, 6 = 300x, 7 = 1076x and 8 = 582x. Calibration bars : 1 to 5 = 200 µ , 6 = 50 , 7 = 10 µ and 8 = 20µ).
Abbreviations are explained in legend for Plate 3.

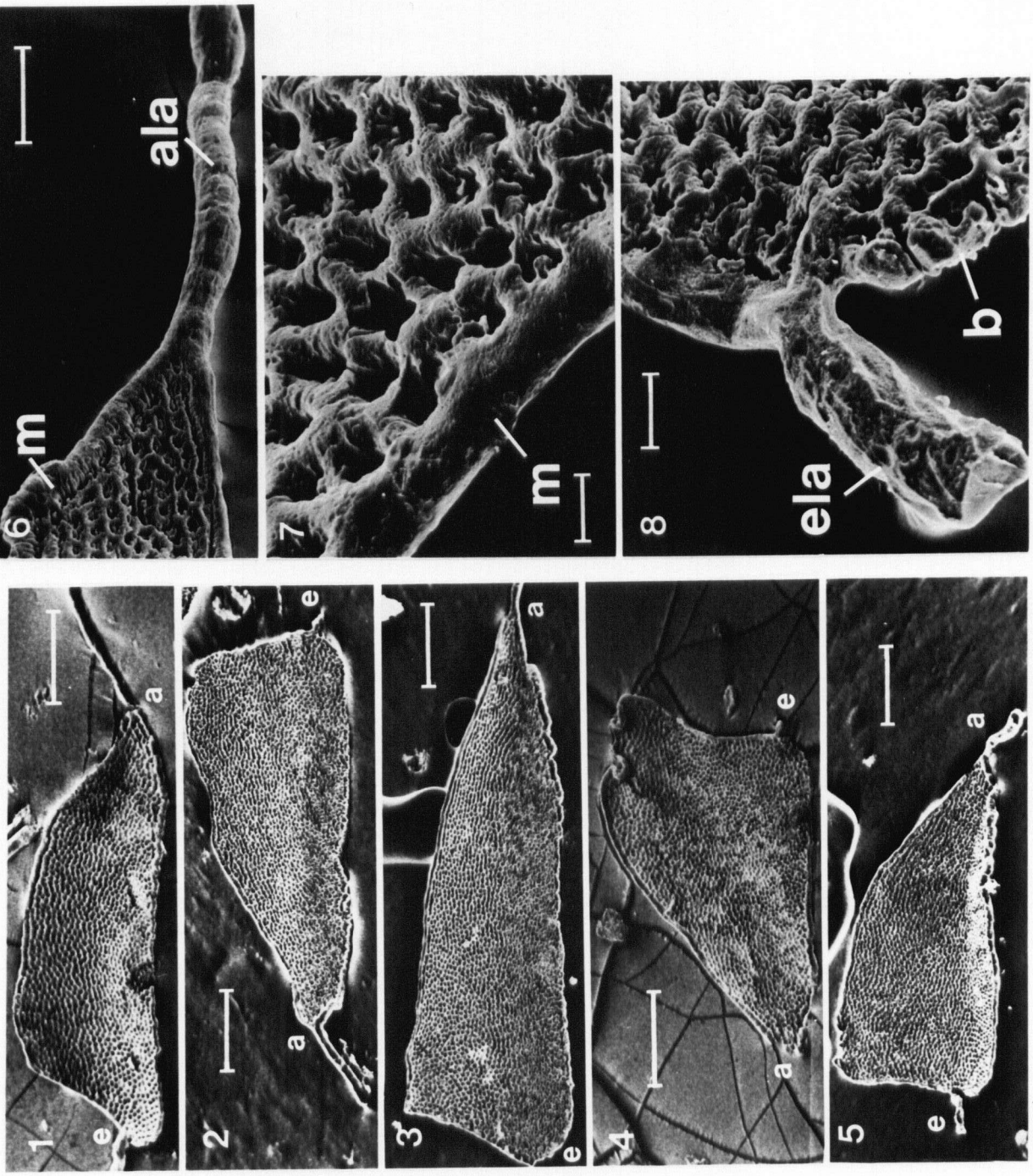
1
e
a
2
a
e
3
a
e
4
e
a
5
e
a
6
m
ala
7
m
8
ela
b

PLATE 9

Histological cross sections of the gill filament in more detail than shown in Plate. 3. A - the afferent side, B and C the efferent side of the filament. (A and C = 155x, bar = 100µ : B = 650x, bar = 20µ).

Abbreviations are explained in legend for Plate 3.

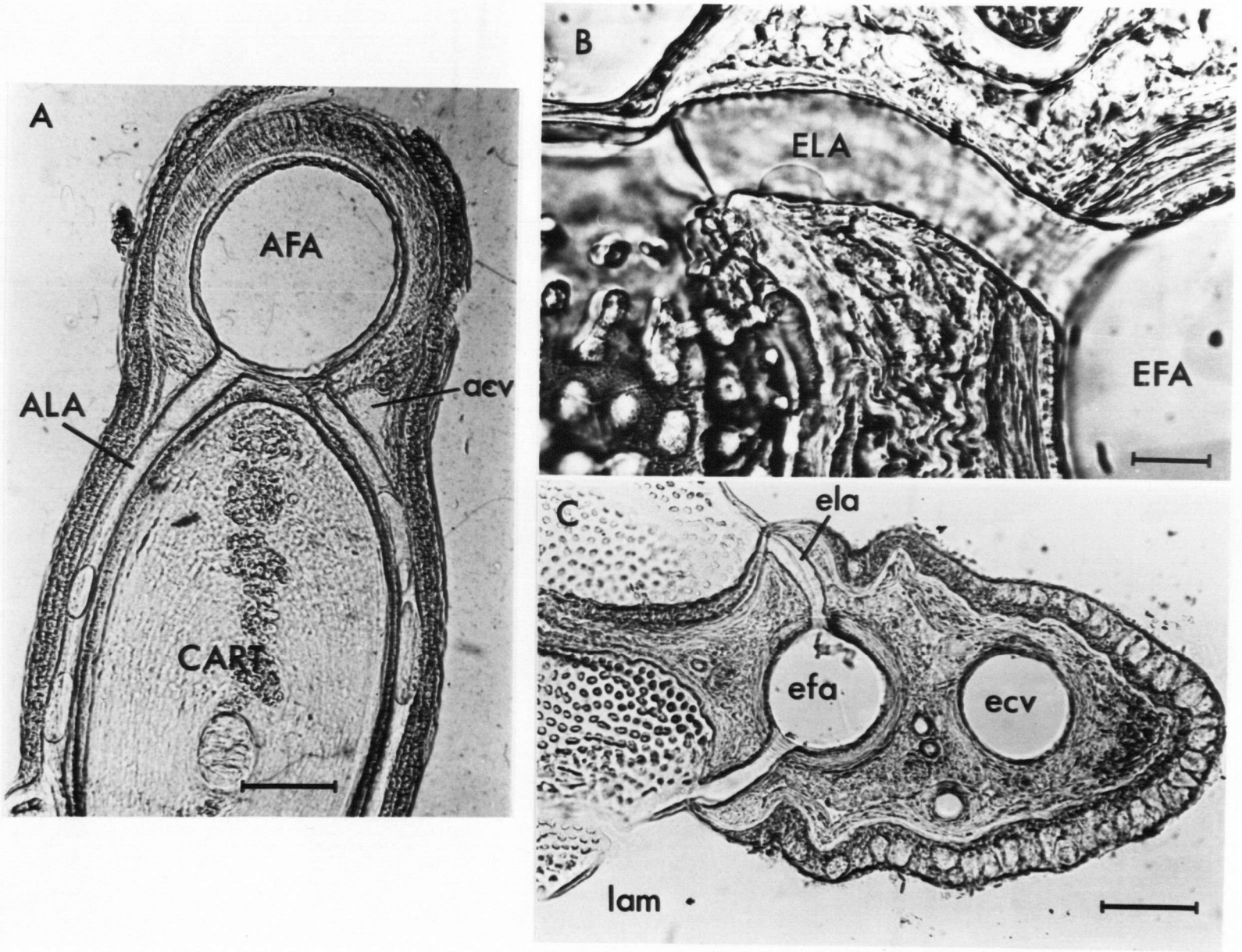
A
AFA
ALA
aev
CART
B
ELA
EFA
C
ela
efa
ecv
lam

PLATE 10

A methyl methacrylate corrosion cast of a gill filament revealing the general arrangement of the vasculature. Some lamellae have been removed to reveal the structure of the venolymphatics (vl) and central sinus (cs) which lie in between the opposing lamellae. In C note the stubs of the ECV to CS connecting vessels because the ECV was removed. (Magnifications : A = 67x, B = 121x and C = 188x. Calibrations bars A = 200 µ , B = 100 µ and C = 50 µ).

Abbreviations are explained in legend of Plate 3.

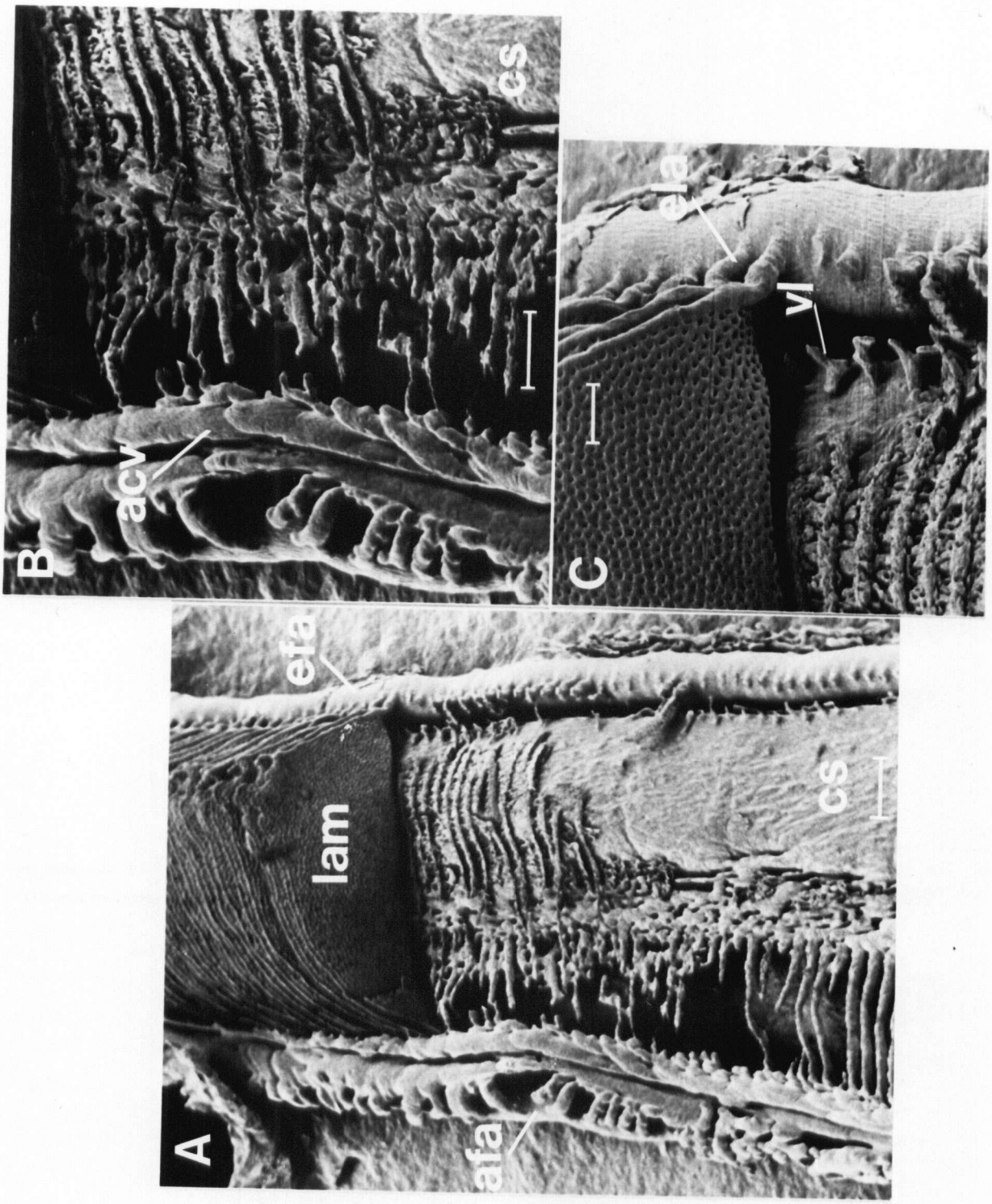
A
afa
efa
lam
cs
B
acv
es
C
es
vl

PLATE 11

A detailed view of the corrosion casts of the vessels on the afferent side of the filament.

A/ A general view. Note the parallel series of central venolymphatic vessels connecting the acv to the cs (73x, bar = 200μ).

B/ Close up view of the origin of the afferent lamellar arterioles (ala) in the proximal region of the AFA . Note the dorsal and ventral vessels have separate origins and the slight taper of the vessel towards its base (460x, bar = 20μ).

C/ As B above, but in the distal region of the AFA. Note the single point of origin for dorsal and ventral ALAs.

D/ A fracture section of the filament cast to reveal the dorsal and ventral arrangement of the paired ACVs. (146x, bar = 100μ).

E/ The diffuse network of vessels interconnecting the pair of main ACVs. This was dissected out from the AFA, which would normally lie inside (392x, bar = 20μ).

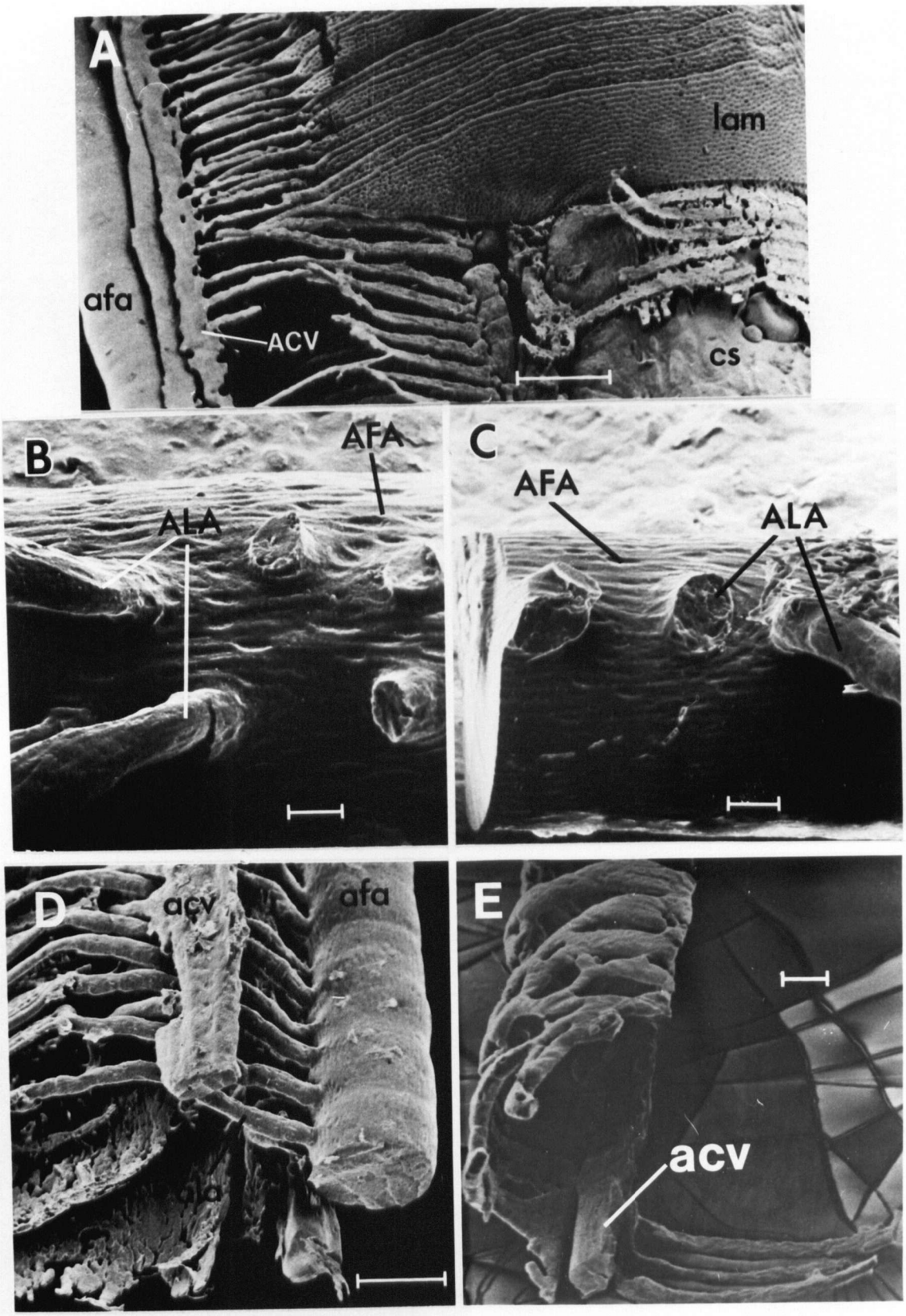
A
lam
afa
ACV
cs
B
AFA
ALA
C
AFA
ALA
D
acv
afa
ala
E
acv

PLATE 12

A detailed view of the corrosion casts of the vessels on the efferent side of the filament.

A/ A side view of the EFA to demonstrate the parallel alignment of the main ECV and the meandering nature of smaller ECVs (200x, bar = 50μ).

B/ A dorsal view of the EFA to show the nature and spacing of the EFA to ECV connections. Note the indentations on the EFA are continued on this connection, unlike the section of the ECV in A (146x, bar = 100μ).

C/ Dorsal view of the filament to show the small vessels between the ECV and the central sinus (cs). Note these vessels interdigitate between the ELAs (331x, bar = 50μ).

A
bm
efa
ecv
B
ela
C
cs
ela
ecv

PLATE 13

A detailed view of the corrosion casts of the vessels in the central region of the filament. The high degree of filling of the central sinus filling was achieved by retrograde casting procedures.

A/ A fracture section of the filament to demonstrate the large proportions that the central sinus (cs) can attain (141x, bar = 100μ).

B/ A view of the diffuse network of central venolymphatics (cvl) which lie in between and separate from the lamella (lam) and the central sinus. (See also Plate 11 A). Note the basal lamellar channel and the more defined nature of the cvl that is underneath (258x, bar = 50μ).

C/ A more detailed view of the base of the lamella and the cvl than in B (1132x, bar = 10μ).

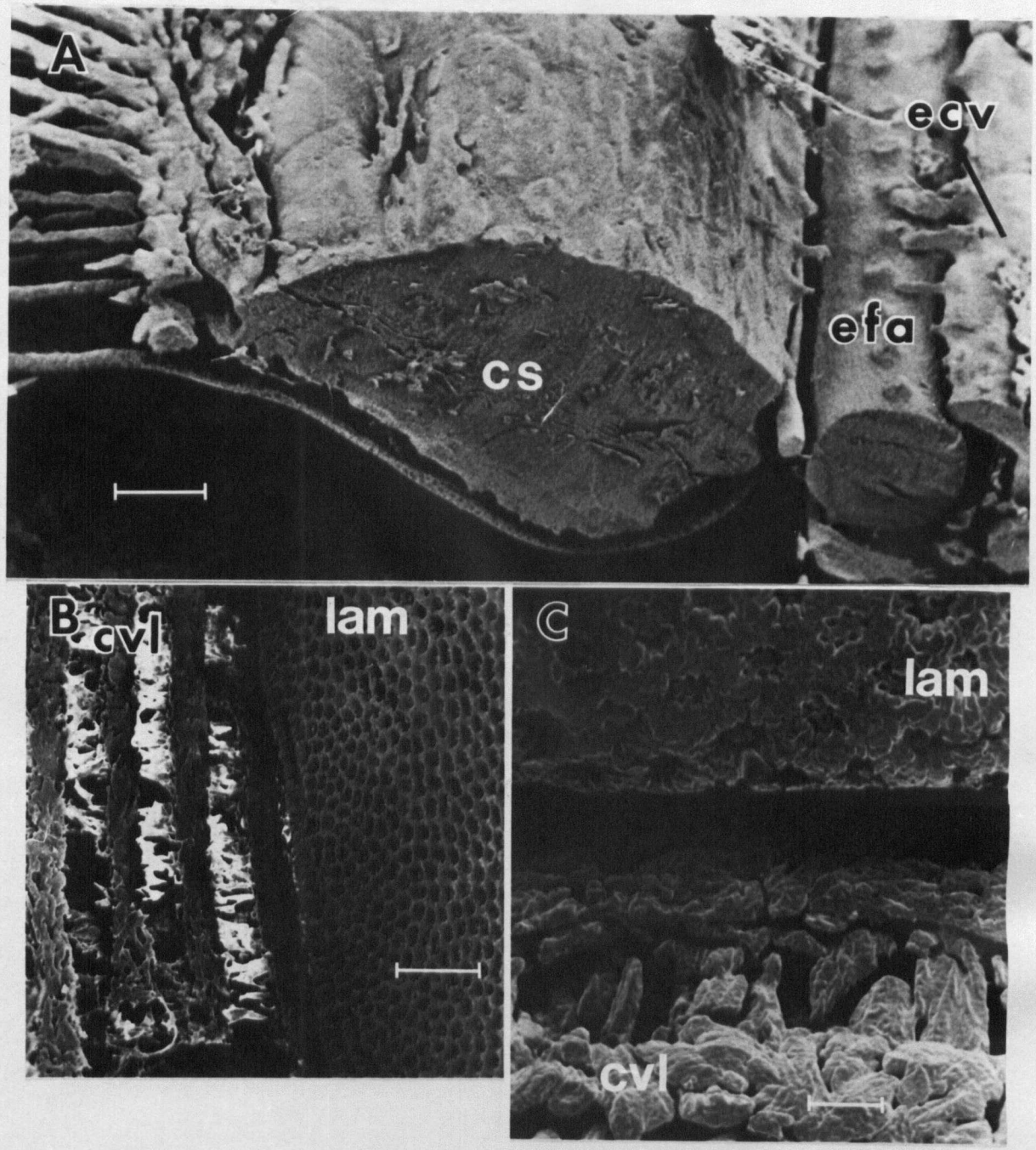
A
ecv
efa
cs
B
cvl
lam
C
lam
cvl

Lamellar casts with silicone elastomer over a range of static transmural pressure gradients

The vascular space to tissue ratio (VSTR) for lamellae 5 mm from the base of the filament did not change over the 20 to 70 cm H_2O transmural pressure range and has a mean value of 88.1% ± 0.3 (n=65 for 3 fish at 4 transmural pressures) (Fig.6) The pillar cell shape changed somewhat depending upon its location in the lamellar sheet (Table II, Plate 14) but the VSTR was not affected. 1,609 individual measurements of the lamellar vascular sheet thickness were made. The mean sheet thickness, $\bar{h}$, increased lineraly with ΔP_{lam} within the pressure range 30 to 60 cm H_2O (Fig. 7). The compliance coefficient (α) from this relationship is 0.07μ .cm H_2O^{-1}. The α value was much reduced at ΔP_{lam} values in excess of 60 cm H_2O. At ΔP_{lam} values of 20 cm H_2O all lamellar channels were not filled in some lamellae (Plate 15), but only lamellae with all channels filled were included in the analysis. No lamella channel was seen with a thickness less than 5.2μ.

The sheet thickness is non-uniform with respect to the lamellar height (Fig. 8). There is a progressive thickening of the vascular sheet at increasing distances from the lamellar basal channel, which is true at all the transmural pressures examined (Fig. 8). For analysis, the lamellar channels were separated into 3 equal areas containing 4 to 8 lamellar channels, but the two most basal and the two most marginal channels were treated

separately: hence the 5 lamellar regions in Figures 8 and 9. The basal region includes some channels which lie within the filament epithelium (Plates 4 and 15). For each region the α value was dependent upon the absolute pressure, but for a given ΔP_{lam}, the α value varied between the 5 regions analysed (Fig. 9). At a low ΔP_{lam} the α value was generally greatest in distal regions, but very low in the basal region. Thus the vascular sheet thickness increases preferentially in distal regions of the lamella when ΔP_{lam} is increased from 20 to 50 cm H_2O. Over a 20 to 70 cm H_2O ΔP_{lam} change, the increase in the absolute values for vascular thickness was about the same in all the five regions examined (Fig. 8).

In some sections the filament arteries were measured in cross-section. The diameter measurements at the two extreme pressures (20 and 70 cm H_2O) in the three fish examined were not significantly different (Table II).

FIGURE 6

Mean values for the lamellar vascular tissue space ratio, VSTR, in three fish (○ = 3.3 kg, △ = 3.6 kg, □ = 3.8 kg weight) over a wide range of transmural pressures, ΔP_{lam}. Vertical bars represent standard errors of each point (only the maximum range is indicated) and the number of observations for each point is indicated along side. The horizontal line is the mean value of 88.1% for all the VSTR values.

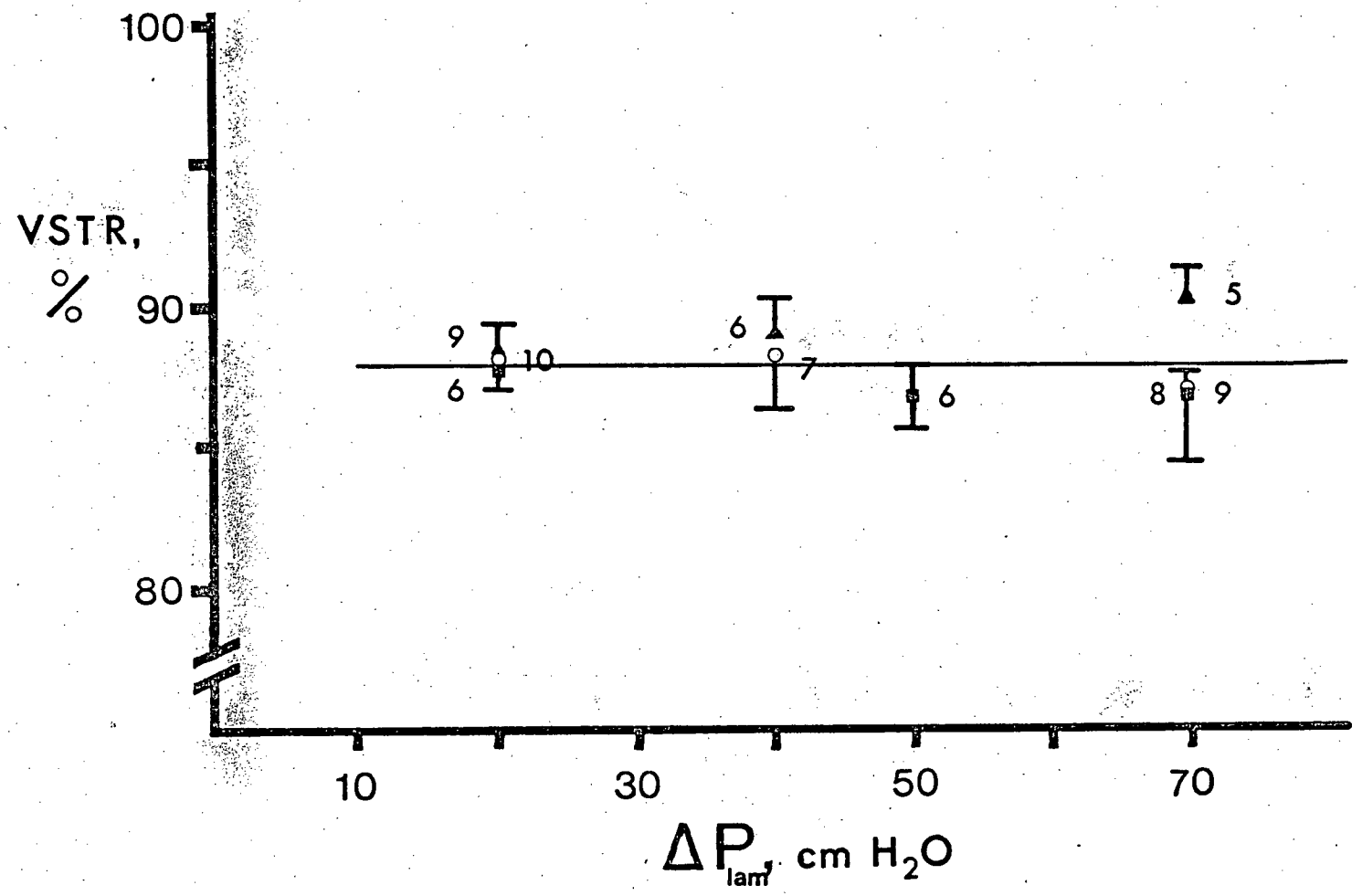
100
90
80
VSTR,
%
9
10
6
6
7
6
5
8
9
10
30
50
70
ΔP_lam, cm H2O

TABLE II

A. The variation in pillar cell cross sectional area expressed as planar area. The pillar cells were grouped according to three locations on each lamellae: afferent, central and efferent.

B. The mean diameters of the afferent and efferent filament arteries from silicone elastomer casts at two transmural pressures of 20 and 70 cm H_2O. The measurements were made from histological sections taken 5.0 mm from the base of filaments 10 to 20 mm long taken from 3 ling cod. The measurements at each pressure are not significantly different.

TABLE IIA

Pillar cell location	area (μ^2) ± s.e	(n)
Afferent	18.4 ± 1.1	(16)
Central	23.0 ± 0.8	(29)*
Efferent	21.6 ± 1.2	(14)*

*Indicates a significant difference (95 % C.I.) from the mean value for the afferent location.

TABLE IIB

Transmural pressure, cm H 0	Artery diameter, μ, ± s.e.(n)	
	afferent filament	efferent filament
20	218 ± 2.6 (59)	205 ± 4.1 (30)
70	214 ± 5.8 (62)	198 ± 4.3 (62)

PLATE 14

Histological plan views of gill lamellae as used for VSTR analysis. Note the regular arrangement of pillar cells (pc), but that the pattern and size of the pillar cells varies with the region of the lamella selected A = central, B = afferent region of the lamella. (725x, bar = 20 μ).

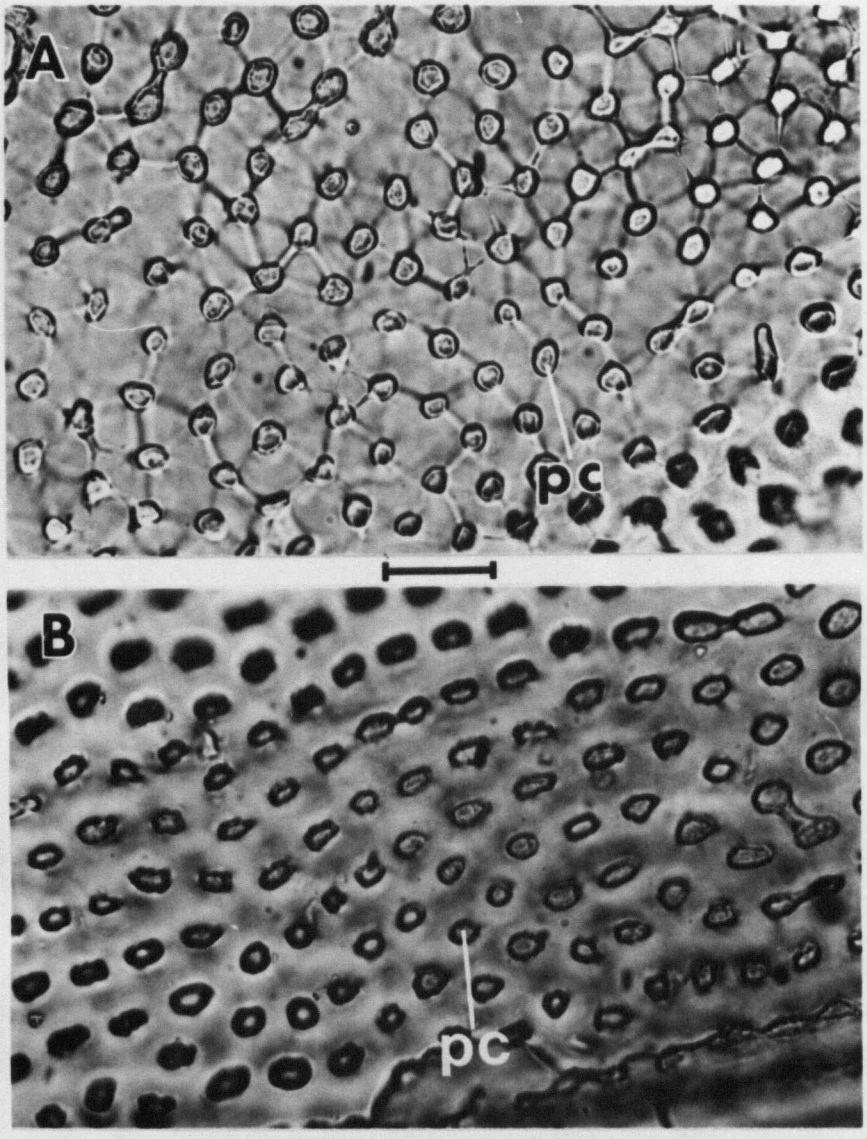
A
pc
B
pc

FIGURE 7

Mean values ± s.e. of lamellar vascular sheet thickness measurements, $\bar{h}$, at different transmural pressures, ΔP_{lam}. The regression line is for $\bar{h}$ values for ΔP_{lam} values between 30 and 60 cm H_2O only and is given by

$$\bar{h} = 8.31 + 0.07\ \Delta P_{lam}$$

For an explanation of the other symbols see the legend of Figure 6.

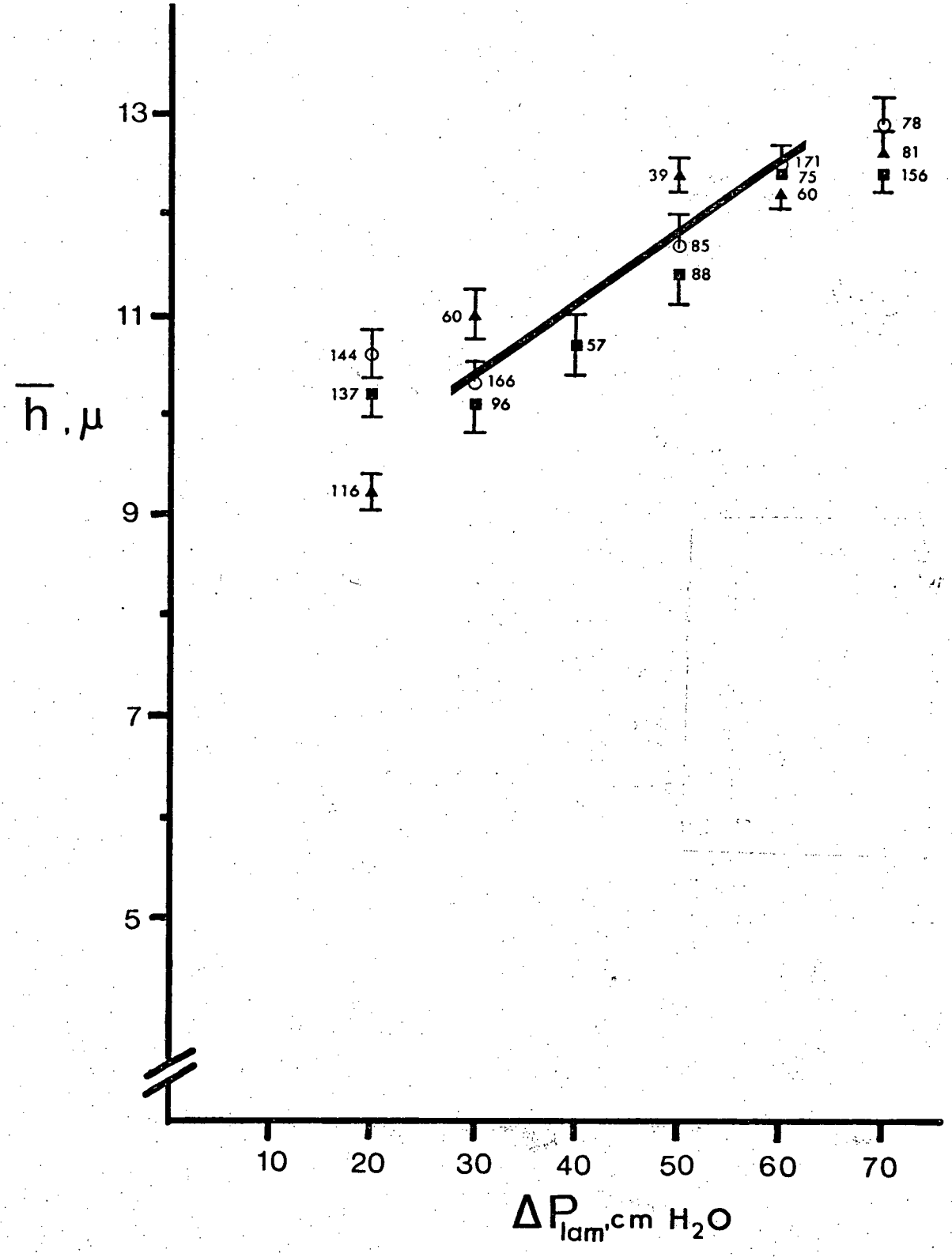
13
11
9
7
5
$\overline{h}$, μ
144
137
116
60
166
96
57
39
85
88
171
75
60
78
81
156
10
20
30
40
50
60
70
ΔP_{lam}, cm H_2O

FIGURE 8

Mean lamellar vascular sheet thickness, $\bar{h}$, for 5 lamellar regions at 3 different transmural pressures, 20, 50 and 70 cm H_2O. Note how closely the lines for 20 and 70 cm H_2O parallel each other, while at 50 cm H_2O the shape is much different. (See discussion for explanation)

● = basal 2 channels **o** = basal area

■ = marginal 2 channels

Δ = central area □ = distal area

Vertical bars represent ± s.e.

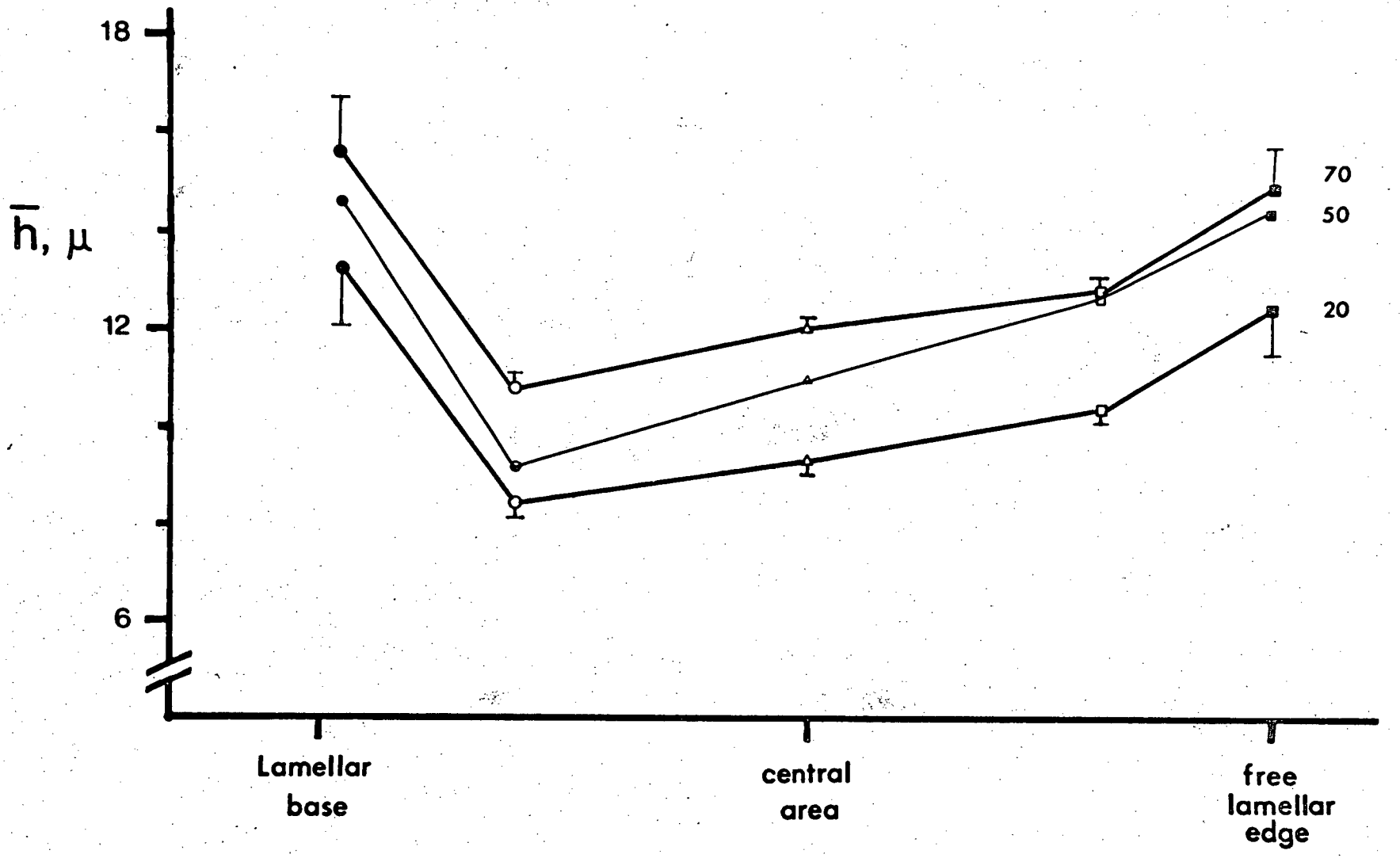
18
12
6
$\bar{h}$, μ
70
50
20
Lamellar base
central area
free lamellar edge

FIGURE 9

Changes in mean lamellar vascular sheet lamellar thickness, $\bar{h}$, with transmural pressure, ΔP_{lam}, for different regions of the lamella. This demonstrates the variation of the compliance coefficient, α , with the region of the filament and absolute pressure, since α represents the gradient of each line. Vertical bar represent ± s.e.

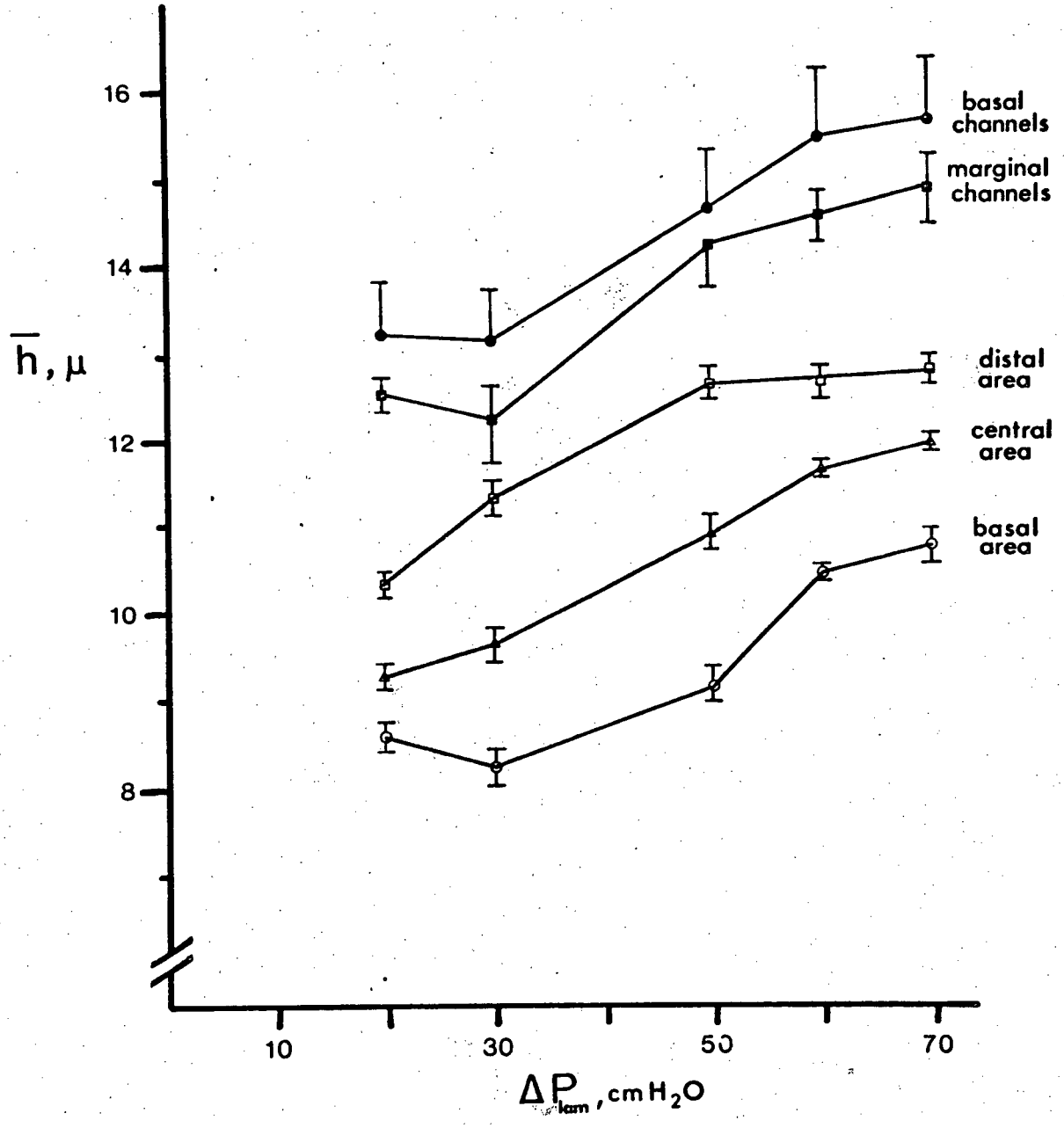
16
14
12
10
8
$\overline{h}$, μ
basal channels
marginal channels
distal area
central area
basal area
10
30
50
70
ΔP_{lam}, cm H_2O

PLATE 15

Histological cross sections of gill lamellae to show the size of the blood channels. The vessels were cast under different transmural pressures (ΔP_{lam}), A = 20 cm H_2O B = 40 cm H_2O and C = 60 cm H_2O. Note that some vessels are collapsed (arrows) at 20 cm H_2O and that the vessels are large at higher ΔP_{lam}. (725x, bar = 20 µ).

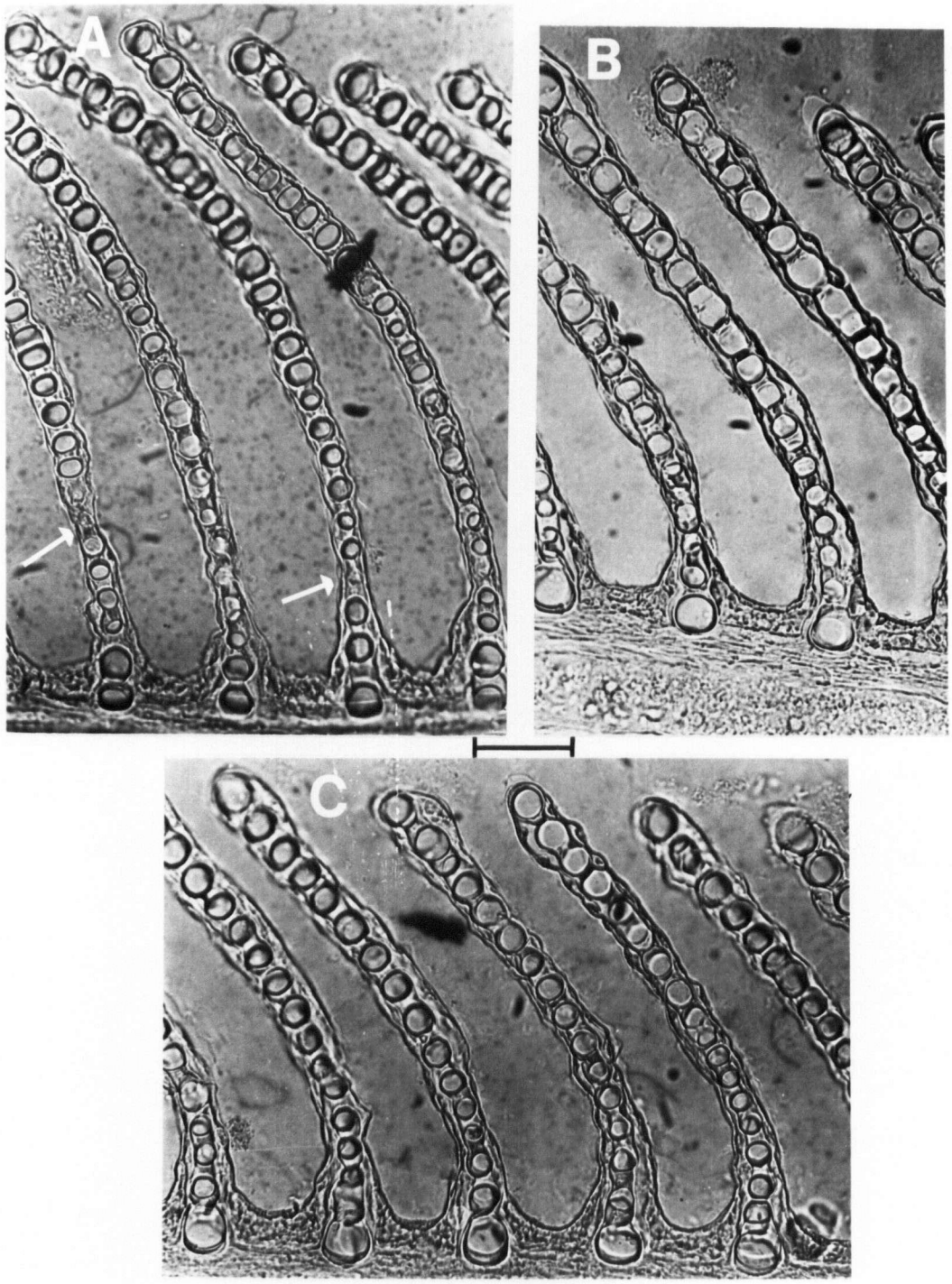
A
B
C

The geometry of the branchial vessels

The branchial vasculature is a complex network. These results are based on selected measurements which I believe are representative samples that can be extrapolated to the whole gill. The filament was considered as a unit with variable length Similarly, lamellar units were considered to vary with respect to their position on a filament and the overall length of the filament on which they were found. The geometry of the gill vasculature is summarised in Table III. The data are drawn largely from measurements made on one corrosion cast of a 4 kg ling cod. The lamellar vascular sheet thickness data are drawn from the silicone casting experiments.

Lamellar surface area: The planar vascular surface area of individual lamellae is greater on longer filaments (Fig. 10) and the total lamellar surface area increases with filament length (Fig. 11) The area of individual lamellae is also dependent upon its position on the filament. However, the lamellar area is almost linearly distributed along the filament length, regardless of the absolute filament length (Fig. 12). Even though figure 12 displays a slightly "S" shaped relationship, 60% of the total lamellar area is found on the proximal 60% of the filament.

The total gill lamellar vascular surface area for a 4 kg ling cod is 1.38 m^2 or 345 $mm^2.g^{-1}$. This value assumes a total number of filaments of 3760 (Fig. 2); a mean

filament length for the gill of 14.4 mm (Fig. 3) and a total lamellar surface area for a 14.4 mm filament of 367 mm^2 (Fig. 11). This area value is based on planar surface areas, but the peripheral channels are, however, rounded. The effect of the peripheral vessel curvature was estimated by tracing the outside of the vessels in Plate 15, which is representative of a mid-lamellar cross-section. The planar surface area was increased by 6%, but this percentage would clearly vary from lamella to lamella, since the overall shape of lamellae varies.

Lamellar volume: This was calculated from the weights of corrosion casts. The total lamellar unit volume for a filament increases proportionately with the filament volume and is 63% of the latter (Fig. 13). Both volumes increase exponentially with $V \propto L^3$ filament length. The filament volume combines lamellar, arterial and venolymphatic volumes. The total volume of all the lamellar units of a 4 kg ling cod was 3.34 ml. This value was derived from figure 13 where the total lamellar volume for a 14.4 mm filament = 0.9 µl (Fig. 13). Lamellar volume was also estimated from their geometry. Total lamellar volume in this case was 4.85 ml (Table IV). Assuming only 60% of lamellae are perfused at rest (Section III) and a resting cardiac output of 0.8 $ml.sec^{-1}$ (Section II), the transit time of blood through the lamellae is calculated to be between 2.5 and 3.6 seconds, for the estimated and weighed lamella volumes respectively.

Afferent filament artery: The diameter of the base of the AFA increases linearly on filaments of increasing length, but a doubling in diameter is accompanied by a quadrupling of the length (Fig. 14a). The AFA artery also tapers along its length. The relationship between the % decrease in AFA diameter along the filament length is displayed in Fig. 14b. The relationship is non-linear. There is almost no taper over the proximal 20 to 30% of the filament. At a location 60% along the filament length the AFA has tapered by 10-30% (Fig. 14b).

TABLE III

The geometry of the gill vessels in a 4 kg ling cod, Ophiodon elongatus. The data were derived from measurements made on a methyl methacrylate corrosion cast of the branchial basket. Filament numbers were counted and lamellar numbers were extrapolated for a mean filament length of 14.4 mm using figure 4.

TABLE III

Vessel	Diameter (μ)	Number	Length (cm)	Total X sectional area (cm^2)	Volume (ml)
Ventral Aorta	4000	1	3.0	0.126	0.378
Afferent Branchial Artery	2500	8	5.0	0.393	1.97
Afferent Arch Artery	700	16	7.5	0.0616	0.462
Afferent Filament Artery	200	3760	1.44	1.18	1.70
Afferent Lamellar Arteriole	20	1.94×10^6	0.045	6.10	0.274
Lamella 60%	10	1.16×10^6	0.1	29.0	2.9
100%	10	1.94×10^6	0.1	48.5	4.85
Efferent Lamellar Arteriole	28	1.94×10^6	0.009	1.19	0.010
Efferent Filament Artery	190	3760	1.5	1.07	1.61
Efferent Arch Artery	700	16	7.5	0.0616	0.462
Afferent Branchial Artery	2000	8	5.0	0.251	1.25

FIGURE 10

The planar vascular surface area of lamellae for a range of filament lengths. Each point represents a determination for an individual lamella at a measured distance from the filament base. The filaments were taken from the 2nd gill arch of 4 kg ling cod. N.B. The effect of marginal vessel curvature would be to increase surface area values by about 6% (See P.67).

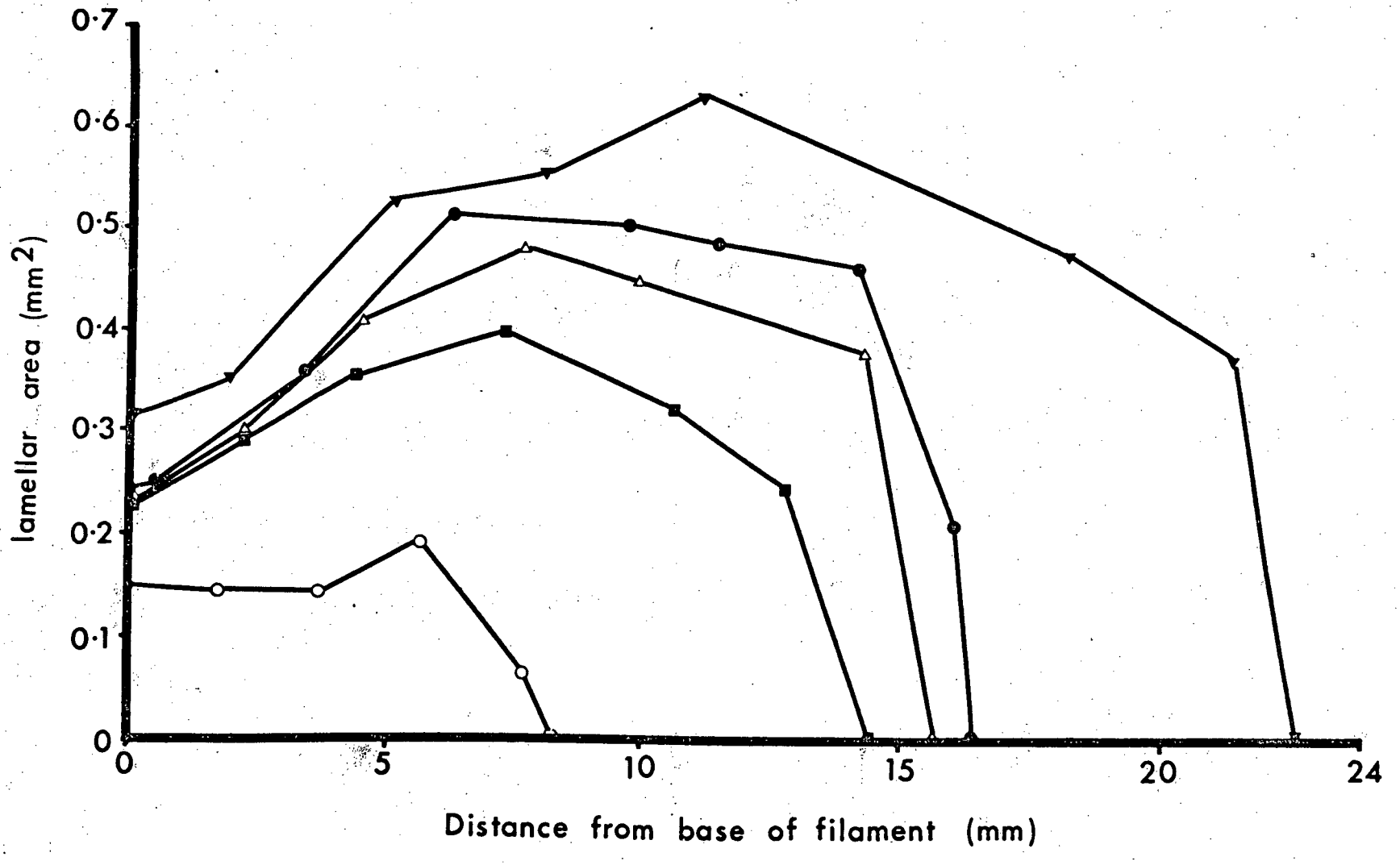
0·7
0·6
0·5
0·4
0·3
0·2
0·1
0
lamellar area (mm²)
0
5
10
15
20
24
Distance from base of filament (mm)

FIGURE 11

The total lamellar vascular surface area (planar) for the complete range of filament lengths found on a 4 kg ling cod. This relationship was established using an integration of the relationships showing in Fig. 7, plus other similar relationships not included in that graph. The line was fitted by eye. N.B. The effect of the marginal vessel curvature would be to increase the areas by approximately 6%.

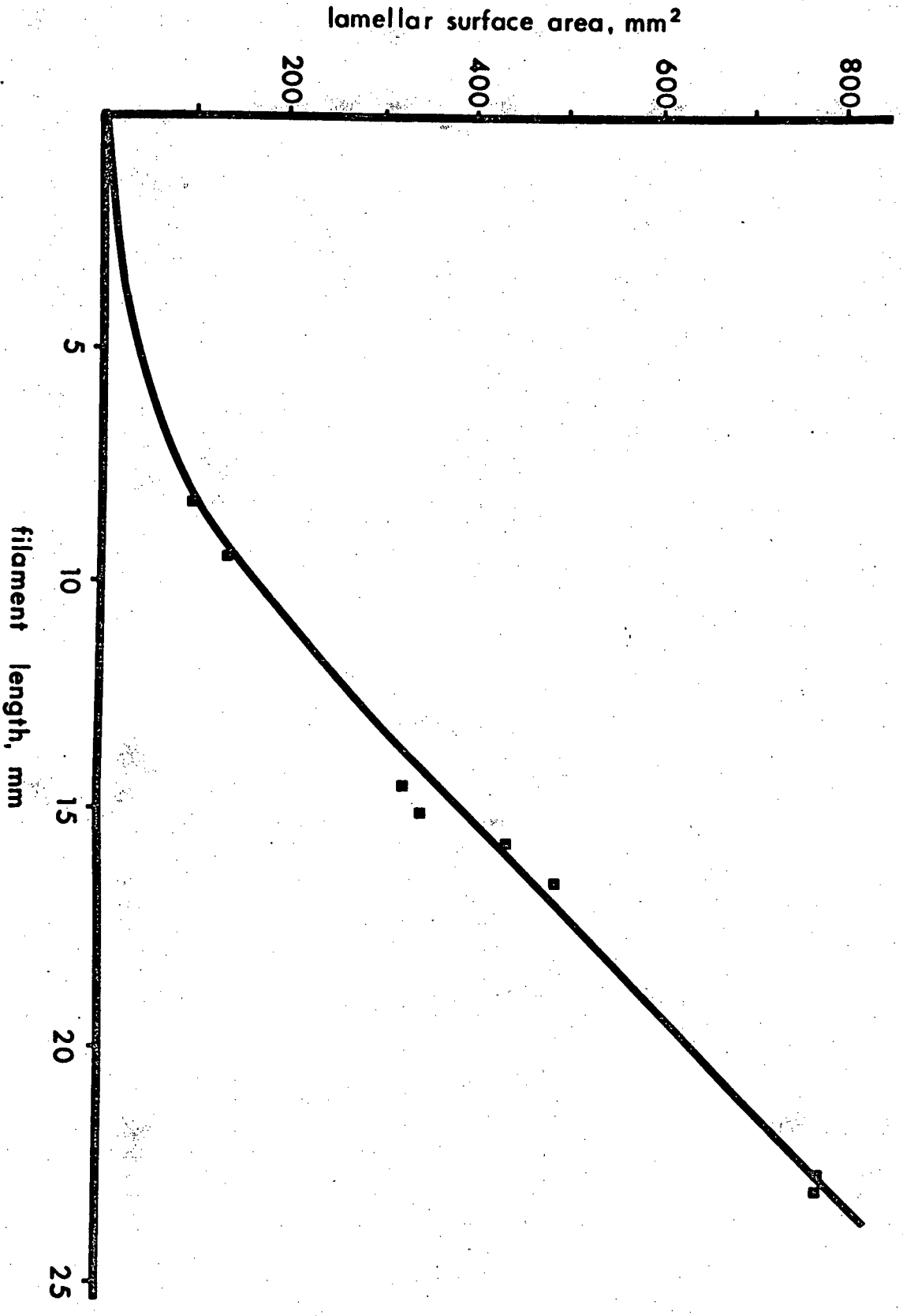
lamellar surface area, mm²
200
400
600
800
filament length, mm
5
10
15
20
25

FIGURE 12

Results of lamellar surface areas from Fig. 10 and others (n = 9 filaments of different lengths), that are expressed as percentages. Note the slight "S" shape relationship, but that 60% of the total lamellar area is found in the proximal 60% of the filament length. Data were taken from all four filaments, which show a similar relationship for % area to % length.

% TOTAL LAMELLAR SURFACE AREA
0
50
100
% FILAMENT LENGTH
0
50
100

FIGURE 13

The exponential relationship between total filament volume and total lamellar unit volume with respect to filament length. The results are from weights of plastic casts and each point represents a different filament. Length refers to the combined lengths of two filaments with equal length that opposed each other on the anterior and posterior hemibranchs (See Materials and Methods). The lines were fitted by eye.

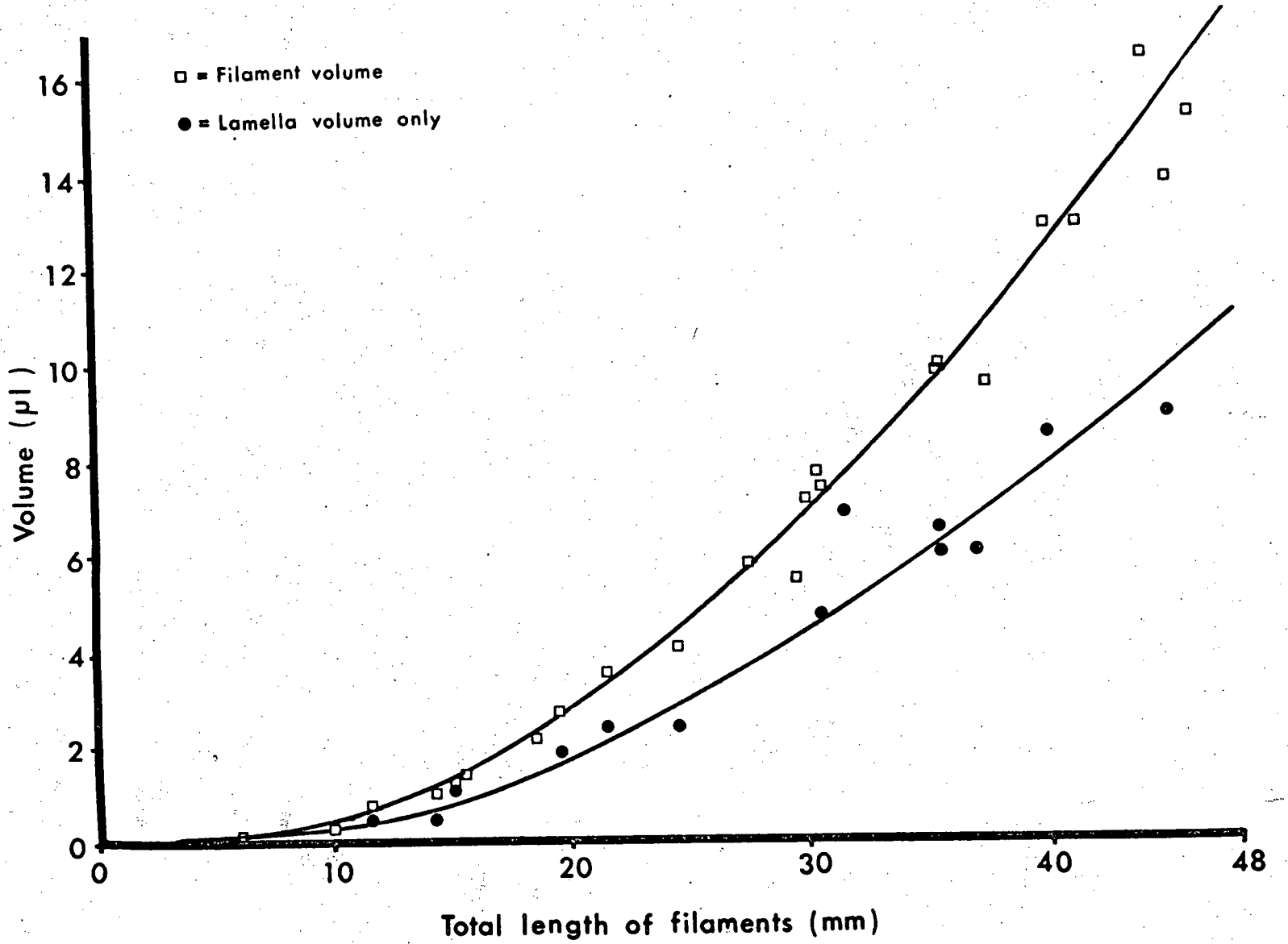
□ = Filament volume
● = Lamella volume only
Volume (µl)
0
2
4
6
8
10
12
14
16
0
10
20
30
40
48
Total length of filaments (mm)

FIGURE 14

The geometry of the afferent filament artery from vascular corrosion casts.

A/ The diameters of the base of vessels versus their length (n = 17 filaments), to show that shorter filaments have narrower afferent filament arteries at their base.

B/ The afferent filament artery tapers along its length in a non-linear fashion. Over the proximal 20 to 30% of its length there is little or no taper. The amount the vessel has tapered by the position 60% along its length is indicated by the broken line, i.e. there has been only a 10 to 30% decrease in its dimensions.

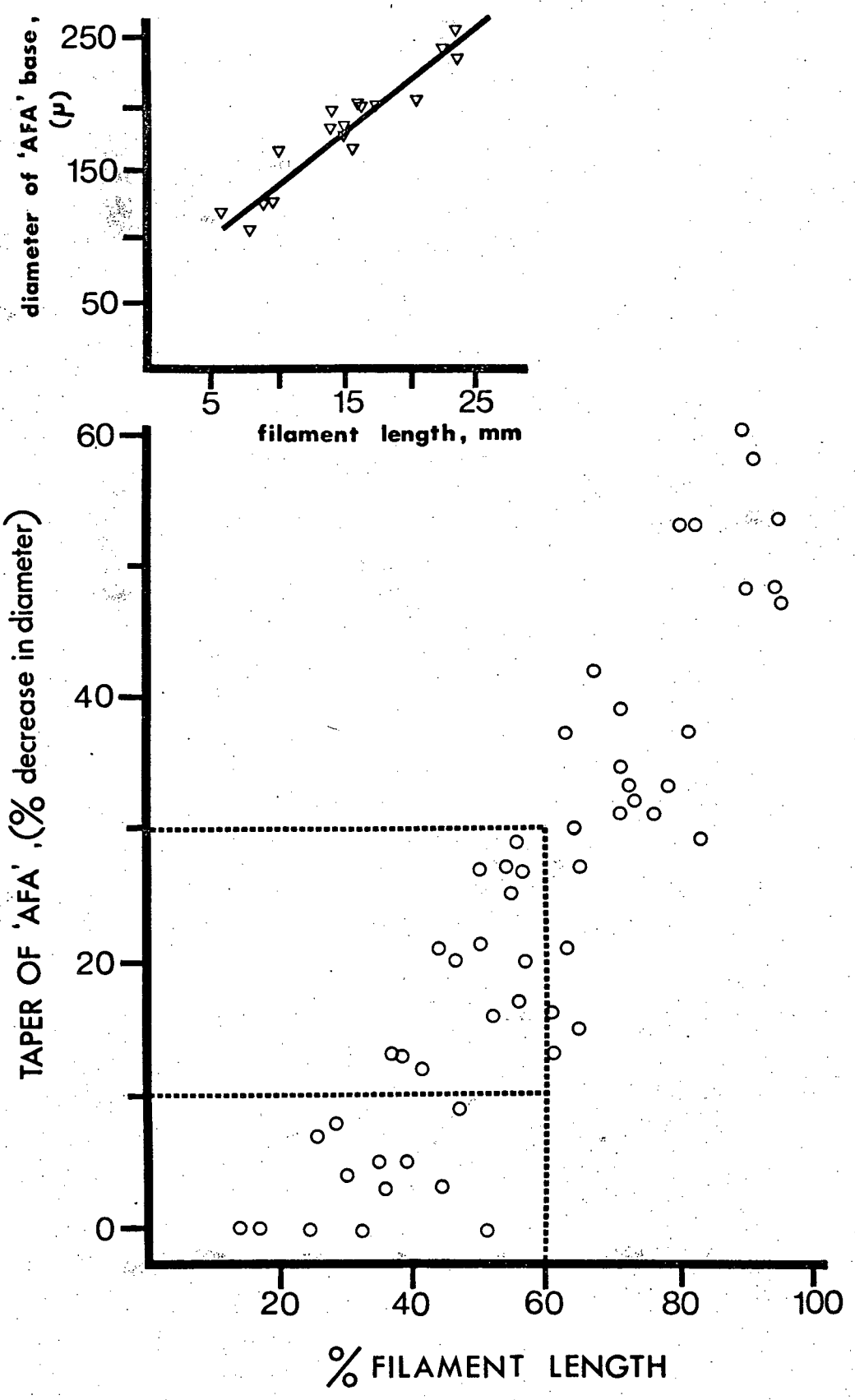
diameter of 'AFA' base, (μ)
250
150
50
5
15
25
filament length, mm
TAPER OF 'AFA', (% decrease in diameter)
60
40
20
0
20
40
60
80
100
% FILAMENT LENGTH

DISCUSSION

The pattern of respiratory vascular pathways in ling cod gills differs little from those previously described for other teleosts (See Introduction for references). Ling cod, if anything, have a less complex vessel arrangement than other teleosts. For instance, in ling cod the AFA is simply tapered and round in cross-section, whereas ampullae are present in carp and trout (Hyrtl, 1838; Riess, 1881; Campbell et al., in preparation). Furthermore, there are no connections between the AFA and central sinus which have been previously reported for Anguilla anguilla (Steen and Kruysse, 1964; Dunel and Laurent, 1977). These differences highlight some of the species variation amongst teleosts. A striking difference between ling cod and trout is in the nature of the venolymphatic arrangement. In trout small, meandering capillaries connect the EFA with both the ECV and the central sinus (Campbell et al., in preparation; Vogel et al., 1976; Vogel, 1978). By contrast Ophiodon have regular but short EFA to ECV connections, which have a larger diameter and also possess a smooth muscle coat. My findings support the general observation that marine fish have better developed venolymphatic network than freshwater fish (Steen and Kruysse, 1964).

A simple functional summary of the vascular flow through ling cod gills is now proposed. (See Plate 16 for a composite diagram of the vascular pathways in the gill filament). All the cardiac output passes through the gill lamellae. At the

PLATE 16

A schematic cross section through the gill filament to demonstrate the arrangement of the vasculature contained within. Blue represents venous blood in the respiratory vasculature and red represents arterial blood in the same system. The venolymphatics are in yellow. The filament support cartilage is colored green.

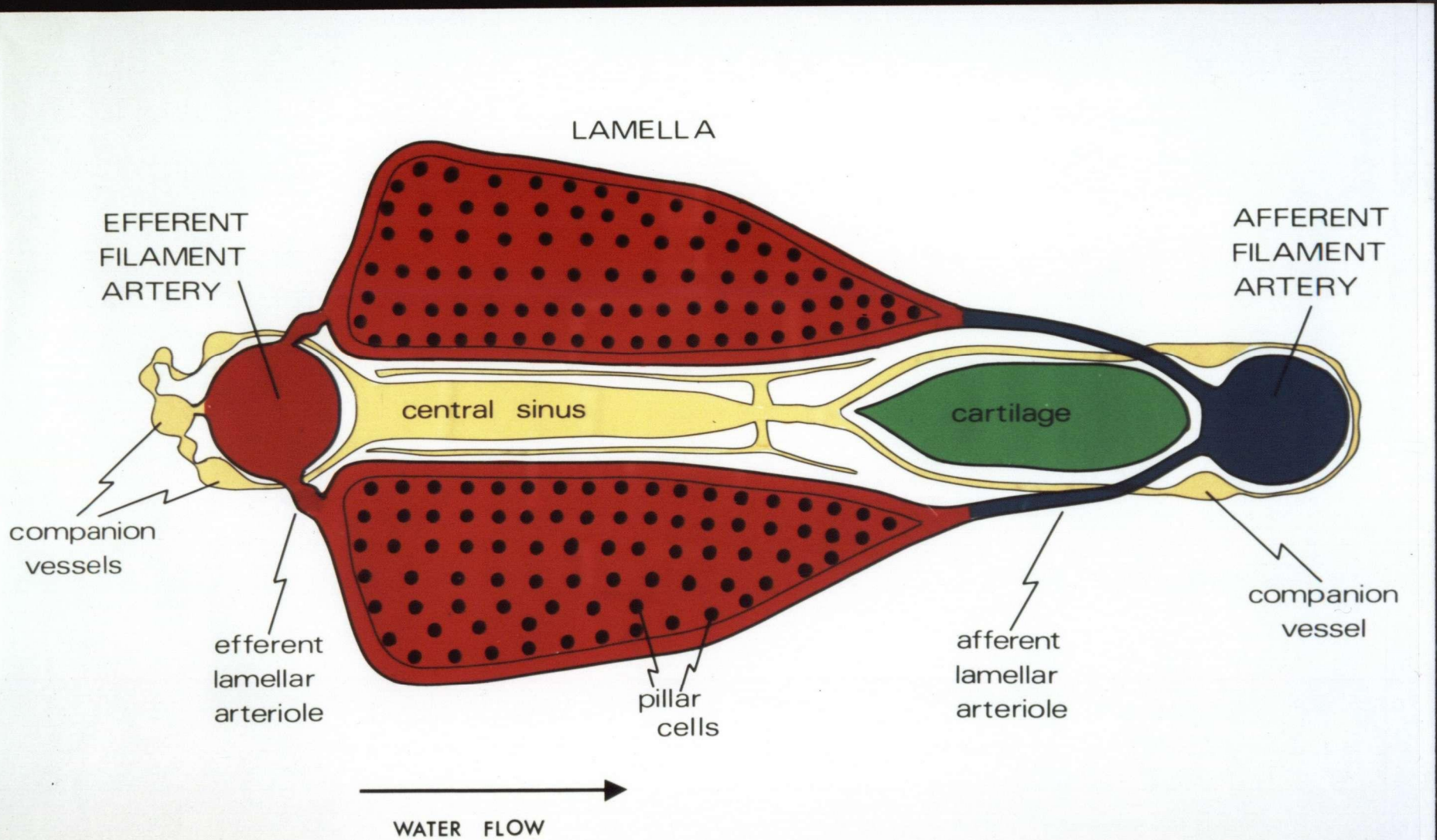
LAMELLA
EFFERENT FILAMENT ARTERY
AFFERENT FILAMENT ARTERY
central sinus
cartilage
companion vessels
efferent lamellar arteriole
pillar cells
afferent lamellar arteriole
companion vessel
WATER FLOW

lamellae there will be some lymph formation which drains via extracellular channels between the pillar and epithelial cells into the central sinus. Oxygenated blood enters the efferent filament artery and thence to the efferent arch arteries. The efferent flow from the gill arches may take one of several routes depending on which arch is considered. In all arches flow can pass into the dorsal aorta, with lesser amounts passing to the head region (including the pseudobranchs) and into the hypobranchial supply. A portion of the oxygenated blood in the efferent filament artery also enters the main efferent companion vessels. This oxygenated blood is distributed to the filament and arch tissues and returns directly to the sinus venosus. The central sinus is drained via the afferent companion vessels. The venolymphatic system returns directly to the heart. How flow is generated in the afferent companion vessel is problematic since there are at least three high resistance (i.e. narrow) channels between the efferent filament artery and ACV. Like mammalian lymphatics, flow is probably driven by arterial pulsations and filament movements and it is aided by non-return valves. Veno-lymphatic flow is discussed in more detail in Section II.

Lamellar blood flow

Two independent relationships were derived for the lamellar vascular sheet. First, mean lamellar vascular sheet thickness ($\bar{h}$) varies directly with the transmural pressure

(ΔP_{lam}) over a typical in vivo pressure range ($\bar{h}$ = 8.36 + 0.07 ΔP_{lam}). Second, vascular space to tissue ratio (VSTR) does not vary with ΔP_{lam}. By deriving these equations it is now evident that the lamellar vascular sheet is quite compliant but, at the same time, anisotropic. In addition, the lamellar vascular sheet behaves in a manner predicted by sheet blood flow theory (Fung and Sobin, 1969).

The similarities between capillary structure and blood flow in the lungs and gills are now confirmed. In fact the two vascular beds appear more alike than previously thought since blood flow in both is best described as a sheet flow. The 88.1% VSTR for ling cod compares well with the 91% for mammalian alveoli (Sobin et al., 1970). A ratio of 80% was determined for frogs by Maloney and Castle (1969) using different methods. The possibility now exists that sheet blood flow is found in the respiratory circulation of all vertebrates. The compliance of the lamellar vascular sheet is high (α=0.07μ .cm H_2O^{-1}) and is comparable to the alveolar sheet in greyhound lungs (21 to 31 kg), where α = 0.079μ .cm H_2O^{-1} when ΔP_{lam} = 25 cm H_2O. The cat alveolar sheet is even more compliant (α = 0.21μ .cm H_2O^{-1}). The h value for the lamellae of ling cod (about 3.5 kg) is greater than that for lung alveoli of cats (3 to 5 kg) (Sobin et al., 1972). There is also less resistance to blood flow in the branchial circulation than in the pulmonary or other systemic vascular beds. These two facts are no doubt related, since resistance is inversely proportional to h^4.

A gill lamella has a non-uniform vascular sheet thickness and the greatest h values are associated with distal lamellar regions. Since α values for each region of the lamella are dependent upon the absolute ΔP_{lam}, h does not increase uniformly from region to region as ΔP_{lam} rises. This situation is more complex than that for lungs, where h is uniform for a given alveolus. The α value has a constant value in cat lungs, but does however vary with ΔP_{alv} in greyhound lungs: at 25 cm H_2O, α = 0.079μ .cm H_2O^{-1} and at 10 cm H_2O, α= 0.12 μ.cm H_2O^{-1} (Glazier et al., 1969).

The non-uniform properties of the gill lamellae have some important consequences with respect to intralamellar blood flow patterns. Considering only passive distributions of flow, blood flow will always be greatest in central and distal regions of the lamellae since h is greatest here for all ΔP_{lam} (Fig. 8). The effect of raising blood pressure will be to alter intralamellar flow patterns (Table IV). Fluctuations in blood pressure will alter ΔP_{lam}, since blood pressures are about 50 times those pressures associated with normal gill ventilation. In Table IV the proportion of blood flow to the basal areas is compared with the remainder of the lamella. These calculations show that if ΔP_{lam} is increased and flow (i.e. $\dot{Q}$) is raised, then blood flow is shunted preferentially to the central and distal regions. Intralamellar shunting of blood flow can therefore occur automatically as a result of elevated $\dot{Q}$ and blood

pressures.

It can now be seen how elevated Q and blood pressures can increase the diffusing capacity of fish. First through intralamellar shunting of blood to regions of the lamella associated with reduced diffusion distances. Gaseous exchange is diffusion limited and the diffusion barriers are well documented (Hughes and Perry, 1976; Piiper et al., 1977). Between the blood and environment there are three barriers. One of these, the epithelial thickness, clearly increases significantly at the base of the lamella, presumably as support for the lamella fold. Furthermore, up to 5 lamellar channels may be buried in the filament epithelium (Plates 4 and 15). The diffusion distances are thus much greater in basal regions than in distal regions. Intralamellar shunting is therefore directed away from regions of high diffusion distances and hence the overall gill diffusion capacity will be raised. Although the estimated quantity of blood shunted may appear small (Table IV), the increases in diffusing capacity will be more pronounced. The marginal channel has a much larger 'free' surface area than other lamellar channels (the curvature of the marginal channel increases the planar surface area of the lamella by at least 6%).

Secondly, when ΔP_{lam} is raised and h increases, the diffusion barrier thickness must decrease by a corresponding amount because the VSTR does not change. The VSTR is a measure of the pillar cell size in relation to the vascular sheet dimensions. Since the pillar cell dimensions do not change with ΔP_{lam}, then the diffusion barrier must alter to accommodate

TABLE IV

A summary of the changes in flow that can occur without any change in resistance when ΔP_{lam} is raised. The basal regions are compared with the remainder of the lamella. Flow was assumed to be proportional to the fourth power of the vascular sheet thickness, and h values were taken from figure 3. The second column summarises how these flow changes are regionally distributed.

TABLE IV

	% increase in absolute flow			Distribution of flow %		
ΔP_{lam}, cm H_2O	20	50	70	20	50	70
Basal regions	0	52	122	40	31	36
Central, distal and marginal regions	0	115	156	60	69	64

increases in vascular sheet thickness.

Thirdly, overall lamellar blood volume is increased with elevated ΔP_{lam} and Q. This in itself increases the lamellar diffusing capacity. Danzer et al. (1968) consider the increased aveolar capillary volume the major reason for an elevated diffusing capacity of the human lung during exercise. Although they consider changes in membrane thickness of little importance in this respect, lung membranes are extremely thin. The lamellar diffusion barrier, however, may be 10 fold that of the alveoli and in fish, membrane changes clearly have a greater potential to alter diffusion capacitance, as presented above. These three mechanisms which increase gill diffusing capacity with elevated Q and blood pressure may, therefore, enable exercising fish to increase in oxygen uptake 5 fold, when gill surface area is only increased by 50%. The relative importance of each of the three mechanisms must still be established.

Clearly intralamellar shunting can occur passively as a result of changes in ΔP_{lam} and flow to the lamella. Whether intralamellar shunting is always a passive (automatic) phenomenon needs to be discussed. Intralamellar shunting has been suggested in the past based on visual observations of lamellar flow (Steen and Kruysse, 1966; Richards and Fromm, 1969) and that pillar cells might be contractile and as a result 'actively' control lamellar blood flow (Bettex-Galland and Hughes, 1973). This conclusion was based on the orientation of thin filaments in pillar cells before and after ATP treatment (Hughes and Grimstone, 1965;

Bettex-Galland and Hughes, 1973). That pillar cells contract has often been postulated to explain increased gill resistance, but the actual likelihood of *in vivo* pillar cell contraction was questioned by Richards and Fromm (1969). It is also questioned here.

There is no direct evidence that humoral or neural influences affect pillar cell contractility *in vivo* and any future studies must show that any changes in lamellar dimensions and flow cannot be accounted for by changes in ΔP_{lam}. Acetylcholine has been cited (speculation, not direct observation) as having a contractile effect on pillar cells (Steen and Kruysse, 1966), but this is unlikely to be of importance *in vivo* because the pillar cells are not innervated (Hughes and Grimstone, 1965; Newstead, 1965 and 1967; Gannon, 1972). Acetycholine released into the circulation is rapidly destroyed by cholinesterase. Other factors like oxygen level or the level of circulating catecholamines may affect pillar cell tension, but this has yet to be demonstrated in fish. At present there is no reason to conclude that changes in intralamellar flow are anything but passive (automatic) responses to changes in transmural pressure.

Lamellar blood channels display the phenomenon of critical closure at low ΔP_{lam}. The concept of critical closure of small vessels was first established by Burton (1951) and Nicol *et al.* (1951). It has since been observed in mesenteric vessels by Lamport and Baez (1962), contested on

theoretical grounds by Peterson (1962) and demonstrated by Fung and Sobin (1972) in pulmonary alveoli. At a ΔP_{lam} of about 20 cm H_2O many lamellae were observed with no silicone in some basal and central channels of otherwise filled lamellae (Plate 8). All lamellar channels had been previously exposed to a higher ΔP_{lam} during the preliminary silicone perfusion and unfilled channels were never seen at a ΔP_{lam} exceeding 30 cm H_2O. These unfilled channels must have collapsed at the low ΔP_{lam}. Wood (1974a) examined the critical closing pressure for trout gills in vitro, but incorrectly considered the differences between input and output pressures instead of ΔP_{lam}. Re-analysis of his results reveals that many gill preparations displayed critical closing at pressures of 15 to 25 H_2O for ΔP_{lam}, which is in agreement with my work. Because vessels can collapse at pressures above ambient explains my observation that no vessels were open below h = 5.2μ. Similar observations have been made for the mesentery and alveoli. Critical closing pressures are associated with vessels not being open below 5μ (mesentery; Lamport and Baez, 1962) and 2.5μ (alveoli; Fung and Sobin, 1972). Not all lamellae, nor all lamellar channels collapsed at the overall ΔP_{lam} of 20 cm H_2O (Fig. 15). Thus not all vessels have the same critical closing pressure. The sigmoid curve of Figure 7 can now be explained. There is no sharp cut off at h = 5.2μ for two reasons. First, h is a mean value of a non-uniformly thick vascular sheet. Second, only

completely filled lamellae were analysed at low ΔP_{lam} and thus lamellae with low critical closing pressures were selected. At high a ΔP_{lam}, increases in h are limited by the finite curvature of the lamellar sheet (Fung and Sobin, 1972).

Whether critical closure occurs *in vivo* is speculative, unlike the mammalian situation. Collapsed lamellar vascular channels would be advantageous in some situations e.g. osmotic exchange with the water could be minimised or when lamellae were damaged or parasitised. That the lamellar vascular sheet can collapse would appear to be an important reason for maintaining dorsal aortic pressure *in vivo*, and in experimental situations "*in vitro*".

In conclusion, sheet blood flow theory can be applied to lamellar blood flow in fish gills. Intralamellar shunting can occur passively as a consequence of pressure changes. The importance of intralamellar shunting in teleosts is that the diffusion capacity for respiratory exchange can be varied.

Predictions on sites of gill resistance

It is possible to calculate the resistance to flow in the gills and determine sites of high resistance within the gill vascular network, based on the previously described morphology and vessel geometry of the gills. Sites of high resistance will be influential in the pattern of blood flow through the gills. Fung and Sobin (1977) have summarised the equations they developed for determining resistance in sheet flow systems and these equations can be applied to the lamellae. The equations I have adapted are as follows:

Lamellar resistance, R_{lam}, is given by

$$R_{lam} = \frac{C}{h_a^3 + h_a^2 h_v + h_a h_v^2 + h_v^3} \qquad (1)$$

where h_a and h_v are the sheet thicknesses at the afferent and efferent ends of the lamella.

and $$C = \frac{4\eta k f \bar{L}^2 \alpha}{SA} \qquad (2)$$

where η = kinematic viscosity, k and f are constants determined by the geometry of the pillar calls, $\bar{L}$ is the average length of the lamellar capillary channels, α is the compliance coefficient, S is the VSTR value and A is the lamellar area. Flow, Q, is given by

$$Q = \frac{1}{C}(h_a^4 - h_v^4) \qquad (3)$$

Mean sheet thickness, h, is given by

$$h = h_o + \alpha \Delta P_{lam} \qquad (4)$$

where $h_o = 8.31\,\mu$ and $\alpha = 0.07\,\mu$ .cm H_2O^{-1} for ling cod.

Blood flow in the remaining gill vessels, the afferent and efferent arteries and arterioles, is probably Poiseuillian and can therefore be described by Poiseuille's equations. Poiseuille's equation states that flow, Q,

$$= \frac{\Delta P\ r^4 \pi}{8L}$$

where ΔP is the pressure drop along a vessel of length L and of radius r. This was verified by calculating 'a' for these vessels. 'a' was less than 0.8 where 'a' $= \sqrt{\frac{2\pi\omega}{\eta}}$ and ω = angular frequency (McDonald, 1960).

The relationship between Q and resistance is complex because the vascular system is compliant. If input pressure increases Q will rise, but as the vessels are compliant they expand. So resistance falls as pressure rises, since resistance is inversely proportional to the fourth power of the vessel radius. Thus in this analysis I have assumed a constant cardiac output = 44 ml.min^{-1} (See section II) and a constant input pressure, where ΔP_{lam} = 45 cm H_2O, to permit the calculation of pressure drops along vessels in the gills. At constant pressure and flow the gill resistance is inversely related to the pressure drop. In the case of the lamellae, resistance and flow were calculated directly from the dimensions of the gills.

The pressure drop between the ventral and dorsal aortae

is 13 cm H_2O *in vivo* (see section II). This value represents the sum of the pressure drops in individual vessels of the gills. Below I have made a partial account for this pressure drop by making calculations for the vessels of the gill filament only. Detailed information of the values used in the calculations is presented in Appendix I.

The lamellae: In the equations dealing with sheet flow (1,2,3 and 4) only R_{lam} and h_v are unknowns. Assuming 60% lamellar perfusion, h_v was calculated to be 11.44 μ and R_{lam} to be 7.65×10^3 cm $H_2O.min.ml^{-1}$. Thus ΔP_{lam} on the efferent side of the lamella was 44.71 cm H_2O. Therefore the pressure drop across the lamellae is very small, 0.29 cm H_2O (45 to 44.71 cm H_2O). From equation (1) the effect of raising ΔP_{lam} from 45 to 65 cm H_2O on lamellar blood volume was calculated. The $\bar{h}$ would increase from 11.44 to 12.86 μ, which represents a 12% increase in capillary volume.

Afferent filament artery: These vessels have many lengths and radii in any gill bed. As a result not all filaments receive the same amount of flow. As an AFA has arteriole branches along its length, flow will diminish along the length. Furthermore the vessel tapers along its length. This variability hampers calculation of ΔP for the AFAs. It was therefore assumed that flow to any filament was dependent upon the number of lamellae

it supported. Blood flow to any filament is then proportional to its length since lamellae are evenly spaced (Fig. 12). Vessel radius is also directly related to filament length (Fig. 14). A representative AFA (or filament) was selected to represent the gill bed and this vessel had a length equivalent to the mean filament length for the whole gill. For a 4 kg ling cod the AFA was 14.4 mm in length and had a 100 μ radius. Furthermore the effects of vessel taper and flow loss to branching arterioles on vessel resistance nullify each other, assuming 60% lamellar perfusion (Appendix I). The representative AFA used in these calculations was therefore considered to be of a uniform diameter.

ΔP = 2.1 cm H_2O for the afferent filament arteries under the above conditions. The resistance of the representative AFA is 1.84×10^2 cm $H_2O.min.ml^{-1}$.

The lamellar arterioles: The efferent lamellar arterioles have a relatively uniform length and range of diameters on any filament. Because of the bulbar swelling in the ELA, its radius can range from 11 to 15 μ. By assuming the minimum radius for the vessel an overestimate of the pressure drop was determined to be 0.15 cm H_2O with 60% of lamellae perfused. The resistance of the vessel is 3.95×10^3 cm $H_2O.min.ml^{-1}$.

The afferent lamellar arterioles have complex variations in their geometry. Vessel length can be as much as 700 μ in proximal locations and as short as 120 μ distally. Distal

arterioles have diameters up to 6 μ narrower than proximal vessels and some ALAs have a narrower region at their point of origin from the AFA (Plate 11). In addition flow cannot be estimated accurately because of bifurcations in the vessel. These bifurcations may supply two lamellae on the same side of the filament or, more commonly and in distal regions, they may supply a pair of dorsal and ventral lamellae. The variations in ALA geometry and flow prevent a general calculation of ΔP and resistance, as presented above. Instead the calculations were made using representative dimensions of ALAs from proximal, central and distal locations (see Appendix I). The values for these calculations are presented in Table V, along with values for the other filament vessels as calculated above. The calculated resistances and pressure drops for ALAs will be underestimates since it was assumed one ALA supplied one lamella and the vessels had uniform diameters. This underestimation would be greatest for the distal ALAs since they were all bifurcated.

In the gills the ALAs are clearly the major resistance site and the major pressure drop occurs here (Table V). The ALAs, therefore, have an ideal geometry to control input pressures to the lamellae and thus determine intralamellar flow patterns. A 25% reduction in the diameter of a distal ALA would increase resistance to 4.98×10^5 cm H_2O.min.ml^{-1} and ΔP to about 15 cm H_2O given no other changes. Thus critical

TABLE V

A summary of the calculations of vascular resistance, pressure drop across vessels (ΔP) and blood transit times in gill filament vessels. Three calculations were made for afferent lamellar arteriles in proximal, central and distal locations of the filament because their geometry is different for various regions of the filament. See text and Appendix I for details of the calculations.

TABLE V

		Resistance (cm H_2O.min.ml^{-1})	ΔP (cm H_2O)	Blood transit time (sec)
Afferent filament artery		1.84×10^2	2.1	2.1
Afferent lamellar arterioles	Proximal	1.27×10^5	4.8	0.34
	Central	1.21×10^5	4.6	
	Distal	1.33×10^5	5.0	
Lamella		7.65×10^3	0.29	2.5 to 3.6
Efferent filament artery		3.95×10^3	0.15	0.01

closure pressure for lamellar channels and indeed for the whole gill (Wood, 1974a) would be attained. Fine control of ALA diameter might be achieved neurally. ALAs receive adrenergic innervation in other teleosts, but this has yet to be established for Ophiodon. An afferent arteriole control site of capillary blood pressure is consistent with findings for other microcirculatory systems (see Section II).

Morgan and Tovell (1973) concluded that the afferent filament artery restricted flow to distal lamellae because its taper reduced lamellar input pressures. They, however, did not consider that AFA branching reduces flow along the AFA. My findings lend no support to their conclusion or that AFAs control input pressures or flow to lamellae. A greater than 50% reduction of vessel diameter over the whole vessel length is needed to develop a sufficient pressure drop that critical closure pressures are reached in the lamellae. Arterial vessels rarely alter their diameter more than 50% (Petersen, 1962).

Of the 13 cm H_2O pressure drop across the branchial vessels in vivo, my calculations reveal that 9.6 cm H_2O or more is due to vascular resistance in the filament. I assume here that the pressure drop in the EFA is similar to that determined for the AFA. The small pressure drop across the lamellae may be surprising to some authors who previously considered that the capillary bed regulated gill blood flow patterns. The calculations presented here for lamellar resistance do not support this contention. With such a small ΔP across lamellae, a high pressure associated with ventilation (the other component

of the transmural pressure) could have important effects on intralamellar flow patterns. This may be why ventilation-perfusion synchrony occurs in Ophiodon during stress when ventilation pressures rise up to 5 cm H_2O. Ventilation-perfusion synchrony occurs in other fish during stressful conditions (Randall, 1967; Hughes, 1972; Roberts, 1975).

Blood transit times through filament vessels are also shown in Table V. They were calculated using a constant flow and the vessel volumes presented in Table IV. Lamellar transit time represents the residence time of red blood cells at the gas exchange site. The time of 2.5 sec is higher than, but of the same order as the 1 sec transit time in mammalian lungs (West, 1977). In mammalian lungs the degree of gaseous exchange is determined by ventilation and perfusion rates (perfusion limited) since the alveolar diffusion barriers are so thin. If the alveolar barrier is thickened by disease, gas exchange is severely reduced i.e. the system approaches diffusion limitations. Considering that lamellar diffusion distances are 10 times greater than in alveoli, but that red blood cell residence time is only 2 to 3 times greater, it is possible that lamellar gaseous exchange is diffusion limited in ling cod. Fisher et al. (1969) and Randall (1976) have concluded that lamellar gaseous exchange is diffusion limited for other teleosts.

In summary, I have demonstrated in this section that all cardiac output passes through the lamellae in ling cod. The

venolymphatic flow in the gill filaments must be derived entirely from efferent vessels and lymph formation. I predicted from calculations based on vessel geometry, that ALAs are the major resistance site in the gills and consequently determine the lamellar input pressure and ΔP_{lam}. Intralamellar blood flow patterns can now be predicted from ΔP_{lam}, since lamellar flow is best described by sheet blood flow equations. The vascular sheet of a lamella is compliant, but since its compliance varies regionally, intralamellar shunting of blood flow can occur automatically as P_{lam} and Q change. When resting blood pressures are elevated, intralamellar shunting occurs away from the base of the lamella, towards regions of reduced epithlial thickness. Since gaseous exchange is apparently diffusion limited in ling cod, intralamellar shunting enhances gaseous exchange. Lamellae have a critical closure pressure and whether they are perfused or not is determined largely by the input pressure. The resistance associated with distal lamellae is greater than for proximal lamellae. Thus distal lamellae are less likely to be perfused. If distal lamellae were not normally perfused *in vivo*, then elevated ventral aortic blood pressures in ling cod would alter the pattern of gill blood flow in two ways: a) recruitment of distal lamellae, b) intralamellar blood flow changes. Both flow alterations, as pointed out, enhance O_2 transfer. The predictions outlined in this Section are now tested experimentally *in vivo* and *in vitro* in subsequent sections.

SECTION II

AN EXAMINATION OF GILL BLOOD FLOW CHARACTERISTICS AND GILL RESISTANCE AND HOW THEY CHANGE IN VITRO AND IN VIVO

Blood flow to the gills in resting ling cod.

Micropressure measurements *in vivo*, anaesthetised ling cod

Micropressure measurements in isolated, perfused holobranchs and the effect of adrenergic and cholinergic drugs on gill resistance

The *in vivo* effects of intravascular administration of adrenergic and cholinergic drugs on gill resistance and gill blood flow in resting ling cod.

INTRODUCTION

In recent years mammalian microcirculations have become better understood as a result of direct studies of blood flow and blood pressure in small arteries, arterioles and capillaries. Blood pressures can be measured in small vessels by micropuncture; a technique pioneered by Landis (1934). Landis measured average capillary blood micropressures with pipets of 8 to 15 μ tip diameter. Only recently, however, have accurate, pulsatile micropressure measurements been made in small blood vessels (Weiderhielm et al., 1964). Weiderhielm et al. developed a high fidelity, automatic, servonulling device which used pipets as small as 0.1 μ tip diameter. Weiderhielm's device has since been refined both electronically and mechanically (Intaglietta et al., 1970; Intaglietta, 1973). The major insight gained from micropressure measurements is that major pressure drops (major sites of resistance to flow) can be located. Furthermore, flow directions can be assigned from pressure measurements within a system, given the vascular arrangement as well as input and output perfusion pressures.

Micropressure studies have been limited primarily to mammalian systemic vascular beds that were easily accessible, visible and relatively stable or free from movement e.g. the bat wing (Weiderhielm and Weston, 1973), the rabbit mesentery and omentum (Zweifach and Lipowsky, 1977). From these and many other studies it is now recognized that capillary blood flow is

pulsatile with a pressure pulse of the order 1 - 2 cm H_2O. A general finding is that the major site of vascular resistance is located in precapillary arterioles; a conclusion also made by Landis (1934). Thus the arteriolar resistance reduces capillary blood pressure to about 20 mm Hg, which represents only 15 to 20% of the central systemic blood pressure. Furthermore, it is now held that the intracapillary pressure is largely regulated at input sites or precapillary sphincters which may be located in the arteriole (Nicoll, 1971). This concept is supported by the work of Fronek and Zweifach (1975). They examined the effect of vessel dilation on micropressures by administering isoprenaline and demonstrated that arterioles as small as 20μ would dilate and produce major resistance changes. Lundvall and Jarhult (1974) also report adrenergic dilation of precapillary sphincters. If arterioles are regulating capillary pressure, they will also control flow to the capillary bed. Sobin et al. (1977) have concluded that smooth muscle in pulmonary arterioles of fetal and new born mammals is concerned only with pulmonary blood flow regulation. I have also been able to witness slow arteriole pulsations of myogenic origin in mammalian mesenteric vessels (through the courtesy of Dr. Intaglietta and co-workers). The arteriole contractions would stop blood flow without complete vessel constriction and divert flow to a nearby branch.

Regulation of intracapillary blood pressure is clearly of prime importance to mammals since it sets the transcapillary

blood pressure. This pressure will determine transcapillary fluid exchange i.e. the rate of lymph formation (Starling, 1896; Landis 1934; Weiderhielm, 1968), and, in the lungs at least, both the distribution of blood flow and capillary blood volume (Fung and Sobin, 1977). Intracapillary pressure will be largely determined by the arteriole resistance.

Do similar mechanisms for regulating intralamellar pressures exist in fish? The branchial vascular flow dynamics in teleosts differ in a number of important respects from the pulmonary and systemic circulation in mammals. The branchial vascular bed reduces the central blood pressure by only 25 - 30% in most teleosts, including Ophiodon (Randall, 1970; Stevens et al., 1974). The intralamellar blood pressures are therefore comparatively high: generally at least 30 cm.H_2O which is the outflow blood pressure measured in the dorsal aorta. Lamellar capillary blood pressure should also be quite pulsatile; this again is predicted from the pulsatility of dorsal aortic blood pressure. I predicted in Section I that the major resistance to gill blood flow was the afferent lamellar arteriole. If this is true, ALA resistance would determine the preferential perfusion of proximal lamellae and the ΔP_{lam} which affects intralamellar blood flow and the rate of lymph formation. Clearly, it is important to confirm that ALA is the major resistance site in the dynamic situation. The micropressure system, as developed for mammalian investigations, was therefore used to examine pressure within gill filament vessels and

establish the major resistance site.

Alterations in vascular dimensions are reflected in measurements of gill resistance. Gill resistance (Rg) may be altered by direct vascular actions of hormones, through neural activity or a myogenic feedback system. The isolated perfused gill or holobranch has been used extensively in the past to study the effects of adrenergic and cholinergic drugs on Rg. It is clear that intravascular infusion of adrenaline reduces Rg *in vitro*, however a controversy surrounds the exact nature of the adrenergic response (Krawkow, 1913; Mott, 1951; Randall and Stevens, 1967; Richards and Fromm, 1969; Randall *et al.*, 1972; Wood, 1974a). In trout, at least, it appears there are α-adrenergic constrictory and β-adrenergic dilatory receptors in the gills (Wood, 1975). The exact site of these receptors has yet to be localised but it is known that adrenergic fibres innervate afferent lamellar arterioles (Gannon, 1972). Catecholamine infusion will also reduce flow into the venolymphatics in trout (Girard and Payan, 1976) possibly through α-adrenergic vasoconstriction of connecting vessels (Dunel and Laurent, 1977). Acetylcholine infusion *in vitro* markedly increases gill resistance (Ostlund and Fange, 1962; Wood, 1975). Attempts to localise the site of acetylcholine action in the gill were not successful (Steen and Kruysse, 1964; Richards and Fromm, 1969; Klaverkamp and Dyer, 1974) until quite recently (Smith, 1977; Dunel and Laurent, 1977). Smith provided good experimental evidence that acetylcholine causes a major vasoconstriction at

the base of the EFA in trout; a site which probably corresponds to a marked constriction seen in plastic vascular corrosion casts of trout EFAs (Campbell et al., in preparation; Smith, 1976) and other teleosts (Dunel and Laurent, 1977).

Gill blood flow and changes in gill resistance have not been examined extensively in vivo. Studies such as Stevens et al. (1972), Jones et al. (1974) and Chan and Chow (1976) have examined blood flow in teleosts in some detail, but not branchial blood flow specifically. Stevens et al. (1972), working with Ophiodon concentrated largely on cardiac function and demonstrated that the heart rate was under vagal control. It varied widely with water temperature and had the major influence on Q. Also, increased vagal activity was associated with exercise and with disturbing the fish. They showed an α-adrenergic systemic vasoconstriction, but concluded that the associated cardiac responses were reflexogenic. Jones and co-workers (1974) compared a hydraulic circulatory model with measured cardiovascular variables from Gadus morhua and examined the importance of vascular compliance in pulsatile blood flow. They concluded branchial blood flow was both continuous and pulsatile. They also discussed the significance of matching stroke volume with gill blood volume and concluded stroke volume rarely exceeded gill blood volume. Chan and Chow (1976) made an extensive investigation of the pharmacological effects on cardiovascular function in Anguilla japonica using intravascular

injections of most known vasoactive agents. They measured a variety of arterial and venous blood pressures, but were unable to calibrate their Doppler flow meter to allow accurate measurement of Q changes.

A number of cardiovascular investigations have also been made on dogfish. The works of Satchell (1962), Kent and Peirce (1975 and 1978) and the recent experimental series by Butler and Taylor (1975) and Taylor et al. (1977) have been particularly useful since they highlight the remarkable similarities in cardiovascular responses between teleosts and elasmobranchs. For example, the vagally mediated bradycardia in response to environmental hypoxia has been examined extensively in both fish groups. (See Smith and Jones (1978) and Daxboeck and Holeton (1978) for references).

Vagal innervation of the teleost heart is well established. The cardiac vagus carries largely cholinergic fibres and a negative chronotropic vagal tone exists during resting states in a number of teleosts, but not in Salmo gairdneri (Randall, 1970). Adrenergic cardiac excitation is also evident in some teleosts and both positive inotropic and chronotropic effects are believed to be mediated by β -receptors in the heart (Gannon and Burnstock, 1969; Randall, 1970; Chan and Chow, 1976; Holmgren, 1977). Adrenergic cardiac stimulation may be due to endogenous catecholamine levels (Wahlqvist and Nilsson, 1977) or via vagal stimulation (Gannon and Burnstock, 1969). Vagal stimulation appears more complex than a simple negative

chronotropic effect since in trout, at least, the vagus also carries some adrenergic excitatory fibres (Yamauchi and Burnstock, 1968; Gannon and Burnstock, 1969). Gannon (1972) and Cobb and Santer (1973) both document a small cardiac acceleration after vagal stimulation of the heart was stopped. Kulaev (1958) and Rudinov (1959), as reported by Chan and Chow (1976), found that the effect of stimulating reduced numbers of vagal fibres (produced by sectioning vagal branches one by one) was to change the elicited bradycardia to a tachycardia.

Previous investigations have, therefore, provided information on control of cardiac activity *in vivo* and on general blood flow in teleosts. The investigation of gill blood flow has not, however, been detailed enough for an analysis of how patterns of gill blood flow change. For this reason pre- and post-branchial blood pressures were monitored along with Q and heart rate in resting *Ophiodon*. Ventilation rate and amplitudes were also monitored. Micropressure measurements were made in filament vessels in anaesthetised fish and in isolated gill arch preparations to localise the major site of gill resistance. The effects of adrenergic and cholinergic agonist drugs on gill resistance and blood flow were also examined by injections into the ventral aorta of resting ling cod and drug infusions into isolated gill arch preparations. Thus *in vivo* and *in vitro* experiments were carried out to a) confirm that the ALA was the major resistance site to gill blood flow, b) establish whether vascular changes alter the balance of vessel resistances sufficiently to alter gill blood flow patterns.

MATERIALS AND METHODS

Intravascular administration of adrenergic and cholinergic agonists in vivo

Adrenergic and cholinergic agonist drugs were injected intravascularly *in vivo* via indwelling catheters in resting fish. An attempt was made to observe any effects on the gill vasculature. Thus the agonists were administered through the ventral aortic catheter and would pass through the gills before reaching the heart or systemic circulation. All drug injections were made in concentrated form, using a 0.1 to 0.25 ml carrier volume of heparanised saline. The final blood concentrations ($g.ml^{-1}$) of the drugs, based on a 5% blood volume, were 1×10^{-7} ACH (O-acetylcholine chloride, B.D.H.); 1×10^{-7} NAD (L-arterenol bitartrate, Sigma); 1×10^{-8} to 10^{-7} ISOP (DL-isoproterenol HCl, Sigma); 1×10^{-8} to 10^{-7} CARB (carbachol, K + K) and 1×10^{-6} to 10^{-5} ATROP (atropine alkaloid, N.B.C.). These concentrations were selected after trials which determined the minimum dosage required to produce an observable response. Higher concentrations often promoted struggling of the fish. ACH and NAD are naturally occuring neuro-transmitters and both are metabolised within several minutes. ISOP and CARB, however, are synthetic agonists which are slowly metabolised in a period of up to 1 hr. Recovery periods were allowed between successive drug injections. The

recovery period was 1 hr following NAD or ACH and 2 to 3 hr or overnight following ISOP or CARB administration. Recovery periods were rigorously adhered to and were prolonged if there was any doubt concerning the fish's recovery. ATROP is known to produce a prolonged muscarine cholinergic blockade in other fish (Randall, 1970). Hence, after ATROP treatment in ling cod, further experiments were considered to be on fish with a cholinergic blockade.

Micropressure measurements in the gill filament vasculature

These measurements were made on isolated perfused holobranchs and *in vivo* on anaesthetised or narcotised, restrained fish.

Isolated perfused holobranch protocol: Five holobranchs were prepared as previously described (See general methods). The whole branchial basket was cleared *in situ* using saline delivered from a Harvard pulsatile infusion pump, but only the first or second holobranchs were used. A pulsatile inflow, (Q_i) of 1.25 $ml.min^{-1}.Kg^{-1}$ was maintained throughout the experiment. The saline was not prefiltered and it was gased with carbogen. Drugs for adrenergic or cholinergic stimulation of the holobranch vasculature were introduced by way of a 3-way tap, which allowed a 30 to 60 sec perfusion with saline containing an agonist. The agonist drug concentrations ($g.ml^{-1}$) of perfusate were 10^{-6} to 10^{-7} NAD and 10^{-7} to 10^{-8} for ISOP and ACH.

Input perfusion pressure (P_i) and output perfusion pressure (P_o) were monitored, which allowed calculation of overall gill resistance (Rg) = $(P_i-P_o)/Q_i$. The outflow (Q_o) from the efferent arch artery cannula was measured periodically under control conditions, but always during drug perfusions.

In vivo procedure: These experiments were performed on 10 ling cod that had been routinely prepared for blood flow and blood pressure measurements (See general methods). The animal was immobilised prior to the experiment with either 2% urethane added to the aquarium or with an intraperitoneal injection of curare (3 $mg.Kg^{-1}$). The immobilised fish was supported in a body holder, with its gills irrigated, and was rotated onto one side. The gill filaments were made accessible for micropuncture by removing part of one operculum. Individual filaments were stabilised for micropuncture by a holding device manoeuvered around them with a micromanipulator. The holding device consisted of a length of PE 260 tubing, which fitted freely around the filament. It had many windows cut out to allow free access for water and for the entry of micropipets.

Micropressure instrument preparation and measurement protocol

The micropressure system, its calibration and the analysis of the measurements are discussed in detail in Appendix II.

The principles of the micropressure system and its operation followed the servonulling techniques of Weiderhielm et al. (1964) and Intaglietta (1973). A micropressure 4 system (I.P.M., San Diego) servonulling device was used in conjunction with bevelled micropipets. Individual micropipets were made from scrupulously cleaned borosilicate glass capillary tubing (0.1 mm O.D. and 0.08 mm ID; Corning, New York) on a vertical pipet puller (model 700 C, David Kopf Instruments, Tujunga, Ca.). The micropipet tip diameters were regularly 2 to 4μ . Micropipets were filled with triple filtered (0.45μ, Millipore) 1M NaCl. The tip was filled overnight by capillarity and the stem of the micropipet was back-filled from a syringe. Any air bubbles in the stem were always removed at this stage by carefully flicking the pipet stem. The tips were remarkably hardy to this procedure and the cleanliness of the inside of the stem was reflected in the ease with which air bubbles were removed. Pipet bevelling greatly facilitated micropuncture, therefore each pipet was sharpened on one or, occasionally, two sides with a BV-10 micropipet beveller (Sutter Instrument Co., Los Angeles). The micropressure system was calibrated against pressures from a static column of water. The frequency response of the system, was always in excess of 10Hz and was tested using the 'pop' test

(McDonald, 1960) in a specially designed chamber issued by the manufacturers (IPM, San Diego) for this purpose. The micropressure system was nulled at the seawater or saline surface in all experiments. The micropipet was manoeuvered with a manual Narashige variable angle micromanipulator and its progress was followed with a Leitz operating microscope.

In vivo micropunctures were made on both afferent and efferent sides of gill filaments located near to the bed in the arch on the first and second gill holobranchs. Micropunctures were made up to 3 hrs after the fish was immobilised, but experiments were terminated when the fish either began voluntary movements (2 to 3 hours) or Q became unstable and declined, as was the case with curarised fish after 1 to 2 hr. Blood pressures and Q were monitored continuously throughout the experiment. In vitro micropunctures were made in the same regions of the isolated gill holobranch and the experiments lasted 2 to 3 hrs.

Analysis

Ventral aortic (VA) and dorsal aortic (DA) pressures are described by their mean and pulse pressures where pulse = systole - diastole and mean = diastole + 1/3 pulse. All pressures are expressed in cm H_2O unless stated otherwise (1 cm H_2O = 0.098 kPascals). Stroke volume (ml) was determined from the area under the pulsatile flow recording. High chart speeds, 5 $mm.sec^{-1}$, were used to improve the accuracy of area measurements. Beat to beat heart rate was determined from the

flow record and is expressed in beats.min^{-1}. Cardiac output (ml.min^{-1}), Q, is the product of stroke volume and heart rate. Q and stroke volume are expressed per kg fish weight (ml.Kg^{-1} and ml.min^{-1}.Kg^{-1} respectively). Gill resistance, Rg, is defined as VA mean - DA mean/Q and systemic resistance, Rs, is defined as DA mean/Q. The resistance units are cm H_2O.min.Kg.ml^{-1}. The Rg, therefore, assumes the major resistance in the lamellar units where all Q passes (Section I). The Rs assumes venous return to the heart is at ambient pressure (see Randall, 1968; Randall, 1970). The cardiovascular data were compiled, initially graphed and statistically analysed using a PDP 11 computer. The grouped data were expressed as mean values ± standard error (s.e.) from n "individual" observations on m fish, unless otherwise stated. An "individual" observation represents single measurement for any given variable. A 95% confidence limit was used as a test of significance with the Student 't' test.

Graphical treatment of data

In all graphs displaying in vivo data the single points are "individual" values wherever possible i.e. there may be an overlap of "individual" values and thus some points may represent more than one "individual" value. The mean resting value of the variable being graphed is indicated by the broken horizontal line. The standard error for the mean resting value is represented by vertical bars, but often the standard error

lies within the actual point. The mean resting value is used as a point of reference, since no statistical inference can be made from this type of graphical treatment. The graphs are presented to illustrate the trends for qualitative changes with time (or oxygen content, Section IV). Quantitative changes are dealt with in the tables, where statistical comparisons are made.

RESULTS

Branchial blood flow and respiration in unanaesthetised resting ling cod

The resting state

Fish were observed in the sea at depths up to 30 m. They rest on the sea floor propped on their large pectoral fins. Each ventilation was perceptable only by slight opercular movements that were separated by several seconds. In the holding aquaria fish adopted a similar resting behaviour, spending long periods stationary on the bottom. In the experimental aquarium buccal cavity movements during ventilation in resting fish were hardly perceptable to the eye. The mouth remained slightly open but was sealed during buccal compression (Fig. 15) by the buccal flap. The period of reduced pressure in the opercular cavity was visually correlated to opercular abduction. The differential pressure gradient across the gills is small, less than 0.4 cm H_2O at its highest and is at ambient pressure during the respiratory pause prior to inhalation (Fig. 15). The ventilation rates ranged from 6 to 16.min^{-1} with a mean value = 11.9 ± 0.4 (n = 60 for 8 fish). Heart rate often fluctuated from beat to beat, but $\dot{Q}$ was unchanged. Heart rates between fish ranged from 22 to 35 beats.min^{-1} which was a greater variation than the beat to beat fluctuations. Ventral aortic blood flow was continuous throughout the cardiac cycle at resting heart rates. The diastolic portion of flow was not steady and

characteristically declined with time (Fig. 16). Thus at lower heart rates, end diastolic flow and pressure were reduced. Fluctuations in VA pressure were often greater than those in DA mean pressure. Between 24% and 30% of VA mean pressure was lost to the gill bed resistance (ΔPg mean/VA mean) and the ventral aortic pressure pulse (VA pulse) was damped by about 60% (ΔPg pulse/VA pulse) (Table VI).

TABLE VI

A/ Measured cardiovascular variables in resting ling cod. Data is derived from resting values prior to all treatments in 8 fish. Values expressed as mean values ± standard error for the 103 observations. VA mean, VA pulse, DA mean and DA pulse are the mean and pulse pressures in the ventral aorta and dorsal aorta expressed in cm H_2O.

B/ Summary of calculations based on the variables measured in Table VIA. $Q = SV \times HR$, ΔPg = VA mean - DA mean, ΔPg pulse = VA pulse - DA pulse. $Rg = \Delta Pg/Q$, Rs = DA

Abbreviations are explained above.

TABLE VI

A/

Heart rate beats.min^{-1}	29.8 ± 0.4
Stroke Volume ml.kg^{-1}	0.37 ± 0.008
VA mean	52.6 ± 0.4
VA pulse	12.4 ± 0.2
DA mean	39.6 ± 0.3
DA pulse	6.0 ± 0.2

B/

Cardiac output, Q. ml.min^{-1}.kg^{-1}	10.91 ± 0.22
Rg	1.24 ± 0.04
Rs	3.86 ± 0.12
ΔPg	13.1 ± 0.4
ΔPg pulse	6.4 ± 0.2

FIGURE 15

Typical records for simultaneous recordings of respiratory and cardiovascular variables. There is a respiratory pause in the opercular (o.p.) and buccal cavities (b.p.) as indicated by the period of ambient pressure (atm.) in both cavities. Buccal and opercular ventilation pressures and dorsal aorta blood pressure (DA) are all measured in cm H_2O above ambient pressure. Pulsatile flow in the ventral aorta (Q, $ml.min^{-1}$) illustrates the continuous diastolic flow. Heart rate (h.r., $beats.min^{-1}$) is shown as an on-line beat to beat record.

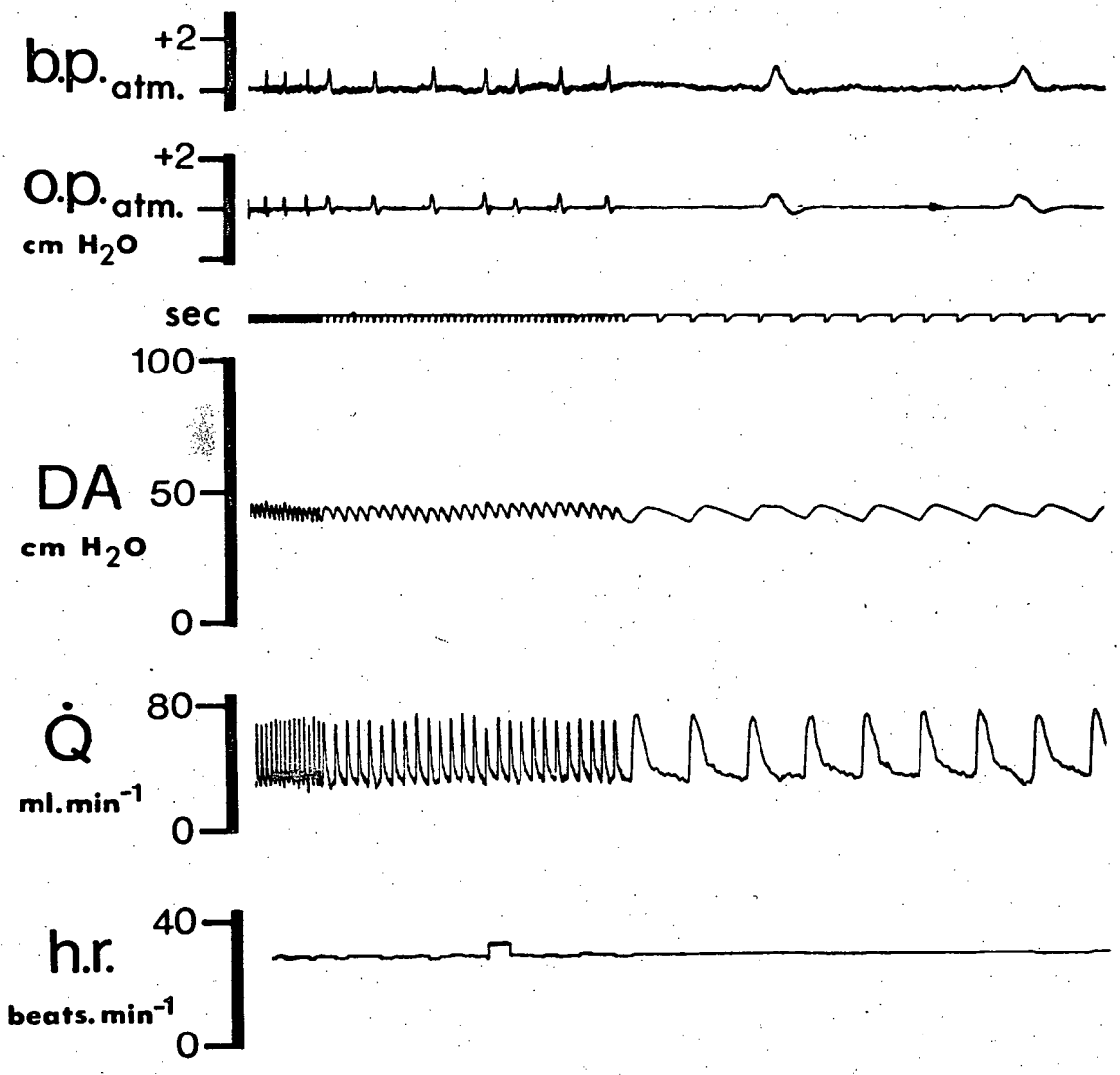
b.p. atm.
+2
o.p. atm.
cm H2O
+2
sec
100
DA
50
cm H2O
0
Q̇
80
ml.min-1
0
h.r.
40
beats.min-1
0

FIGURE 16

A typical record of the cardiovascular variables in a resting ling cod. Note the continuous diastolic flow and the effect of breathing on the flow recording during diastole. Boo! represents a shock (banging). Note the zero flow during diastole. All abbreviations are explained in legend for Fig. 15. VA is ventral aortic pressure.

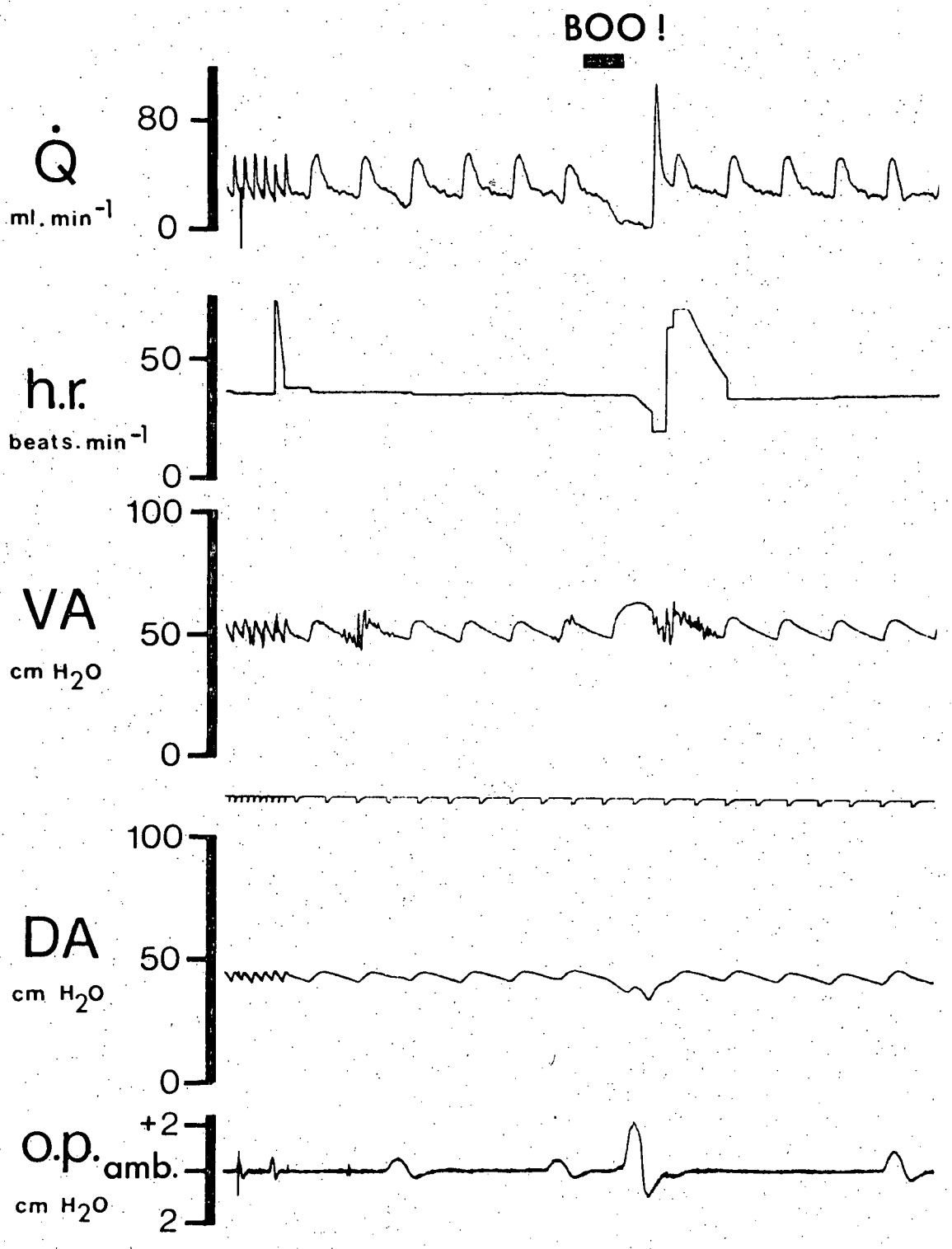
BOO !
Q̇
ml. min⁻¹
80
0
h.r.
beats. min⁻¹
50
0
VA
cm H2O
100
50
0
DA
cm H2O
100
50
0
o.p.amb.
cm H2O
+2
2

Observations on anaesthetised ling cod

There was often a marked change in the intensity of the red coloration to the gill filaments along their length, usually occuring about midway along the filament. The distal filamental regions were lighter in colour than the proximal half of the filament and this difference was more pronounced on the afferent rather than the efferent side of the filament. These colour differences were attributed to different degrees of blood oxygenation, with the lighter regions corresponding to greater oxygenation.

The opercular and filament muscles were not always completely immobilised by anaesthesia. Large opercular movements were abolished, but smaller, rhythmic movements often persisted. The filaments also displayed small, anterio-posterior oscillatory movements, which were enhanced if gill irrigation was stopped. The filaments also had very slight pulsatile movements which were synchronised with the blood pulse. This pulsatility was easily seen when the pressure sensitive micropipet touched the filament, and in fact the pulsatility caused artifacts during some micropressure measurements .

During urethane anaesthesia Q was maintained close to resting levels, even though heart rate was reduced (Table VII, cf Table VI). Rg was elevated but Rs was reduced (Table VII). Both resistance values are associated with a reduced DA pressure.

If gill irrigation flow was reduced or stopped, then the fish would develop an immediate bradycardia. Normal heart rates would return when gill irrigation was restored to the normal flow rates.

TABLE VII

Mean values ± s.e. for the cardiovascular variables recorded from 5 ling cod under deep urethane anaesthesia during the 9 micropressure recordings that were made. Mean blood pressures are presented and Rg = VA mean - DA mean/Q and Rs = DA mean/Q in cm H_2O.min.kg.ml^{-1}.

TABLE VII

Cardiac output, Q. ($ml.min^{-1}.kg^{-1}$)	10.7 ± 0.3
Heart rate ($beats.min^{-1}$)	20.5 ± 1.2
Ventral aortic (VA) pressure (cm. H_2O)	49.2 ± 1.8
Dorsal aortic (DA) pressure (cm. H_2O)	22.8 ± 0.7
Gill resistance, Rg	2.48 ± 0.09
Systemic resistance, Rs	2.14 ± 0.04

Gill filament micropressure measurements

In vivo ling cod: Nine recordings of pulsatile micropressures were made in 5 anaesthetised ling cod at various locations along the afferent and efferent sides of the filament length. Two recordings, one afferent and one efferent, were less than the DA pressure (Fig. 17). For the remaining measurements, the micropressures associated with the afferent side recordings were all greater than those on the efferent side. The afferent side records were 70 to 95% of the VA pressure, but the two efferent records were only slightly above the DA pressure. These two groups clearly represent blood pressures in the afferent and efferent respiratory network.

Six other micropressure measurements were made on curarised fish, but were not included in the analysis because either Q was much reduced, or the DA catheter was no longer patent. On one occasion a curarised fish displayed an interesting response when the filament was touched by the advancing micropipet. Both VA and DA pressures would immediately rise by 2 to 3 cm H_2O for about a 1 minute period, presumably representing a touch reflex.

Isolated perfused holobranchs: In vitro the micropipets were less prone to blockage and movement compared to in vivo because the preparation was more easily manipulated and more stable. As a result better quality recordings were obtained (Fig. 17),

there was a higher ratio of successful micropunctures and micropressures could be recorded for up to several minutes, unlike *in vivo* where the recording time was several seconds.

The 22 micropressure records that were made *in vitro* are summarised in Fig. 17. Three categories of pressure, similar to the *in vivo* recordings, are evident. By comparison, however, the efferent micropressures and output pressures are reduced due to the high overall gill resistance of the preparation (Rg = 6.16 ± 0.33, n = 20). The afferent micropressures were also comparatively reduced and clearly reflect an elevated resistance to flow in vessels afferent to the gill lamellae.

ACH perfusion for 30 to 60 sec caused Rg to rise in 90% of the 24 trials, with an accompanying rise in P_i. Q_o was reduced and sometimes ceased during the peak ACH response. Micropressure recordings after ACH administration were usually invalidated by filament movements associated with the rising Rg that dislodged the micropipet. In two instances, however, the efferent micropressure rose after ACH perfusion (Fig. 16b and Fig. 18). On 5 other occasions the efferent micropressure was also rising before the pipet became dislodged.

No successful continuous micropressure recordings were made during adrenergic infusion. Filament movements again accompanied gill resistance changes. Rg decreased with adrenergic stimulation, n = 5 for NAD and n = 6 for ISOP, or did not change, n = 2 for ISOP. NAD perfusion caused a marked fall in P_i and rise in P_o. The pressure changes accompanying ISOP treatment were similar, but very small.

FIGURE 17

A summary of the micropressure measurements made in the afferent and efferent sides of the gill filament in anaesthetised ling cod (IN VIVO) and in isolated perfused holobranchs from ling cod (IN VITRO). Each micropressure point represents an average value for a single micropuncture. a) In vivo micropressures are expressed as a percentage of the ventral aortic mean blood pressure (va) that was measured at the same time. The average value for all dorsal aortic mean blood pressures (da) is similarly expressed with the standard error indicated by the vertical bars (n = 9 for 5 fish). b) In vitro micropressures are expressed as percentages of the input mean pressure. The vertical bars indicate the standard error of the average value for all output mean pressures (n = 22). The ranges of micropressures which are greater than da or output pressure is enclosed by solid lines. Pulsatile micropressures that were below this range are indicated by ∇. The micropressure recorded after ACH administration is indicated by o.

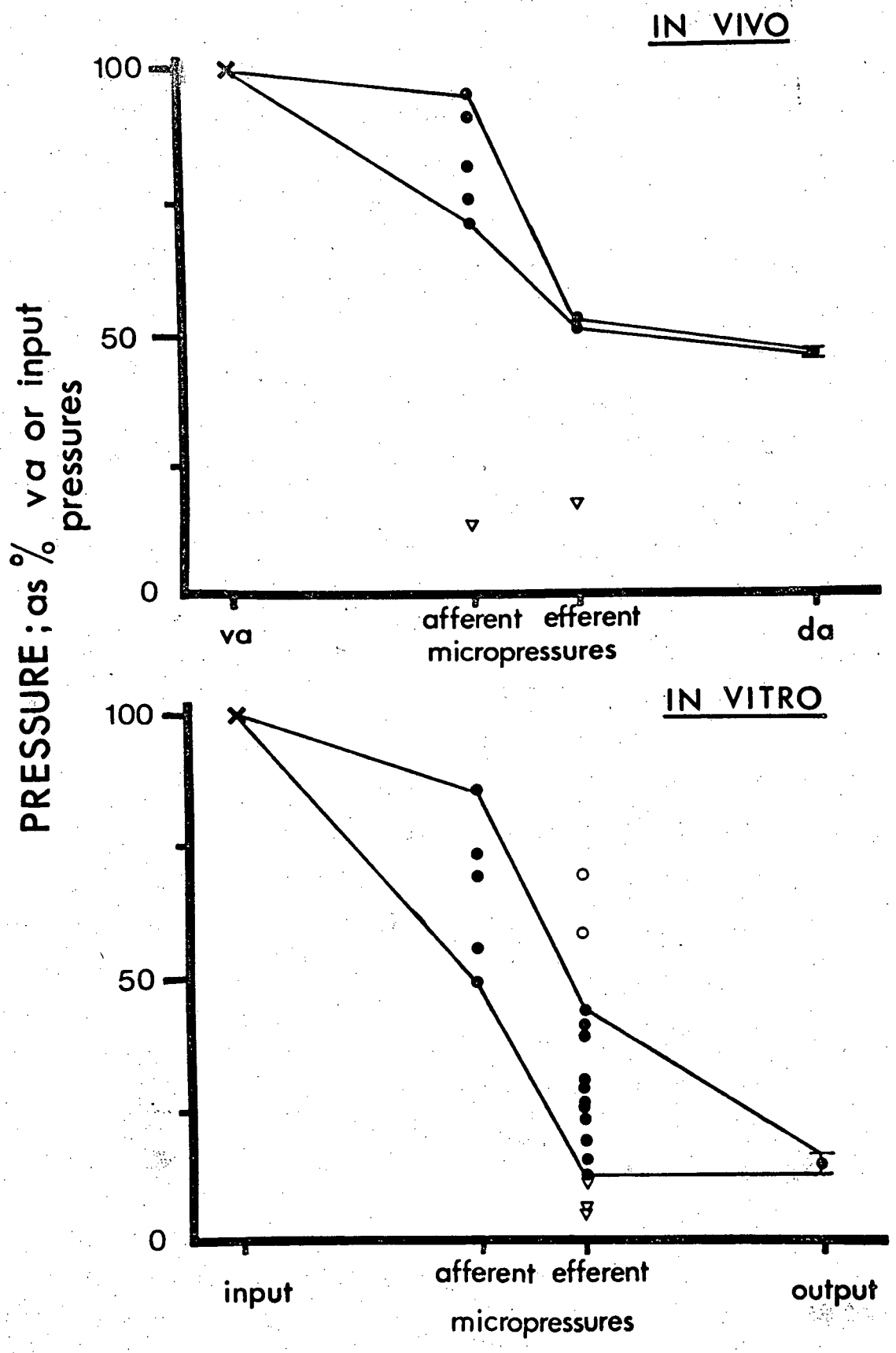
IN VIVO
100
50
0
PRESSURE; as % va or input pressures
va
afferent efferent micropressures
da
IN VITRO
100
50
0
input
afferent efferent micropressures
output

FIGURE 18

Examples of typical micropressure recordings. a) an *in vivo* record of pulsatile pressure from the afferent venolymphatics with accompanying ventral and dorsal aortic blood pressures, cm H_2O, and cardiac output, Q, $ml.min^{-1}$. Note the filament movement artifacts in the micropressure record after the 4th pulse. b) an *in vitro* record of an afferent filament micropressure with input and output perfusion pressures. c) an *in vitro* record of efferent micropressure and the effect of ACH perfusion (1×10^{-7} $g.ml^{-1}$ for 30 sec). The decline in P_o was accompanied by a near zero outflow. All pressures are in cm H_2O.

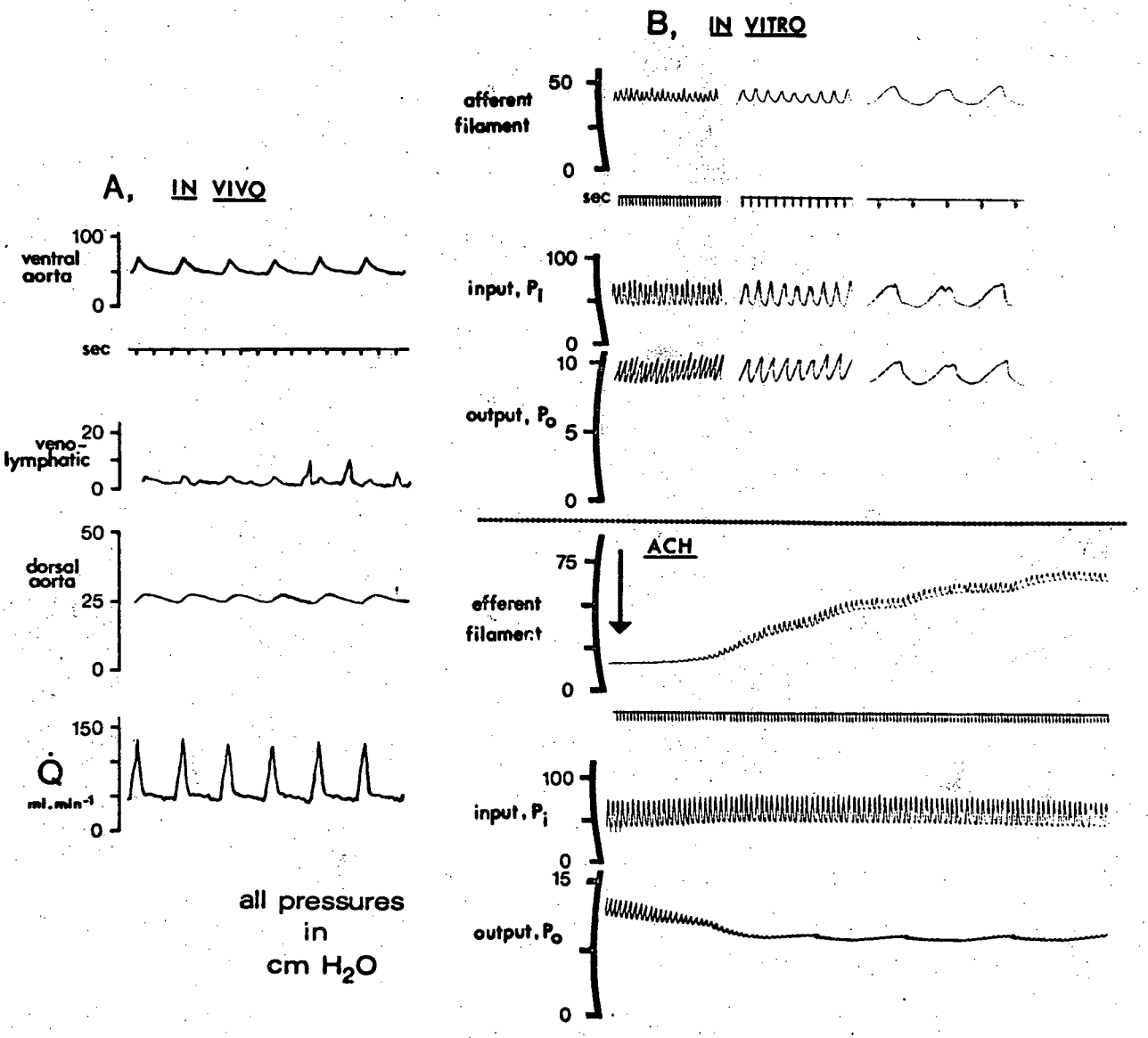
A, IN VIVO
100
ventral aorta
0
sec
20
veno-lymphatic
0
50
dorsal aorta
25
0
150
Q̇
ml.min⁻¹
0
all pressures in cm H2O
B, IN VITRO
50
afferent filament
0
sec
100
input, Pi
0
10
output, Po
5
0
ACH
75
efferent filament
0
100
input, Pi
0
15
output, Po
0

The effect of intravascular injection of adrenergic agonists in resting ling cod

NORADRENALINE (NAD): The response to NAD administration into the ventral aorta was rapid and began after 20 to 30 sec of the injection. The response was reproducible with blood pressures and blood flow increasing simultaneously (Fig. 19). At the peak pressor response to NAD, the mean $\dot{Q}$ was elevated 42% above the resting value. The pattern of VA blood flow during the cardiac cycle was also changed since both systolic and diastolic flows increased. Specifically, peak systolic flow was greater and diastolic flow rate remained almost constant, unlike its normal decline with time during rest (Fig. 19). These changes resulted in the mean stroke volume increasing by 34%

After NAD injection Rg decreased by 30% of the mean resting value (Table VIII, Fig. 20). In individual fish Rs either did not change or increased as a result of the injection. Overall, there was no significant change in mean Rs values (Table VII). There was an increase in mean blood pressures but the pressure drop across the gills did not change. VA and DA pulse pressures also increased. However, there was a much greater damping of the pressure pulse by the gills, Δ Pg pulse, indicating an increase in the total gill compliance (Table VIII).

Ventilation characteristically changed after a NAD injection. There was a noticeable pause in ventilation which coincided with the rise in $\dot{Q}$ and VA mean pressure (Fig. 19).

FIGURE 19

The effect of a noradrenaline injection (NAD) into the ventral aorta of a ling cod on cardiovascular and respiratory variables that were monitored simultaneously. Cardiac output (Q), $ml.min^{-1}$, increases due to systolic and diastolic flow changes. (Compare expanded traces 1, resting, and 2, peak response). In this fish there was also an increased heart rate. Note also the synchronous rise in VA and DA pressures (cm H_2O). From the pressure measurements in the opercular cavity (op) (cm H_2O) the brief respiratory pause at the onset of the pressor response can be seen.

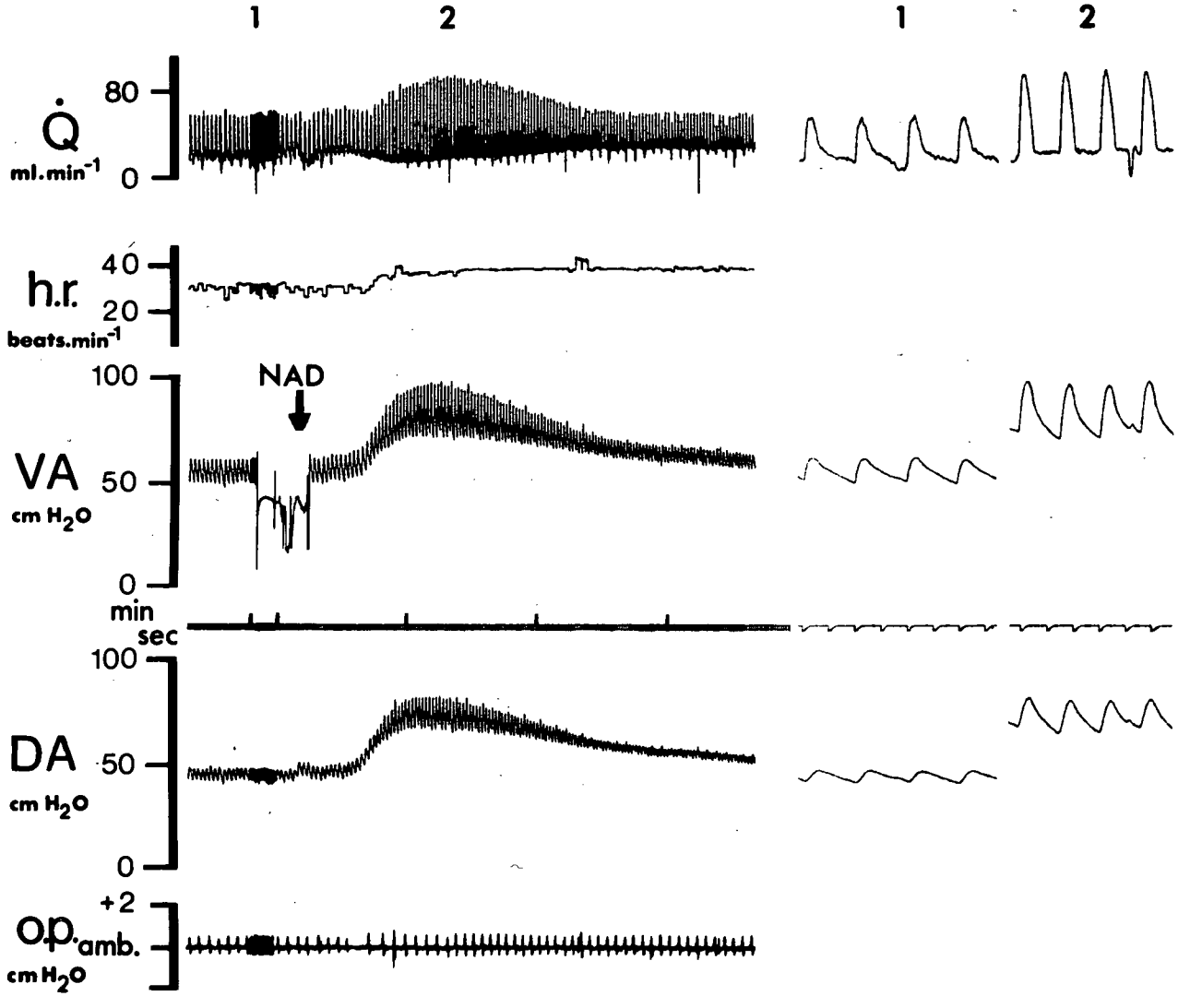
1
2
1
2
80
0
Q̇
ml.min⁻¹
40
20
h.r.
beats.min⁻¹
NAD
100
50
0
VA
cm H2O
min
sec
100
50
0
DA
cm H2O
+2
op.amb.
cm H2O

TABLE VIII

A/ The effect of a noradrenaline (NAD) injection into the ventral aorta in 8 ling cod (12 observations) on measured cardiovascular variables. The rest and peak response values are compared statistically, * significant difference. The abbreviations are explained in Table VI.

B/ The affect of a noradrenaline injection into the ventral aorta on cardiovascular variables calculated from those measured in Table VII A above.

TABLE VIII

A/

	Rest (n=22)	Peak (n=12)
Heart Rate beats.min^{-1}	30.6 ± 1.0	32.9 ± 2.2
Stroke Volume ml.kg^{-1}	0.356 ± 0.014	0.477 ± 0.039*
VA mean	52.6 ± 0.8	74.7 ± 2.6*
VA pulse	12.2 ± 0.5	24.3 ± 1.8*
DA mean	39.4 ± 0.8	60.9 ± 2.0*
DA pulse	6.1 ± 0.4	12.5 ± 1.2*

B/

	Rest	Peak
Cardiac output, Q ml.min^{-1}.kg^{-1}	10.7 ± 0.4	15.2 ± 1.1*
Rg	1.26 ± 0.07	0.88 ± 0.06*
Rs	3.81 ± 0.22	4.35 ± 0.37
ΔPg	13.3 ± 0.7	13.8 ± 1.4
ΔPg pulse	5.0 ± 0.4	11.8 ± 1.0*

FIGURE 20

A summary of the analysis of the effect of noradrenaline injection (NAD) into the ventral aorta in 8 fish upon cardiac output, Q, stroke volume, S.V. and gill resistance, Rg. Time (sec) is measured from the completion of the injection.

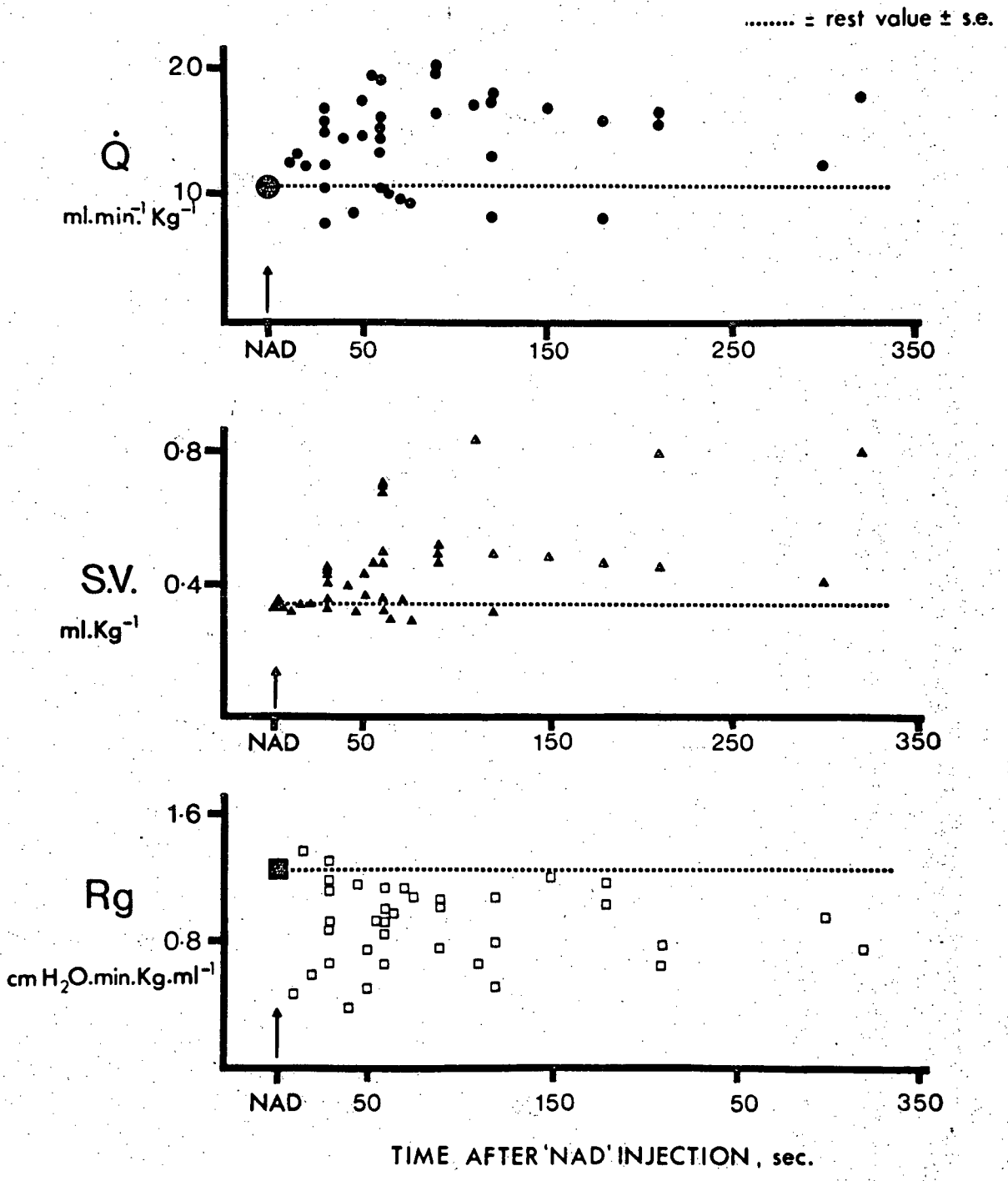
..... = rest value ± s.e.
Q̇
ml.min⁻¹ Kg⁻¹
20
10
NAD
50
150
250
350
S.V.
ml.Kg⁻¹
0·8
0·4
NAD
50
150
250
350
Rg
cm H₂O.min.Kg.ml⁻¹
1·6
0·8
NAD
50
150
50
350
TIME AFTER 'NAD' INJECTION, sec.

ISOPRENALINE (ISOP): ISOP injected into the ventral aorta produced, in general, small initial changes during the first 100 sec. The Q was elevated slightly due to an increased stroke volume (Fig. 21, Table IX). Both Rg and Rs were reduced significantly during the initial 100 sec (Table IX). During the 100 sec after ISOP injection the pressure drop across the gills (Δ Pg mean) was not altered, but there was an increased damping of the pressure pulse, ΔPg pulse (Table IX).

The biphasic response to ISOP injections was characterised by a significant elevation of heart rate after $t = 100$ sec (Table IX, Figs. 21 and 22) and Q returning to a rest value. Rg and Rs were both at values in between those of rest and their reduced values when $t < 100$ sec.

FIGURE 21

A summary of the analysis of the effect of isoprenaline (ISOP) injection into the ventral aorta of 8 fish upon cardiac output (Q), heart rate (hr), stroke volume (sv) and gill resistance (Rg). Time (sec) is measured from the completion of the injection.

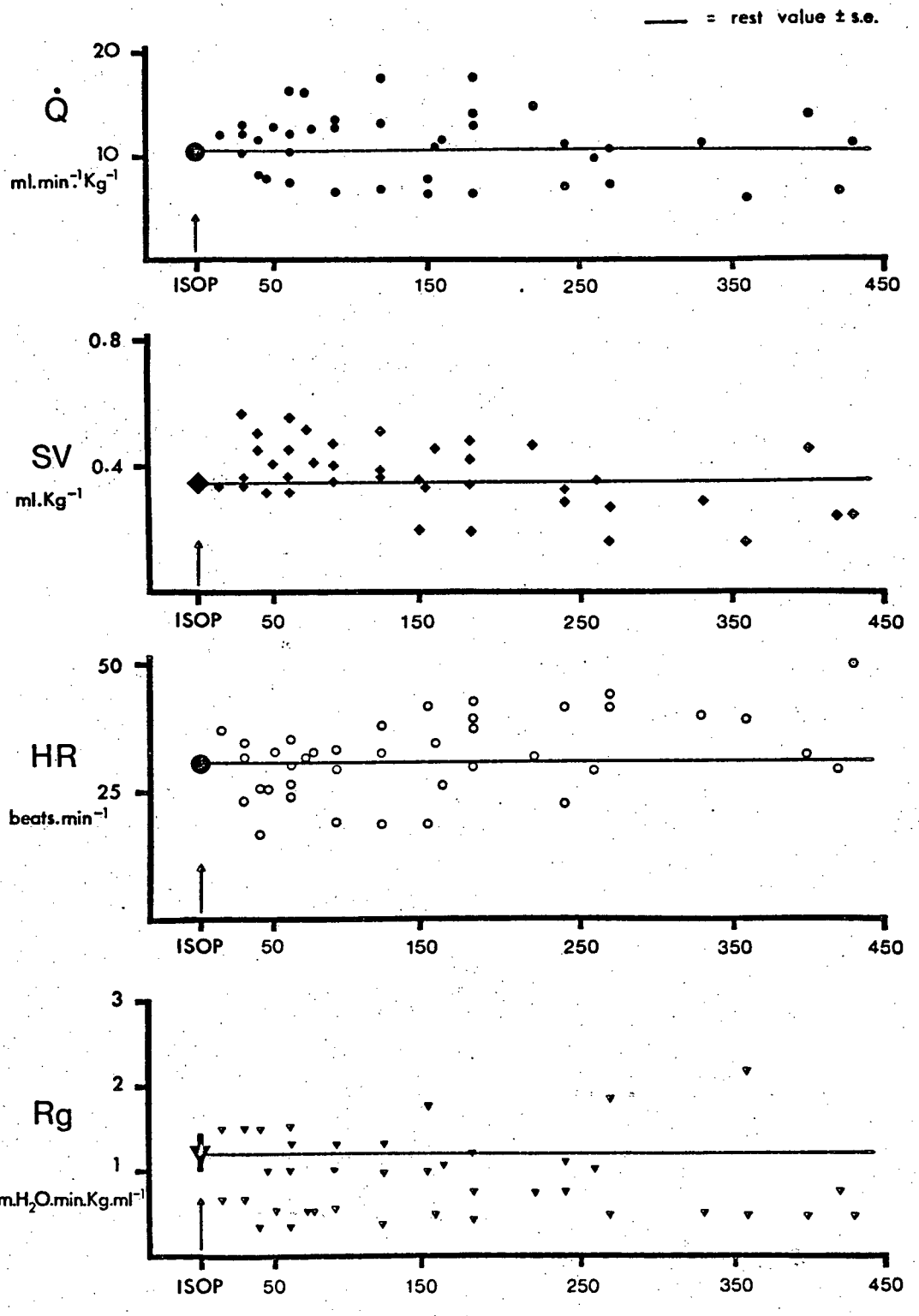
—— = rest value ± s.e.
Q̇
ml.min⁻¹Kg⁻¹
20
10
SV
ml.Kg⁻¹
0.8
0.4
HR
beats.min⁻¹
50
25
Rg
cm.H₂O.min.Kg.ml⁻¹
3
2
1
ISOP
50
150
250
350
450
TIME AFTER 'ISOP' INJECTION, sec.

TABLE IX

A/ The effect of an isoprenaline (ISOP) injection into the ventral aorta in 8 ling cod (10 observations) on measured cardiovascular variables. The rest values are compared with all values when t <100 sec and t> 100 sec after injection. * denotes statistical difference. The abbreviations are explained in Table VI.

B/ The effect of a isoprenaline injection into the ventral aorta on cardiovascular variables calculated from those measured in Table IX A above.

TABLE IX

A/

	Rest(n=18)	t<100sec(n=17)	t>100sec(n=22)
Heart Rate beats.min^{-1}	30.2 ± 0.9	29.7 ± 0.8	34.9 ± 1.9*
Stroke Volume ml.kg^{-1}	0.352 ± 0.023	0.401 ± 0.022*	0.313 ± 0.023
VA mean	50.8 ± 0.7	47.5 ± 1.1*	44.1 ± 0.8*
VA pulse	13.1 ± 0.4	14.7 ± 0.9*	11.7 ± 0.8*
DA mean	39.4 ± 0.9	36.3 ± 1.2*	34.4 ± 0.8*
DA pulse	6.2 ± 0.3	6.6 ± 0.5	5.3 ± 0.5*

B/

	Rest	t<100sec	t>100sec
Cardiac output, Q ml.min^{-1}.kg^{-1}	10.5 ± 0.6	11.8 ± 0.7*	10.6 ± 0.8
Rg	1.19 ± 0.13	0.92 ± 1.10*	1.00 ± 0.12
Rs	4.13 ± 0.38	3.34 ± 0.30*	3.63 ± 0.32
ΔPg	11.5 ± 0.8	11.1 ± 1.2	9.7 ± 0.9*
ΔPg pulse	6.9 ± 0.4	8.1 ± 0.6*	6.4 ± 0.6

FIGURE 22

The effect of an isoprenaline (ISOP) injection into the ventral aorta of a ling cod on cardiovascular and respiratory variables which were monitored simultaneously. Note the biphasic response of cardiac output (Q, $ml.min^{-1}$) and heart rate (h.r., $beats.min^{-1}$) during periods '2' and '3' as compared to rest, period '1'. Expanded traces of period '1', '2' and '3' are also shown. In period '2' heart rate characteristically decreases and stroke volume increases, whilst in period '3' heart rate increases and stroke volume is decreased. During these responses DA and VA mean pressures ($cm\ H_2O$) were reduced, but pulse pressures are elevated during period '2'. Ventilation is indicated by opercular pressures ($cm\ H_2O$) and does not change.

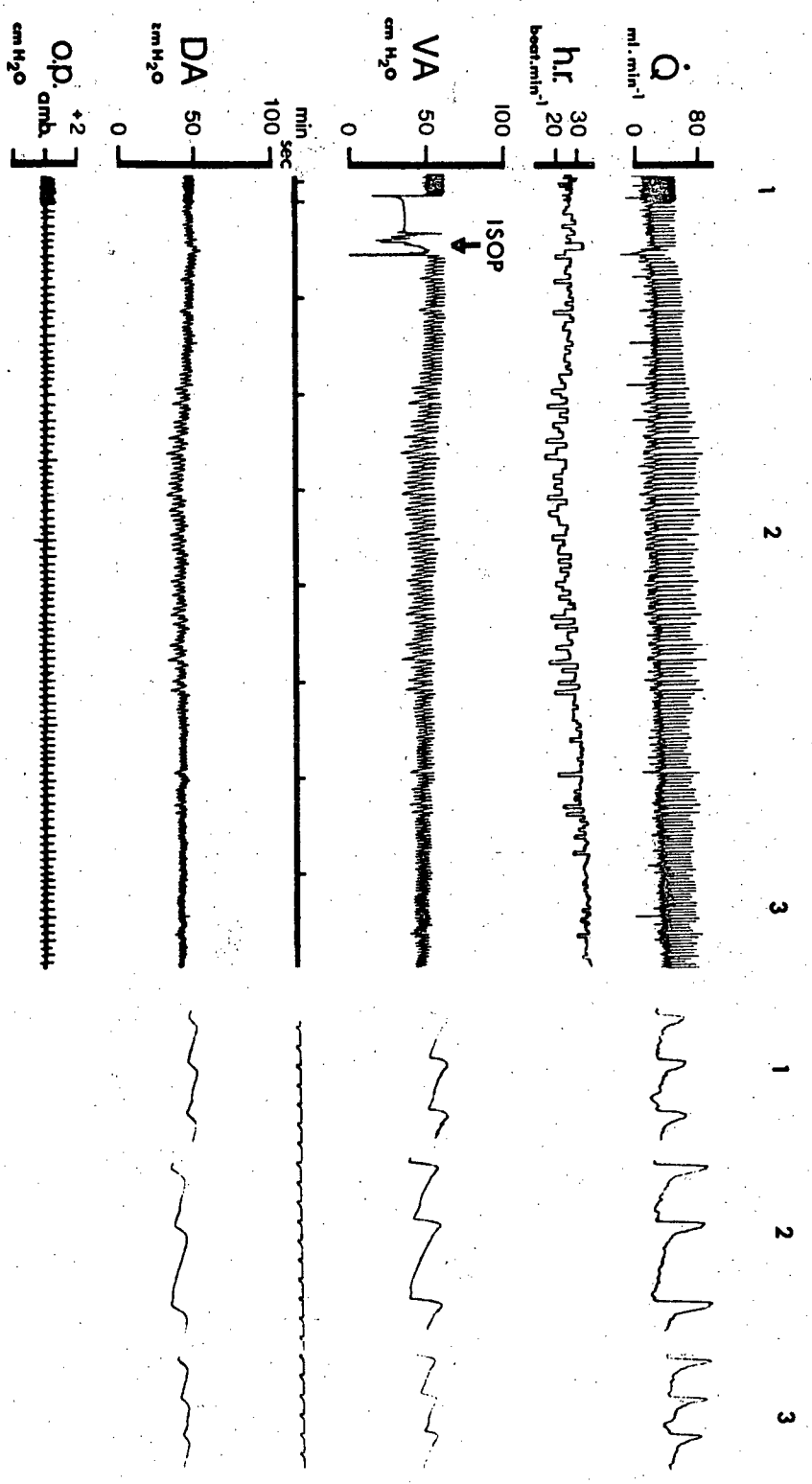
Q̇
ml.min⁻¹
80
0
h.r.
beat.min⁻¹
30
20
VA
cm H₂O
100
50
0
ISOP
min
sec
100
DA
cm H₂O
50
0
o.p.
cm H₂O
+2
amb.
1
2
3
1
2
3

The effect of intravascular administration of cholinergic agents in resting ling cod

ACH injection into the ventral aorta produced a peak response within 50 to 60 sec of injection (Figs. 23 and 24). The extent of the response to ACH injection varied from fish to fish. The Q and stroke volume both increased significantly, but the mean heart rate did not change (Table X). The peak systolic flow was elevated and the diastolic flow did not decline with time. Therefore the shape of the ventral aortic flow pulse was changed to a pattern resembling that seen during the peak response to a NAD injection. There was marked increase in Rg, but Rs did not change (Table X). During the peak response VA and DA pulse pressures were elevated, and ΔPg pulse was also increased. Ventilation rates were increased after an ACH injection.

Carbachol (CARB) injections produced peak responses in blood flow and pressure similar to the ACH responses. However, CARB, which remains longer in the circulation, reduced heart rate dramatically, to 12 to 15 beats.min^{-1} after about 90 to 120 sec. The Q was also reduced below resting values at this time.

One hour after an atropine (ATROP) injection heart rate had gradually risen to a steady state value of about 45 beats. min^{-1} (n=3 fish). There were no beat to beat heart rate fluctuations and this peak heart rate was sustained for at least 2 hrs. (This was the final experiment before sacrificing the fish). The Q was not changed by ATROP injection. Ninety minutes after the ATROP injection a CARB injection into the dorsal aorta

had no effect on heart rate, Q or Rg, unlike the unatropinised fish. The Rs however decreased by 15% about 30 sec after the injection with corresponding reductions in VA and DA mean pressures (Fig. 25). Ventilation rate was increased slightly above the pre-CARB injection rate.

FIGURE 23

The affect of an acetylcholine injection (ACH) into the ventral aorta of 2 different ling cod (a) and (b). Note the variability in the peak pressor response between fish. In (a) the cardiac output ($\dot{Q}$), $ml.min^{-1}$, changes are small with heart rate (hr), $beats.min^{-1}$, increasing slightly, if anything. DA mean pressure, cm H_2O, was depressed and the opercular pressure (op) record indicates that ventilation rate increased. In (b) only cardiac output and VA and DA pressure are shown, with areas '1' and '2' displayed with an expanded time scale. The pressor response of ACH is evident with DA pressures also increasing slightly. $\dot{Q}$ increased markedly through increased stroke volume, with blood flow being elevated during both the systolic and diastolic periods.

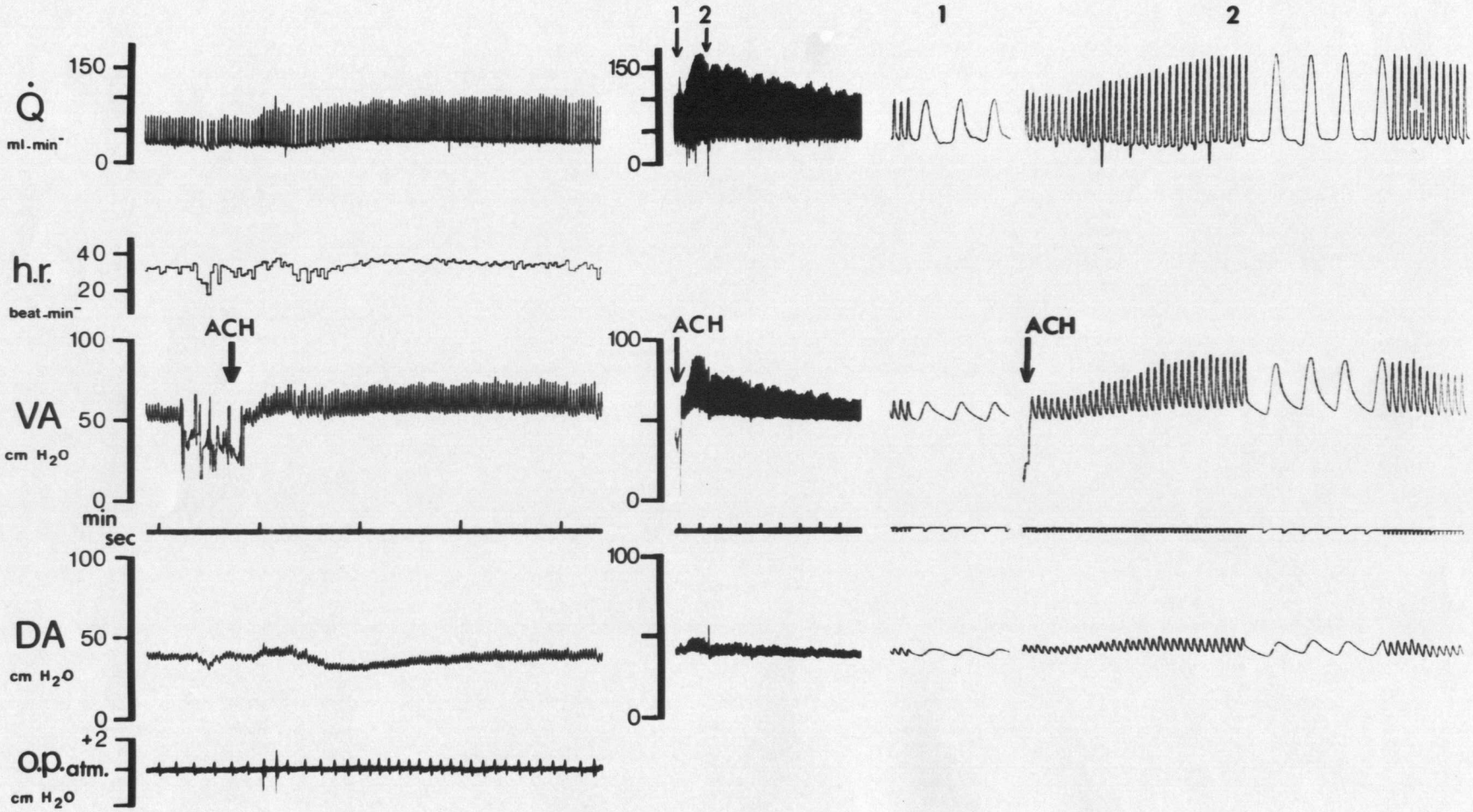
Q̇
ml.min⁻
150
0
1
2
1
2
h.r.
beat.min⁻
40
20
ACH
ACH
ACH
VA
cm H2O
100
50
0
min
sec
DA
cm H2O
100
50
0
100
0
o.p.
cm H2O
+2
atm.

TABLE X

A/ The effect of an acetylcholine (ACH) injection into the ventral aorta in 8 ling cod (11 observations) on measured cardiovascular variables. The rest and peak response values are compared statistically, * significant difference. The abbreviations are explained in Table VI.

B/ The effect of an acetylcholine injection into the ventral aorta on cardiovascular variables calculated from those measured in Table X A above.

TABLE X

A/

	Rest(n=30)	Peak(n=11)
Heart Rate beats.min^{-1}	29.1 ± 0.7	29.1 ± 1.2
Stroke Volume ml.kg^{-1}	0.400 ± 0.016	0.440 ± 0.020*
VA mean	52.7 ± 0.6	63.7 ± 2.0*
VA pulse	12.4 ± 0.4	22.4 ± 2.3*
DA mean	39.7 ± 0.6	42.3 ± 1.4*
DA pulse	6.0 ± 0.3	7.9 ± 0.6

B/

	Rest	Peak
Cardiac output, Q ml.min^{-1}.kg^{-1}	11.5 ± 0.1	12.7 ± 0.6*
Rg	1.16 ± 0.08	1.71 ± 0.19*
Rs	3.60 ± 0.16	3.25 ± 0.23
Δ Pg	13.2 ± 0.9	22.2 ± 2.2*
Δ Pg pulse	6.4 ± 0.3	14.5 ± 2.1*

FIGURE 24

A summary of the analysis of the effect of acetylcholine (ACH) injection into the ventral aorta of 8 ling cod upon cardiac output (Q), gill resistance (Rg) and the drop in mean pressure over the gills (ΔPg). Time (sec) is measured from the time of completion of the injection.

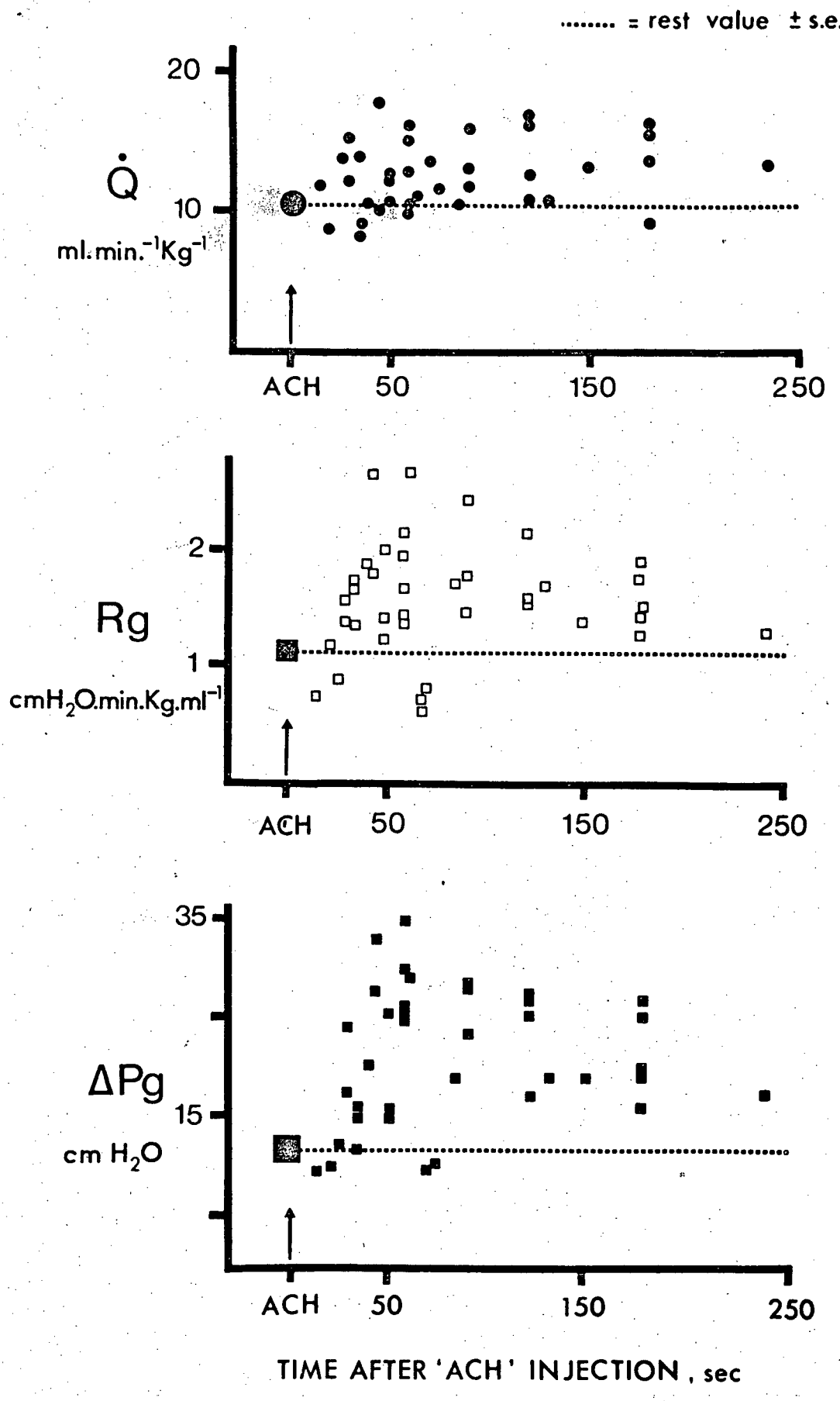
..... = rest value ± s.e.
20
10
$\dot{Q}$
ml.min.$^{-1}$Kg^{-1}
ACH
50
150
250
2
1
Rg
cmH$_2$O.min.Kg.ml^{-1}
ACH
50
150
250
35
15
ΔPg
cm H$_2$O
ACH
50
150
250
TIME AFTER 'ACH' INJECTION , sec

FIGURE 25

The effect of a carbachol injection (CARB) into the dorsal aorta of a previously atropinised ling cod. Heart rate (hr, beats.min^{-1}) and cardiac output (Q, ml.min^{-1}) do not change, but ventral (VA) and dorsal (DA) aortic pressures are reduced. Ventilation rate increases, as indicated by the buccal pressure (b.p., cm H_2O) record. The expanded trace is a demonstration of the zero flow calibration using a pneumatic cuff. The cuff was inflated over the time period indicated by the thick horizontal bar on the Q record.

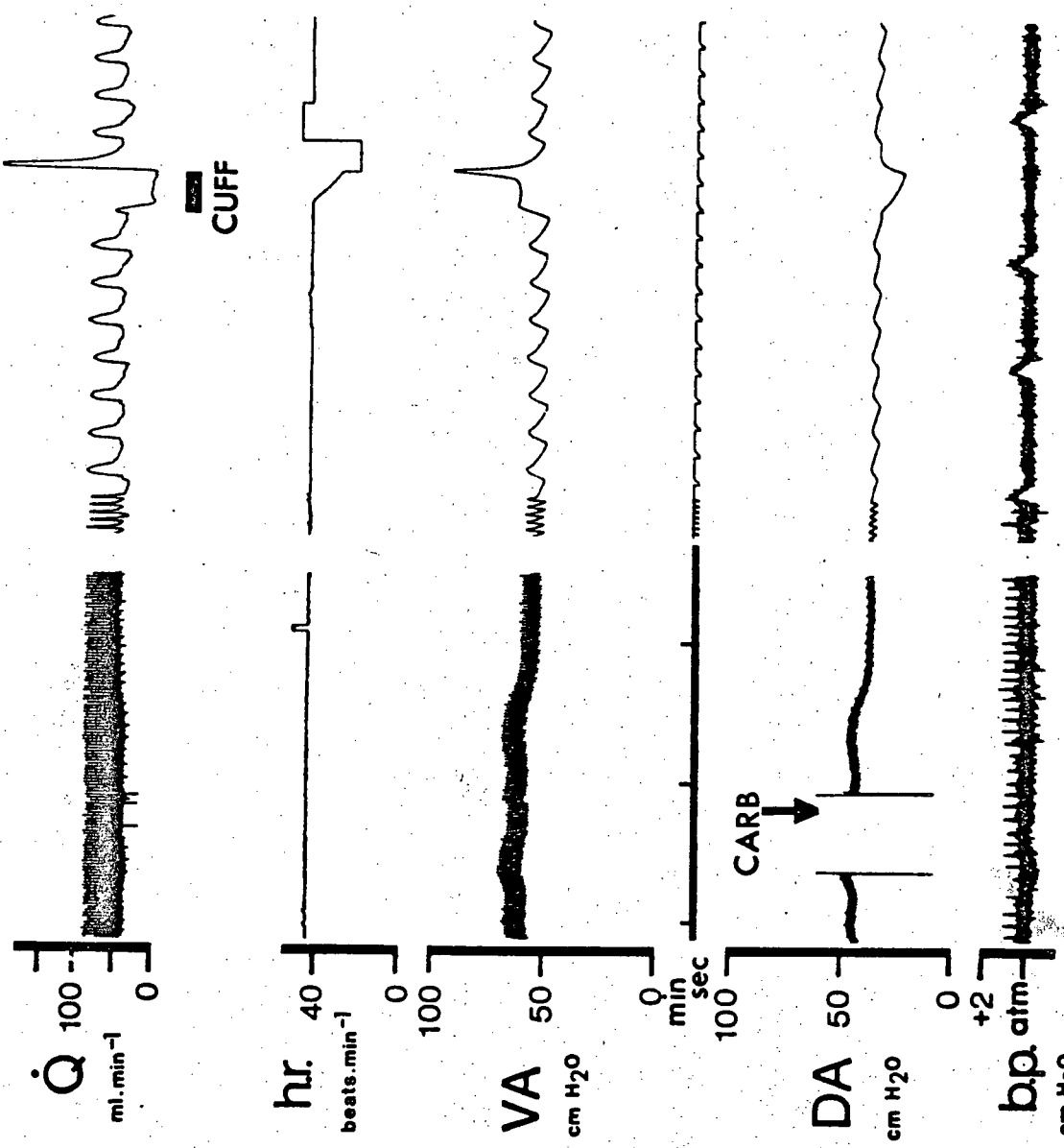
ATROPINISED
CUFF
CARB
Q̇
ml.min⁻¹
100
0
hr.
beats.min⁻¹
40
0
VA
cm H₂O
100
50
0
min
sec
DA
cm H₂O
100
50
0
bp.
atm
cm H₂O
+2

DISCUSSION

The resting ling cod

A detailed *in vivo* examimation of cardiovascular variables pertaining to branchial blood flow was made with *Ophiodon elongatus* using simultaneous measurements of pre- and post-branchial blood pressures, and Q. The findings of the present study are generally consistent with other *in vivo* studies in teleosts (Stevens *et al.*, 1972: Jones *et al.*, 1974; Chan and Chow, 1976). Ventral aortic flow and, therefore, gill blood flow are continuous even during diastole due to the Wind-kessel effect of the large bulbus arteriosus. Blood pressures and Q have similar values to those measured (or calculated) for other teleosts. A Q value of 5.9 $ml.min^{-1}.Kg^{-1}$ was reported by Stevens *et al.* (1972) for smaller specimens of *Ophiodon* (1 to 4 kg). They also reported a heart rate of 47 $beats.min^{-1}$ and a ventilation rate of 26.8 $breaths.min^{-1}$. Such high rates and low Q values were only found in disturbed or traumatised fish in my study. A slightly higher water temperature (13°C) was used by Stevens *et al.*, which may explain, in part, the high cardiac and respiratory rates. Q in resting *Gadus morhua* is 52 $ml.min^{-1}$ (5 fish weighing 2 to 3 kg) (Jones *et al.*, 1974). Although no mean weight was given for *Gadus*, it is apparent that Q is greater in *Gadus* than in *Ophiodon*. The interspecific difference in Q is expected since free swimming fish will have higher Q than bottom dwelling fish. Trout for instance, have

a similar resting Q to Gadus of about 20 $ml.min^{-1}.kg^{-1}$ (as calculated by the Fick principle, Stevens and Randall, 1967b).

In the resting ling cod the heart rate varies from beat to to beat, but Q changes little since there are compensatory changes in stroke volume. These observations can be explained in terms of Starling's Law of the heart. According to Starling's law, stroke volume can be altered intrinsically and is related to the degree of stretching of atrial muscle fibers when the chamber is filled. Greater atrial filling will produce higher stroke volumes and greater atrial filling can be achieved by a reduced heart rate, elevated venous pressures, or both. The general applicability and the importance of Starling's law of the heart in resting teleosts has been discussed by Randall (1970). Recently, Short and co-workers (1977) made an extensive study of cardiac activity in dogfish and established the importance of Starling's law in these elasmobranchs.

The ΔPg mean represents only a 25% to 30% loss of VA pressure, which suggests that the gills have an unusually low resistance to flow for a capillary network compared to mammalian microcirculations. The reason for this may be due to lamellar sheet flow since h is high, almost double that found for cat pulmonary microcirculation (See Section I). The pressure pulse, is, however, damped by 60%, which is not at all surprising given the compliant nature of the microvascular bed (Sections I and III). The importance of systemic compliance on damping of the DA

pulse pressure (Jones et al., 1974) was not examined here.

Ventilation in ling cod did not appear to differ in any major respect from previous descriptions of teleost ventilation patterns (Ballintijn and Hughes, 1963; Shelton, 1970), although it was not examined thoroughly in this study. Ophiodon have buccal and opercular ventilation pumps. The buccal pumping and the opercular suction phases generated the greatest hydrostatic pressure changes, but resting ventilatory pressures never exceeded 1 cm H_2O. Ventilation rates could be as low as 6 to 7 breaths.min^{-1} in some fish that had been left undisturbed for many hours. The mean ventilation rate (12 breaths.min^{-1}) is low compared with the trout, for instance, where the rate is commonly 60 breath.min^{-1}. The quiet ventilatory pattern of Ophiodon correlates well with its benthic habitat (Shelton, 1972).

Micropressure measurements and gill resistance

This study applied the micropressure techniques to both respiratory vessels and the fish microcirculation for the first time. Its application was clearly restricted by movement artifacts and the inability to see the pipet inside the vessels. In vivo the sensitivity of the gill to irrigation, the instability of the gill filaments within the water current and the incomplete response of the gill filament and opercular muscles to anaesthesia were unresolveable problems. Consequently many of the micropuncture recordings were not used because of

uncertainty concerning their validity (Appendix II). The *in vitro* preparation was technically more suitable, but possessed slightly different perfusion characteristics compared to *in vivo*. The filament movements associated with Rg changes following drug infusion were unfortunate, and the gill lamellae were far too flexible for micropuncture measurements. Despite the above limitations the high fidelity of some *in vitro* micropressure recordings (Fig. 18b) was indeed encouraging.

A general pattern for the pressure distribution within the filament vasculature was established both *in vivo* and *in vitro*. This pattern shows that the major resistance to flow resides within the lamellar unit and that the combined resistance of the afferent branchial arteries is small. These conclusions help substantiate predictions made in Section I.

The absolute pressure loss in the branchial arteries and in the lamellar unit cannot be established with certainty since the micropressure measurements may not have been made from only the filament arteries, i.e. some measurements could have been made in lamellar arterioles. Nevertheless a good idea of the possible range of resistances can be deduced from figure 17. In the anaesthetised fish VA blood pressure was reduced by 56% due to the total gill resistance. As little as 10% of Rg was due to the resistance of the afferent branchial arteries, which agrees with that reported in Section I where AFA resistance was calculated as 16% of Rg. The lamellar unit, on average, accounted for over half, (58%) of Rg (a value derived by comparing the

average of all afferent and all efferent micropressures). Similar conclusions to these can be made *in vitro*. In this case the lamellar unit was on average 44% of Rg (a maximum value of 73%). It is also clear that afferent and efferent artery resistances were increased in isolated holobranch preparations, which probably accounts for the overall reduction in the lamellar component to overall Rg. The afferent arteriole is clearly the major resistance in the lamellar unit and the hypothesis that the major site of gill resistance is the afferent lamellar arterioles has now received some experimental support.

In *Ophiodon* it appears that the proximal filament is more greatly perfused than distal filament under certain *in vivo* conditions, assuming that the light coloration of distal lamellae in anaesthetised fish was due to slower flowing, fully oxygenated blood (See Section III also). A similar, tentative conclusion was also made by Davis (1972) who made visual observations and took infra red films of trout gills. Blood flow control at the ALA explains the difference between proximal and distal lamellar perfusion since distal ALAs have a higher resistance to flow due to their geometry (Section I). Davis (1972) also concluded that an adrenalin injection increased the perfusion of the filament tip as well as the filament as a whole. Increased perfusion of the tip region would involve lamellar recruitment. However, the mode by which ALAs would control lamellar recruitment is still speculative since lamellar recruitment could occur automatically with increased blood pressure, blood flow or both. In addition

there may be autonomic control of ALA size, since in trout the vessels have adrenergic innervation. Randall (1976) postulated β- adrenergic dilation of distal ALAs to increase lamellar perfusion. In actuality a combination of these two controls is expected.

Drug injection studies

The response to any drug injection *in vivo* is complex and its interpretation is, therefore, difficult and to some degree speculative. Drugs injected into the ventral aorta pass through the gill in about 15 to 20 seconds (Section I). Thus, branchial vascular responses to such injections should have a time lag of this order. I analysed peak responses, but peak responses developed over a period of 30 to 60 sec. Thus by combining all peak responses with up to 100 sec delay after the injection I included all responses that were branchial in origin. *In vitro* branchial vasodilation and vasoconstriction are easily demonstrable with drug infusions since Q_i is constant. The demonstrated branchial vasoactive effects of agonists drugs *in vitro* were also utilised in the analysis of *in vivo* responses to the same agonists. Lag times for a response were helpful in evaluating the sites of drug action as indicated by the observations on the cardiac effects of synthetic agonist drugs injected into the ventral aorta. The inotropic effect of ISOP on the heart and the negative chronotropic effect of CARB both occured about 2 minutes after injection. This time lag is

consistant with estimated of circulation times for teleosts (Davis, 1970).

In vivo distinction must be made between direct agonist actions and reflexogenic (hemostatic?) mechanisms. Randall and Stevens (1967), for instance, noted reflexogenic vagal stimulation of the heart after adrenaline injections in trout. Lutz and Wyman (1932) reported that an increased VA pressure in dogfish elicited a vagally mediated bradycardia, as did Mott (1951) with eels. Furthermore, Satchell (1962) reported that a bradycardia was evoked during hypoxia when VA pressure also increased. I will attempt to make my distinction by using known vasoactive actions from in vitro responses and time lag of the response. For example, a NAD injection in Ophiodon had the direct agonist effect of reducing Rg, but the associated increase in Q must be reflexogenic since the time lag of the response precludes recirculatory effects of NAD on the heart.

Under the steady state pulsatile perfusion conditions of the in vitro experiments ACH markedly increased Rg. In vivo, ACH injected into the ventral aorta also caused a marked branchial vasoconstriction in ling cod since Rg rose markedly (Table X). The presence of a cholinergically mediated branchial vasoconstriction is in agreement with previous in vitro and in vivo investigations in teleost species (See Introduction).

A specific site of branchial cholinergic vasoconstriction has been hypothesised (Smith, 1977; Dunel and Laurent, 1977), which is located at the base of the efferent

filament artery. A number of observations in my study are consistant with their hypothesis. Firstly, there are vascular constrictions at the base of the EFA in ling cod (Section I) similar to those observed in other teleosts. Secondly, ACH infusion in vitro resulted in flow being diverted from normal efferent pathways, since outflow via the efferent artery decreased markedly with inflow unchanged; an observation also recorded by Smith (1977). The observation can be explained by increased venolymphatic flow due to cholinergic constriction at the EFA base, because EFA to venolymphatics connections are located upstream to this site. An alternative arguement is that a general cholinergic constriction in all arteries elevates Rg, similar to the action demonstrated on strips of large branchial arteries (Klaverkamp and Dyer, 1974). Smooth muscle also surrounds the short vessels connecting the EFA to the ECV and, therefore, these vessels would also be constricted, thus preventing venolymphatic flow if the major response was a general cholinergic vasoconstriction. Thus, while some general cholinergic vasoconstriction may occur, it cannot account for the observed reduction in efferent artery outflow. Lastly, the efferent micropressures consistently rose after ACH treatment in the isolated holobranch preparations. Since Q_o fell at the same time, the cholinergic constriction site must be downstream of the pressure measurements. The site could either be at the base of the EFA, again, or within the efferent arch artery. A general response in the EAA can be argued against because it would require extensive cholinergic innervation of the

EAA or circulating levels of acetlycholine. The possibility of hormonal ACH actions in teleosts has been discussed and rejected (Wood, 1975), but nothing is known about the distribution of cholinergic fibres in the gills. Whether the site of cholinergic action is the base of the EFA or not will have to await localisation of cholinergic terminals.

The observation that gill filaments move with ACH infusion in vitro may be important in producing Rg changes. The base of the EFA lies close to the cartilage which surrounds the gill arch. It is possible that the base of the EFA could be physically constricted by the cartilage when the arch hemibranchs are spread out. Whenever perfused holobranchs were being set up, the orientation of the arch bend, which affected the spread of hemibranchs, was important since some manipulations would raise P_i independent of other factors. Smith (1976) has actually noted the difficulty of infusing viscous fluids past the base of the efferent filament artery in trout. Thus filament movements may be important in the Rg elevation after ACH administration.

What is certain is that branchial vasoconstriction is localised to the efferent gill arteries in ling cod and will result in elevated EFA intravascular pressure unless flow is reduced. Consequently, intralamellar pressure (ΔP_{lam}) and lamellar input pressures will also rise in the whole filament. These elevated pressures initiate lamellar recruitment, intralamellar shunting and increased lamellar blood volume

automatically. It is postulated, therefore, that cholinergic vasoconstriction at the base of the filament initiates changes in blood flow of the whole filament. Input flow must be maintained or elevated in face of the increased Rg, however, for these flow pattern changes to be effected.

In vivo after the VA injection of ACH, $\dot{Q}$ increased reflexogenically, which effected the lamellar recruitment, lamellar volume changes and intralamellar shunting initiated by branchial vasoconstriction. The ACH injection was also associated with elevated ventilation rates and pumping pressures (Fig. 23) which increase gill ventilation ($\dot{V}g$). Vagal and cholinergic neurones have been implicated with respiratory control (Hughes and Shelton, 1962; Roberts, 1975), but my experiments provide no evidence for mechanism behind the increase in $\dot{V}g$. Increased $\dot{V}g$, however, increases O_2 delivery to the gills which is fundamental to enhancing O_2 transfer in fish. I, therefore, concluded that the branchial actions of ACH are all geared towards initiating conditions for increased O_2 transfer, which are effected by increased $\dot{Q}$ (reflexogenic) and $\dot{V}g$.

The heart in ling cod has cholinergic receptors which reduce heart rate if stimulated - note the effects of CARB injections. The heart also receives cholinergic tone since atropine injections resulted in a sustained tachycardia: a result which agrees with previous findings for Ophiodon (Stevens et al., 1972), carp (Randall, 1968) and Gadus morhua (Holmgren, 1977). The resting trout lacks vagal tone (Stevens and Randall,

1967a). It is interesting that no heart rate higher than the atropinised rate was ever observed in my experiments. And that the characteristic beat to beat heart rate fluctuations were abolished by atropine. Cholinergic tone is probably mediated via vagal cardiac innervation as in other fish. Consequently, if the general cholinergic nerve activity increased in ling cod, then a bradycardia and an efferent branchial vasoconstricton could all be expected to follow immediately. Decreased cholinergic activity would increase heart rate and $\dot{Q}$, if stroke volume was maintained.

It is clear that intravascular infusion of catecholamines reduces Rg *in vitro* and *in vivo* in ling cod. My findings agree with previous results for catecholamine injections in teleosts both *in vivo* and *in vitro*. ISOP, a pure β - adrenergic agonist, produced only a small Rg change *in vitro*. In trout gills β - adrenergic dilation produces more marked Rg reductions (Wood, 1975). Why is there this difference? When comparing results of different experiments one must consider the vascular properties of the *in vitro* preparation and the perfusion conditions. Wood controlled input pressures with reduced inflow rates. I used normal inflow rates and input pressures were high. I suggest that under the conditions of my *in vitro* preparation the vessels had little or no vascular tone and only small dilatory responses were possible. Vascular tone is defined as the ability of a vessel wall to maintain its diameter over a range of internal pressures.

NAD, a potent α- and β - adrenergic agonist, produced a greater reduction in Rg than did ISOP in my experiemnts. There are two possible explanations for this. First NAD could be α - dilatory and β - dilatory in Ophiodon. Since only α - constrictory receptors have been found previously in teleost gill vasculature (Wood, 1975), this explanation is unlikely. An α - constrictory and β - dilatory action is the other possibility, but how can α - constriction decrease gill resistance? In gills α - constriction has only small effects on overall perfusion pressures (Wood, 1975). Therefore vessel diameters are unlikely to be altered greatly by α - constriction. If, instead, the α - constriction effect is to stiffen afferent arterial vessel walls, i.e. increase vascular tone, the pressure profile in the gills would be altered. Pulse pressures would be larger which would raise lamellar input pressures. Higher input pressures would overcome critical closure pressures and recruit lamellae, in addition to increasing the lamellar volume. Both changes reduce Rg with constant Q_i conditions. The hypothesis of α - constriction conferring branchial vascular tone is given support by comparing vascular properties in vivo and in vitro. Gill arch preparations are noted for their lack of vascular tone, high compliance and high resistance to flow (Wood, 1974b; visual observations; Section III). The findings of Payan and Girard (1977) can also be interpreted to suggest either a lack of or a reduced vascular tone in vitro since phentolamine and propanolol (α - and β - adrenergic antagonists, respectively) had little

affect on gill perfusion pressures or flow by themselves. In vivo, gill resistance is low (Table VI) and gill vascular tone does exist (Wood, 1974b, Helgason and Nilsson, 1973) contrary to the suggestions of Randall and Stevens (1967). In resting fish branchial vascular tone may in fact be due to circulating catecholamines which are at sufficient levels to elicit tonic vascular effects (Nakano and Tomlinson, 1967; Mazeaud et al., 1977). It is concluded that the branchial vasculature in Ophiodon possess β - dilatory and α - constrictory receptors.

In resting ling cod VA injections of NAD and of ISOP produced different responses. NAD had a marked pressor effect, but ISOP produced a depressor effect. One explanation for this is that the systemic circulation possesses α - adrenergic receptors, which produce a very potent vasoconstriction (Stevens and Randall, 1967; Wood and Shelton, 1975; Stevens et al., 1974). The coeliac artery is one specific site of adrenergic vasoconstriction in teleosts (Holmgren, 1978). NAD injected into the ventral aorta in my experiments increased Rs, in most ling cod. In the remainder, Rs was not changed by NAD injection and in these the pressor response was a result of Q being elevated.

NAD administration in ling cod in addition to branchial vasodilation will bring about lamellar recruitment and intralamellar shunting because of its pressor effects and elevation of Q. Lamellar recruitment can apparently be qualitatively assessed by changes in pulse pressures since the

lamellae are complaint vascular sheets (Section I). Perfusion of additional complaint vascular beds in parallel raises the overall gill compliance and increase the damping of the pressure pulse across the gills. The ΔPg pulse was increased with administration of catecholamines into resting ling cod. Notably, the greatest increase in ΔPg pulse occured with NAD administration, which correlates well with the NAD pressor response that greatly enhanced lamellar recruitment.

Cardiac output increased reflexogenically in response to catecholamine injections into the ventral aorta. The elevated $\dot{Q}$ was a result of increased stroke volume, as there was little change in heart rate. ΔPg mean, however, was relatively unchanged as a result of Rg and $\dot{Q}$ changes. In other words the changes in $\dot{Q}$ and Rg were compensatory or automatically matched. A decrease in Rg can be due to lamellar recruitment and/or vasodilation. Lamellar recruitment will increase filament blood volume the greatest, since the lamellae contain the majority of the blood (Fig. 13, Section I). The recruited lamellae will thus be largely responsible for accommodating the increased $\dot{Q}$. I, therefore, postulate that the increased $\dot{Q}$ closely matches lamellar recruitment, in which case increased Rg only reflects the branchial vasodilation. Thus the NAD injections produced greater lamellar recruitment and branchial vasodilation than ISOP since the increases in input pressures, $\dot{Q}$ and ΔPg pulse were greater. Clearly changes in branchial blood flow patterns occur in response to catecholamines through increase input pressure

and $\dot{Q}$.

The venolymphatics

Little is known concerning flow in the venolymphatic system of teleost gills. The results presented here and in Section I provide some information on venolymphatic flow in ling cod. Blood flow is derived from the efferent filament arteries and can proceed through a series of narrow connecting vessels between the ECVs, CS and ACVs (Section I). Lymph formed at the lamellae enters the interstitial space between the epithelium and capillary endothelium. The interstitial space apparently drains into the central sinus by separate channels lying beneath the lamellae. These channels have not been observed before in other teleosts. Valve-like structures exist at the base of the lamellae in the interstitial space in trout (Campbell et al., in preparation). Such valves, if present in ling cod, would prevent reflux of lymph from the central sinus to the lamellar interstitial space.

The CS and ACVs are relatively free of red blood cells and the ECVs contain reduced rbc numbers compared to arterial blood. A high rate of lymph formation would produce this situation in the venolymphatics. Plasma skimming would also reduce rbc numbers in the venolymphatics. The small vascular connecting vessels are ideal for excluding red blood cells but allowing plasma through. In trout Vogel et al. (1976) noted that

the openings of venolymphatic connecting vessels are surrounded by microscopic "hairs". These hairs could serve to exclude red blood cells in trout, but they have not been looked for in ling cod. Blood flow from the EFA to the main ECV may be controlled in ling cod by the smooth muscle that surrounds the connecting vessel.

Based on the micropressures measured here, venolymphatic flow is driven by low pressures. This conclusion could be predicted from the presence of narrow inter-connecting vessels of the venolymphatics. The micropressures were pulsatile, confirming that venolymphatic flow is pulsatile. Mammalian lymphatic systems are low pressure and have a pulsatile flow. Increased pulsatility is known to enhance lymphatic flow in mammals (Parsons and McMaster, 1938; McMaster and Parsons, 1938; Ruszyak et al., 1967). Some lymphatics can propel fluid by their own intrinsic activity and increased lymphatic transmural pressure will increase the rate of lymph propulsion (McHale and Roddie, 1976). Arterio-lymphatic interactions also influence lymph flow since in mammalian lungs lymphatic flow is enhanced by the arterial pulse pressure (Shephard and Kirklin, 1969; Nicolaysen and Hauge, 1977). Furthermore non-pulsatile arterial lung perfusion resulted in lymph accumulation which was associated with reduced oxygen consumption. Arterio-lymphatic interactions may also occur in the gill filament, and it is predicted that the pulsatile nature of arterial flow could have important effects on venolymphatic flow. This prediction is

examined in Section III. Venolymphatic flow in gills might also be under neural or humoral control mechanisms, since in trout, α-adrenergic constriction decreases venolymphatic volume (Girard and Payan, 1976; Payan and Girard, 1977; Dunel and Laurent, 1977). The importance of maintaining venolymphatic flow in the filament is quite simple. If lymph formed at the lamellae were to accumulate, O_2 transfer would be limited because of increased diffusion distances.

In summary I have demonstrated experimentally that the ALAs are the major resistance site to gill blood flow and distal lamellae are not perfused under certain in vivo conditions. Changes in vascular dimensions through cholinergic and adrenergic actions initiate alterations in gill blood flow patterns. Gill resistance is altered by the vascular changes, but flow pattern changes are effected by Q regulation. Increased Q in vivo will therefore be associated with lamellar recruitment and intralamellar shunting, which increase the gill diffusing capacity. The changes in flow pattern associated with increased Q and input pressure were not visualized, but are assumed to occur automatically based on previous findings. It is necessary to experimentally confirm that flow changes do occur automatically with Q and pressure changes. This confirmation was carried out in Section III by observing lamellar perfusion in isolated gill arches.

SECTION III

AN EXAMINATION OF THE VASCULAR RESISTANCE AND COMPLIANCE AS THEY AFFECT GILL BLOOD FLOW USING IN VITRO PREPARATIONS

The effects of alterations in pressure, flow and pulse rate of gill blood flow patterns in the isolated, perfused holobranch

Pressure/volume curves for the bulbus arteriosus and ventral aorta

INTRODUCTION

In the previous Sections it was demonstrated that pre-lamellar arterioles control lamellar blood. A delicate balance exists between the overall resistance of each parallel lamellar unit and the distal lamellae may not be perfused under certain conditions. Furthermore the pattern of flow distribution within a single lamella is not uniform. In these situations an increase in $\dot{Q}$ and in gill input pressure is predicted to alter gill blood flow patterns in such a way that O_2 transfer is enhanced. Is this truly the situation? Exercising trout do show marked changes in $\dot{Q}$ and VA pressure which are also associated with an elevated $\dot{M}o_2$ (Stevens and Randall, 1967a and b; Kiceniuk and Jones, 1977). However the direct effects of increased $\dot{Q}$ and input pressure on observed patterns of gill blood flow have not been studied. Such an investigation was made here using the isolated perfused gill preparation, where lamellar perfusion can be observed directly. Also, only the passive properties of the vessels were examined when perfusion conditions were changed, since in vitro gill preparations have little or no vascular tone (Section II), and they are denervated.

Our understanding of gill blood flow control has benefited from many studies using an in vitro isolated perfused holobranch or head preparation (Ostlund and Fange, 1962; Richards and Fromm, 1969; Wood, 1974b and 1975; Bergmann et al., 1974

Forster, 1976; Payan and Girard, 1977). These preparations have also been used to investigate gill ion transfer (Payan and Matty, 1975; Pic et al., 1974 a and b; Girard and Payan, 1976; Payan, 1978). If input pressure and Q can alter blood flow patterns, then care must be taken in selecting in vitro perfusion conditions. At the very least, perfusion pressures should be high enough to avoid critical closure of lamellar blood channels (Section I). Yet in all these previous investigations in vivo pressures and flow regimes were largely ignored. Teleost fish, in vivo, have neither constant Q nor constant gill perfusion pressure. Blood flow is pulsatile and the DA blood pressure is of the order of 20 to 40 cm H_2O. It is reassuring that recently Shuttleworth (1978) did consider the in vivo state of blood flow and lamellar perfusion in the design of his isolated, perfused holobranch preparation, as did Wood et al. (1978). The direct effects of pulsatile flow and pressure changes on the pattern of gill blood flow clearly need to be examined and the results of this investigation may well affect the interpretation of previous in vitro experiments.

Interpretation of in vitro results can be complicated by the nature of the perfusion conditons (Section II). The quantitative nature of vascular responses is definitely affected by perfusion conditions. For example, in the perfused mammalian kidney preparation, pressor responses using constant Q perfusions were 2 to 5 times lower than responses with constant pressure perfusion (Khajutin, 1964). There are also difficulties

applying *in vitro* results to *in vivo* conditions because of different perfusion conditions. *In vitro* adrenergic and cholinergic drug infusions will mimic possible neural vascular control, but they only inform us whether vessels constrict or dilate. *In vivo* administration of these drugs produces more complex responses than a resistance change e.g. changes in pulsatility and Q (Section II). If pulsatility and Q can also change gill blood flow patterns, then clearly the extrapolation of *in vitro* findings to the discussion of how branchial adrenergic and cholinergic effects alter blood flow patterns *in vivo* must be approached carefully. Indeed, I suggested in Section II that in addition to altering Rg, Q must also be maintained or elevated to alter perfusion patterns. It is surprising then, that previous interpretation and application of *in vitro* findings rarely considered or acknowledged the differences in perfusion pressures and flows between the *in vivo* and the *in vitro* situations.

In teleosts blood flow remains pulsatile throughout the gills. Lymphatic flow is also pulsatile. It has already been suggested in Section II that arterial pulsatility could affect Mo_2 by its effect on lymphatic flow, based on the observed arterio-lymphatic interactions in mammalian lungs. It is noteworthy that the filament venolymphatics are extensive in ling cod (Section I), and that the pulse pressures throughout the gill bed, in particular the lamellar capillaries, are comparatively high (Section II). Is pulsatility *per se*, therefore, important in determining branchial blood flow patterns? Furthermore, to

what extent can pulsatility of blood flow be controlled?

Arterial pulsatility is determined largely by the action of the heart. Blood flow is, however, depulsed - a Wind kessel effect - by the elastic bulbus arteriosus (Randall, 1968; Satchell, 1971; Jones et al., 1974). In a number of teleosts there is sympathetic innervation of the smooth muscle of the bulbus (Gannon, 1972; Watson pers. comm.). It is possible then, that sympathetic release could alter the tone of the bulbus arteriosus and thus modulate the degree of blood flow depulsation. The effect of pulsatility per se on branchial blood flow patterns and whether or not the bulbus can contribute to the control of pulsatility were examined here.

In this Section I conducted investigations on how alterations in pulsatile flow, pressure and pulse rate passively affect gill perfusion and patterns of lamellar perfusion by using the isolated holobranch preparation.

MATERIALS AND METHODS

In vitro isolated holobranch perfusion: the effect of alterations in pressure, flow and pulse rate on gill blood flow patterns

The clearing, preparation and cannulation of the isolated gill holobranchs has been described in the general methods. The perfusion protocol was as follows.

Each arch was perfused separately in a constant temperature (11°C) saline bath using a Watson-Marlow pulsatile perfusion pump (Fig. 26). Inflow (Q_i) was controlled with a series of precalibrated, interchangeable tubes and the variable pulse rate of the pump. Input pressure (P_i) was monitored within 2 cm of the gill arch using a Statham P23Db pressure transducer and a Brush chart recorder. The afferent cannula resistance was measured after each experiment and deducted from mean P_i values. Outflow from the efferent arch vessel (Q_o) was measured by drop counting and outflow pressure (P_o) was set by the height of the cannula above the saline level of the preparation (Fig. 26). Thus Q_i, pulse rate (hence stroke volume) and P_o could be manipulated, whilst mean P_i and Q_o were the measured variables. Excessive pulse pressures that were generated by the pump were damped by a "Wind-Kessel" which consisted of an air filled syringe as a side branch of the main perfusion line (Fig. 26). "Resting" values for pulse rate (30 min^{-1}), Q_i to each arch (1.25 to 1.5 $ml.min^{-1}.kg$ body $weight^{-1}$) and P_o (30 to 40 cm H_2O) were based on

FIGURE 26

A schematic diagram to represent the *in vitro* perfusion system used. The perfusate inflow and perfusion bath were both kept at constant temperature by water jackets. The Wind-kessel consisted of an air-filled syringe, the volume of which could be adjusted to vary the damping of input pulse pressure. P_o = output pressure and the height of the efferent catheter above the saline.

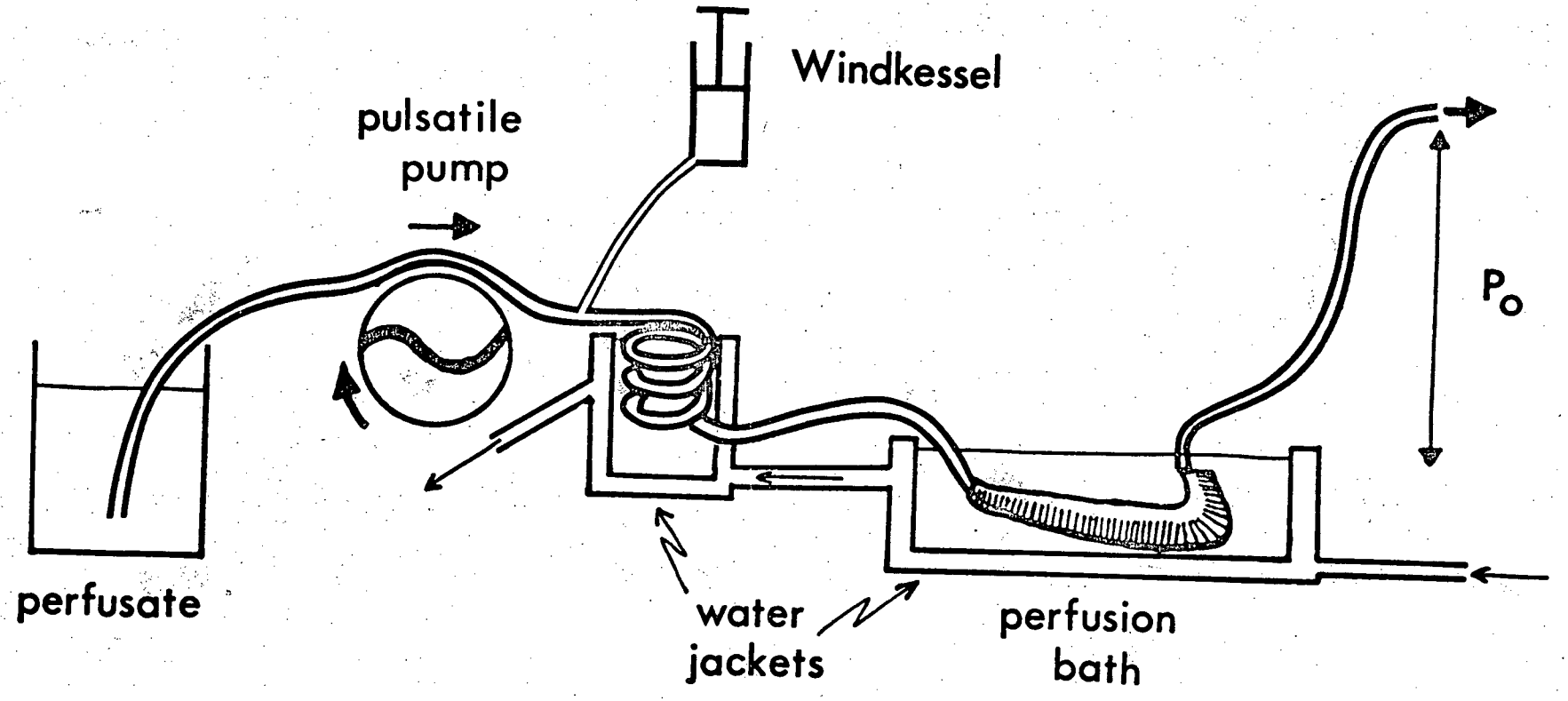
Windkessel
pulsatile
pump
P_o
perfusate
water
jackets
perfusion
bath

the *in vivo* measurements from ling cod. Similarily, pulse rates of $45.min^{-1}$ and $15.min^{-1}$ approximate the maximum heart rate (atropinised) and the minimum heart rate (hypoxic bradycardia) recorded in ling cod (see Sections II and IV).

Typically, each holobranch was initially perfused at resting Q_i and pulse rate, while P_i gradually fell and Q_o gradually rose with time towards stable values. After equilibration (10 to 15 min), individual manipulations were made to pulse rate/stroke volume, Q_i or P_o, while recording P_i and Q_o. The subsequent effects on lamellar recruitment were determined. To visualize the number of lamellae perfused after a given manipulation, a 1 to 2 min equilibration period was allowed, then a Prussian Blue dye suspension was introduced to the inflow. This procedure also served to demonstrate successful afferent cannulations since dye never leaked from the afferent side of the preparation. The particulate dye lodged in the lamellar capillary channels to indicate the flow pathways at that time. Perfusion was stopped immediately since P_i was rising due to vessel occlusion. The distribution of dye was observed by clearing the gill tissue in methyl salicylate after alcohol dehydration. The intact holobranch was photographed and the extent of dye penetration along the filament length, as well as the total length were measured in every 10th filament, which were isolated and viewed under a microscope. The dye penetrated along a portion of the afferent filament artery and entered all lamellae connected to that segment of artery containing dye.

There was no evidence of dye in the remaining length of filament or lamellae. Since the lamellae are evenly distributed along the filament (Fig. 4, Section I), the percentage of lamellae perfused was calculated from the extent of dye penetration along the filament expressed as percentage of total filament length.

Six holobranchs were routinely used from each fish; the fourth gill arches, which were smaller than the rest and had an excessive amount of cut tissue, were not used. Holobranchs lacking Q_o or that had excessively high P_i values, were not used. The experiments were conducted over a 2 to 3 hours period proceding gill removal, thereby minimising experimental time and the associated changes in the characteristics of the gills with time. Storing the holobranchs in ice-cold saline was helpful in this respect.

The pressure/volume curves for the bulbus arteriosus and ventral aorta

It is difficult to separate the bulbus arteriosus from the ventral aorta. Therefore the pressure/volume curves were established for the intact bulbus arteriosus and ventral aorta vessel from two ling cod and six rainbow trout. The vessel length was measured *in situ* in the anaesthetised fish prior to being excised *in vivo* and cleared of blood. The vessel was cannulated at both ends with PE 200 tubing and placed into a perfusion bath containing the appropriate oxygenated saline at 9 to 10°C. The vessel was stretched to and held at its *in vivo* length. The bulbus catheter was connected to a constant flow Harvard infusion syringe pump and, via a side arm, to a Statham P23Db pressure transducer (Fig. 27). The pressure transducer signals were amplified and recorded on a Harvard chart recorder. Infusion rates comparable to those found *in vivo* were established in preliminary trials, since the shape of pressure/volume curves vary with the rate of increase of internal volume (Bergel, 1961a and b; Fung, 1972). The major experiments were performed on vessels from trout, for which the filling time could be approximated to those associated with resting heart rates found in trout (Randall, 1970). Filling of the ling cod vessel was at best 2 to 3 times slower than *in vivo* because of the limited delivery speed of the syringe pump compared to the large vessels from the specimens used. For this reason only the control pressure/volume curve was established in 2 ling cod so that its general similarity with the trout vessel could be ascertained.

FIGURE 27

A schematic diagram of the water-jacketed, saline-filled perfusion bath used for examining the pressure/volume curves of the bulbus arteriosus and ventral aorta vessel.

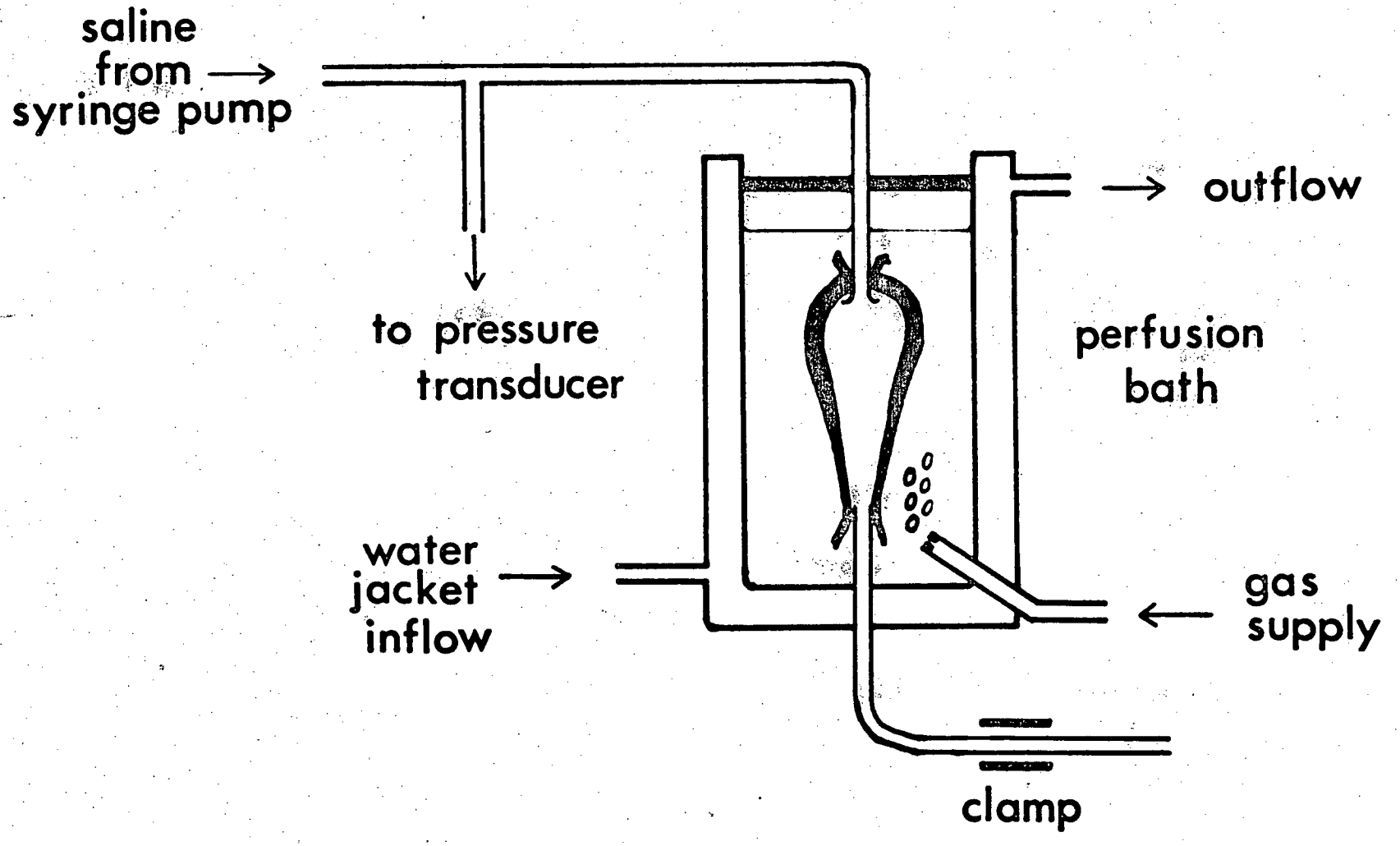
saline
from
syringe pump
to pressure
transducer
outflow
perfusion
bath
water
jacket
inflow
gas
supply
clamp

Each experiment with the trout vessel consisted of a series of preliminary vessel distensions, control saline distensions and the testing of an agonist drug. For each vessel ACH, ISOP and NAD were tested in sequential experiments and in the final experiment the saline bath was progressively deoxygenated with N_2 gas while a series of distensions were made. The protocol adopted for each experiment was; infusion started with the vessel collapsed to a negligible volume and the outflow cannula clamped. The internal pressure was monitored on the chart recorder and infusion was stopped at an internal pressure no greater than 100 cm H_2O. The internal pressure was released immediately. Five preliminary distensions ensured a pre-stretching of the excised tissue prior to determining any series of pressure/volume curves (Fung, 1972). Three control curves were determined first. Then an agonist drug was added to the saline bath (1×10^{-4} mg.l^{-1} final concentration) and three to five distensions made afterwards. The bath and vessel were washed thoroughly with three changes of fresh saline and the vessel was freely perfused. After 15 min a final saline change preceded the next experiment. When all three agonist drugs had been tested, the saline was progressively deoxygenated for the final experiment in which four to six distensions were made over a 5 to 10 min period. The repetition of the control curves with saline before each drug experiment ensured that the preparation did not deteriorate. All results from any preparation that developed a leakage part way through the experimental series were

discarded. The pressure/volume curves were constructed directly from the pressure recordings since volume was directly related to time at the calibrated, constant flow rates of the syringe pump.

RESULTS

The effect of alterations in pressure, flow and pulse rate on the lamellar blood flow in isolated, perfused holobranchs

A total of 52 successful gill perfusion preparations from 10 ling cod were studied. Cardiac output in resting ling cod at 11°C is about 10 $ml.min^{-1}.kg^{-1}$. The isolated arches were perfused initially at 1/8th the estimated cardiac output given the weight of the donor fish. At this initial flow rate, referred to as "resting Q_i", the mean input pressure (P_i) was between 70 to 95 cm H_2O. The gill resistance to flow, Rg (calculated from $\Delta Pg/Q_i$, where $\Delta Pg = P_i - P_o$), was initially high, but fell to a stable value 10 to 15 min after the onset of perfusion.

A stepwise increase in P_o resulted in smaller changes in P_i. At low levels of P_o, an increase caused a fall in P_i whereas at high levels an increase P_o resulted in a small rise in P_i (Fig. 28). Clearly, as ΔPg falls with increasing P_o and, as Q_i is constant, Rg also falls with increasing P_o (Fig. 28b).

The ratio of Q_o to Q_i was between 30 and 88% at the time of dye injection. Saline was, therefore, also lost from the preparation via other outlets or by filtration. There were never any leaks in the afferent portion of the system and all saline must, therefore, enter the secondary lamellae. Fluid could be lost by filtration but this is probably not a major pathway

because when P_i increased the difference between Q_o and Q_i decreased (Fig. 29b). Thus there is more than one outflow channel in the efferent circulation but fluid was only collected from the efferent branchial artery. The ratio of Q_o:Q_i was also increased by raising Q_i and/or increasing the pulse rate (Fig. 29a). Elevation of P_o at constant Q_i initially decreased Q_o which then returned to the original level. If, however, P_o was greater than 30 cm H_2O the pre-change Q_o was not always attained.

The progressive deoxygenation of the perfusate with N_2 gas failed to produce any change in P_i or Q_o in three preparations.

Changes in lamellar perfusion patterns

Under "resting" perfusion conditions 66.8% ± 3.0 (n = 10) of all lamellae were perfused. In any one holobranch the % perfusion varied slightly from filament to filament. In particular, filaments in the region dorsal to the bend in the arch usually had slightly more lamellae perfused than elsewhere on the arch (Plate 17). There was no obvious correlation between the number of lamellae perfused and gill resistance Rg (Fig. 30). There was a significant change in lamellar perfusion with increases in Q_i, P_i and pulse rate (Figs. 31 and 32).

The effect of increased Q_i and P_i: In preparations with a

50 to 100% increase ($\bar{x}$ = 76.9%) in Q_i and an elevated P_i lamellar perfusion was increased from 66.8% to 77.8 ± 3.0, n = 13) (Fig. 31). Not all filaments of one arch showed the same increase in lamellar perfusion. Q_i was increased through either increasing stroke volume or pulse rate. The changes in Q_i were controlled by me and resulted in changes in P_i. However, the change in Q_i and P_i, although in the same direction were not in phase. Typically when Q_i was increased P_i initially rose by a mean of 37.9%, (range 15 to 55%) and overshot its latter, stable increase 23.5% above the initial level (range 8 to 42%) (Fig. 29).

The effect of increased P_o and P_i: In this system, elevation of P_o, and the consequent limited rise in P_i, did not alter % lamellar perfusion but ΔP_g fell proportionately (Fig. 29).

The effect of changes in pulse rate/stroke volume at constant Q_i

Increased rate/decrease stroke volume: The % lamellae perfused was reduced ($\bar{x}$ = 59.3% ± 6.0) in 5 out of 6 preparations when pulse rate was increased to 45.min^{-1}, but Q_i was maintained at or close to a resting value by decreasing stroke volume (Fig. 32). Under these conditions, pulse pressure was reduced and mean P_i always increased 4 to 10 cm H_2O.

Increased stroke volume/decreased pulse rate: When stroke volume was doubled and Q_i kept constant by decreasing pulse rate to 15.min^{-1}, pulse P_i was also increased as a result. The mean P_i always decreased by 2 to 10 cm H_2O after these manipulations. These changes resulted in a mean of 68.2 ± 2.9% (n = 9) of the lamellae being perfused, a value similar to that at resting stroke volumes. Increased stroke volume/decreased pulse rate per se can increase lamellar perfusion since in 6 of the 9 preparations there was always an increase in lamellar perfusion (Fig. 32). Considering only these six preparations, lamellar perfusion was 73.1 ± 1.4% compared with 66.8 ± 3.0% of the total number of lamellae under "resting" conditions. In one experiment, stroke volume was slightly less than doubled and Q_i was, therefore, below the resting value. Here the % lamellae perfused was again higher than resting values.

FIGURE 28

The effect of stepwise increases in P_o on the mean P_i and ΔPg (or k.Rg where $k = 1/Q_i$ at resting Q_i).
a) absolute values of P_o vs mean P_i: each point represents the mean value ± 1 s.e. of n observations (n above points), except at P_o = 60 cm H_2O, where the range of the two values is indicated; b) the decrease in ΔPg across the holobranch with increasing P_o. Each point represents the value for $P_i - P_o$ taken from Fig. 28A at each P_o.
Note: 1 cm H_2O = 0.098 kPa.

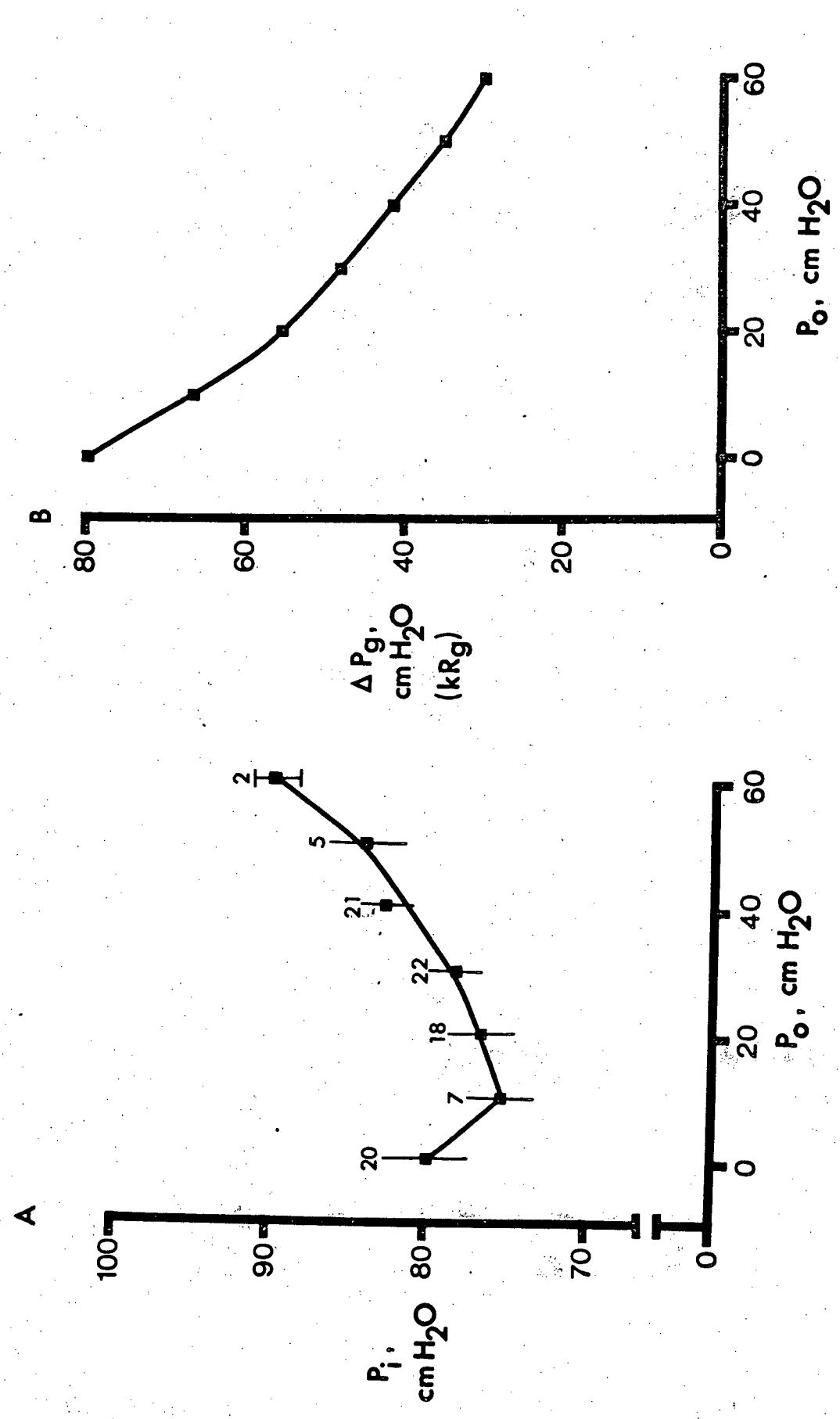
A
100
90
80
70
P_i, cm H_2O
2
5
21
22
18
7
20
0
20
40
60
P_o, cm H_2O
B
80
60
40
20
ΔP_g, cm H_2O (kR_g)
0
20
40
60
P_o, cm H_2O

FIGURE 29

A/ A typical recording of P_i when pulse rate was elevated from 30 to 45 pulses.min^{-1} at the arrow. Q_i was not changed from the resting value but Q_o:Q_i increased.
Note the x5 increase in chart speed.

B/ A typical recording of the effect of elevating Q_i to 150% resting flow by elevating pulse rate in a stepwise fashion from 30 to 45 pulses.min^{-1}, upon P_i and the ratio Q_o to Q_i. The time trace is in seconds and minutes.

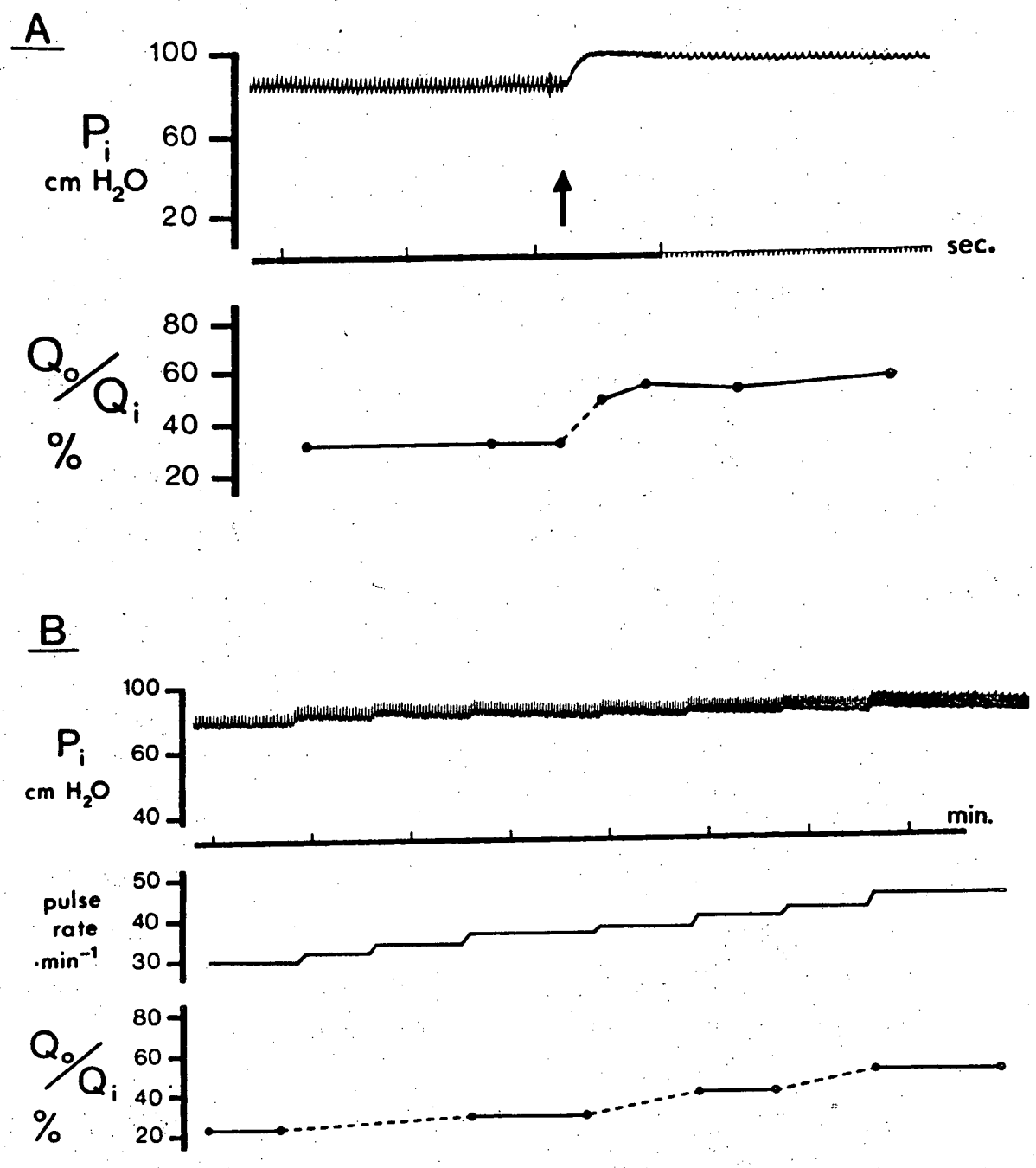
A
100
60
20
P_i
cm H_2O
sec.
80
60
40
20
Q_o/Q_i
%
B
100
60
40
P_i
cm H_2O
min.
50
40
30
pulse
rate
·min^{-1}
80
60
40
20
Q_o/Q_i
%

PLATE 17

A/ An isolated holobranch of Ophiodon elongatus illustrating dye distribution in the arch filaments. The placement of the ligatures can be seen at either end of the arch. The dye within the afferent branchial artery (top of plate) is also visible.

B/ A magnified image of a filament tip displaying the filling of the afferent filament artery and some secondary lamellar channels traversing the filament. Note the completely clear vessels at the tip.

C/ A more central region of a filament at higher magnification showing clearly the filling of the base of the lamellar vessels.

a.

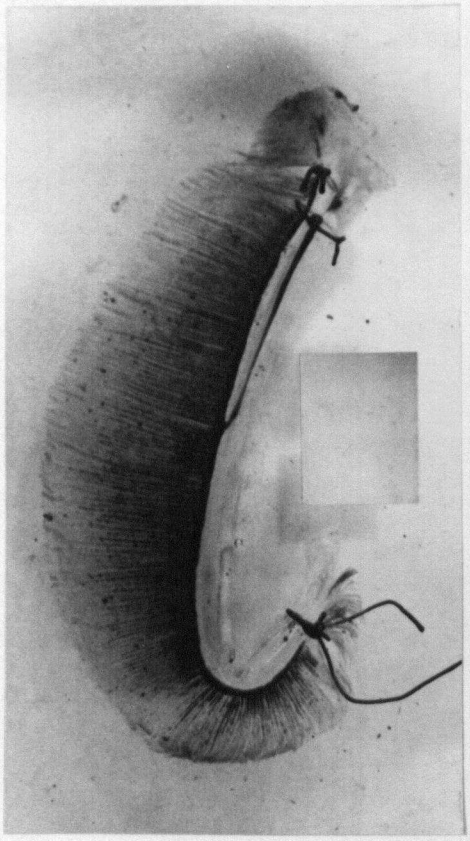

b.

c.

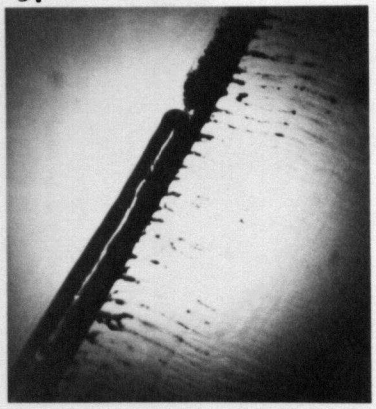

FIGURE 30

Gill resistance, $\Delta P_g/Q_i$ (or Rg) should be directly correlated with the reciprocal of the number of lamellae perfused (n) as indicated by the continuous line, if the gills are a simple ohmic resistance

$$\frac{1}{Rg} = \frac{n}{R_{lam}}$$

since the lamellar are a parallel array. Each point represents the values for one holobranch preparation and overall the points represent the complete range of perfusion conditions examined here. There is no correlation of these points.

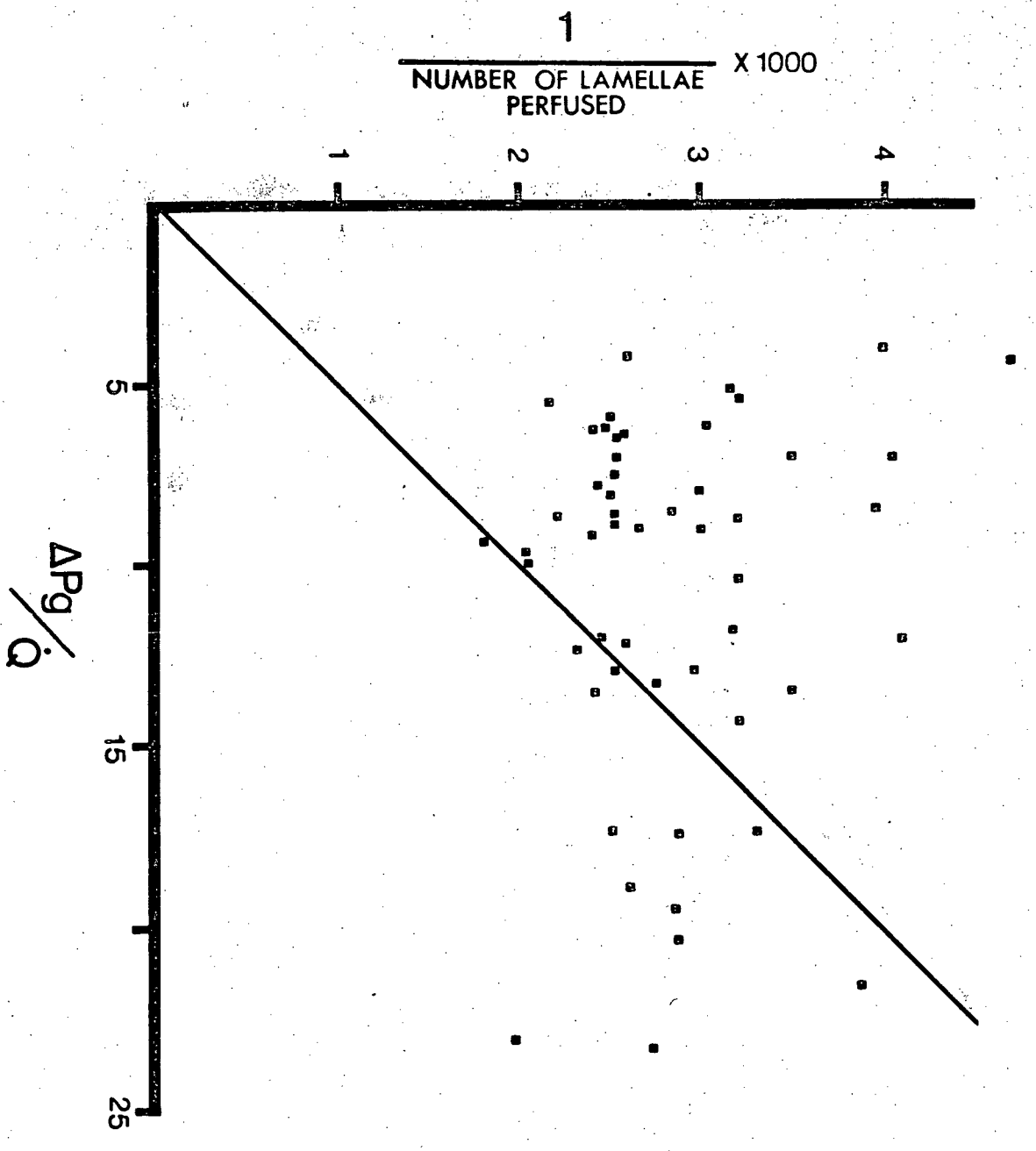
1
NUMBER OF LAMELLAE PERFUSED
X 1000
1
2
3
4
5
15
25
ΔPg/Q̇

FIGURE 31

A 3-dimensional representation of the effect of elevated Q_i, expressed as a ratio of resting Q_i (=1) on % lamellae perfused and on the input pressure P_i. Each point represents one holobranch preparation, where ✗ = resting Q_i and pulse rate, ● =elevated Q_i at a pulse rate of 45 pulses.min^{-1} and ▲ = elevated Q_i at a pulse rate of 30 pulses.min^{-1}.

Note: The length of the solid lines connecting each point in X/Z plane represents the % lamellae, as indicated on the Y-axis of the figure. The broken lines are projections of the Y-coordinate onto the X/Z plane. This is not a standard 3 - D plot. However it allows simultaneous representation of 3 variables, when each point is independent of the other points. With resting perfusion conditions 67% of lamellae are perfused. A line for 67% perfusion is projected on the X-Y plane.

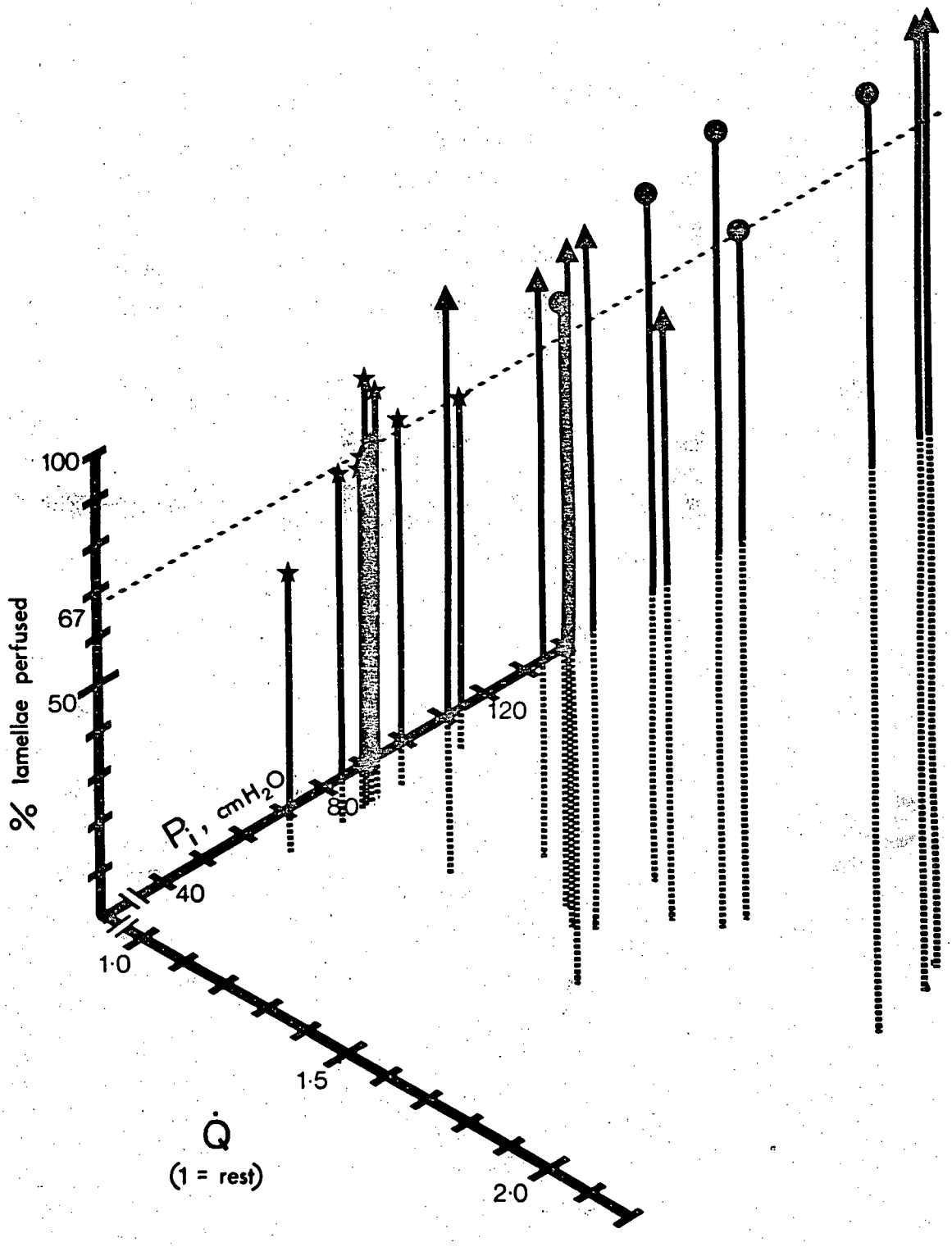
100
67
50
% lamellae perfused
P_i, cmH_2O
40
80
120
1·0
1·5
2·0
$\dot{Q}$
(1 = rest)

FIGURE 32

A summary of the effects upon lamellar recruitment of altering pulse rate with stroke volume adjusted to maintain Q_i at resting levels. Each point in the 3-dimensional representation is one holobranch preparation where ● = 45 pulses.min^{-1}, ⊛ = 30 pulses.min^{-1} and ✳ = 15 pulses.min^{-1}. See legend of Figure 31 for further explanation of figure.

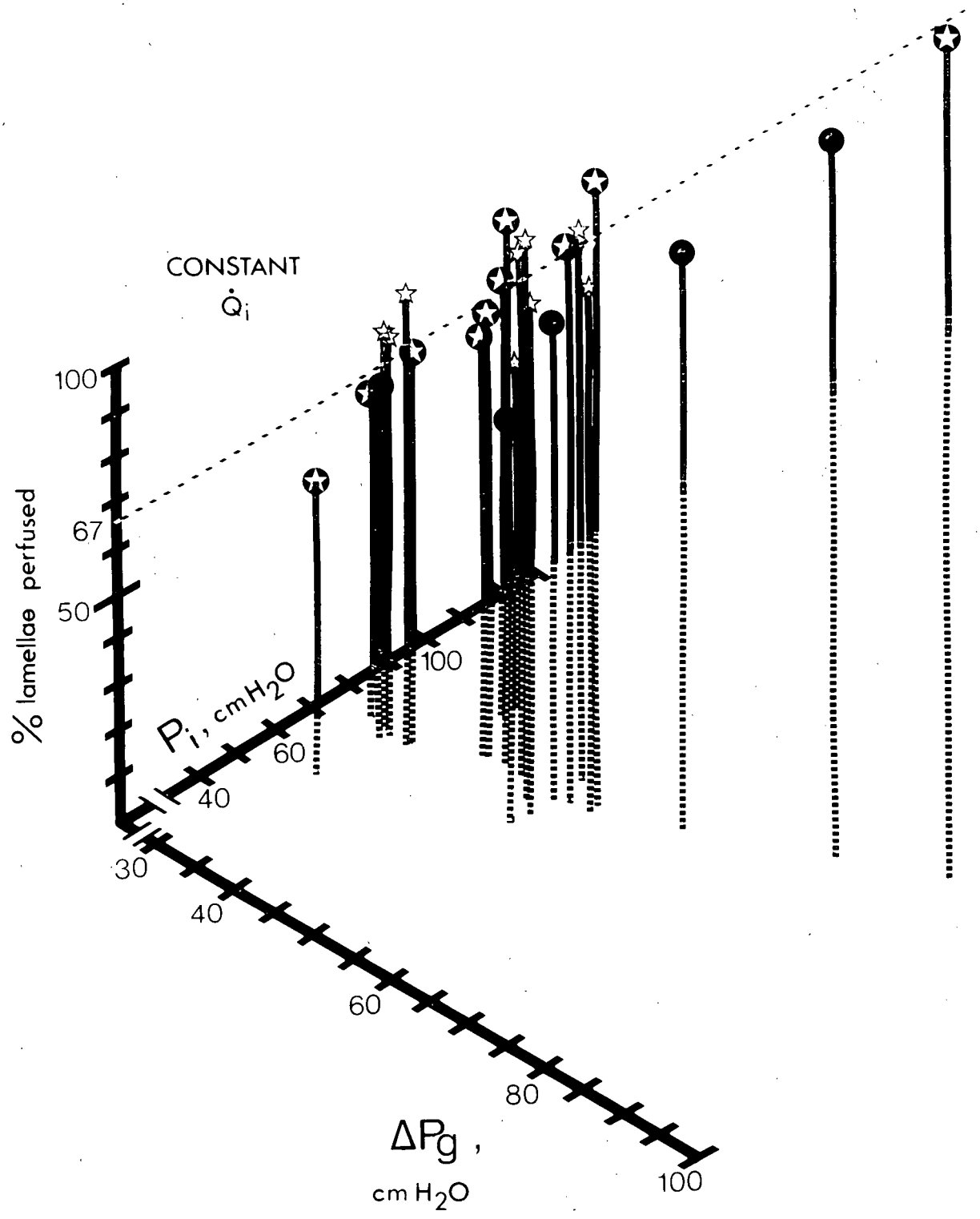
CONSTANT
$\dot{Q}_i$
100
67
50
% lamellae perfused
P_i, cm H_2O
40
60
100
30
40
60
80
100
ΔP_g,
cm H_2O

Pressure/volume curves for the bulbus arteriosus and ventral aorta vessel

During surgery when these vessels were exposed, expansion of the vessel could be observed with each ventricular ejection of blood. The bulbus arteriosus was always distended more than the ventral aorta. The reproducibility of the vessels distentions can be seen in figure 33. The pressure volume curves show that the vessels from trout and ling cod have a high compliance at pressures between 40 and 60 cm H_2O (Fig. 33). The ling cod vessels had a high compliance up to pressures of 75 cm H_2O, but these vessels were distended at reduced rates to those found *in vivo*. The effects of adrenergic and cholinergic agonist drugs for vessels from trout are summarised in figure 34. Acetylcholine decreased the vessel compliance over the 40 to 60 cm H_2O pressure range. The β - agonist isoprenaline increased compliance more than noradrenaline, an α - and β - agonist, over the same pressure range. Hypoxia increased vessel compliance to the greatest extent and its progressive effects are shown in more detail in figure 34b.

FIGURE 33

A) Typical pressure/volume curves for the bulbus arteriosus and ventral aorta vessel in trout. The distensions were performed at rates associated with *in vivo* conditons.

'1' = 3 initial saline control curves.

'2' = 3 curves after ACH treatment.

'3' = 3 saline control curves about 1 hr after the initial controls and subsequent ACH treatment.

B) Three pressure/volume curves for the ling cod vessel with saline filling rates that were 2 to 3X slower than those encountered *in vivo*.

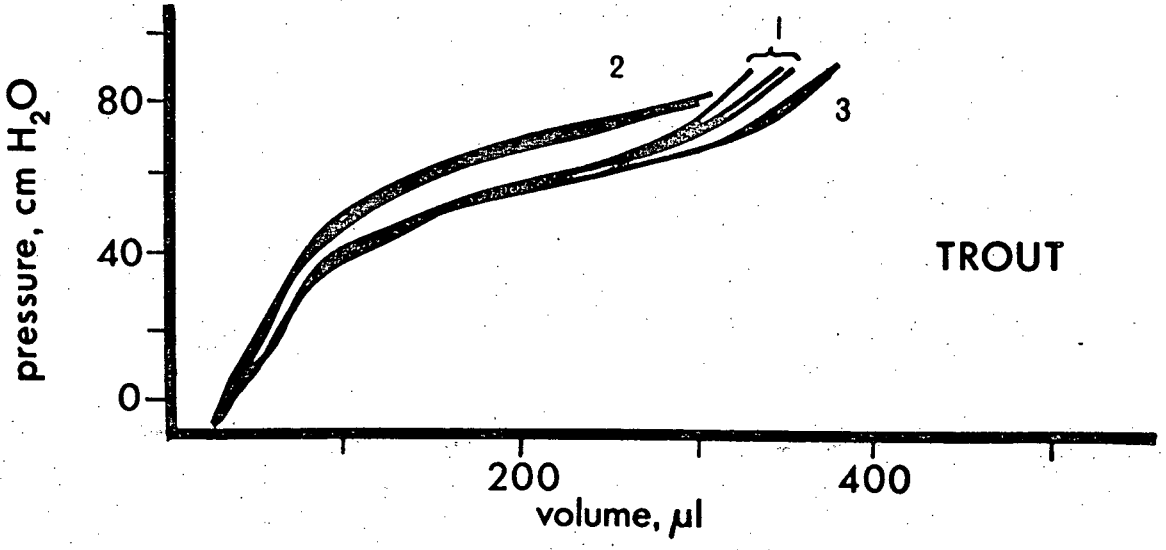
pressure, cm H_2O
80
40
0
1
2
3
200
400
volume, µl
TROUT

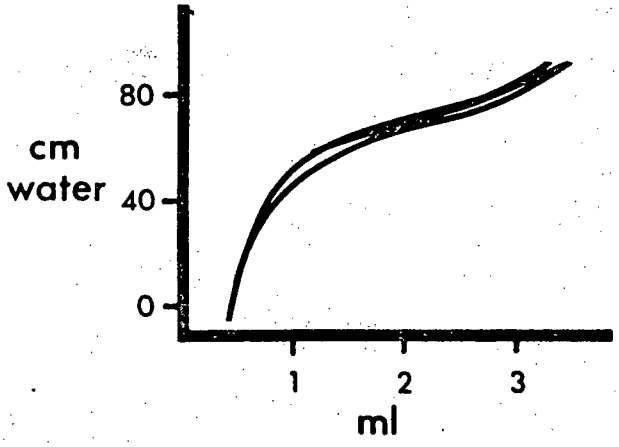
cm
water
80
40
0
1
2
3
ml
LING
COD

FIGURE 34

A) A summary of the effects of adrenergic and cholinergic treatment, and hypoxia on the pressure/volume relationships of the bulbus arteriosus and ventral aorta of trout. These curves are representative of the changes found in all experiments.

B) The effect of progressive hypoxia (in the direction of the arrow) on the vessel compliance.

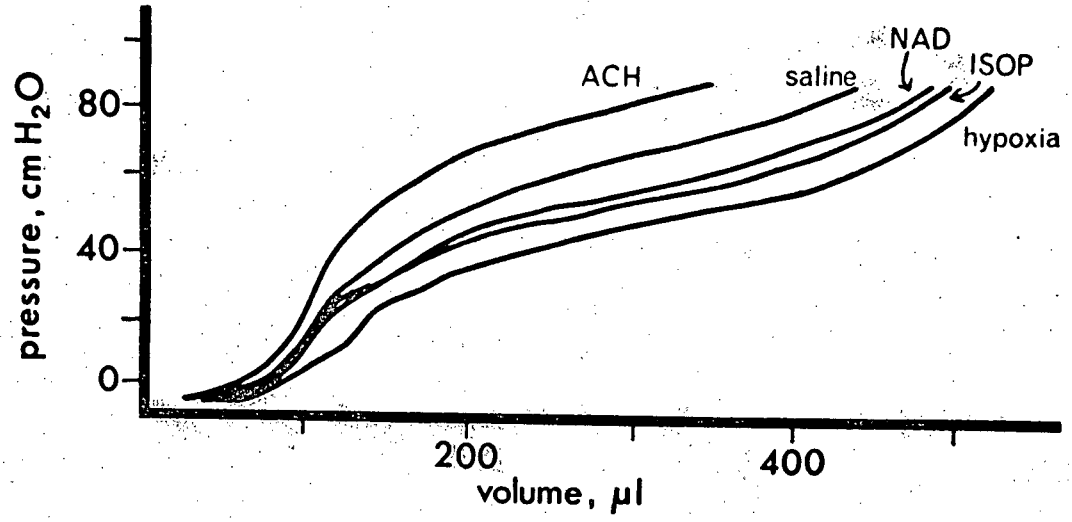
ACH
saline
NAD
ISOP
hypoxia
pressure, cm H_2O
80
40
0
200
400
volume, µl

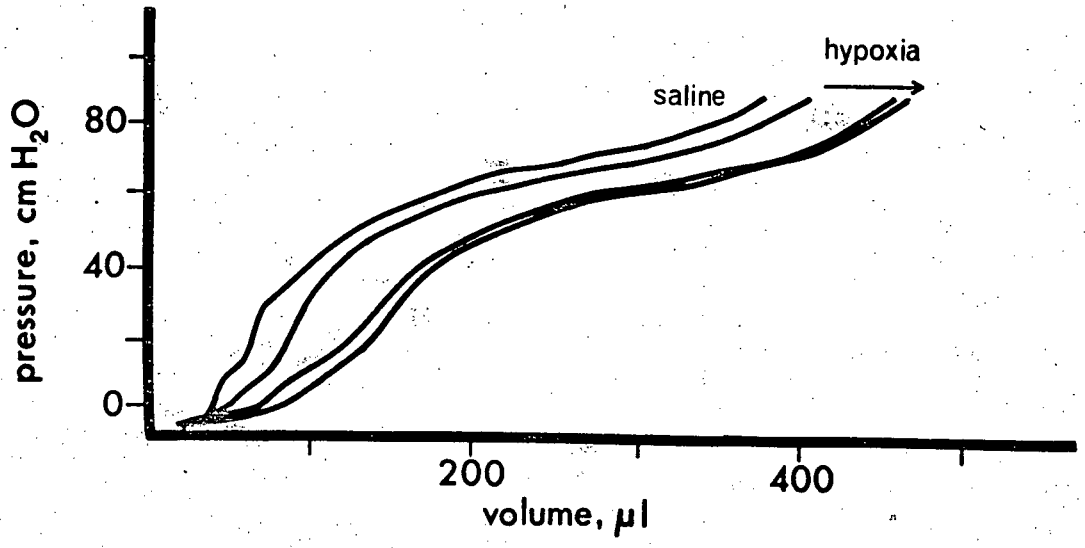
hypoxia
saline
pressure, cm H_2O
80
40
0
200
400
volume, µl

DISCUSSION

Lamellar perfusion is not complete in the isolated perfused holobranch when Q_i, P_o, pulse rate and pulse P_i are comparable to *in vivo* resting values for ling cod. The obtained value of 67% perfusion, is in good agreement with the 60% lamellar perfusion in resting rainbow trout (Booth, 1978). The agreement may well be closer, since "resting Q_i" in the isolated gill arch was slightly high, if anything, due to some filaments at either end of the arch not being perfused. Q_i was based on perfusion of complete holobranchs, as *in vivo*. Interestingly, the mean value for lamellar perfusion was 59.3% in experiments with high pulse rate/low stroke volume perfusion. It is possible then that resting ling cod like trout, perfuse a minimum of 60% of their gill lamellae.

Increased Q_i and P_i brought about lamellar recruitment. So too did increased stroke volume/decreased pulse rate. However, increased Q_i and P_i had the greater effect on lamellar recruitment. In fish, exercise is accompanied by elevated Q and VA pressures (Stevens and Randall, 1967a and b; Stevens *et al.*, 1972; Section IV). Fish in hypoxic conditions, however, maintain Q in the face of a bradycardia by increasing stroke volume (Holeton and Randall, 1967a and b; Taylor *et al.*, 1977; Section IV). These *in vivo* changes in blood flow and pressure in the ventral aorta could lead to changes in the number of gill lamellae perfused in a purely passive manner in the

above situations without the involvement of any local neural or humoral responses within the gill.

Lamellar recruitment in the isolated gill of ling cod occurs by perfusion of the more distal lamellae on each filament. Q_i and P_i could not be varied independently in my experiments and it cannot be determined if recruitment is related to changes in flow alone, pressure alone or both together. The following is an explanation of a possible way by which changes in pressure may lead to lamellar recruitment. The size of the filament afferent artery and the change in flow along its length are such in ling cod that each lamellar arteriole along a filament is subject to almost the same input pressure (Sections I and II). The critical closure pressure for any lamellar arteriole will be set by its overall resistance and its vascular tone (Burton, 1951). The resistance of distal afferent lamellar arterioles is greater since they are slightly narrower than proximal ones and supply more than one lamella, and it is likely then that their critical closure pressure is also greater. If the critical closure pressure of arterioles does increase towards the distal end of the filament then a rise in P_i will result in the recruitment of distal lamellae. <u>In vitro</u> vascular compliance must also be considered. The arterioles will remain patent, once opened, at pressures below the opening pressure (Busby and Burton, 1965). Thus increases in pulse pressure which elevated peak (systolic) pressure above the critical closure pressure, will also cause

lamellar recruitment even though there may be no change in mean pressure. Thus both the rise in VA pressure during exercise and the marked rise in VA pulse pressure during hypoxia in fish may account for the lamellar recruitment that has been observed in trout during hypoxia (Booth, pers. comm.) and hypothesized during exercise (Jones and Randall, 1978).

My hypothesis above explains how mean pressure and peak systolic pressure *per se* overcome critical closing pressures. Unfortunately it does not explain why increased pulse rate/decreased stroke volume conditions reduced lamellar perfusion, when mean pressure rose slightly and offset any reduction in systolic pressure, and why there was increased lamellar perfusion with low pulse rate/high stroke volume conditions. A fall in interstitial pressure could lower the pressure for critical closure in the arterioles. In ling cod there is an extensive venolymphatic drainage of the gills and an increase in lymph flow could decrease interstitial pressure. Many of the lymphatic vessels in the gill are in close association with filament arteries such that there may be a mechanical interaction between the vessels, in particular the afferent companion vessels and filament arteries and arterioles (Plate II, Section I). The effect of the arterio-venolymphatic interaction in trout gills on Rg has been briefly discussed by Smith (1977). Volume changes in the compliant filament vessels *in vitro* that are associated with the pulse pressure may then promote lymphatic drainage. Thus if the pressure pulse increases

then there may be more adequate venolymphatic drainage and a fall in interstitial pressure resulting in a fall in the critial closure pressure of the lamellar arterioles. More effective lymphatic drainage may then by its effect on interstitial pressure lead to lamellar recruitment.

If there are arterio-venolymphatic interactions then venolymphatic flow would alter when arterial flow was changed. In this series of perfusion experiments only the outflow from the EFA (Q_o) was measured. Q_o, although always less than Q_i, increased if either P_i, Q_i or pulse rate was raised. The afferent branchial artery was cannulated and this vessel supplies only the lamellar arterioles. All of Q_i passes through the secondary lamellae and lamellar filtration was not a major alternate pathway for fluid loss. Thus the saline, having perfused the lamellae enters the efferent filament vessel and flows out either by the cannula inserted in the afferent branchial artery or via some other pathway. The efferent circulation gives rise to a recurrent nutrititive supply to the filament that forms a part of an arch venolymphatic drainage and also a hypobranchial arterial supply to the ventral branchial muscles. Both vessels pass ventrally down the gill arch (Fig. 35). The hypobranchial artery was tied off separately and also ligatures were tied around both the afferent and efferent cannulae to seal off the venolymphatic drainage in the arch.

FIGURE 35

Schematic representation of the circulation through the gill lamella and the body of the gill filament indicating the sites of cannulation. (Based on Section I).

→ = flow direction of perfusate

γ = ligature

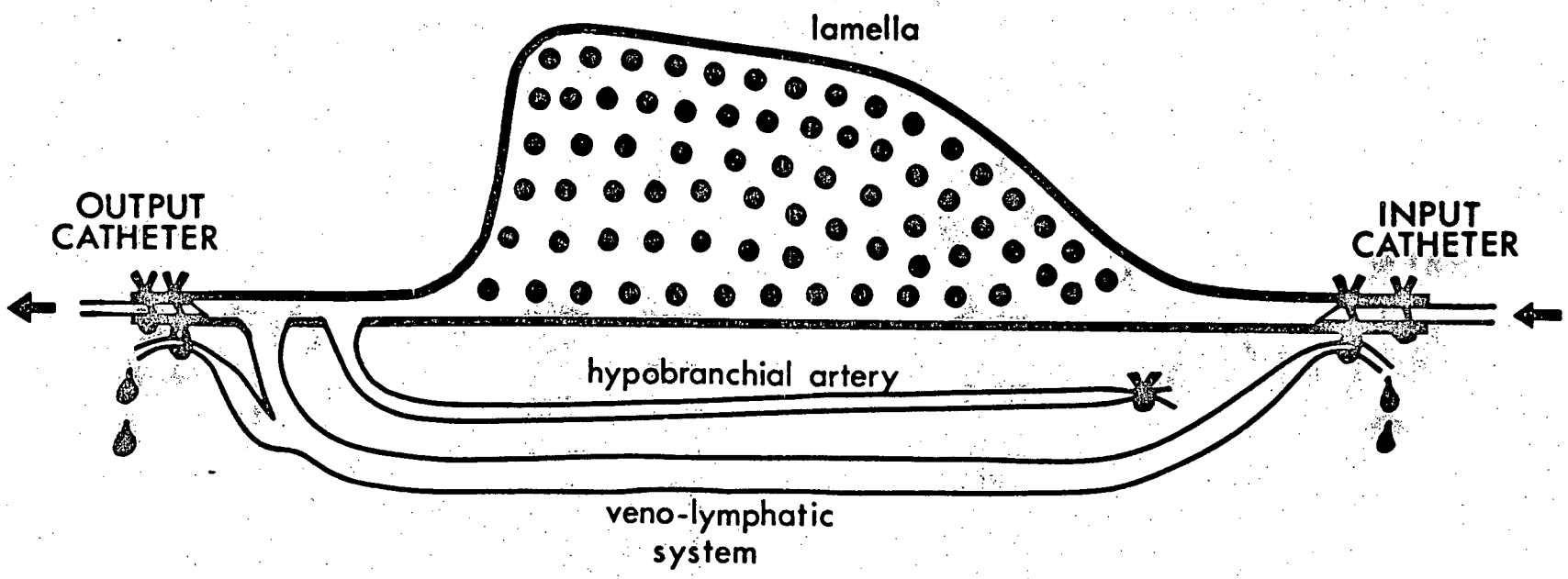
lamella
OUTPUT CATHETER
INPUT CATHETER
hypobranchial artery
veno-lymphatic system

It seems probable, however, that saline leaked out via this venolymphatic supply. Why then should an increase in P_i be associated with a decrease in venolymphatic outflow? One answer is that at higher arterial pressures, compliant arterial vessels expand and compress the venolymphatic vessels, thereby raising the resistance to flow in the venolymphatic system and thus reduce venolymphatic outflow. Such interaction would occur where the lamellar arterioles and venolymphatic vessels interdigitate (See Plates 11 and 12, Section I). Hence the observation that high arterial pulse rates reduced venolymphatic flow is consistant with the concept of the concept of arterio-venolymphatic interactions.

In vitro gills do not act as simple ohmic resistance (Fig. 30) and it is clear that gill compliance must be taken into account (Fig. 29). Under constant flow conditions, a stepwise elevation of P_o decreased Rg without lamellae recruitment and the changes in mean P_i were much smaller than P_o. Vessel dimensions must therefore increase to lower Rg. The extent to which compliance affects overall Rg can be estimated. In these gill perfusion experiments, when Q_i was elevated by a mean value of 76.9%, lamellar perfusion increased from 67.8% to 76.5%. If the gills were a simple ohmic resistance, the mean P_i should have increased by 55%. In fact, mean P_i only rose an average of 37.9%, to later stabilise at 23.5% above the average pre-change mean P_i. When Wood et al. (1978) elevated P_o

in their gill preparation, Rg was decreased and there was little effect on P_i. Clearly, then, the range of the gill compliance *in vitro* and its effect on Rg is indeed considerable. There is, however, an important difference between the vessel tone *in vivo* and *in vitro*. *In vitro* there is little or none, whilst *in vivo* the muscular lined arch and filament arteries and arterioles have resting adrenergic tone (Helgason and Nilsson, 1973; Wood, 1974b; Table III, Section I). The lamellae lack vascular tone and are very compliant (Section I). Swelling of the lamellae and of vessels lacking tone would account for the number of lamellae perfused not being proportional to Rg when pressures and flow regimes are changed.

Decreases in Rg cannot now be taken as unequivocal evidence for lamellar recruitment *in vitro*. They only indicate a change in the pressure profile across certain portions of the gill vasculature that result from changes in vessel dimensions. Of course lamellar recruitment *may* still occur as a result of the changes in the pressure profile. These findings clearly support the predictions made in Section II concerning changes in gill blood flow patterns. It was concluded that elevated Q actually effected the lamellar recruitment, that was initiated by Rg or input pressure changes which represent changes in vessel dimensions. In my experiments in Section III, Q_i was not altered when Rg was lowered and no recruitment was observed. Elevations in $\dot{Q}$ have now been associated with lamellar recruitment *in vivo* and *in vitro*.

The consequences of these findings are important to the interpretation of results in other investigations using *in vitro* preparations. P_i, Q_i, Q_o P_o, pulse rate/stroke volume must all be considered. The pressure needed to overcome critical closure of afferent lamellar arterioles as well as lamellar channels (Section I) will dictate how much of the surface area of the gills is available for diffusion. Arterio-venolymphatic interactions within the gill must also be considered when designing *in vitro* perfusion experiments. In the past these factors were not usually considered. Thus the quantitative interpretation of *in vitro* pharmacological studies will, for instance, be affected by the pressure and flow regimes since *in vitro* vascular compliance is high and vessels will be more or less dilated depending on the regime chosen. In ion and water transport studies the selection of appropriate flows and pressures is imperative, since diffusing capacity will be affected by the number of lamellae perfused and ΔP_{lam}. The ΔP_{lam} dictates capillary fluid filtration rates and low lymphatic clearance rates will increase lamellar diffusion distances. All these changes affect passive exchange quantitatively.

Pulse rate and pulsatility are also important in determining branchial blood flow patterns because of arterio-venolymphatic interactions. Pulsatility will be altered by the tone of the branchial vessels and the bulbus arteriosus. The bulbus was demonstrated to act as a Wind-kessel over a

range of pressures similar to resting VA blood pressures. The degree to which blood flow is depulsed by the bulbus can be altered however, by adrenergic and cholinergic agonists, and hypoxic conditions. What is the importance of these observations in vivo? Changes in VA pulse pressure in the intact fish will depend on a large number of factors, of which the properties of the bulbus is only one. However, with no other changes, adrenergic stimulation would increase depulsation. Hypoxia would have a similar effect, but cholinergic stimulation would increase pulsatility. If blood pressures are elevated at the same time as bulbus stimulation, then an adrenergic action would increase pulsatility, as would a cholinergic action. Adrenergically mediated bulbus compliance changes in vivo appear feasible, since a number of teleosts have sympathetic innervation of the bulbus (Gannon, 1972; Watson, pers. comm.). Sympathetic pathways have not been examined in Ophiodon. Whether cholinergic alterations occur in vivo is speculative since nothing is known concerning cholinergic innervation of the bulbus. The sympathetic innervation of the bulbus in trout is derived as a branch of the largely cholinergic cardiac vagus nerve (Gannon, 1972) and therefore cholinergic innervation may also be present. The effect of hypoxia on the bulbus arteriosus is viewed as an hypoxic vasodilation through reduced vascular tone. Haswell et al. (1978) reported a similar phenomenon in the branchial vasculature of trout. I found no hypoxic vasodilation in isolated perfused gill arches but my preparations had little or

vascular tone, which explains the apparent discrepancy. The importance of hypoxic vasodilation and whether it even occurs *in vivo* is unknown.

In summary, I have now demonstrated that not all lamellae will be perfused in resting ling cod. Increases in Q and input pressure will recruit lamellae automatically, as will condition of reduced heart rate/high stroke volume (pulsatility). Mean and pulse pressures also affect venolymphatic flow rates. Since increases in Q and input pressure will also increase ΔP_{lam} the following changes in gill blood flow patterns can therefore occur in ling cod. Lamellar recruitment, intralamellar shunting, increased lamellar volume and the associated reduced epithelial thickness, and increased venolymphatic flow and associated reduced lamellar intersitial space. All these changes can increase diffusing capacity. They were, however, all demonstrated *in vitro*, *in situ* or *in vivo* when drugs were administered. Do they occur naturally *in vivo*? It is predicted that if O_2 demands increase or O_2 availability decreases one or more of these changes in gill blood flow will be brought about to maintain O_2 transfer at the gills. This prediction is tested in Section IV.

SECTION IV

A STUDY OF GILL BLOOD FLOW AND ITS REGULATION IN OPHIODON ELONGATUS IN VIVO

In vivo monitoring of blood flow and ventilation during the struggle responses.

The effect of an hypoxic and an hyperoxic environment on the cardiovascular system, gill ventilation and oxygen uptake.

INTRODUCTION

Randall et al. (1967) showed that exercise and hypoxia in trout was associated with a change in gill transfer factor for oxygen, To_2, (see page 250 for definition). The increase in transfer factor was subsequently suggested to be caused by changes in branchial blood flow (Randall, 1970; Jones and Randall, 1978). In particular it was suggested that there were changes in both the number of lamellae perfused and the distribution of blood within each lamella.

Gaseous exchange in fish gills is diffusion limited (Fisher et al., 1969; Randall, 1976; Scheid and Piiper, 1976) and lamellar recruitment and the redistribution of blood within the lamella enhance the conditions for diffusion such that elevated $\dot{Q}$ and $\dot{V}g$ (gill ventilation) are associated with increased $\dot{M}o_2$ during exercise (Stevens and Randall, 1967a and b). The capacity of the gills to transfer gases must be enhanced during exercise otherwise the increases in O_2 delivery (ventilation) and removal (blood perfusion) would be pointless. Thus the increases in $\dot{Q}$, $\dot{V}g$ and To_2 are coupled during exercise to enhance $\dot{M}o_2$. During hypoxia To_2 and $\dot{V}g$ are increased to maintain $\dot{M}o_2$ at reduced levels of O_2 in the water (Holeton and Randall, 1967a and b).

Changes in lamellar recruitment have been observed during hypoxia in trout (Booth, pers. comm.) and I have demonstrated a number of ways in which cardiovascular changes

increase gill surface area (lamellar recruitment) and alter diffusion distances (increased sheet thickness, intralamellar shunting and lymphatic drainage) (Sections I, II and III). From the information we have, some of the mechanisms that bring about these changes are evident. All changes in lamellar perfusion can now be explained in terms of automatic changes related to alterations in blood flow and input pressure to the lamellae (Section III). There are no observations of direct humoral or neural actions on the lamellar capillary sheet *per se*.

Humoral agents do, however, produce the changes in blood flow and pressure and some of these effects have been determined for ling cod (Section II). Cardiac output can be regulated by humoral agents affecting heart rate and stroke volume. Cholinergic agonist drugs have negative chronotropic effects, and resting heart rates are influenced by a cholinergic tone. Positive inotropic effects are apparently mediated by β-adrenergic receptors in the heart. The pressor effects produced by ACH and NAD injection *in vivo* were largely a result of direct vascular actions of the drugs, whilst the increased $\dot{Q}$ was reflexogenic, as it could not be accounted for by recirculation of the drugs to the heart. The cardiovascular changes in that were mediated by NAD and ACH in ling cod were concluded to produce alterations in gill blood flow patterns, which would alter To_2 (Section II). Similar cardiovascular changes have been previously demonstrated to affect To_2 in other fish. Adrenaline infusion increased arterial oxygenation *in vitro* in

trout (Wood et al., 1978). Also intravenous injection of adrenaline increased arterial Po_2 and O_2 content in restrained eels (Steen and Kruysse, 1964). These changes in To_2 associated with adrenaline infusion could also be explained in terms of alterations in branchial blood flow and pressure causing automatic changes in lamellar recruitment and perfusion, based on my findings for ling cod.

Thus, whilst I now have reasonably detailed information on how blood flow and pressure may be regulated in ling cod, there are few data on how Mo_2 is affected by blood flow and pressure changes in vivo. The following questions are therefore addressed in this Section. What cardiovascular changes are made in vivo to ensure an O_2 supply that meets tissue demands and how are these changes regulated in vivo. Two experimental approaches were used to answer these questions. In the ocean ling cod are bottom dwellers, and the nearest they appear to come to exercise is burst type swimming. An analogous response was examined here to establish what cardiovascular changes accompany an increased O_2 demand. Secondly, the cardiovascular responses to hypoxia and hyperoxic environments were established to determine what changes can be evoked if environmental O_2 availability is reduced or increased.

MATERIALS AND METHODS

Exposure to hypoxic or hyperoxic water

Routine surgery was performed on 6 ling cod and blood flow and pressures were monitored continuously (See general methods). Gill ventilation and the water oxygen tension (Po_2) were monitored during the experiments. For each experiment the inflowing water to the aquarium was made progressively hypoxic or hyperoxic with N_2 or O_2 gases, respectively. The changing Po_2 stabilized after about 10 min and was maintained at this level for a further 10 to 20 min. The total exposure time was 30 min, or less if the fish struggled excessively. The fish were then returned to normoxic water conditions in a similar but more rapid fashion. The normoxic water Po_2 (160 to 170 mm Hg) was slightly higher than ambient because of a small air leak in the main salt water pump of the building. After each experiment fish were allowed to recover for several hours or overnight prior to further experiments.

Oxygen uptake ($\dot{M}o_2$) determinations

$\dot{M}o_2$ determinations were made on five other fish that had been very lightly anaesthetised (MS222) when being placed into the aquarium and had then been allowed to recover and acclimate overnight. The sealed aquarium was darkened except at one end to allow visual observation of the fish. The gas tension of inflowing water could be altered with O_2 or N_2 gases

(Fig. 36). Mo_2 was measured in two ways. First, using a constant flow-through system (usually 2 $l.min^{-1}$), inlet and outlet water samples were taken simultaneously. The oxygen tensions of the water samples were measured using the Radiometer O_2 electrode.

$$Mo_2 = \frac{\Delta Po_2 . \alpha o_2 . flow}{wt}$$

where Mo_2 was measured in ml $O_2.hr^{-1}.Kg^{-1}$; Po_2 is the difference in the inlet and outlet water oxygen tensions measured simultaneously; αO_2 is the oxygen bunsen solubility constant for 23 o/oo seawater at 10 to 11°C. (Green, 1965). Flow ($l.hr^{-1}$) was measured by regular outflow collection during the experiment. The fish was weighed (kg) prior to the experiment.

A closed box system was also used to measure Mo_2. Here the water was recirculated (Fig. 36) and the fish gradually reduced the water Po_2 due to its own consumption. Water samples were collected at 5 minute time intervals and the water Po_2 measured

$$Mo_2 = \frac{(Po'_2 - Po''_2)\ \alpha\ o_2 . V}{t}$$

where Po'_2 and Po''_2 are water oxygen tensions at the first and second samples of a given time period, t (hr.) and V is the volume of water in the recirculating system = (19.6 - fish wt) in litres.

FIGURE 36

A schematic diagram of the sealed experimental holding aquarium used for measurements of oxygen uptake in ling cod. The plexiglass container was round and darkened. One end was clear to allow visual observations. An aerated water supply could flow directly to the aquarium or be diverted through a gas stripper. Alternatively the water inside the aquarium could be recirculated with the pump.

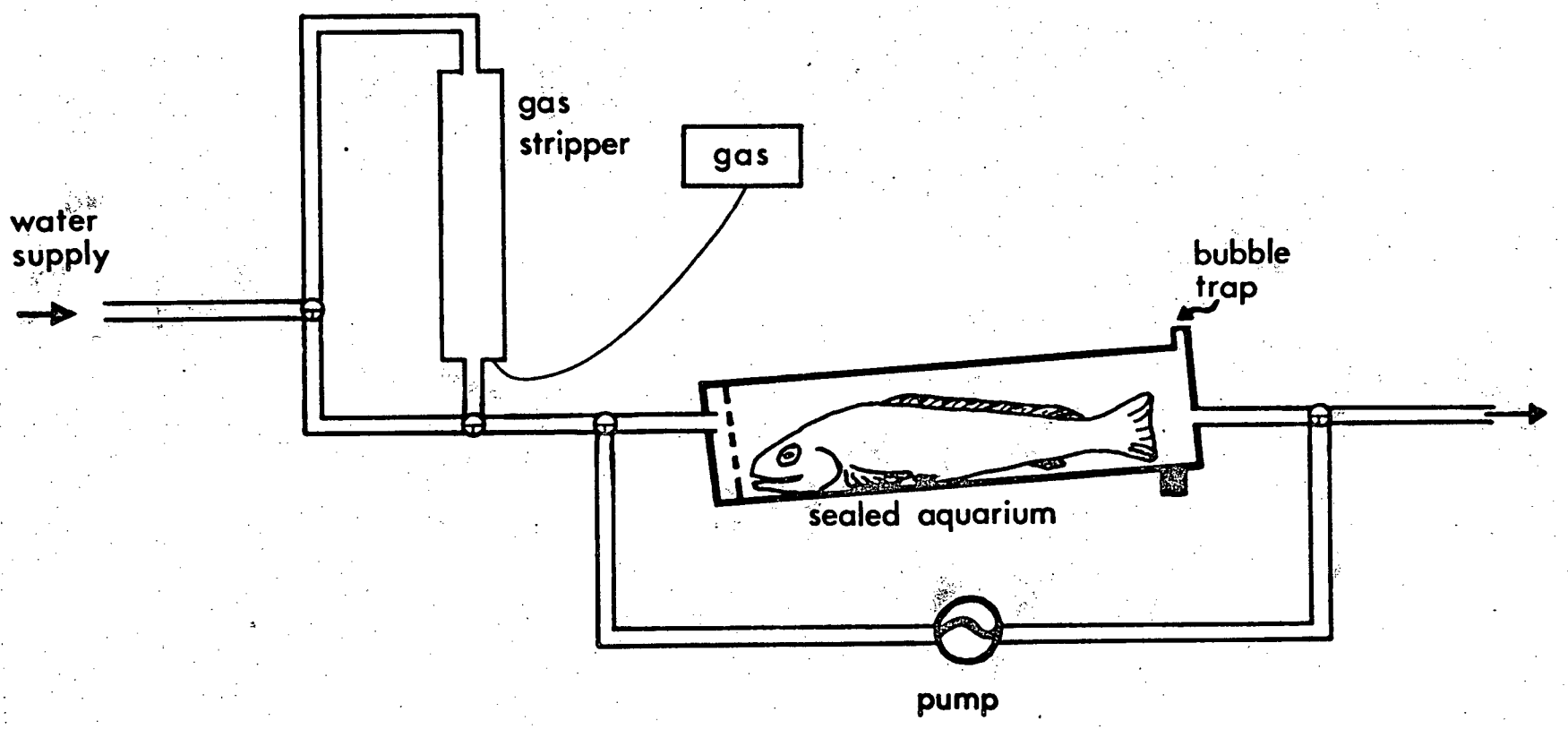
gas
stripper
gas
water
supply
bubble
trap
sealed aquarium
pump

Experimental protocol used during Mo_2 determinations: At least five Mo_2 determinations were made at a normoxic Po_2 for each fish using the flow-through system. These determinations were made during a 30 min period and preceded the experiments using the closed box system.

The effect of hypoxic water conditions on Mo_2 was examined using the closed box system. A 3 min equilibration period was allowed whenever the recirculating system was started. During this time all air bubbles were removed from the system. The first water sample was taken after this 3 min period, followed by two others, 5 min and 10 min later. The Mo_2 was calculated for each 5 min period. This first set of two Mo_2 determinations was made near to normoxic water conditions. The recirculating water was then made progressively hypoxic and further Mo_2 determinations were made. To reduce the water Po_2 the aquarium was flushed with deoxygenated water for 2 minutes. A three minute equilibration period followed the restarting of the pump, before the second set of two Mo_2 determinations were made. Typically each set of Mo_2 determinations was separated by about 6 minutes, during which time the water Po_2 was reduced 5 to 10 mm Hg. This protocol was repeated and four or five sets of Mo_2 determinations were made on each fish as the water became progresively more hypoxic. Progressive hypoxia was stopped at a Po_2 of 20 mm Hg, or when the fish appeared disturbed. Flushing of the aquarium with deoxygenated water prevented CO_2 accumulation in the

recirculating water as well as producing stepwise reductions in water Po_2. Ventilation rate was measured by observing and counting opercular movements over 1 min. period during all Mo_2 determinations. Ventilation amplitude was visually assessed at the same time, where 0.5 = little discernible movement and 5 = maximum flaring of the buccal and opercular cavities.

For details of analysis and graphical techniques see Materials and Methods, Section II.

RESULTS

The struggle response

The resting behaviour of ling cod in the ocean and the resting values for cardiovascular variables and gill ventilation in ling cod have been presented (Section II). Resting ling cod have an $\dot{M}o_2$ of 22.8 ± 0.6 ml $O_2.hr^{-1}.kg^{-1}$ (n=26 for 5 fish). When fish were disturbed in the ocean, they would make 1 or 2 quick lateral tail movements and 'glide' to a new resting position a few meters away. In the holding aquaria I observed a similar behaviour pattern. Similar movements are also used for feeding, which I observed both in the ocean and in the holding aquaria. The fish lie in wait and then pounce quickly on a passing fish. In the experimental aquarium movements were limited but the ling cod's characteristic sharp lateral tail movements were not prevented. The tail movements were visually associated with characteristic respiratory and cardiovascular changes were the "struggle response" (See p14 also). Many struggles were observed and recorded during this investigation. The nature of the struggle generally moved the flow probes or cannulae, which caused artifacts.

Complete artifact free records of all cardiovascular and respiratory variables during struggles were therefore difficult to obtain. Four representative struggles from two different fish were, however, obtained and were suitable for the detailed analysis that was performed here.

Ventilation rate and amplitude both increased after the tail beat of a struggle (Fig. 37). Fish that were seen to struggle frequently had higher $\dot{M}o_2$ values than the more quieter fish (see variability in resting $\dot{M}o_2$ values in Fig. 41 later). During a struggle cardiovascular variables displayed very striking patterns when they changed (Figs. 37 and 38). The tail beat was associated with a) a reduced $\dot{Q}$; b) a marked bradycardia and c) an elevated stroke volume of up to twice the resting value. The bradycardia developed gradually over the two to eight heart beats prior to the tail beat. Stroke volume was elevated during this period and $\dot{Q}$ was maintained. The reduction in $\dot{Q}$ at the tail beat was a very brief and sudden event, with $\dot{Q}$ rising equally rapidly after the first tail beat up to a value 70 to 80% above the resting value. Increased $\dot{Q}$ was largely a result of a tachycardia (of 45 beat.min^{-1} maximum), but stroke volume was still elevated somewhat, albeit declining. Heart rate and stroke volume usually showed reciprocal changes during this phase of the struggle. The $\dot{Q}$ returned to a resting value about 100 sec after the tail beat in three of the struggle responses analysed. In one of the struggle responses, however, $\dot{Q}$ was re-elevated about 1 min after the initial tail beat. Here the stroke volume and heart rate increased in phase with each other and there was no tail beat.

Gill resistance (Rg) remained remarkably stable for most of the time during the struggle (Fig. 31) considering the fluctuations in $\dot{Q}$. The Rg did, however, increase considerably prior to and at the time of the tail beat, but only for several seconds. The increased Rg was associated with the bradycardia.

The Rs also rose just prior to the tail beat, but fell markedly at the time of and after the tail beat (Fig. 39). Rg increased during the second, delayed elevation in $\dot{Q}$ (Fig. 39). As a consequence of the relatively stable Rg during the struggle, the pattern for the ΔPg mean pressure resembled that of $\dot{Q}$ (Fig. 40). The damping of the pressure pulse (ΔPg pulse) displayed a pattern similar to that of stroke volume (Fig. 40), and was also increased when $\dot{Q}$ was elevated during a struggle.

Fish did occasionally struggle for sometime after atropine had been injected via the dorsal aorta, but the elevation of $\dot{Q}$ following the tail beat became much reduced compared to unatropinised fish. The atropine injection gradually blocked changes in cardiac rate and after 1 hr there was no bradycardia associated with tail beats (Fig. 37b). In fact heart rate remained elevated above resting values (Section II). In atropinised fish, tail beats were associated with only small changes in ventilation, unlike resting fish (Fig. 37).

Atropinised fish developed another response where Q was elevated (Fig. 37c). This response was only noticed in atropinised fish (3 fish), and it was much akin to the response produced by a NAD injection into the ventral aorta of resting fish (See Fig. 19). The increased $\dot{Q}$ was not associated with any body movement, unlike the struggle response, and there were major elevations in VA and DA pressures (Fig. 37c). The amplitude and rate of ventilation was noticably unchanged during this response, except for the ventilatory pause at the begining of the response (Fig. 37c).

FIGURE 37

Records of cardiovascular and respiratory varibles taken simultaneously during three types of "struggle response" typically seen in ling cod. In all cases $\dot{Q}$ = cardiac output ($ml.min^{-1}.kg^{-1}$), hr = beat to beat heart rate ($beats.min^{-1}$), VA = ventral aorta blood pressure (cm H_2O), DA = dorsal aorta blood pressure (cm H_2O), OP = opercular pressure (cm H_2O). All pressures were measured from ambient pressure (amb). The start of tail movements are indicated by solid vertical bars at the bottom of the figure.

A. The first trace shows a struggle with a single tail beat and the second trace illustrates the effect of several tail beats.

B. The effect of atropine injection with time (+ 15 min, + 24 min and + 48 min). The cardiovascular events associated with tail movements are reduced, there is a tachycardia with no beat to beat rate fluctuations.

C. Two records of a response peculiar to atropinised fish (+ 65 and + 95 min after injection) which caused elevations in $\dot{Q}$ and blood pressures. This response was not associated with a tail movements and can be contrasted with Fig. 37A and compared with Fig. 19.

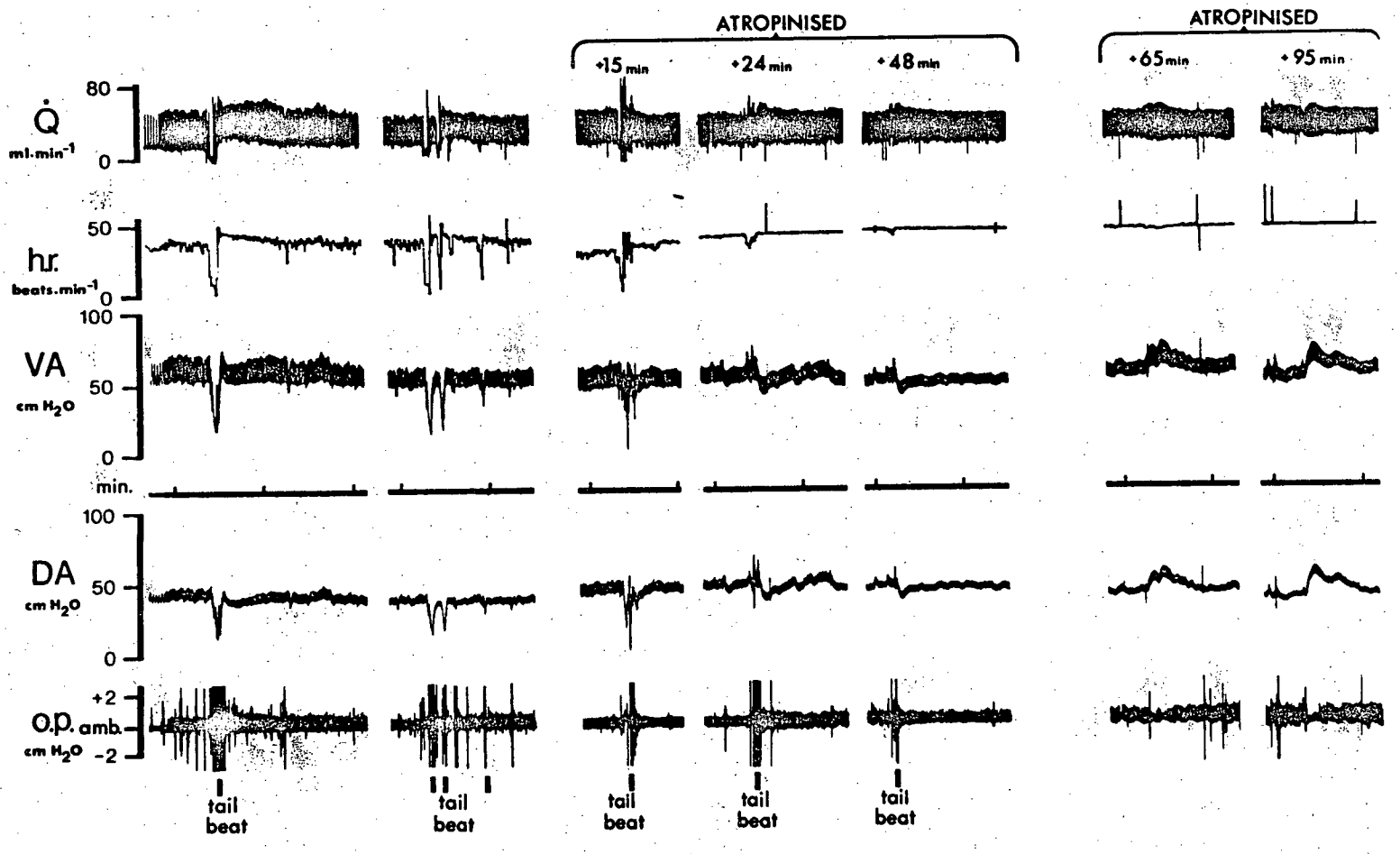
ATROPINISED
ATROPINISED
+15 min
+24 min
+48 min
+65 min
+95 min
Q̇
ml.min⁻¹
80
0
hr.
beats.min⁻¹
50
0
VA
cm H2O
100
50
0
min.
DA
cm H2O
100
50
0
O.P.
cm H2O
+2
amb.
-2
tail beat
tail beat
tail beat
tail beat
tail beat

FIGURE 38

A summary of the analysis of the cardiovascular variables during four typical struggle responses in ling cod. All values were measured simultaneously. Each point represents an individual value for cardiac output ($\dot{Q}$), stroke volume (S.V.) and heart rate (h.r.). The resting value for each variable is also known. The tail movements started when t = 0.

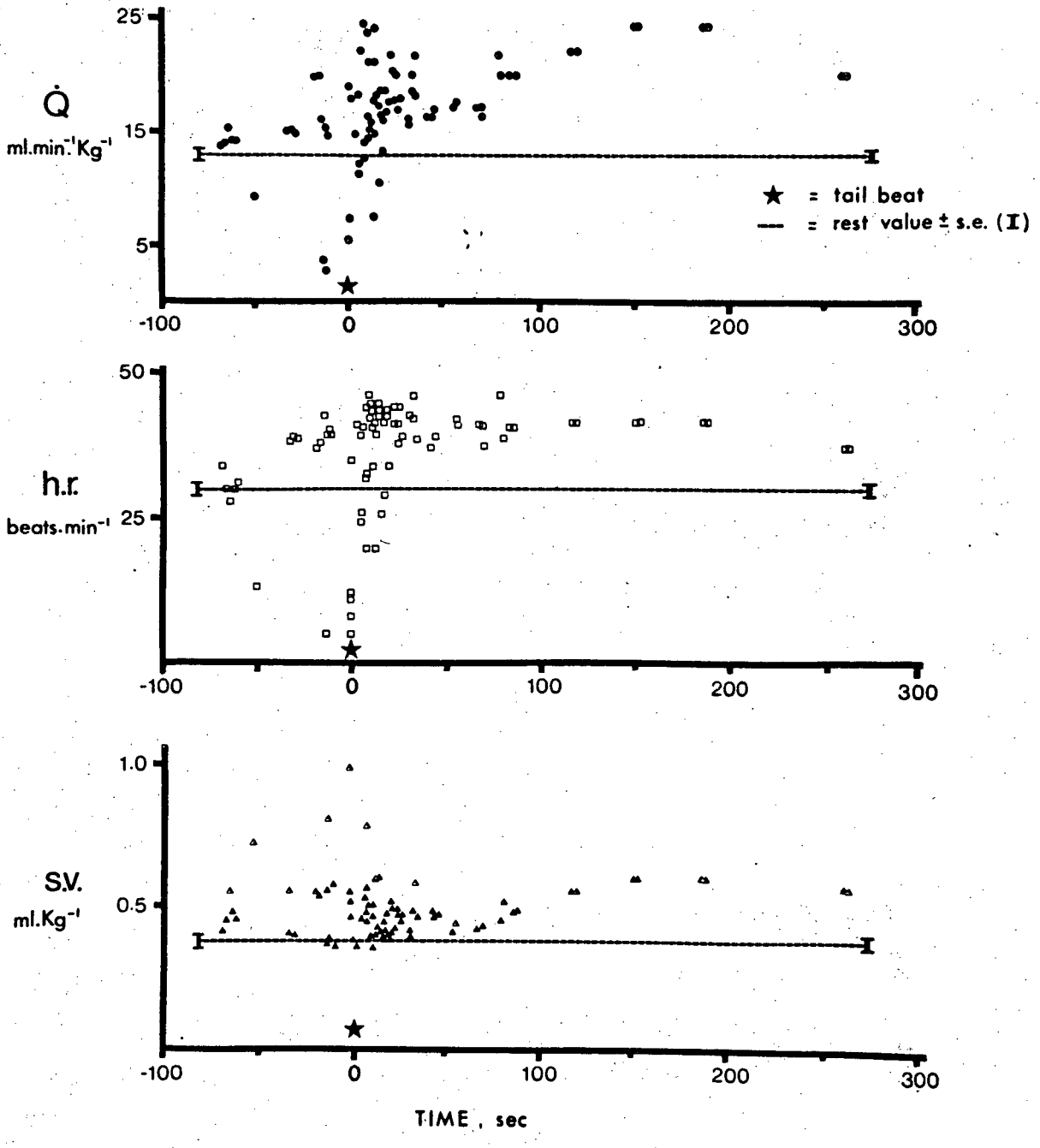
Q̇
ml.min⁻¹Kg⁻¹
25
15
5
★ = tail beat
— = rest value ± s.e. (I)
h.r.
beats.min⁻¹
50
25
S.V.
ml.Kg⁻¹
1.0
0.5
-100
0
100
200
300
TIME, sec

FIGURE 39

A summary of the analysis of the resistance to blood flow in the branchial (Rg) and systemic (Rs) circulations during four typical struggle responses in ling cod. See the legend of figure 38 for further explanation of this figure.

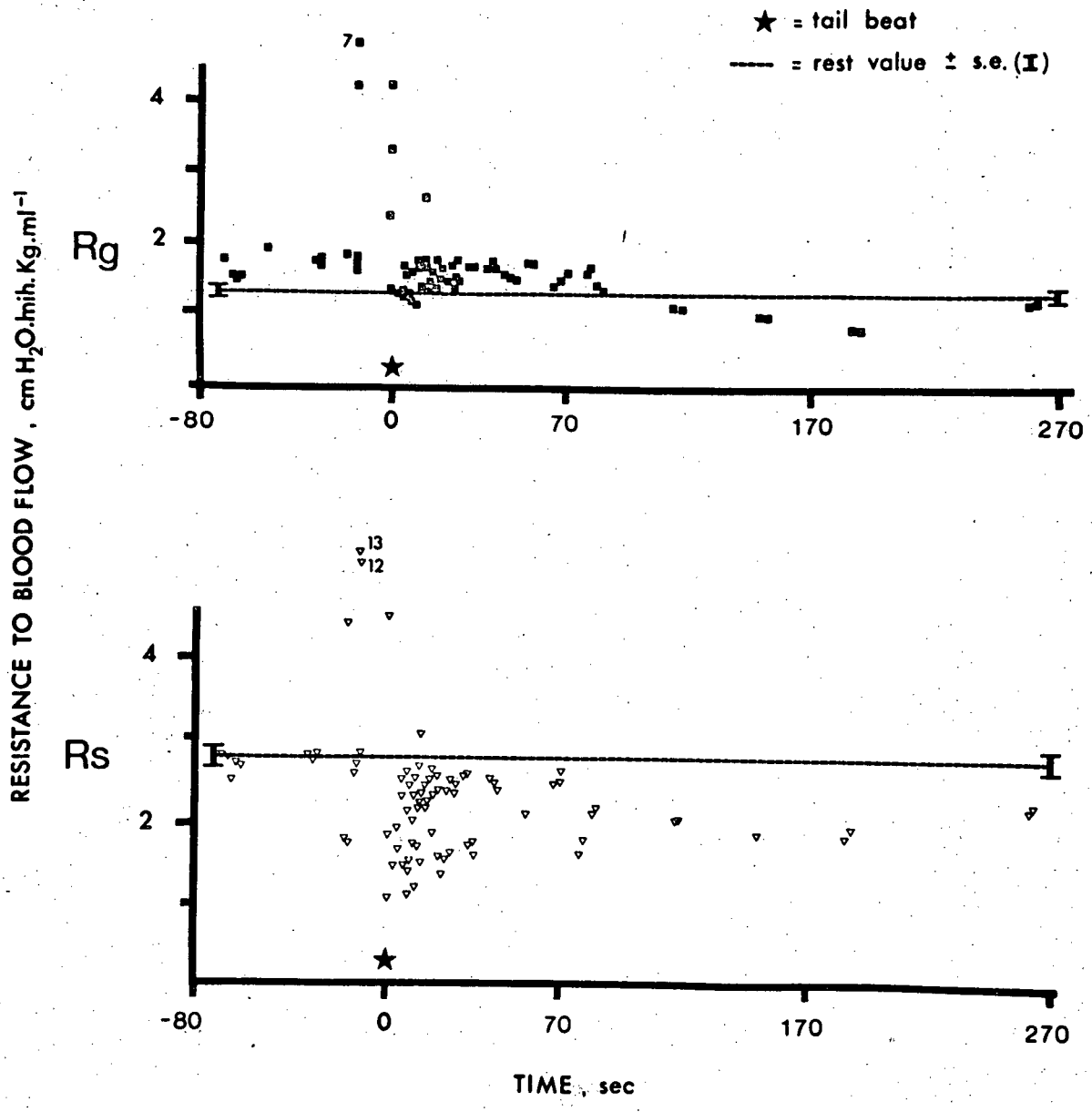
★ = tail beat
—— = rest value ± s.e. (I)
RESISTANCE TO BLOOD FLOW , cm H2O.hih.Kg.ml-1
Rg
Rs
7
13
12
4
2
-80
0
70
170
270
TIME , sec

FIGURE 40

A summary of the analysis of changes in blood pressures across the gill bed during four typical struggle responses in ling cod. ΔP_g mean is the change mean blood pressures across the gills. ΔP_g pulse is the change in pulse blood pressure, which indicates the degree of damping of pulsatile flow. See the legend of figure 38 for further explanation of this figure.

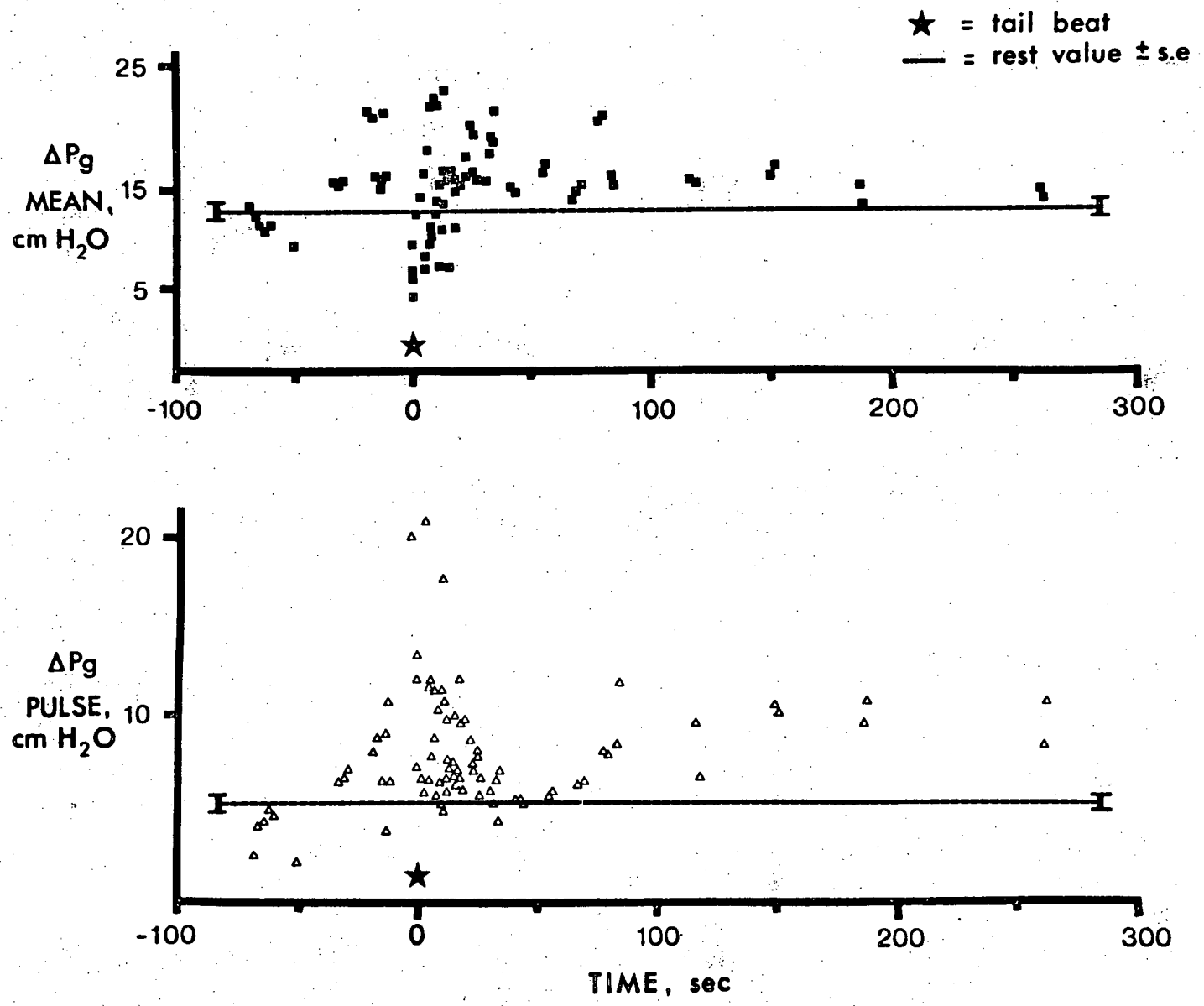
★ = tail beat
— = rest value ± s.e
ΔPg MEAN, cm H2O
25
15
5
-100
0
100
200
300
ΔPg PULSE, cm H2O
20
10
-100
0
100
200
300
TIME, sec

The effects of exposure to hypoxic water

Ventilation: Increases in ventilation rates and amplitude accompanied progressive hypoxia, but these changes were out of phase with each other (Fig. 41). Ventilatory amplitude increased before ventilation rate as the water Po_2 was reduced. Furthermore, maximum ventilatory amplitude i.e. full distension of the buccal and opercular cavities, was attained at a water Po_2 of 70 to 80 mm Hg, whilst peak ventilation rate (30 breaths.min^{-1}) was reached at 50 - 60 mm Hg water Po_2. The maximum ventilatory activity was sustained at water Po_2 levels as low as 20 mm Hg.

Oxygen uptake: The Mo_2 was elevated during progressive hypoxia and reached a peak value when the water Po_2 was 70 to 80 mm Hg (P_{crit}). The Mo_2 at P_{crit} was 51.3±11.7 ml $O_2.hr^{-1}.kg^{-1}$ (n=5 fish), but the range of P_{crit} exceeded resting values by 75% to 300%. Below a water Po_2 of 40 mm Hg, Mo_2 was reduced (Fig. 41).

Cardiac output: This was usually maintained or slightly elevated when the water Po_2 was above 70 to 90 mm Hg (Fig. 42). Fish would struggle during the hypoxic exposure (Fig. 43), but these struggles have been analysed separately (see above) and are not included here. The Q was reduced when the water Po_2 was below 60 to 70 mm Hg and it was reduced to 69% of the resting value at

the termination of the progressive hypoxia (t=O, Table XI), when the water Po_2 was as low as 20 mm Hg. The Q was reduced as a result of a marked bradycardia. The effect of the bradycardia on Q was, however, greatly offset by a concomitant increase in stroke volume (Fig. 42 and Table XI).

Upon progressive reoxygenation of the hypoxic water Q was elevated above resting values; although the water Po_2 was below normoxic levels. The Q was elevated as a result of a tachycardia and a small increase in stroke volume. The subtle increase in stroke volume displayed by each fish was not evident when the mean values were statistically compared (Table XI) due to the large range values for stroke volume between fish. The fish did not struggle at a reduced water Po_2 when the water was being progressively reoxygenated after hypoxic exposure.

Gill resistance (Rg) and systemic resistance (Rs): The Rg changes during progressive hypoxia were not marked until water Po_2 tensions were below 70 mm Hg, when Rg became elevated, with a peak value at about 40 mm Hg (Fig. 44). Hypoxic exposure was terminated at a water Po_2 below 40 mm Hg, and Rg had generally declined from the peak value but was still elevated above the rest value (Table XI, Fig. 44). The Rs increased more markedly than Rg during hypoxia and also displayed at peak value at about a water Po_2 of 40 mm Hg (Fig. 44, Table XI). Rs also declined in some fish at Po_2 values lower than 40 mm Hg.

During the first five minutes of the reoxygenation of the hypoxic water Rs was reduced significantly, despite below normoxic Po_2 levels (Table XI). The Rg, however, was at a value in between the elevated value at t = 0 and the resting value (Table XI).

During progressive hypoxia the ΔP_g pulse was increased compared to that in resting fish. The ΔP_g was also elevated during the reoxygenation of hypoxic water when Q was elevated (Table XI).

FIGURE 41

The effect of environmental hypoxia on oxygen uptake (Mo_2) and ventilation rate and amplitude (arbitrary units) in 5 ling cod. The oxygen uptake during progressive hypoxia for each fish is presented as a continuous line. These determinations were made in the "closed box" system. The Mo_2 values joined by a vertical line at the normoxic Po_2 are resting values determined using the "flow-through" system. Each point for the ventilation variables is an individual value, but many values overlap.

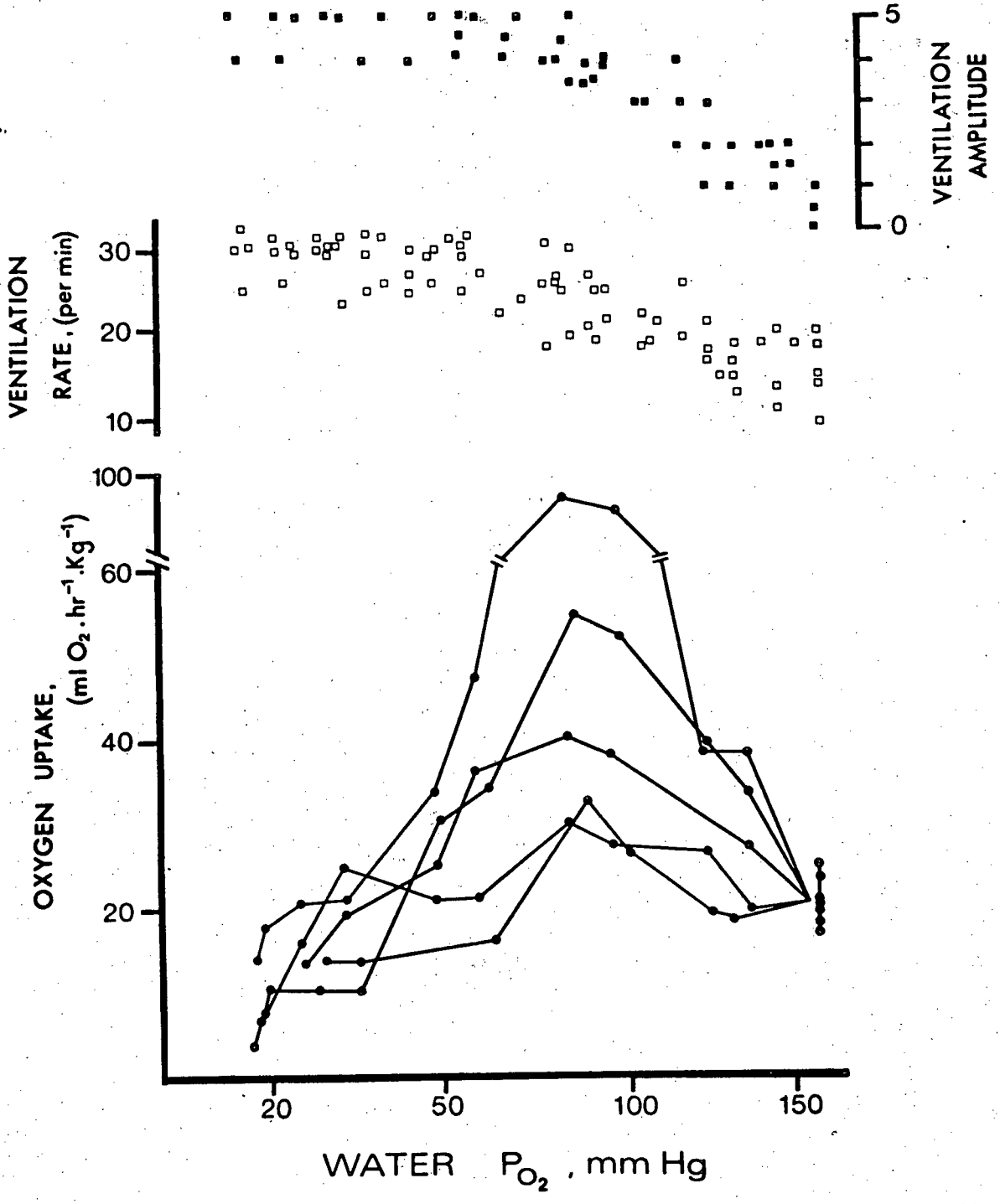
VENTILATION AMPLITUDE
5
0
VENTILATION RATE, (per min)
30
20
10
OXYGEN UPTAKE, (ml O_2 . hr^{-1} . Kg^{-1})
100
60
40
20
20
50
100
150
WATER P_{O_2} , mm Hg

FIGURE 42

A summary of the analysis of cardiac output (Q), heart rate (h.r.) and stroke volume (S.V.) during the progressive hypoxic exposure in 6 ling cod. Individual values are plotted and the resting value is indicated as a reference.

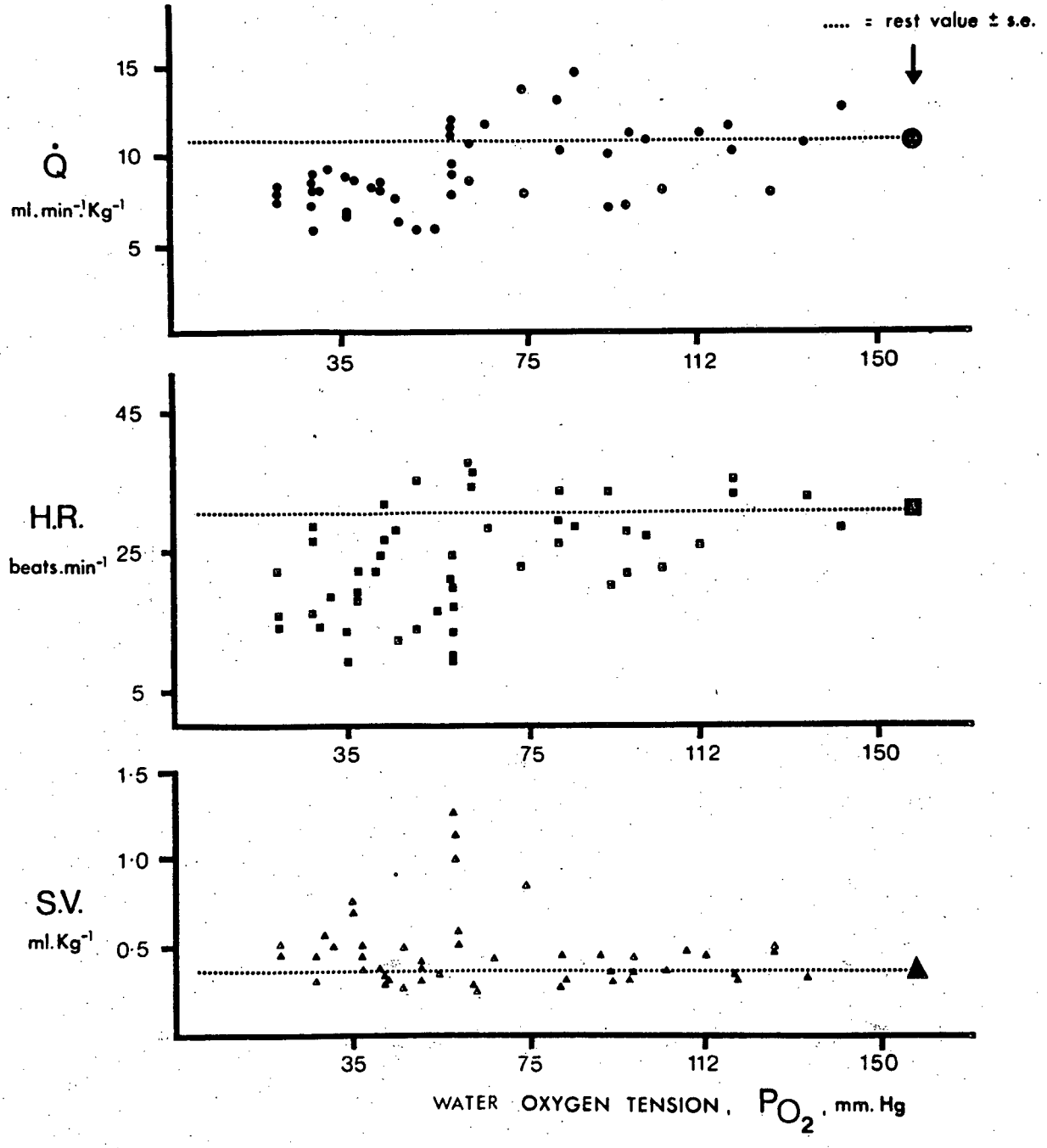
..... = rest value ± s.e.
$\dot{Q}$
ml.min⁻¹Kg⁻¹
15
10
5
35
75
112
150
H.R.
beats.min⁻¹
45
25
5
35
75
112
150
S.V.
ml.Kg⁻¹
1·5
1·0
0·5
35
75
112
150
WATER OXYGEN TENSION, P_{O_2}, mm. Hg

FIGURE 43

The cardiovascular responses of a ling cod to exposure to progressive environmental hypoxia and then reoxygenation of the water. The four selected areas are taken from a continuous record. "Rest" is prior to the experiment "N_2 on" represents the start of water deoxygention. The "9th min" is a selected trace continuing from the 9th min of exposure to progressive hypoxia. The "15th min" section displays the termination of the hypoxic exposure in the 18th min (t = 0) when N_2 was turned off and "air turned on". It can be seen that reoxygenation was much faster than deoxygenation. Note the synchrony between the heart beat and breathing during the 9th min of progressive hypoxia. See Fig. 37 for explanation of abbreviations used.

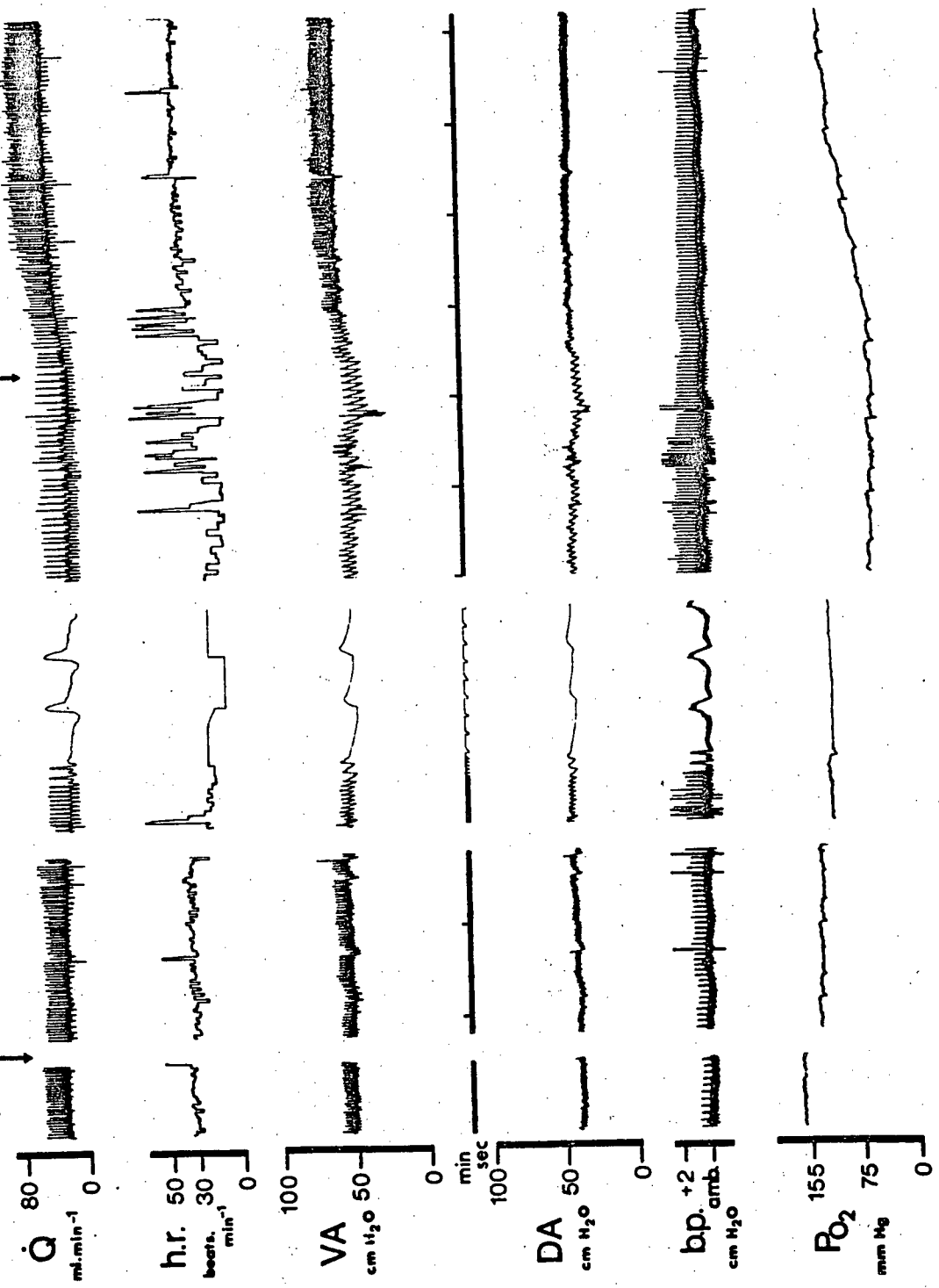
REST
N2 on
9th min
15th min
AIR on
t=0
Q̇
ml.min-1
80
0
h.r.
beats. min-1
50
30
0
VA
cm H2O
100
50
0
min
sec
DA
cm H2O
100
50
0
bp.
cm H2O
+2
amb.
PO2
mm Hg
155
75
0

TABLE XI

A/ The effect of hypoxia on mean values s.e. (n values) for measured cardiovascular variables in 6 ling cod. Resting values were obtained prior to the exposure, and are statistically compared with t = 0 values (representing the termination of progressive hypoxia) and t = +1 to +5min values (representing the first 5 min of reoxygenation of hypoxic water). Statistical differences are indicated by *. VA mean, VA pulse, DA mean and DA pulse are the mean and pulse pressures (cm H_2O) in the ventral aorta and dorsal aorta.

B/ The affect of hypoxia on cardiovascular variables calculated from those variables measured in Table XI A above. $\dot{Q}$ = SV x HR, ΔPg = VA mean - DA mean, ΔPg pulse = VA pulse - DA pulse. Rg = $\Delta Pg/\dot{Q}$, Rs = DA mean/$\dot{Q}$.

Abbreviations are as explained above.

TABLE XI

A/

	Rest(n=18)	t=0(n=6)	t=1to+5(n=14)
Heart Rate beats.min^{-1}	29.4 ± 0.9	12.1 ± 1.2*	32.8 ± 1.9*
Stroke Volume ml.kg^{-1}	0.384 ± 0.015	0.696 ± 0.108*	0.421 ± 0.028
VA mean	51.7 ± 0.5	46.0 ± 1.6*	57.7 ± 1.5*
VA pulse	12.2 ± 0.5	22.3 ± 1.8*	15.5 ± 0.9*
DA mean	38.5 ± 0.6	32.5 ± 1.3*	38.4 ± 1.1
DA pulse	6.1 ± 0.3	7.4 ± 0.8*	6.0 ± 0.2

B/

	Rest	t=0	t=1 to 5 min
Cardiac output,Q ml.min^{-1}.kg^{-1}	11.2 ± 0.4	7.7 ± 0.5*	13.0 ± 0.7*
Rg	1.20 ± 0.09	1.88 ± 0.23*	1.49 ± 0.61
Rs	3.58 ± 0.20	4.67 ± 0.19*	3.23 ± 0.19
ΔPg	13.3 ± 0.8	13.6 ± 1.2	18.9 ± 1.3*
ΔPg pulse	6.1 ± 0.4	8.5 ± 1.5*	9.7 ± 0.7*

FIGURE 44

A summary of the analysis of the resistance to blood flow through the gill (Rg) and systemic (Rs) circulations during the progressive hypoxic exposure in 6 ling cod. Individual values are presented and the resting value is indicated.

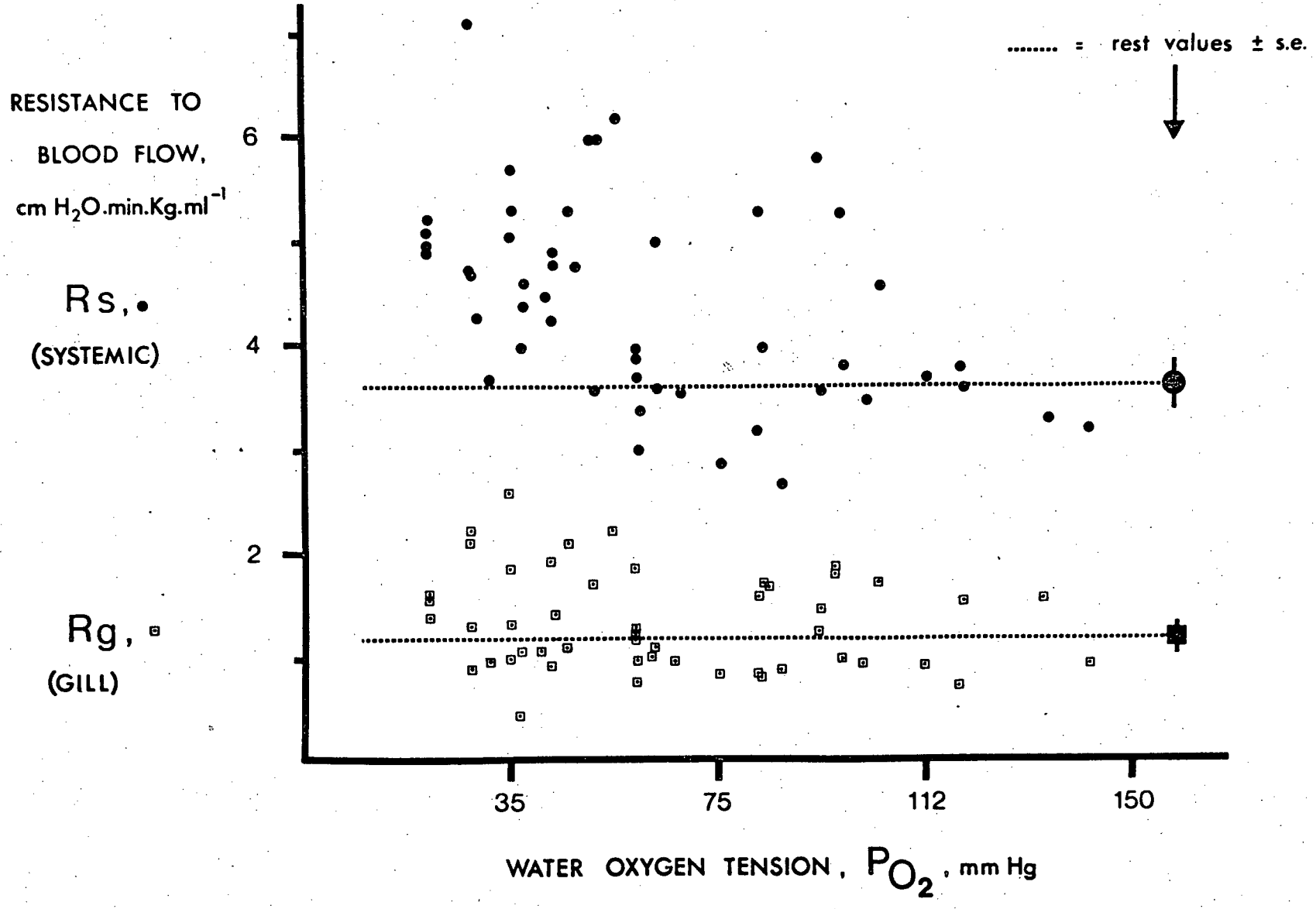
RESISTANCE TO BLOOD FLOW, cm H_2O.min.Kg.ml^{-1}
Rs, •
(SYSTEMIC)
Rg, ▫
(GILL)
6
4
2
35
75
112
150
..... = rest values ± s.e.
WATER OXYGEN TENSION, P_{O_2}, mm Hg

The effects of exposure to hyperoxic water

Progressive hyperoxia up to 90% O_2 saturated produced few cardiovascular changes. There were small changes in the mean values for VA mean and DA mean pressures at t = 0. (Table XII). Only in one of the four experiments were $\dot{Q}$ and stroke volume reduced markedly.

TABLE XII

A/ The affect of hyperoxia on measured cardiovascular variables in 4 ling cod. For an explanation of the abbreviations see Table XI.

B/ The effect of hyperoxia on cardiovascular variables calculated from those variables measured in Table XII A above.
See Table XI for an explanation of the abbreviations used.

 TABLE XII

A/

	Rest (n=12)	t=0 (n=4)	t=1to+5min (n=8)
Heart Rate beats.min^{-1}	29.5 ± 0.9	27.3 ± 1.7	28.9 ± 0.8
Stroke Volume ml.kg^{-1}	0.348 ± 0.026	0.303 ± 0.041	0.309 ± 0.025
VA mean	53.2 ± 0.5	49.4 ± 0.7*	50.4 ± 1.1*
VA pulse	11.9 ± 0.3	11.4 ± 0.4	11.1 ± 0.4*
DA mean	40.8 ± 1.0	38.1 ± 2.1	38.1 ± 1.2*
DA pulse	5.4 ± 0.4	4.6 ± 0.7	5.0 ± 0.5*

B/

	Rest	t=0	t=1to+5min
Cardiac output, Q ml.min^{-1}.kg^{-1}	10.2 ± 0.8	8.5 ± 1.6	9.0 ± 0.9
Rg	1.27 ± 0.10	1.61 ± 0.54	1.29 ± 0.18
Rs	4.00 ± 0.21	4.48 ± 0.25	4.23 ± 0.23
ΔPg	12.4 ± 0.9	11.3 ± 1.6	11.9 ± 0.7
ΔPg pulse	6.4 ± 0.1	6.9 ± 0.3	6.1 ± 0.3

DISCUSSION

The struggle response in ling cod

My visual observations confirm that the struggle response analysed here is one form of exercise normally found in ling cod. The struggle response is characterised by a tail movement. A bradycardia precedes, and an increase in $\dot{Q}$ follows the tail movement. Stevens et al., (1972) made observations on exercising and disturbed ling cod, but their analysis was less detailed and they only reported the marked bradycardia and concurrent reduction in $\dot{Q}$. Increased $\dot{Q}$ during swimming has also been observed in trout (Stevens and Randall, 1967b; Kiceniuk and Jones, 1977) and dogfish (Piiper et al., 1977).

The analysis presented here revealed two striking points. First, cardiovascular changes during the struggle show patterns which reveal clear interrelationships between the variables. Heart rate and $\dot{Q}$ shared a similar pattern. Stroke volume had a different pattern to heart rate, but it was similar to the pattern of ΔP_g pulse. In ling cod, therefore, heart rate has the major influence on $\dot{Q}$. This conclusion differs from those for trout and dogfish, where increases in $\dot{Q}$ during exercise are largely brought about through increased stroke volume (Stevens and Randall, 1967b; Kiceniuk and Jones, 1977; Piiper et al., 1977). Secondly, during the struggle response, Rg changes were small compared with flow changes except for the brief, but dramatic rise in Rg prior to and at the tail beat. Similarly in exercising trout Rg remains relatively unchanged (Stevens

and Randall, 1967) or increases (Kiceniuk and Jones, 1977). The elevated $\dot{Q}$ during struggling will recruit lamellae, which is consistent with the observed increase in the damping of the pressure pulse. Lamellar recruitment and no other changes should, however, reduce Rg.

Why does lamellar recruitment not alter Rg during the struggle response if the major gill resistance resides in the lamellar unit? $\dot{Q}$ must be elevated to effect lamellar recruitment. One explanation is that the increased flow is the same or nearly the same as the increased blood volume of the gills, as a result of lamellar recruitment and increased vascular sheet thickness (Section I), and thus any potential change in Rg is offset. This explanation is supported by calculations of increased flow and potential changes in Rg due to lamellar recruitment in my experiments. Resting ling cod probably perfuse about 60% of their lamellae at rest (Section III) and if during a struggle all lamellae were perfused, Rg could decrease by 66% with no other changes. During the struggle response $\dot{Q}$ is increased by 70 to 80%, which would clearly offset the potential effect of lamellar recruitment on Rg. Any discussion of the important changes in vascular dimensions during the struggle response would be speculative since little is known concerning vascular compliance *in vivo*, except that the lamellae are the major gill compliance site.

The tail beat does not initiate the struggle response. There is a preceding bradycardia which indicates some anticipation of the tail beat. The bradycardia reduces $\dot{Q}$ even though stroke volume is increased due to increased filling times and assuming

unimpeded venous return. The bradycardia can result from an increase in cholinergic tone to the heart. The Rg also increased concurrently. Increased Rg can be produced by a cholinergically mediated branchial vasoconstriction (Section II). It is proposed that the observed bradycardia and increased Rg are both produced by a short-lived increase in vagal cholinergic activity. Atropine, which blocks cholinergic receptors, prevented the bradycardia and the increase in Rg during a struggle response.

The elevated $\dot{Q}$ and tachycardia displayed by exercising trout or dogfish may be related excitatory cardiac effects of circulating catecholamines during exercise. These hormones are known to increase during exercise in trout (Randall et al., pers. comm.) and also during stress in salmon (Mazeaud et al., 1977), Gadus (Nilsson et al., 1976) and dogfish (Butler et al., 1978). The importance, if any, of adrenergic mechanisms during the struggle response in Ophiodon is difficult to determine. However, the second, delayed elevation of $\dot{Q}$ has many similarities to cardiovascular excitation through circulating catecholamines (Section II), in which there is elevated $\dot{Q}$, elevated VA mean pressure, no change in ΔP_g mean and an increased damping of the pressure pulse. The simultaneous elevations of stroke volume and heart rate, without tail beats, indicates an adrenergically mediated inotropic effect in addition to a loss of cholinergic tone to the heart (Section II). Ling cod are also apparently capable of adrenergically mediated cardiovascular responses. In atropinised fish spontaneous cardiovascular changes occur without a tail beat. There is an elevated $\dot{Q}$ and pressor response without any heart

rate change (Fig. 37), which are very similar to the cardiovascular changes brought about by a NAD injection into the ventral aorta of resting ling cod. There is even the characteristic respiratory pause associated with the initiation of the pressor response (Fig. 37). It is interesting that Stevens et al., (1972) noted that exercise in atropinised ling cod was accompanied by an elevated $\dot{Q}$ and no heart rate changes. Ling cod, therefore, probably can and do release catecholamines during stressful situations like other fish.

I propose that the struggle response in ling cod is largely cholinergically mediated and results in lamellar recruitment with a matched elevation in blood flow. Increased $\dot{Q}$ also alters intralamellar flow to further increase diffusing capacity. The increased diffusing capacity, $\dot{Q}$, and $\dot{V}g$ permit an elevation in $\dot{M}o_2$ to meet the increased tissue O_2 demands during the struggle.

Exposure to hypoxic water

During hypoxia ling cod elevated their $\dot{M}o_2$ as much as threefold and maintained $\dot{M}o_2$ levels even at water Po_2 as low as 40 mm Hg. My observations show a peak $\dot{M}o_2$ associated with maximum ventilatory activity at the water P_{crit} of 70 mm Hg. Qualitatively similar observations have been made for trout (Holeton and Randall, 1967 a and b). Ling cod can elevate or maintain their $\dot{Q}$ at Po_2 levels above the P_{crit}. The effect of periodic struggles is to further increase $\dot{Q}$ by 70 to 80% for short periods (see above). Struggling, which occurred to a

variable extent, is therefore in itself an important response to hypoxia. Oxygen delivery to and O_2 removal from the gills are clearly increased during hypoxia.

It is clear that the increased perfusion during hypoxia cannot per se account for the observed threefold elevation in $\dot{M}o_2$. The rate of diffusion must also change, which would involve changes in surface area, diffusion distances and Po_2 gradients. Thus diffusion limitations must be operative during hypoxia in ling cod, a conclusion first made for trout (Randall et al., 1967). This conclusion is consistent with gas transfer in fish being diffusion limited (Fisher et al., 1969; Randall, 1976; Piiper and Scheid, 1976).

How then do observed cardiovascular changes in ling cod relate to the altered To_2 during hypoxia? The noted cardiovascular events are those associated with the bradycardia and those with struggling. These observed cardiovascular events can promote lamellar recruitment, intralamellar shunting, lamellar volume changes and elevated venolymphatic flow, as will be deduced below. All these changes increase the gill diffusing capacity (Section III). The effects of struggling on To_2 have already been discussed in detail. Lamellar recruitment occurs during hypoxia when the fish struggles. Bradycardia per se will also promote lamellar recruitment based on the in vitro findings (Section III) since this is a condition of high stroke volume/low heart rate. The bradycardia probably maintains a higher

percentage of lamellae perfused in between struggles than are perfused during resting states. If this is the case then a condition of high lamellar perfusion will exist during hypoxia in ling cod, which is similar to the observed lamellar recruitment during hypoxia in trout (Booth, pers. comm.). A high pulse pressure/low heart rate condition also enhances venolymphatic flow (Section III). Improved venolymphatic flow may result in better drainage of the lamellar interstitial space. If this is true, then the blood-water diffusion barrier will be reduced during hypoxia.

The increase in Rg during hypoxia is due to a cholinergically mediated vasoconstriction of the branchial outflow arteries (Section II). As discussed above this alters gill blood flow patterns through an elevated ΔP_{lam}, provided $\dot{Q}$ is elevated. During hypoxia $\dot{Q}$ is elevated at Po_2 levels above the P_{crit}, but at Po_2 levels below the P_{crit}, $\dot{Q}$ is no longer maintained and $\dot{M}o_2$ is no longer maximal (Fig. 41). O_2 delivery, however, remains maximal. As $\dot{Q}$ falls, so will ΔP_{lam} and lamellar recruitment. It is suggested that because ling cod are unable to maintain $\dot{Q}$ below the P_{crit}, Rg is increased to compensate and thus maintain the ΔP_{lam} to some degree. This strategy is successful to an extent since below the P_{crit}, oxygen uptake can still be elevated (Fig. 41).

Ling cod lack a coronary blood supply and thus myocardial O_2 supply is derived from the venous blood. Hypoxia in

trout is associated with reduced venous Po_2 levels (Holeton and Randall, 1967b), which is likely to be true for ling cod as well. If it does occur and there are no other changes, myocardial hypoxia will develop. Myocardial hypoxia will reduce the force of cardiac contraction in fish (Gesser, 1978). One strategy which may maintain myocardial O_2 supply is to increase blood residence time in the heart through a bradycardia. This strategy however involves a compromise between maintaining myocardial activity and reducing $\dot{Q}$ since the heart rate has the major influence on $\dot{Q}$. Ling cod, however, can maintain a certain degree of status quo in the face of bradycardia, because $\dot{Q}$ can be maintained with increased stroke volumes (Starling's law). With progressive hypoxia venous Po_2 levels must ultimately fall so low that prolonged residence times can no longer maintain myocardial O_2 supply, and $\dot{Q}$ is reduced.

The cholinergically mediated cardiovascular changes associated with hypoxia are similar to those observed to precede the tail movements during the struggle response in ling cod. In other fish (tench; Randall and Shelton, 1962, and dogfish; Kent and Pierce, 1975) the hypoxic bradycardia is prevented by atropine injection. Thus these changes appear widespread amongst fish. In the preceding discussion it was suggested (not demonstrated) that these cholinergically mediated changes enhanced lamellar recruitment, reduced diffusion distances and helped maintain cardiac performance, all of which affect To_2. The

findings of Taylor et al., (1977) add credence to these suggestions since they have established the importance of cholinergic mechanisms in maintaining To_2 during hypoxia in dogfish. In their work, at any given level of environmental hypoxia, the arterial Po_2 was always lower in dogfish in which cholinergic mechanisms had been prevented by atropine injection or vagi sections, compared with intact fish. Since the qualitative and quantitative cardiovascular responses to hypoxia are similar in both ling cod and dogfish, it is likely that the cholinergically mediated changes also have important effects on To_2 in ling cod.

The analysis of cardiovascular responses of ling cod to aeration of hypoxic water is difficult to interpret since the water Po_2 increased rapidly. There were, however, significant cardiovascular changes (Table XI, Fig. 43), which resembled those observed after NAD had been injected into the ventral aorta of resting ling cod (Section II). Heart rate reached 45 beats.min^{-1}, $\dot{Q}$ increased up to 50%, stroke volume was elevated, there was a pressor response and ΔPg pulse increased. Such changes will change the pattern of gill blood flow, increase the gill diffusing capacity and, therefore, the gill To_2 would be increased. These changes are consistent with the observed increase in $\dot{M}o_2$ in ling cod during the aeration of hypoxic water. A possible involvement of adrenergic mechanisms in the flow and pressure changes associated with the increase in transfer factor cannot be discounted.

Hyperoxia was not associated with marked cardiovascular changes. Although conditions for oxygen diffusion are greatly enhanced in this experimental situation, no changes in gill perfusion were apparent. It is suggested, therefore, that resting ling cod perfuse a minimum number of lamellae, which would be about 60% based on the observations made in Section III.

In conclusion the hypoxic response and the struggle response of ling cod have remarkable similarities with respect to their associated cardiovascular and ventilatory changes. Both responses will increase the number of lamellae perfused, alter the perfusion within each lamella and reduce diffusion distances. These changes increase the diffusing capacity of gills. Vg and $\dot{Q}$ are also elevated which accounts for $\dot{M}o_2$ being increased. The struggle response involves a tail beat, which increases venous return, and cholinergic mechanisms that alter $\dot{Q}$ and Rg prior to and at the tail beat, thus initiating the changes in blood flow through the gills. The subsequent increase in $\dot{Q}$ with reduced cholinergic activity, effects the changes in gill blood flow patterns. There may also be a catecholamine release after the tail beat associated with struggling. The hypoxic response involves a cholinergically medicated cardiovascular responses during progressive hypoxia, which are interrupted by numerous struggles. The aeration of hypoxic

water may be accompanied by catecholamine release and no cholinergic effects.

GENERAL DISCUSSION

AND

SUMMARY

Lamellar recruitment and intralamellar shunting were proposed in the past as possible ways in which blood flow might be altered in teleost gills. This study has confirmed these two hypotheses. During the course of my work, Booth (pers. comm.) also experimentally established that lamellar recruitment occurs in trout. Respiratory (lamellar) bypass as found in Anguilla, does not occur in Ophiodon. In addition to demonstrating two patterns of blood flow, my study has presented observations which permit an explanation of how these alterations in gill blood flow patterns might be regulated in vivo. The thesis has emphasised passive properties of blood vessels, paricularly the lamellar capillary sheet which allow passive changes in blood flow patterns, and the importance of ΔP_{lam}. Overall, I have revealed a number of the intricacies of branchial circulation and its regulation in Ophiodon, which can be applied to other teleosts, provided the often very important interspecific differences are also considered.

Resting ling cod perfuse about two thirds of their lamellae, and these are the proximal lamellae. Critical closure of small vessels, afferent lamellar arterioles, lamellar channels or both, in distal regions of the filament is apparently central to this condition. Blood flow through the lamellae is best described by sheet flow. The conditions of lamellar blood flow are, therefore, analagous to pulmonary blood flow in mammals and possibly amphibians, thus patterns of capilary blood flow in respiratory exchange sites show evolutionary convergence.

Lamellar recruitment

Lamellae can be recruited automatically when input pressure and/or flow are elevated. Lamellar recruitment does not cause marked changes in Rg, which can be related to changes in resistance to flow in the input and output branchial vessels instead. The lamellae are very compliant vascular sheets with a low resistance to flow. Consequently overall gill compliance will increase with lamellar recruitment, and blood flow will be damped. In vivo elevations in Q are accompanied by increased damping of the pressure pulse, ΔPg pulse. It is suggested, therefore, that an increase ΔPg pulse is associated with lamellar recruitment. Thus ΔPg pulse measurements can be used to qualitatively describe changes in lamellar perfusion, given the compliance characteristics of the lamellar sheet. More accurate predictions of lamellar recruitment could be obtained if VA and DA blood flow patterns were compared for phasic differences. The afferent filament artery does not have a major role in controlling lamellar recruitment in Ophiodon. Its resistance to flow is significant but I disagree with the proposal of Morgan and Tovell (1973) that the vessel taper has a major effect on resistance, because flow is reduced along the vessel length. Morgan and Tovell (1973) apparently did not consider these flow changes. In resting ling cod the afferent lamellar aterioles have the controlling influence in perfusion

of individual lamellae. These vessels will also set ΔP_{lam} which is extremely important to intralamellar flow (see below).

Fish recruit more lamellae when oxygen demands increase. We now have a clearer idea of what mechanisms may bring this about *in vivo*. Elevations of $\dot{Q}$ and/or arterial blood pressures can bring about lamellar recruitment automatically. So too does a reduced heart rate/increased stroke volume condition, but to a lesser extent. The reason for these cardiovascular changes producing lamellar recruitment has been explained based on my *in vitro* observations. The explanations are that a) the higher critical closure pressures associated with distal lamellar units are overcome by elevated systolic blood pressures (changes in pulse pressure) or by elevated mean pressure *per se*. In the compliant lamellar units positive feedback occurs when P_{lam} is raised since the vascular sheet thickness increases and resistance falls. Hence blood pressures need not be continually elevated for lamellar recruitment. b) Because of arterio-venolymphatic interactions in gill filaments, increased venolymphatic flow rates during high pulse pressure/low heart rate perfusion conditions may reduce critical closure pressures. The nature of the cardiovascular changes that I observed during the *in vivo* responses to stress in ling cod, hypoxia and struggling, is such that both the above mechanisms could operate *in vivo*. The resulting lamellar recruitment is important in accounting for the elevated Mo_2 observed in these situations.

In ling cod, the changes in $\dot{Q}$ and/or blood pressures that produce lamellar recruitment are a result of adrenergic and cholinergic actions. Heart rate has the major influence on $\dot{Q}$ in ling cod. Reduced cholinergic tone to the heart or adrenergic cardiac excitation increase $\dot{Q}$. Increased cholinergic tone reduces heart rate, but stroke volume and pulse pressures are elevated and $\dot{Q}$ is maintained provided venous return is maintained. Tail beats may be important in increasing venous return to elevate stroke volume. The branchial vasculature, excluding the lamellar vascular sheet, is also directly affected by cholinergic and adrenergic actions. In vivo gill outflow arteries vasoconstrict through localised cholinergic actions, which raise Rg. In struggles the brief period of elevated Rg will raise the filament blood pressure (a back pressure), and overcome the higher critical closure pressures associated with the distal lamellae. This leads to lamellar recruitment if $\dot{Q}$ is subsequently elevated. The importance of elevating $\dot{Q}$ at the same time as changing Rg was demonstrated in vitro where decreasing Rg alone did not bring about lamellar recruitment. Branchial vasodilation occurs through adrenergic actions and reduces Rg. Vasodilation of input vessels reduces critical closure pressures and may be neurally mediated adrenergic vasodilation of afferent lamellar arterioles. Release of catecholamine stores also occurs in ling cod and the humoral adrenergic actions cause a systemic vasoconstriction with a resulting pressor response, in addition

to branchial vasodilation. The pressor response and the branchial vasodilation led to lamellar recruitment with the accompanying increase in $\dot{Q}$. When critical closure pressures are lowered or elevated blood pressures exceed them, lamellar recruitment can occur. Lamellar recruitment should potentially reduce Rg, unless the increase in $\dot{Q}$ closely matches these potential Rg changes. This appears to be the situation with humoral adrenergic actions in ling cod. Catecholamine injection causes little change in ΔPg, even though lamellar recruitment and vasodilation will occur (Sections II and III). Since lamellae contain the greater blood volume of the filament (Section I), $\dot{Q}$ increases must therefore closely match the volume of lamellae recruited. This correlation clearly emphasises the reason for no Rg changes accompanying lamellar recruitment and the importance of elevating $\dot{Q}$ *in vivo* and *in vitro* to effect lamellar recruitment. Such a situation may well be best regulated if the lamellar recruitment occured automatically with Q and pressure elevations.

The matching of $\dot{Q}$ with lamellar recruitment has an important consequence in gaseous exchange: red blood cell transit time through the lamellae is unaltered by these cardiovascular changes. Such a situation might be expected since blood oxygenation is dependent on residence time of red blood cells in the lamellae when exchange is diffusion limited. Lamellar transit time in resting ling cod is about 2 seconds (Section I) which approximates to the resting frequency of the

heart beat. Clearly if alterations in Q occur through stroke volume changes that are matched to lamellar recruitment, then transit time remains proportional to heart rate. During hypoxia, therefore, when there is lamellar recruitment, increased stroke volume and a bradycardia, the lamellar transit time is increased. This situation facilitates O_2 transfer in the face of reduced partial pressure gradients. Such a situation was predicted by Randall (1970). During struggles when Q is elevated through heart rate and stroke volume increases, the relationship between lamellar transit time and heart rate is altered. Lamellar transit time *per se* is not altered though.

Intralamellar shunting

Mo_2 in ling cod is increased up to three fold during hypoxia. Resting ling cod perfuse about 60% of their lamella. If lamellar perfusion became maximal, then the surface area for gaseous exchange would be increase by about two-thirds. Thus maximal lamellar perfusion will only increase To_2 by two-thirds if there are no other changes, and this does not account for observed increases in Mo_2. Intralamellar shunting and the associated changes in the lamellae with increased ΔP_{lam} (Section I) must, therefore, contribute significantly to increasing Mo_2. Intralamellar shunting is a redistribution of blood flow within a lamella and occurs because in ling cod the compliance, epithelium and vascular sheet thickness of the lamellae are non-uniform. Intralamellar shunting can easily be

envisaged as an automatic phenomenon as ΔP_{lam} rises now that I have described lamellar blood in terms of sheet flow. Simply, flow is proportional to resistance, which is proportional to lamellar vascular sheet thickness to the fourth power. Sheet thickness, and thus flow, are always greater in distal regions of the lamella. This relationship is true at all ΔP_{lam}. The distal regions are associated with higher diffusion capacities since in epithelial diffusion distances are greater in basal regions. The distal regions of the sheet are more compliant at low ΔP_{lam} than basal regions. Thus as blood pressure rises the lamellar vascular sheet thickens more in the distal region and alters the ratio of resistances and flow between the distal and basal regions. Therefore, intralamellar shunting to distal lamellar regions occurs automatically when ΔP_{lam} rises and, as a consequence, the gill diffusing capacity increases. Adrenergic and cholinergic cardiovascular actions cause pressor responses, as described above, which raise ΔP_{lam} and increase gill diffusing capacity in this manner. Other effects of raising ΔP_{lam} are that lamellar volume is increased (a 12% rise with a 20 cm H_2O increase in ΔP_{lam}) and the epithelium becomes thinner as the lamellar blood sheet thickens. Both changes increase diffusing capacity. The relative contributions of intralamellar shunting, increased lamellar volume and reduced epithelial thickness on increasing diffusing capacity are not known.

As ΔP_{lam} increases so will lymph formation,

however. Fish are noted for their high capillary premeability (Hargens et al., 1974) and furthermore, lamellar capillary blood pressures are high by mammalian capillary standards. Lymph so formed will enter the lamellar interstitial space and, if it is not removed, will increase diffusion distances and decrease diffusing capacity. To fish, increasing ΔP_{lam} is so important in increasing To_2 that there are certain safeguards that appear to prevent lamellar interstitial fluid accumulation associated with high ΔP_{lam}. The lamellar blood flow is highly pulsatile compared to other capillary beds, and because the lamella blood sheet is compliant, this pulsatility drives lymph flow from the interstitium into the central sinus. In addition an increased arterial pulsatility/reduced heart rate condition can promote venolymphatic flow.

The effect of intralamellar shunting on gas transfer can be analysed in more detail in the future as an extension of my findings. Accurate regional measurements of epithelium thickness and blood sheet thickness, and how they change with ΔP_{lam} are needed. Predictions can then be made, as I did, based on the regional variations in lamellar compliance. Important questions to be answered in future investigations are how and why does this regional variation occur? I can speculate on both these points. Firstly the reasons for gill lamellae displaying regional non-uniformity. Is it fortuitous that both α and h are reduced in the base of the lamellae where the epithelium is thicker, or are they related? Alveoli in the cat

lung are noted for a high α value and a very thin epithelium. An alternative is that the properties of the pillar cells are important since they hold the lamellar vascular sheet together under blood pressure and undoubtedly affect the compliance. Pillar cell size does vary regionally (Table III), but whether this corresponds to the regional variations in α would require a more rigorous analysis of pillar cell size than performed here. Collagen fibre content of pillar cells may also be a factor. In some teleosts the pillar cells in basal regions have a higher collagen content than those in distal regions (Newstead, 1967), which is interesting since the lung and blood vessel compliance are both reduced if collagen fibre content is increased (Sobin, pers. comm.; Gosline and Harman, pers. comm.). Newstead's finding appears to correlate well with the less compliant basal lamellar regions in ling cod and regional variations in lamellar compliance may, then, be related to collagen content of pillar cells.

Why does regional variation in compliance and, thus intralamellar shunting exist in fish? Lamellae act as the gaseous and ionic exchange area. Intralamellar shunting may be necessary for this dual function. Resting fish apparently perfuse the minimum number of lamellae to meet tissue O_2 demands. Thereby they minimise diffusional losses of water or ions, which have to be replaced by active processes to maintain an internal homeostasis. Lamellar perfusion is a compromise between $\dot{M}o_2$ and water or ionic loss, and should alter in relation to the demands of a given situation. During swimming

Mo_2 should dictate the nature of lamellar perfusion and this has indeed been demonstrated. Trout during swimming activity tolerate an increased salt efflux and water influx whilst Mo_2 is elevated (Wood and Randall, 1973a and b). Clearly regional variations in lamellar diffusing capacity and the ability to shunt flow between these areas provides the flexibility needed for adjusting lamellar perfusion. Some specialized fishes inhabit hypoxic aquatic environments and obtain their oxygen largely by breathing air using another gas exchange site in addition to that of the gills. Blood flowing through the gills is, therefore, oxygenated and, in hypoxic water, O_2 loss from the blood to the water can occur. In this situation perfusion of regions of the lamella with a high diffusing capacity is a liability. Air breathing fish are noted for large diffusion distances over extensive regions of the lamella and perfusion of these regions would be highly advantageous in a hypoxic aquatic environment (Randall et al., 1979). Some bimodal air-breathing fish when in normoxic aquatic environments, do not air breath and obtain oxygen across the gills. Here perfusion of regions of the lamella with high diffusion capacity is necessary. To air breathing fish, therefore, intralamellar shunting of blood flow may well be a way of life. There is no intra-alveolar shunting of blood flow. In conclusion, it is expected that as fish radiated into different niches and as the relative roles of the gills were altered, the nature of intralamellar shunting altered accordingly by regionally modifying the lamellar vascular sheet compliance.

BIBLIOGRAPHY

ATTINGER, E.O. and F.M. ATTINGER (1973). Frequency dynamics of peripheral vascular blood flow. Am. Rev. Biophys. Bioeng. 2: 7-36.

BALLINTIJN, C.M. & G.M. HUGHES (1965). The muscular basis of the respiratory pump in the trout. J. Exp. Biol. 43: 349-362.

BARER, G., F. MOHAMMED, A. SUGGETT, C. TWELVES (1978). Hypoxic pulmonary vasoconstriction in the ferret. J. Physiol. 281: 40P-41P.

BERGEL, D.H. (1961a). The static elastic properties of the arterial wall. J. Physiol. (Lond.) 156: 445-457.

BERGEL, D.H. (1961b). The dynamic elastic properties of the arterial wall. J. Physiol. (Lond.) 156: 458-469.

BERGMAN, H.L., K.R. OLSON and P.O. FROMM (1974). The effects of vasoactive agents on the functional surface area of isolated-perfused gills of rainbow trout. J. comp. Physiol. 94: 267-286.

BETTEX-GALLAND, M. and G.M. HUGHES (1973). Contractile filamentous material in the pillar cells of fish gills. J. Cell. Sci. 13: 359-370.

BOOTH, J.H. (1978). The distribution of blood flow in the gills of fish: application of a new technique to rainbow trout (Salmo gairdneri). J. Exp. Biol. 73: 119-129.

BURTON, A.C. (1951). On the physical equilibrium of small blood vessels. Am. J. Physiol. 164: 319-329.

BUSBY, D.E. and A.C. BURTON (1965). The effect of age on the elasticity of the major brain arteries. Can. J. Physiol. Pharmacol. 43: 185-202.

BUTLER, P.J. and E.W. TAYLOR (1975). The effect of progressive hypoxia on respiration in the dogfish (Scyliorhinus canicula) at different seasonal temperatures. J. Exp. Biol. 63: 117-130.

BUTLER, P.J., E.W. TAYLOR, M.F. CAPRA and W. DAVIDSON (1978). The effect of hypoxia on the levels of circulating catecholamines in the dogfish Scyliorhinus canicula. J. comp. Physiol. 127: 325-330

CAMERON, J.N. (1974). Evidence for lack of by-pass shunting in teleost gills. J. Fish. Res. Bd. Can. 31(2): 211-213.

CAMPBELL, G., B.J. GANNON and D.J. RANDALL. The vasculature of the gill of the rainbow trout, Salmo gairdneri. In prep.

CHAN, D.K.O. and P.H. CHOW (1976). The effects of acetylcholine, biogenic amines and other vasoactive agents on the cardiovascular functions of the eel, Anguilla anguilla. J. Exp. Zool. 196: 13-26.

COBB, J.L.S. and R.M. SANTER (1973). Electophysiology and cardiac function in teleosts: cholinergically mediated inhibition and rebound excitation. J. Physiol. 230: 561-573.

DANZER, L.A., J.E. COHN and F.W. ZECHMAN (1968). Relationship of Dm and Ve to pulmonary diffusing capacity during exercise. Respir. Physiol. 5: 250-258.

DAVIS, J. C. (1970). Estimation of circulation time in rainbow trout, Salmo gairdneri. J. Fish. Res. Bd. Can. 27(10): 1860-1863.

DAVIS, J.C. (1972). An infrared photographic technique useful for studying vascularisation of fish gills. J. Fish. Res. Bd. Can. 29: 109-111.

DAXBOECK, C. and G.F. HOLETON (1978). Oxygen receptors in the rainbow trout, Salmo gairdneri. Can. J. Zool. 56(6): 1254-1259.

DOELLINGER, Dr. (1837). Ueber die Vertheilung des Blutes in den Kiemen der Fishe. Abhandl. der mathem. physie Klasse Bd II: 784-794.

DUNEL, S. and P. LAURENT (1977). La vascularisation branchiale chez l'Anguille: action résparition d'une résine polymérisable dans les différent compartiments vasculaires. C.R. Acad. Sc. Paris 284: 2011-2014.

FISHER, T.R., R.F. COBURN and R.E. FORSTER (1969). Carbon monoxide diffusing capacity in the bullhead catfish. J. Appl. Physiol. 26(6): 161-169.

FORSTER, M. E. (1976). Effects of adrenergic blocking drugs on the cardiovascular system of the eel, Anguilla anguilla (L). Comp. Biochem. Physiol. 55(1C): 33-36.

FRONEK, K. and B.W. ZWEIFACH (1975). Mircovascular pressure distribution in skeletal muscle and the effect of vasodilation. Am. J. Physiol. 228(3): 791-796.

FUNG, Y.C. (1972). Biomechanics - its foundations and objectives. p. 182 Pub. Prentice-Hall Inc., New Jersey.

FUNG, Y.C. and S.S. SOBIN (1969). Theory of sheet flow in lung alveoli. J. Appl. Physiol. 26: 472-488.

FUNG, Y.C. and S.S. SOBIN (1972). Elasticity of the pulmonary alveolar sheet. Circulation Res. 30: 451-469.

FUNG, Y.C. and S.S. SOBIN (1977). Mechanics of pulmonary circulation in "Cardiovascular Flow Dynamics and Measurements". Ed. N.H.C. Hwang and N.A. Normann. Pub. Uni. Park Press, Baltimore. p665-730.

GANNON, B.J. (1972). Comparative and developmental studies of autonomic nerves in visceral and cardiovascular systems. PhD dissertation, Univ. of Melbourne, Australia.

GANNON, B.J. (1978). Methods of vascular casting for scanning electron microscopy. In: Advances in optical and electron microscopy Vol. 7. In Press.

GANNON, B.J. and G. BURNSTOCK (1969). Excitatory adrenergic innervation of the fish heart. Comp. Biochem. Physiol. 29: 765-774.

GANNON, B.J. and G. CAMPBELL and D.J. RANDALL (1973). Scanning electron microscopy of vascular casts for the study of vessel connections in a complex vascular bed - the trout gill. Proc. 31st E.M. Soc. Am.: 442-443.

GESSER, H. (1977). The effects of hypoxia and reoxygenation on force of development in myocardia of carp and rainbow trout: protective effects of CO_2/HCO_3. J. Exp. Biol. 69: 199-206.

GIRARD, J.P. and P. PAYAN (1976). Effect of epinepherine on vascular space of gills and head of rainbow trout. Am. J. Physiol. 230: 1555-1560.

GLAZIER, J.B., J.M.B. HUGHES, J.E. MALONEY and J.B. WEST (1969). Measurements of capillary dimensions and blood volume in rapidly frozen lungs. J. Appl. Physiol. 26: 65-76.

GOW, B.S. (1972). The influence of vascular muscle on the viscoelastic properties of blood vessels. In: Cardiovascular Fluid Dynamics, Vol. 2. Ed. D.H. Bergel. Pub. Academic Press, New York.

GUYTON, A.C. and A.W. LINDSEY (1959). Effect of elevated left atrial pressure and decreased plasma protein concentration on the development of pulmonary edema. Circulation Res. 7: 649-657.

HARGENS, A.R., R.W. MILLARD and K. JOHANSEN (1974). High capillary permeability in fishes. Comp. Biochem. Physiol. 48: 675-680.

HASWELL, M.S., S.F. PERRY and D.J. RANDALL (1978). The effect of perfusate oxygen levels on CO_2 excretion in the perfused gill. J. Exp. Zool. 205: 309-314.

HELGASON, S.S. and S. NILSSON (1973). Drug effects on pre- and post-branchial blood pressure and heart rate in a free swimming marine teleost, Gadus morhua. Acta physiol. Scand. 88: 533-540.

HOLETON, G.F. and D.J. RANDALL (1967a). Changes in blood pressure in the rainbow trout during hypoxia. J. Exp. Biol. 46(2): 297-306.

HOLETON, G.F. and D.J. RANDALL (1976b). The effect of hypoxia upon the partial presure of gases in the blood and water afferent and efferent to the gills of rainbow trout. J. Exp. Biol. 46(2): 317-328.

HOLMGREN, S. (1977). Regulation of the heart of a teleost, Gadus morhua, by autonomic nerves and circulating catecholamines. Acta physiol. Scand. 99: 62-74.

HUGHES, G.M. (1972). The relationship between cardiac and respiratory rhythms in the dogfish Scyliorhinus canicula. J. Exp. Biol. 57: 415-434.

HUGHES, G.M. and G. SHELTON (1962). Respiratory mechanisms and their nervous control in fish. Advan. Comp. Physiol. Biochem. 1: 13-29. Ed: O. Lowenstein. Pub. Academic Press Inc., New York.

HUGHES, G.M. and A.V. GRIMSTONE (1965). The fine structure of the secondary lamellae of the gills of Gadus pollachius. Q. Jl. micros. Sci. 106: 343-353.

HUGHES, G.M. and T. KOYAMA (1975). Gas Exchange of single red blood cells within secondary lamellae of fish gills. J. Physiol. 246: 82P-83P.

HUGHES, G.M. and S.F PERRY (1976). Morphometric study of trout gills: a light microscopic method suitable for the evaluation of pollutant action. J. Exp. Biol. 64(2): 447-460.

HYRTL, J. Beobachlungen aus den Gebiethe der vergleichenden Gefäfslehre. Medizinische Jahrbucher Osterr Stäätes 24: 232-248.

INTAGLIETTA, M. (1973). Pressure measurements in the microcirculation with active and passive transducers. Microvas. Res. 5: 317-323.

INTAGLIETTA, M., R.F. PAWULA and W.R. TOMPKINS (1970). Pressure measurements in the mammalian microvasculature. Microvasc. Res. 2: 212-220.

JONES, D.R. and D.J. RANDALL (1978). The respiratory and circulatory systems during exercise. In: Fish physiology Ed: W.S. Hoar and D.J. Randall, Vol. 7. Pub. Academic Press, New York p. 425-501.

JONES, D.R., B.W. LANGILLE, D.J. RANDALL and G. SHELTON (1974). Blood flow in dorsal and ventral aortae of the cod, Gadus morhua. Am. J. Physiol. 226(1): 90-95.

KALEY, G. and B.M. ALTURA (1977). Microcirculation Vol. I. Pub. University Park Press.

KEMPTON, R.T. (1969). Morphological features of functional significance in the gills of the spiny dogfish, Squalus acanthias. Biol. Bull, 136: 226-240.

KENT, B. and E.C. PEIRCE II (1975). Reflex control of gill blood flow in Squalus ancanthias. In: "Respiration of Marine Organisms". Ed: CECH, J.J., D.W. BRIDGES, and D.B. HORTON. p. 183 -184.

KENT, B and E.C. PEIRCE II (1978). Cardiovascular responses to changes in blood gases in dogfish shark, Squalus ancanthias. Comp. Biochem. Physiol, 60C: 37-44.

KHAJUTIN, V.M. (1964). Physical properties of vessels and vasomotor regulations. Ed: E.O. ATTINGER. Pub. McGraw-Hill, New York. p. 331-342.

KICENIUK, J.W. and D.R. JONES (1977). The oxygen transport system in trout (Salmo gairdneri) during sustained exercise. J. Exp. Biol. 69: 247-260.

KLAVERKAMP, J.F. and D.C. DYER (1974). Autonomic receptors in rainbow trout vasculature. European J. Pharmacol. 28: 25-34.

LAMPORT, H. and S. BAEZ (1962). Physical properties of small arterial vessels. Physiol. Rev. Supp. 5: 328-345.

LANDIS, E.M. (1934). Capillary pressure and capillary permeability. Physiol. Rev. 14: 404-481.

LAURENT, P. and S. DUNEL (1976). Functional organisation of the teleost gill. I. Blood pathways. Acta. Zool. 57: 189-209.

LUNDVALL, J. and J.J. ARHULT (1974). Beta-adrenergic microvascular dilation evoked by sympathetic stimulation. Acta physiol. Scand. 92: 572-574.

LUTZ, B.R. and L.C. WYMAN (1932). Reflex cardiac inhibition of branchiovascular origin in the elasmobranch Squalus acanthias. Biol. Bull. 62: 10-16.

McDONALD, D.A. (1960). Blood flow in arteries. Pub. W. and J. Mackay and Co. Ltd., Chatham. p. 255.

McHALE, N.G. and I.C. RODDIE (1976). The effect of transmural pressure on pumping activity in isolated bovine lymphatic vessels. J. Physiol. 261: 255-269.

McMASTER, P.O. and R.J. PARSONS (1938). The effect of the pulse on the spread of substances through tissues. J. Exp. Med. 68(1): 377-400.

MALONEY, J.E. and B.L. CASTLE (1969). Pressure-diameter relationship of capillaries and small blood vessels in frog lung. Resp. Physiol. 7: 150-162.

MAZEAUD, M.M., F. MAZEAUD, and E.M. DONALDSON. Primary and secondary effects of stress in fish: Some new data with a general review. Trans. Am. Fish. Soc. 106(3): 201-212.

MONRO, A. (1785). The structure and physiology of fishes explained and compared with those of man and other animals. Univ. of British Columbia special collections.

MORGAN, M. and P.W.A. TOVELL (1973). The structure of the gill of the trout, Salmo gairdneri. A. Zellforsch 142: 147-162.

MOTT, J.C. (1951). Some factors affecting the blood circulation in the common eel (Anguilla anguilla). J. Physiol. 114: 387-398.

MULLER, J. (1839). Vergleichende Anatomie der Myxinoiden III Uber das Gefässystem. Deutsche Academie der Wissenschaften zu Berlin. Abhandlumger: 175-304.

MURAKAMI, T. (1971). Application of the scanning electron microscope to the study of the fine distribution of blood vessels. Arch. histol. Jap. 32: 445-454.

NAKANO, T. and N. TOMLINSON (1967). Catecholamine and carbohydrate metabolism in rainbow trout (Salmo gairdneri) in relation to physical disturbance. J. Fish. Res. Bd. Can. 24: 1701-1715.

NEWSTEAD, J.O. (1965). Fine structure of the respiratory lamellae of teleost gills. Anat. Rec. 153: 393.

NEWSTEAD, J.O. (1967). Fine structure of the respiratory lamellae of Teleostean gills. Z. Zellforschung 79: 396-428.

NICHOL, J., F. GIRLING, W. JERRARD, E.B. CLAXTON and A.C. BURTON (1951). Fundamental instability of the small blood vessels and critical closing pressures in vascular beds. Am. J. Physiol. 164: 330-344.

NICHOLAYSEN, G. and A. HAUGE (1977). Comparison of lung capillary function at pulsatile and non pulsatile perfusion. Proc. 27th Inter. Congr. Physiol. Sci., Paris.

NICHOLL, P.A. (1971). M.C.S. symposium on "The Precapillary Sphincter". Microvasc. Res. 3: 426-427.

NILSSON, S, T. ABRAHAMSON and D.J. GROVE (1976). Sympathetic nervous control of adrenaline release from the head kidney of the cod Gadus morhua. Comp. Biochem. Physiol. 55: 123-127.

OSTLUND, E. and R. FANGE (1962). Vasodilation by adrenaline and noradrenaline and the effects of some other substances on perfused fish gills. Comp. Biochem. Physiol. 5: 307-309.

PARSONS, R.J. and P.D. McMASTER (1938). The effect of the pulse upon the formation and flow of lymph. J. Exp. Med. 68(1): 353-376.

PAYAN, P. and J.P. GIRARD (1977). Adrenergic receptors regulating patterns of blood flow through the gills of trout. Am. J. Physiol. 232(1): H18-H23.

PERMUTT, S. (1965). Effect of interstitial pressure of the lung on pulmonary circulation. Med. thorac. 22: 118-131.

PETERSON, L.H. (1962). Properties and behaviour of the living vascular wall. Physiol. Rev. Suppl. 5: 309-324.

PIIPER, J., D. BAUMGARTEN and M. MEYER (1970). Effects of hypoxia upon respiration and circulation in the dogfish, Scyliorhinus stellaris. Respir. Physiol. 30: 221-239.

RANDALL, D.J. (1967). Sinus arhythmia and bradycardia in fish resulting from deoxygenated wter passing over the gills. XXII Internat. Cong. Physiol. Sci.

RANDALL, D.J. (1968). Functional morphology of the heart in fishes. Am. Zool. 8: 179-189.

RANDALL, D.J. (1976). Gill structure and function: effects of gas on ion exchanges. Physiologist 19(3).

RANDALL, D.J. (1970). The Circulatory System. In: Fish Physiology Vol. 4 Ed: E.S. Hoar and D.J. Randall. Pub. Academic Press, New York p. 132-172.

RANDALL, D.J. and E.D. STEVENS (1967). The role of adrenergic receptors in cardiovascular changes associated with exercise in salmon. Comp. Biochem. Physiol. 21: 415-424.

RANDALL, D.J. and G.F. HOLETON and E.D. STEVENS (1967). The exchange of oxygen and carbon dioxide across the gills of rainbow trout. J. Exp. Biol. 46(2): 339-348.

RANDALL, D.J., D. BAUMGARTEN and M. MALYUSZ (1972). The relationship between gas and ion transfer across the gills of fishes. Comp. Biochem. Physiol. 41: 629-637.

RICHARDS, B.D. and P.O. FROMM (1969). Patterns of blood flow through filaments and lamellae of isolated-perfused rainbow trout (Salmo gairdneri) gills. Comp. Biochem. Physiol. 29: 1063-1070.

RIESS, J.A. (1881). Der Bau der Kiemenblätter bei den Knocherfischen. Acrhiv für Naturgeschichte (Universitats Buchdruckenei). 47: 518-550.

ROBERTS, J.L. (1975). Cardio-ventilatory interactions during swimming, and during thermal and hypoxic stress. In: Respiration of Marine Organisms. Eds: J.J. Cech, D.W. Bridges and D.B. Horton. p. 139-151

RUSZYAK, I., M. FOLDI and G. SZABO (1967). Lymphatics and lymph circulation. Pub. Permagon Press, New York.

SATCHELL, G.H. (1962). Intrinsic vasomotion in the dogfish gill. J. Exp. Biol. 39: 503-512.

SATCHELL, G.H. (1971). Circulation in fishes. Pub. Cambridge University Press, London.

SCHEID, P. and J. PIIPER (1976). Quantitative functional analysis of branchial gas transfer: Theory and application to Scyliorhinus stellaris (Elasmobranchii). In: Respiration of Amphibious Vertebrates. Ed: G.M. Hughes. Pub. Academic Press, London. p. 17-38.

SHELTON, G. (1970). Regulation of breathing. In: Fish Physiology, Vol. 4 Ed: W.S. Hoar and D.J. Randall. Academic Press, New York. p. 293-359.

SHEPHARD, R.B. and J.W. KIRKLIN (1969). Relation of pulsatile flow to oxygen consumption and other variables during cardiopulmonary bypass. J. Thorac. Cardiovasc. Surg. 58: 694-702.

SHORT, S., P.J. BUTLER and E.W. TAYLOR (1977). The relative importance of nervous, humoral and intrinsic mechanisms in the regulation of heart rate and stroke volume in the dogfish Scyliorhinus canicula. J. Exp. Biol. 70: 77-92.

SHOUKAS, A.A. (1977). Constriction of hydraulic cuff occluders for blood vessels. Am. J. Physiol. 232(1): H99-H100.

SHUTTLEWORTH, T.J.(1972). A new isolated-perfused gill preparation for the study of the mechanisms of ionic regulation in teleosts. Comp. Biochem. Physiol. 43: 59-64.

SHUTTLEWORTH, T.J. (1978). The effect of adrenaline on potentials in the isolated gills of the flounder Platichthys flesus). J. Comp. Physiol. B. 124: 129-136.

SKIDMORE, J.F. (1970). Respiration and osmoregulation in rainbow trout with gills damaged by zinc sulphate. J. Exp.Biol. 52: 481-494.

SMITH, D.G. (1976). PhD Dissertation. Melbourne, Australia.

SMITH, D.G. (1977). Sites of cholinergic vasoconstriction in trout gills. Am. J. Physiol. 233: R222-R229.

SMITH, F.M. and D.R. JONES (1978). Localization of receptors causing hypoxic bradycardia in trout (Salmo gairdneri). Can. J. Zool. 56(6): 1260-1265.

SOBIN, S.S., H.M. TREMER and Y.C. FUNG (1970). Morphometric basis of the sheet-flow concept of the pulmonary alveolar microcirculation in the cat. Circulation Res. 26: 397-414.

SOBIN, S.S., R.G. LINDAL and S. BERNICK. The pulmonary arteriole. Microvas. Res. 14: 227-239.

SOBIN, S.S., Y.C. FUNG, H.M. TREMER and T.H. ROSENQUIST (1972). Elasticity of the pulmonary alveolar microvascular sheet in the cat. Circulation Res. 30: 440-450.

STARLING, E.H. (1896). On the absorption of fluids from the connective tissue. J. Physiol. 19: 312-326.

STEEN, J.B. and A. KRUYSSE (1964). The respiratory function of teleost gills. Comp. Biochem. Physiol. 12: 127-142.

STEVENS, E.D. and D.J. RANDALL (1967a). Changes in blood pressure, heart rate and breathing rate during moderate swimming activity in rainbow trout. J. Exp. Biol. 46: 307-316.

STEVENS, E.D. and D.J. RANDALL (1967b). Changes of gas concentrations in blood and water during moderate swimming activity in rainbow trout. J. Exp. Biol. 46: 329-338.

STEVENS, E.D., G.R. BENNION, D.J. RANDALL and G. SHELTON (1972). Factors affecting arterial blood pressures and blood flow from the heart in intact, unrestrained ling cod, Ophiodon elongatus. Comp. Biochem. Physiol. B. 43: 681-695.

TAYLOR, E.W., S. SHORT and P.J. TAYLOR. The role of the cardiac vagus in the response of the dogfish, (Scyliorhinus canicula to hypoxia. J. Exp. Biol. 70: 57-75.

VOGEL, W.O.P. (1978). Arteriovenous anastomoses in the afferent region of trout gill filaments (Salmo gairdneri). Zoomorphologie 90: 205-212.

VOGEL, W., V. VOGEL, and H. KREMERS (1973). New aspects of the intrafilamental vascular system in gills of a euryhaline teleost, Tilapia mossambica. Z. Zellforsch 144: 573-583.

VOGEL, W., V. VOGEL and W. SCHLOTE (1974). Ultra structural study of arteriovenous anastomoses in gill filaments of Tilapia mossambia. Cell Tiss. Res. 155: 491-512.

VOGEL, W., V. VOGEL and M. PFAUTSCH (1976). Arterio-venous anastomoses in rainbow trout gill filaments. Cell Tiss. Res. 167: 373-385.

WAHLQVIST, I. and S. NILSSON (1977). The role of sympathetic fibres and circulating catecholamines in controlling the blood pressure and heart rate in the cod, Gadus morhua. Comp. Biochem. Physiol. 57: 65-67.

WEIBEL, E.R. (1963). Morphometry of the human lung. Pub. Academic Press, New York.

WEIDERHIELM, C.A. (1968). Dynamics of transcapillary fluid exchange. J. Exp. Physiol. 52: 29-63.

WEIDERHIELM, C.A. and B.V. WESTON (1973). Microvascular, lymphatic and tissue pressures in the unanaesthetised mammal. Am. J. Physiol. 224(4): 992-996.

WEIDERHIELM, C.A., J.W. WOODBURY, S. KIRK and R.F. RUSHMER (1964). Pulsatile pressures in the microvasculature of frog mesentery. Am. J. Physiol. 207(1): 173-176.

WEST, J.B. (1977). Ventilation/blood flow and gas exchange. Blackwell Scientific Publications. 3rd edition.

WOLF, K. (1963). Physiological salines for freshwater teleosts. Progr. Fish. Cult. 25: 135-140.

WOOD, C.M. (1974a). A critical examination of the physical and adrenergic factors affecting blood flow through the gills of the rainbow trout. J. Exp. Biol. 60: 241-265.

WOOD, C.M. (1974b). Mayer waves in the circulation of teleost fish. J. Exp. Zool. 189: 267-273.

WOOD, C.M. (1975). A pharamacological analysis of the adrenergic and cholinergic mechanisms of regulating branchial vascular resistance in the rainbow trout, Salmo gairdneri.

WOOD, C.M. (1977). Cholinergic mechanisms and the response to ATP in the systemic vasculature of the rainbow trout. J. comp. Physiol.(B) 122(3): 325-345.

WOOD, C.M. and D.J. RANDALL (1973). The influence of swimming activity on sodium balance in rainbow trout (Salmo gairdneri). J. comp. Physiol. 82: 207-233.

WOOD, C.M. and J.J. RANDALL (1973b). The influence of swimming activity on water balance in rainbow trout (Salmo gairdneri). J. comp. Physiol. 82: 257-276.

WOOD, C.M., B.R. McMAHON and D.G. McDONALD (1978). Oxygen exchange and vascular resistance in the totally perfused rainbow trout. Am. J. Physiol. 234(5): R201-R208.

YAMAUCHI, A. and G. BURNSTOCK (1968). Electron microscopic study on the innervation of the trout heart. J. Comp. Neur. 132: 567-588.

ZWEIFACH, B.W. and H.H. LIPOWSKY (1977). Quantitative studies of microcirculatory structure and function. III.Microvascular hemodynamics of the cut mesentery and rabbit omentum. Circulation Res. 41(3): 380-390.

APPENDIX I

In Section I, I presented a number of results for calculations of the resistance to flow and the pressure drop in gill filament vessels. The values used in those calulations are presented here.

In equation (1), used for determining ΔP_{lam}, the following values were used. $\eta = 4.17 \times 10^{-7}$ cm H_2O.min; k = 13.8; f = 1.8; $\bar{L} = 0.05$ cm; S = 0.881; $\alpha = 7 \times 10^{-6}$ cm. H_2O^{-1}; $h_a = 1.146 \times 10^{-3}$ cm. The total lamellar area is 6.9×10^3 cm^2, but it was assumed that at rest only 60% of the lamellae were perfused. Thus $A = 4.14 \times 10^3$ cm^2.

In Poiseuille's equation (5) $\eta = 0.833 \times 10^{-6}$ cm H_2O.min, i.e. a blood viscosity of 5 cp. For the calculations on the afferent filament artery corrections were made for vessel taper and the loss of flow to branches. Vessel taper increases resistance to flow and resistance was calculated from its inverse relationship to radius to the fourth power. The calculations are presented in Table XIII and they indicate that a taper of 10 to 30% approximately doubles resistance. The AFA tapers to 10 to 30% of its basal diameter by a position 60% of the way along its length (Fig. 14). Equation (6) was developed from a simple electrical analogue to predict the percentage decrease in vessel resistance due to a progressive loss of flow to branches.

$$\% = m - \frac{1}{n} \sum_{k=1}^{k=m-1} k \qquad (6)$$

where n = the total number of lamellar units on a filament and m = the number of lamellar units at any location along the filament length. Using equation (6), a vessel resistance would be 50% lower than if there were no flow loss to branches. The representative geometry used for afferent lamellar arterioles in proximal, central and distal locations was $l = 600\,\mu$ with $r = 10\mu$, $l = 300\,\mu$ with $r = 8.5\,\mu$ and $l = 150\,\mu$ and $r = 7\,\mu$, respectively.

TABLE XIII

The effect of taper on the resistance of flow in a vessel, where resistance is inversely related to radius to the fourth power.

TABLE XIII

% decrease in radius (r)	0	10	20	15	30	40	50
Resistance $x10^3$ ($= r^4$)	1	1.5	2.4	3.16	4.2	7.7	16

APPENDIX II

Discussion of the use of the micropressure system

Many accurate intravascular and intralymphatic pressure measurements have been made with the micropressure system (See Section II for references). The fidelity of the micropressure 4 system (Fig. 45) used here was measured using calibrations against static pressures developed by a column of water and a dynamic test of frequency response using a "pop-test" (McDonald, 1960). Initially each individual pipet was calibrated and the frequency response tested. After many calibrations it was established that, provided the pipet tip was not partially or completely obstructed, a batch of micropipets with similar tip diameters had the same calibration and their frequency response was between 10 to 20 Hz. Therefore, in later experiments only a representative micropipet was calibrated from each batch of pipets and the rest were visually examined for tip size and internal particles. Typically if a micropipet tip was obstructed the system could not be nulled. Such pipets were discarded. A high yield of unobstructed pipets was obtained only if a rigid protocol of cleanliness was adhered to: scrupulous cleaning of the capillary tubing with a series of concentrated acids, methanol and distilled water; triple filtering of all solutions where possible and using dust covers with a relatively dust free room.

Source of measurement error

The micropipet will only record pressures if the tip is unoccluded and on many occasions pipets were discarded because they became blocked or partially blocked with mucus or tissue during the micropuncture. Only two types of pressures could, therefore, be recorded from the micropipet. Those due to a) blood pressures with the tip in a vessel lumen and b) internal volume changes as a result of bending of the pipet tip. Despite all my efforts to stabilise the preparation, movements at the micro level were problematic. Several strict criteria were, therefore, used to distinguish between pressure artifacts from bending and true blood pressures. Of the several hundred micropressure recordings made less than 40 passed this scrutiny. If there was the least doubt concerning a recording it was rejected. Some of the characteristics of bending artifacts are outlined below.

Mean pressure: The greatest blood pressure in the gill filament could be no greater than the ventral aortic (in vivo) or input (in vitro) pressures. Bending could generate even higher pressures.

Wave form: Pulsatility is lost as blood passes through the compliant gill bed. There is also a characteristic shape to the ventral aortic or input pressure pulse. Bending generated pulse pressures which were in excess of afferent pulse pressures and

which possessed a different wave shape. Often reversed saw-tooth shapes and very sharp triangular shapes were seen as artifacts. Particular effort was made to select micropressures with similar wave forms as the input and output pressures. Note Fig. 17, p.116.

Phasic relationships: Bending artifacts were out of phase with true micropressures, either leading afferent or lagging behind efferent pressures.

The location of the micropipet tip was never visualized during pressure measurements since the tip size approaches the resolution of light microscopy and all gill arteries and arterioles are located deep in the tissues. Post-experimental histological examination of filament micropuncture sites was uninformative due to the small size of the puncture, the vastness of the tissue and limited quantities of dye that could be injected into the tissue from the micropipet. It was, therefore, assumed that the micropipet was in a lumen of a vessel if a pulsatile pressure was being recorded and the artifact possibilities had been eliminated. But what vessel was the pipet in? Fortunately, the regular arrangement of the filament vasculature allowed an answer. On either the efferent or afferent side of the filament there are only two types of vessels: venolymphatic and arterial. I made no attempt to distinguish between recordings made in filament arteries and lamellar arterioles on either the afferent or efferent side of the filament. It was also assumed that arterial pressures could not be less than output pressures.

Micropressure measurements were also attempted on trout gills *in vitro* and C-O sole (*Pleuronichthys coenosus*), a flat fish, *in vivo*, but these experiments had no better success than the experiments with ling cod.

FIGURE 45

A schematic representation of A. the fundamental principle of the servo nulling micropressure measurements and B. the experimental setup (as taken from handbook, I.P.M., San Diego, Ca.).

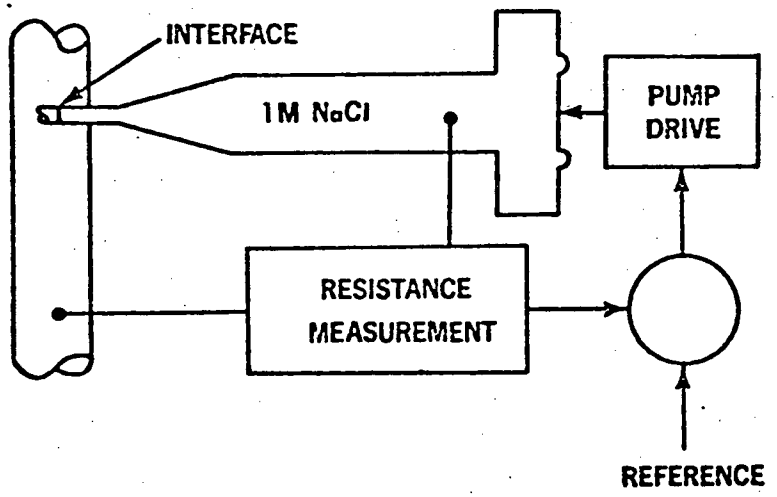
INTERFACE
1M NaCl
PUMP DRIVE
RESISTANCE MEASUREMENT
REFERENCE

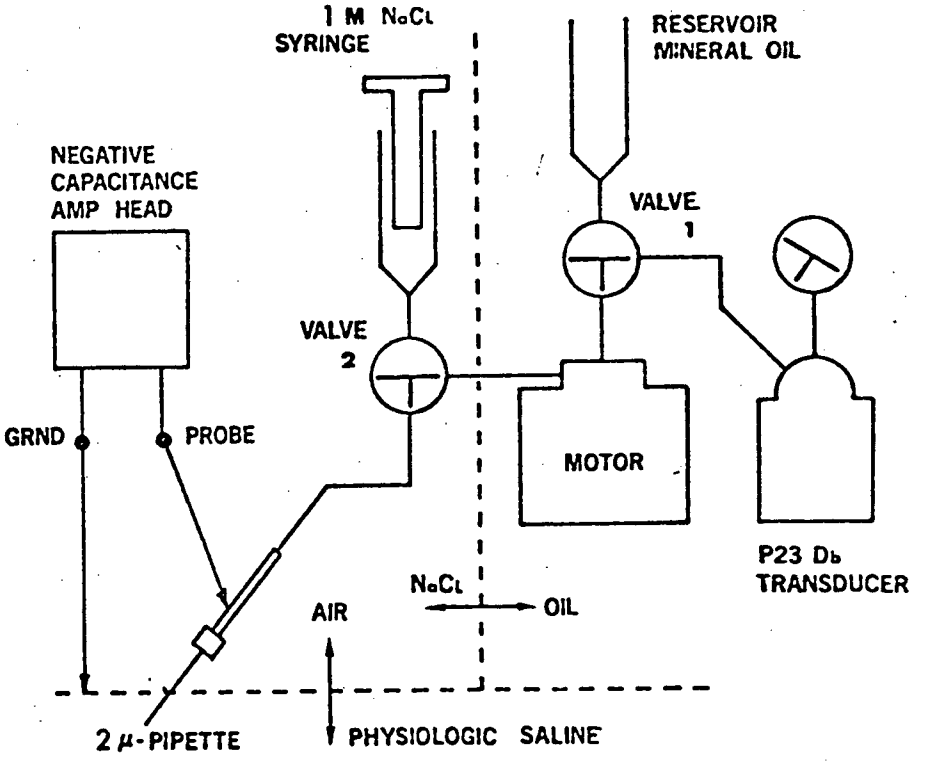
1 M NaCl SYRINGE
RESERVOIR MINERAL OIL
NEGATIVE CAPACITANCE AMP HEAD
VALVE 1
VALVE 2
GRND
PROBE
MOTOR
P23 Db TRANSDUCER
NaCl
OIL
AIR
2 μ-PIPETTE
PHYSIOLOGIC SALINE

APPENDIX III

The transfer factor is a measure of the relative ability of the respiratory surface to exchange gases, and is affected by changes in surface area available for exchange, as well as diffusion distance between blood and water (Randall *et al.*, 1967). The oxygen transfer factor To_2, is defined as

$$To_2 = \frac{Mo_2}{Po_2 \text{ difference between water and blood}}$$

Diffusing capacity of the gills is estimated from morphometric data on the secondary lamellae.

$$\text{Diffusing capacity} = K.\frac{A}{\bar{x}_h}$$

where A is the total surface area of all lamellae and $\bar{x}_h$ is the harmonic mean thickness of the blood to water barrier.